National Library of Canada
Bibliothèque nationale du Canada

Canadian Theses Service
Service des thèses canadiennes

Ottawa, Canada
K1A 0N4

ISBN 0-315-53234-3

STRUCTURAL GEOLOGY AND METAMORPHISM OF ARCHEAN VOLCANIC AND SEDIMENTARY ROCKS AT FENTON LAKE, SLAVE PROVINCE, N.W.T.

BY
R. D. CULLEN

A Thesis
presented to the University of Ottawa in partial fulfillment of the requirements for the degree of Masters of Science in Geology.

Ottawa, Ontario
1989

UNIVERSITÉ D'OTTAWA
UNIVERSITY OF OTTAWA

ABSTRACT

The Fenton Lake portion of the Cameron River volcanic belt is comprised of metamorphosed pillowed and massive flows, with intercalated lenses of felsic volcanic and metasedimentary rocks. The volcanics lie in a steep westerly facing homocline, 1km to 4km across, in fault contact with a complex of older gneissic rocks and younger granitic plutons to the east. The volcanics are overlain to the west by metamorphosed turbiditic greywackes and minor argillites.

The homoclinal volcanic belt abruptly changes trend in the vicinity of Fenton Lake, from northwest to northeast thereby forming an angular outcrop pattern. The development of this pattern is related to a succession of structures.

Deformation of the supracrustal rocks took place in at least four distinct phases. D_1 deformation in the metasediments produced upright to overturned, tight to isoclinal F_1 folds with axial plane parallel foliations rarely apparent. The steep westerly facing homocline in the metavolcanics apparently formed during D_1, accompanied by formation of a bedding - parallel mineral foliation , S_1, associated flattened pillows, and a steeply plunging mineral and pillow

stretching lineation. S_1, in general conformity with the map pattern, changes abruptly in strike from northeast to northwest across a 'fabric front' with the northwest striking foliation apparently overprinting that striking northeast. A later N - S set of S_1 type foliation crosses the other sets within the 'corner' area.

D_2 deformation produced an easterly striking S_2 foliation generally obliterated by later foliations but locally preserved as trails of quartz in biotite and mica in cordierite poikiloblasts, and in metavolcanic rocks as a crenulation cleavage. Map scale F_2 folds are not recognized. D_3 deformation produced minor F_3 folds and an axial planar S_3 foliation in two dominant orientations. S_{3A} strikes northwesterly and a later subset, S_{3B}, strikes northeasterly across both gneissic and supracrustal rocks. S_{3A} and S_{3B} vary from a crenulation cleavage to a penetrative alignment of phyllo-silicates and amphiboles.

Low pressure, high temperature, amphibolite grade metamorphism accompanied intrusion of a late Archean granitic pluton in the northeastern part of the mapped area. Biotite - garnet geothermometry indicates that garnet within the metavolcanic domain began to form at $300^{o}c$ and continued forming to peak temperatures of

570°c within 2 km of the northern granite. Porphyro blasts of biotite, cordierite and garnet are pre- to syn- D_3, indicating that peak temperatures associated with emplacement of the granitic pluton were attained late in the deformational history.

It is suggested that the development of S_1 foliations in contrasting directions parallel to segments of the volcanic homocline indicates sequential development of the segments. The angular arrangement could reflect control of structures by an underlying fault system. Later deformations (D_2 and D_3) and synkinematic emplacement of the granite pluton appear to have resulted in minor modifications to the angular pattern.

INDEX

ABSTRACT i
INDEX iv
LIST OF TABLES vii
LIST OF MAPS vii
LIST OF FIGURES vii
ACKNOWLEDGEMENTS xii

1 INTRODUCTION 1
1.1 Purpose 1
1.2 Location and access 1
1.3 Physiography 4
1.4 Relevant previous work 5
1.4.1 Mapping 5
1.4.2 Geology 6
1.4.3 Zircon Dating 9
1.4.4 Metamorphism 9
1.4.5 Structure 10
1.4.6 Depositional and Evolutionary Models 12
1.5 Field and laboratory work 13

2 GENERAL GEOLOGY 15
2.1 Metamorphism 16
2.2 Deformation 16

3 GRANITIC ROCKS 20
3.1 Sleepy Dragon Complex 20
3.2 Northern Granite 23

4 VOLCANIC ROCKS 25
4.1 Map Pattern 25
4.2 Contacts 25
4.2.1 Volcanic rocks and granitoid gneisses 25
4.2.2 Sedimentary rocks and volcanic rocks 26
4.2.3 Granite and volcanic rocks 28
4.2.4 Gneissic rocks and granite 29
4.3 Lithology 29
4.3.1 Mafic Volcanics 29
4.3.2 Felsic Volcanics 32
4.4 Facing indicators 33
4.5 Mafic Dykes 37
4.6 Alteration 40

5 SEDIMENTARY ROCKS 42
5.1 Introduction 42
5.2 Bedding top indicators 42
5.3 Lithology 45
5.3.1 Sedimentary domain 45
5.3.2 Intervolcanic sedimentary rocks 48
5.4 Petrology 49
5.4.1 Sedimentary domain 49
5.4.2 Intervolcanic sedimentary rocks 51

6	DEPOSITIONAL ENVIRONMENT	54
6.1	Volcanic rocks	54
6.2	Sedimentary rocks	55
7	METAMORPHISM	60
7.1	Introduction	60
7.2	Metasediments	61
7.2.1	Greenschist facies	61
7.2.1.1	Muscovite and Chlorite	61
7.2.1.2	Biotite	62
7.2.2	Amphibolite Facies	68
7.2.2.1	Cordierite Isograd	68
7.3	Metavolcanic rocks	70
7.3.1	Greenschist facies	70
7.3.1.1	Chlorite, Actinolite, Biotite, Albite	70
7.3.2	Amphibolite facies	72
7.3.2.1	Hornblende Isograd	72
7.3.2.2	Anorthite	77
7.3.2.3	Garnet	78
7.3.2.4	Cummingtonite	79
7.3.2.5	Calcic Pyroxene	80
7.4	Sleepy Dragon Complex - metamorphism	81
7.5	Microprobe Analysis	81
7.5.1	Amphibole	82
7.5.2	Garnet - Biotite geothermometry	86
7.5.2.1	Introduction	86
7.5.2.2	Methods	88
7.5.2.3	Results	92
7.5.2.4	Conclusions: Garnet - Biotite Geothermometry	94
7.6	Conclusions	95
8	STRUCTURAL GEOLOGY	97
8.1	Introduction	97
8.2	D_1 Structures	100
8.2.1	Metasedimentary rocks	100
8.2.1.1	Folds	100
8.2.1.2	Structural domains	103
8.2.2	Metavolcanic rocks	103
8.2.2.1	Folds	103
8.2.2.2	Foliation	105
8.2.2.3	Lineations	108
8.2.2.4	Orientations of S_1 and F_1	108
8.2.3	Structural domain relationships	110
8.3	D_2 Structures	111
8.3.1	Metasedimentary rocks	111
8.3.2	Metavolcanic rocks	113
8.4	D_{3A} Structures	115
8.4.1	Introduction	115
8.4.2	Metasedimentary rocks	115
8.4.3	Metavolcanic rocks	118
8.5	D_{3B} Structures	121

8.5.1	Introduction	121
8.5.2	Metasedimentary rocks	121
8.5.3	Metavolcanic rocks	122
8.6	Crystal growth and deformation	122
8.6.1	Metasedimentary Rocks	123
8.6.2	Metavolcanic Rocks	123
8.7	Structures within the Sleepy Dragon Complex	127
8.7.1	Introduction	127
8.7.2	Foliations and mylonites	127
8.7.3	Lineations	131
8.8	Structures within the northern granite	131
9	SUMMARY AND SPECULATIONS	133
9.1	Structural Geology	133
9.2	Metamorphism	135
10	SUGGESTIONS FOR FURTHER WORK	137
10.1	Field Work	137
10.2	Lab Work	139
REFERENCES		140
APPENDIX 1: Microprobe Analysis of Amphiboles		152

TABLE	DESCRIPTION	PG#
1	Geothermometry results for biotite/garnet pairs	89
2	Formulae used to calculate mole fraction	90
3	Margules parameters for garnet solid solutions	93

MAPS	In pocket at back
1	Preliminary geology of the Fenton Lake area at 1:10,000 scale
2	Preliminary structural geology of the Fenton Lake area

FIG #	DESCRIPTION	
1.1	Location Map - Cameron and Beaulieu volcanic belts.	2
1.2	Location Map, Slave Structural Province.	3
1.3	Location Map (in pocket) for sampling, structural domains, and metamorphic isograds.	
2.1	Photograph - Folded mylonite Sleepy Dragon Complex	19
3.1	Photomicrograph - Least deformed Sleepy Dragon Granitic Rock	22
3.2	Photomicrograph of mylonitic foliation, Sleepy Dragon Complex	22
3.3	Photomicrograph - Northern granite	22
4.1	Photograph - Granitic boulders embedded in mafic volcanic rock	28
4.2	Photograph - Northern granite	28
4.3	Photograph - Pillowed basalt flow	28
4.4	Photograph - Extrusive mafic flow unit including pillow breccia, pillow basalt and massive basalt	28

Fig. #	Description	PG#
4.5	Photograph - garnet in outcrop of interflow sediments	28
4.6	Extrusive mafic flow units including pillow breccia, pillowed and massive flows	31
4.7	Pillowed volcanic rock cross section	34
4.8	Strained pillowed volcanic rock	36
4.9	Photograph - Pillowed mafic volcanic rock in cross section	39
4.10	Photograph - vesicular pillowed mafic volcanic	39
4.11a	Photograph - epidote filling fracture and foliation in mafic volcanic outcrop	39
4.11b	Photograph - epidote filling fracture and foliation in mafic volcanic outcrop	39
5.1	Bouma sequence	44
5.2	Photograph - Well bedded sediments with S_{3A} and S_{3B} foliation	47
5.3	Photograph - A, B, E portions of Bouma sequence in outcrop	47
5.4	Photograph - B, E portions of Bouma sequence in thin graded beds	47
5.5	Photograph of A and B or D Bouma divisions in thin bedded sediments	47
5.6	Photograph - Quartz eye porphyry	47
5.7	Photomicrograph - Carbonate rich interflow sedimentary rocks	47
5.8	Photomicrograph - Bedding contact between coarse wacke and pelitic bed	53
5.9	Photomicrograph - Carbonate rich intervolcanic sediment with garnet	53
5.10	Photomicrograph - Coarse grained interflow sedimentary rock	53

Fig#	Description	PG#
6.1	Submarine depositional fan	56
6.2	Photomicrograph - Quartzofeldspathic wacke	58
6.3	Photomicrograph - Poorly sorted sedimentary rock	58
7.1	Map - (in pocket) Cordierite and Hornblende in isograds in the Fenton Lake area with microprobe sample locations	
7.2	Photomicrograph - Biotite with interleaved chlorite	64
7.3	Photomicrograph - Biotite poikiloblasts inside cordierite poikiloblast	64
7.4	Photomicrograph - Biotite poikiloblasts with quartz inclusion trails	64
7.5	Photomicrograph - Biotite porphyroblasts	67
7.6	Photomicrograph - Mineralogy of a greenschist grade metavolcanic rock	67
7.7	Photomicrograph - Alteration of feldspar to sericite	67
7.8	Photomicrograph - Hornblende alteration to chlorite	67
7.9	Divisions of metamorphic grade	73
7.10	Photomicrograph showing tourmaline crystals in metavolcanic rock	76
7.11	Photomicrograph - Garnet poikiloblast in metavolcanic rock	76
7.12	Photomicrograph - Cummingtonite in volcanic rock	76
7.13	Photomicrograph - Calcic pyroxene in metavolcanic rock	76
7.14	Discrimination plots for amphibole composition	83

Fig. #	Description	Pg#
7.15	Discrimination plots for amphibole composition	83
7.16	Discrimination plots for amphibole composition	84
8.1	Outline maps of the study area showing structural trend lines	98
8.2	Stereonet plots of poles to S_0 and S_1 divided into structural domains	101
8.3	Contoured plots of Fig 8.2 stereonets	102
8.4	Sketches of F_{3A} and F_{3B} in outcrop	104
8.5	Photograph - Flattened pillow basalts	107
8.6	Photograph - Elongate pillowed flow rocks	107
8.7	Photomicrograph - Lineation parallel sulfides in metavolcanic rocks	107
8.8	Stereonet plots of poles to S_2, S_{3A}, and S_{3B}	112
8.9	Sketches of F_{3A} and F_{3B} folds in outcrop	114
8.10	Photograph of F_{3A} asymmetrical folds in metasedimentary rocks	117
8.11a	Photomicrograph - S_{3A} parallel phyllosilicates	117
8.11b	Photomicrograph - Biotite poikiloblast containing S_2 parallel quartz inclusion trails	117
8.12	Photomicrograph - Hornblende porphyroblasts in metavolcanic rocks	120
8.13a	Photomicrograph - Polycrystaline quartz clast from intervolcanic sedimentary rock	120
8.13b	Photomicrograph - Intervolcanic sedimentary rock	120

Fig#	Description	Pg#
8.14	Photograph - S_{3A} and S_{3B} foliations in sedimentary rocks	120
8.15	Photomicrograph - S_1 or S_2 parallel hornblende with F_{3B} intrafolial fold and rare S_{3B} parallel hornblende laths.Structural domain B, metavolcanic rock	126
8.16	Photograph - Northerly striking foliation in Sleepy Dragon Granitic rocks	126
8.17	Photograph - Shear bands and F_{3A} folds in Sleepy Dragon Granitic rocks	126
8.18a	Photomicrograph - Recrystallized Sleepy Dragon Granitic rocks	126
8.18b	Photomicrograph - Quartz ribbon lineation in Sleepy Dragon Granitic rock	130
8.19a	Photomicrograph - Mylonitic foliation in Sleepy Dragon Gneiss	130
8.19b	Photomicrograph - Mylonitic foliation in Sleepy Dragon Complex	130
8.20a	Photograph - Vertical lineation in Northern granite	130
8.20b	Photograph - Unlineated surface of Northern granite	130

Acknowledgements

It is my pleasure to here acknowledge the patience, wisdom and expertise of Dr. W. K. Fyson whose tireless effort has made this thesis document possible. Dr. Fyson was always able to direct the effort in the forward direction even as I tried my best to bog it down in endless turnings.

Thanks are due to Dr. Ralph Kretz for his contribution to the work through his impressive knowledge in the fields of petrography and metamorphism. Dr. M. Lambert is thanked for his careful review of the map accompanying this thesis. He also funded the microprobe work, carried out at the Geological Survey of Canada by M. Bonardi.

Sincere thanks to Sue Meunier, Julie (nee) Hayes, George Mrazek, J. F. Tardiff, Ron Hartree and the indomitable Edward Hearne, the technical staff of the University of Ottawa for their help, advice (whether or not solicited) and concern during the preparation of this thesis.

The project was funded under a contract let by the Department of Indian Affairs and Northern Development at Yellowknife, Dr. Bill Padgham, director and produced Economic Geology Series map 1987 - 10.

CHAPTER 1

INTRODUCTION

1.1

PURPOSE

This project was undertaken to study structural geology and metamorphism in the Fenton Lake portion of the Cameron River volcanic belt and adjacent metasedimentary rocks (Figs. 1.1 and 1.2)

This part of the belt is particularly interesting structurally because; 1) the volcanic belt abruptly changes trend from northeasterly to northwesterly and 2) the volcanic succession is in contact with basement gneissic and granitoid rocks (the Sleepy Dragon Complex).

A study of the metamorphism in the area was undertaken to show; 1) the grade of metamorphism, including estimates of temperature based on garnet/biotite geothermometry and 2) the timing of metamorphism in relation to deformation.

1.2

LOCATION AND ACCESS

The Fenton Lake portion of the Cameron River volcanic belt (Fig 1.2) is located 120 km northeast of Yellowknife, N.W.T. in the Slave tectonic province (Fig. 1.1). Access is possible by aircraft only. Depending on the season, floats or skis are neces-

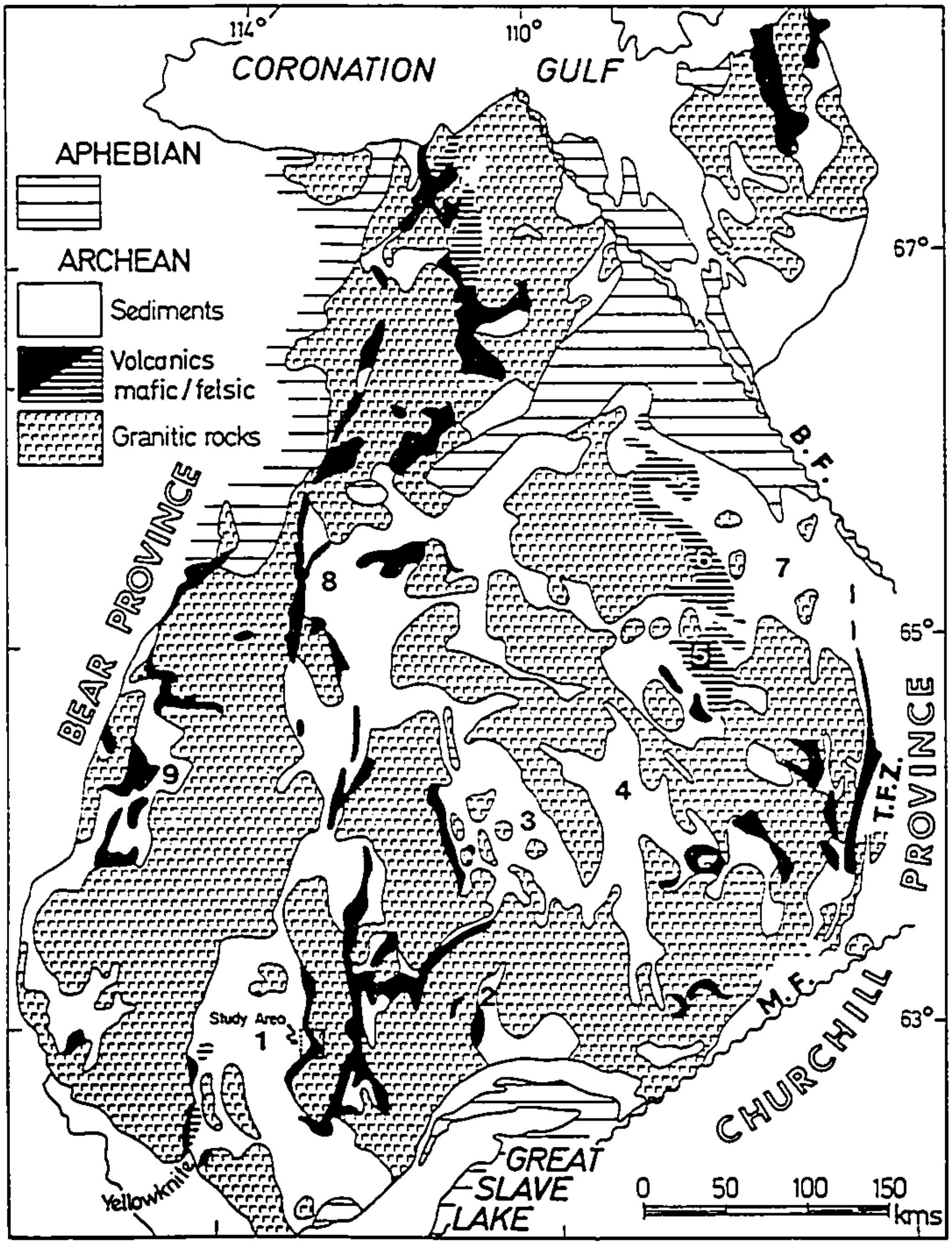

Figure 1.1 Slave Province supracrustal domains with dashed outline of study area near the midpoint of the Cameron River volcanic belt on the eastern side of domain 1, the Yellowknife domain. Other domains, by number are: 2) Benjamin Lake, 3) MacKay Lake, 4) Aylmer Lake, 5) Back River felsic volcanics, 6) Hackett River felsic volcanics, 7) Beechy Lake, 8) Itchen Lake, 9) Indin Lake, 10) Takijug Lake belt. TFZ = Thelon Front Zone. (Figure after Fyson and Helmstaedt, 1988.)

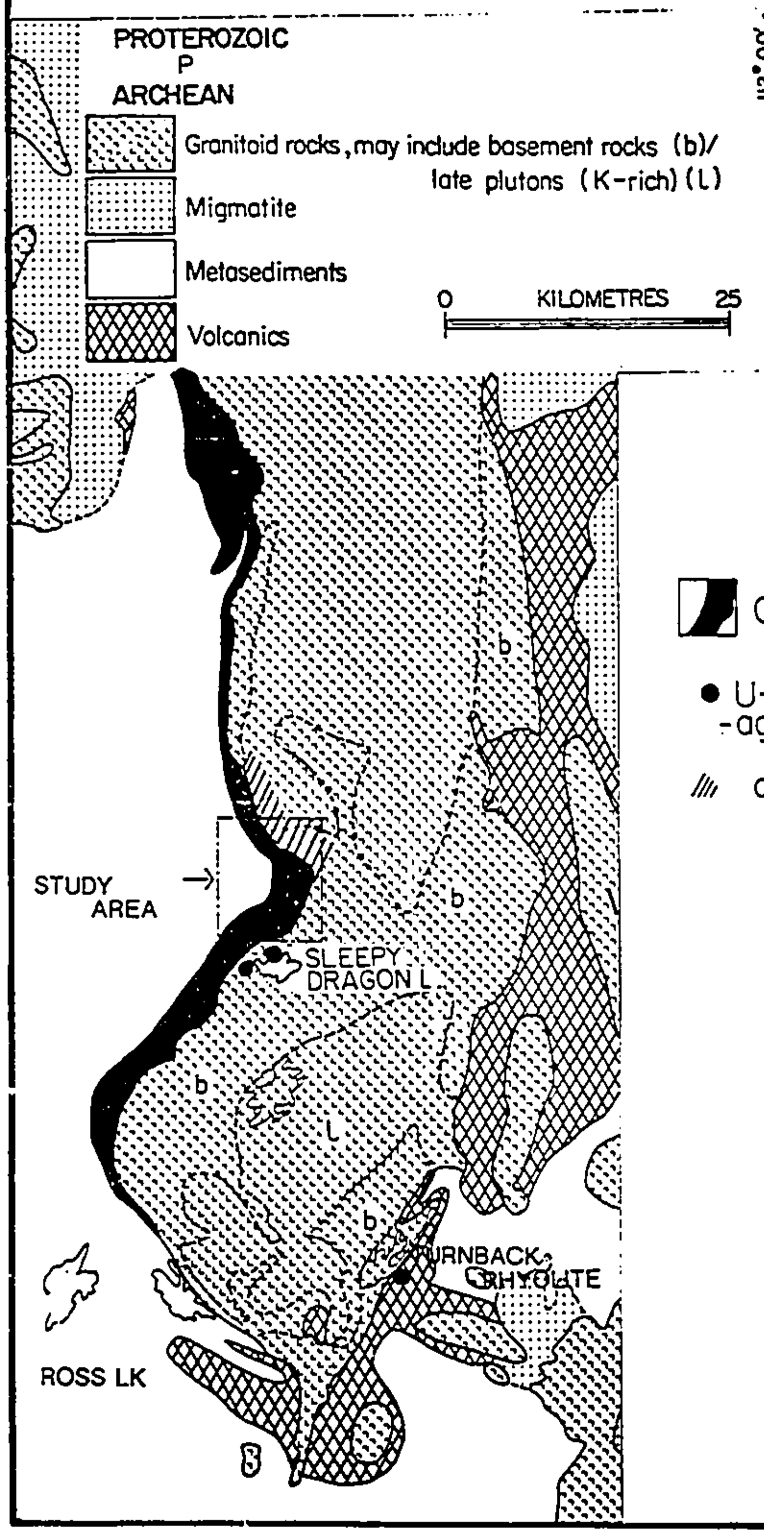

Figure 1.2 Location map for the study area showing the Cameron River volcanic belt and relative positions of the Turnback Rhyolite and Sleepy Dragon Lake zircon sample locations. (Figure after Fyson and Helmstaedt, 1988.)

sary. Helicopter access is also possible from Yellowknife.

1.3

PHYSIOGRAPHY

Fenton Lake lies below the tree line at an elevation of 280m ASL with spot heights of 360m and 390m ASL along the volcanic ridge on the eastern shore of the lake. Rock units have distinct topographic expression relative to each other. Areas underlain by metavolcanic rocks dominate the landscape, rising in cliffs and steep side hills up to 50 meters high above metasedimentary rocks to the west and granitic and gneissic rocks to the east (Map 1). Relief is especially marked along the east striking and parts of the north striking contact with the Sleepy Dragon Complex where the volcanics rise in sheer cliffs. The contact between metavolcanic rocks and the northern granite is seldom as sharp, generally defined by a steep slope eastward from the metavolcanics down to the granitic rocks.

Bedrock is exposed over at least 30% of the area with moss and lichen obscuring some of the details on otherwise well exposed surfaces. Felsic volcanic rocks within the northwest trending arm of the metavolcanics and intervolcanic quartzitic sediments throughout the metavolcanic domain are recessively weathered and outcrop along swamp margins and in deep gullies. Lake shore outcrops generally provide the greatest detail.

1.4

RELEVANT PREVIOUS WORK

1.4.1

Mapping

The geology of the Fenton Lake portion of the Cameron River volcanic belt (Map 1) which lies on the eastern margin of the Yellowknife supracrustal domain, has not previously been considered in detail. However, previous workers have investigated areas within the Yellowknife supracrustal domain that include portions of the belt. Mapping at various scales by members of the Geological Survey of Canada has continued since the late 1930's. The major lithological boundaries were delineated by Henderson in the field season of 1939 (Henderson, 1939). He produced a map at a 1:1,000,000 scale of the greenstone belts, sedimentary rocks and the granites of the area from 112 degrees west to 114 degrees west and lying between the latitudes of 62 and 63 degrees north. His descriptions of the sedimentary volcanic and granitic terrains have served as the model for later workers.

The volcanic rocks of that portion of the Cameron River Belt south of Fenton Lake have been described by Lambert (1977, 1988). The Cameron River volcanic belt north of latitude 63 degrees was mapped on a 1:250,000 scale by Moore et. al.(1951) and more recently at a scale of 1:50,000 by James (1989).

1.4.2

Geology

Henderson (1943) described the textures and composition of the sedimentary rocks[1] of the Yellowknife Supergroup (Henderson, 1985) as dominantly greywacke being comprised of mostly quartz with lesser amounts of feldspar and biotite and having the texture of a medium sand. He also described arkose, quartzite, silt and mudstone with the fine grained of graded units giving good top indications. Noting a minor conglomerate lens at the basal contact with the volcanic rocks east of Ross Lake (Fig. 1.1), Henderson (1939) indicated that granitic cobbles in the conglomerate could have come from the batholithic terrain to the east and represent a period of erosion previous to the extrusion of the mafic volcanic rocks. Henderson(1939) as well as later workers (Fortier,1946,1947; Moore et.al.,1951; Lambert, 1977,

(1. Though all rocks referred to are metamorphosed to greenschist or lower amphibolite grade, protolith names are used for clarity and brevity.)

1988; Henderson, 1981, 1985) have indicated that the contact between the volcanic rocks and the sedimentary rocks appears conformable.

The Cameron River volcanic belt is comprised of basaltic lavas, pillowed flows, pillow breccias, mafic tuffs and volcaniclastics becoming more siliceous and possibly andesitic towards the top of the pile. The volcanics are intruded by felsic and amphibolite dykes and in places intercalated with sediments and felsic lavas. The volcanic dominated assemblage has been assigned to the Beaulieu group (Henderson, 1985). The volcanics , which are mainly steeply dipping reach a maximum apparent thickness of 4000m in the southern part of the Fenton Lake area and thin north and further south to apparent widths of 900 meters and 2800 meters respectively. As noted by Lambert (1988), such measurements apply to the present map pattern only and do not account for possible tectonic thickening or thinning.

The Cameron river volcanic rocks are marginal to gneissic and granitic rocks to the east. The nature of the contact between these lithologies (Units 1 and 4 and unit 2; Map 1) is of interest as the southeastern granitic terrain - the Sleepy Dragon Complex (Davidson, 1972) - appears in part, to be basement to the Yellowknife supracrustal rocks.

Baragar(1966) noted that the composition and texture (plagioclase laths up to 1 1/4 inch long) of mafic dykes that cut the gneissic rocks was repeated in some of the flows within the volcanic pile. He felt that this was evidence that the dykes were feeders to the volcanics which therefore were younger than the gneissic rocks. Neither Baragar(1966) nor later workers in the area (Lambert, 1977,1988, this study), have been able to trace dykes across the contact from the Sleepy Dragon Complex into the volcanics, perhaps indicating that subsequent movement along the contact has accompanied the deformation of the area.

Davidson(1972) found that the cataclastic foliation in the older gneiss adjacent to the Cameron River belt in the vicinity of Sleepy Dragon Lake was truncated by the overlying volcanic rocks which were relatively undeformed and showed no evidence of a similar foliation. Lambert (1977) noted that a NNE trending foliation in the gneissic rocks was conspicuously absent in the overlying volcanic rocks.

Henderson (1985) reported that the conglomerate described by Henderson (1939), was in contact with the gneissic rocks at a point east of Ross lake where the volcanics pinch out. The cobbles appeared similar in composition to the Ross lake granodiorite and may indicate that the granitic rocks contributed detritus to the sediments.

Kusky (1988, 1989) maintains that the granitic and gneissic rocks of the Sleepy Dragon complex are in thrust contact with the volcanics.

1.4.3

Zircon Dating

Recent zircon dating for granitoid gneisses near Sleepy Dragon Lake (Fig. 1.2), within the Sleepy Dragon Complex area (Henderson, 1985) gives an age of 2819 +40/-31 Ma (Henderson and van Breeman, 1987). Vulcanism in the area took place over 100Ma later, based on a U-Pb zircon age of 2665 +/-5 Ma, from the Turnback rhyolite (Henderson and van Breeman, 1987), outcropping to the south and east of the Cameron River volcanic belt (Fig. 1.1).

1.4.4

Metamorphism

Upper greenschist to amphibolite grade metamorphism in Yellowknife group supracrustal rocks is attributed to the intrusion of granite plutons (Henderson,1939). The cordierite isograd in metasediments around the northeastern pluton in the Fenton Lake area, which is attributed to contact style metamorphism (Henderson, 1985) suggests that the younger granites may core a large thermal dome in which supracrustal rocks were heated to amphibolite grade temperatures (Ramsay and Kamineni, 1977)

1.4.5

Structure

Recognition of the nature of deformation in the sedimentary rocks of the Yellowknife supracrustal domain has evolved since the earliest report (Henderson, 1939) that the bedding was folded isoclinally in wavelengths that were dependant on coarseness of deposits, with the larger wavelength folds propagating in the coarser sediments. Fortier (1946) recognized a second generation of cross folds that were generally north trending and a northwest trending cleavage that did not seem to be related to the major structures in the sediments, but may have been related to the cross folds. Fyson (1975, 1981, 1982, 1984a) described the polyphase nature of the deformation in metasediments from a number of localities within the southern part of the Slave Province. Mapping to the west and south of the Fenton Lake area, Fyson (1975) described large, kilometer scale F_1 structures, with smaller 100-200m long F_2 fold hinges overprinting them. A late S_3 north to northwest striking foliation is related to small scale F_3 folds. In a later paper (Fyson, 1984a) he describes the succession of structures in the Yellowknife domain as a progression from large scale F_0 synclines in part marginal to the metavolcanic rocks followed by intermediate scale F_1 folds, both being overprinted by S_2 and S_3 penetrative cleavages, often related to minor folds. The S_3 cleavage is subdivided into 2 sets, an S_{3A} north to northwest trending set, commonly preserved in silty or sandy beds and S_{3B}, a crenulation of S_{3A} most strongly developed in argillites and phyllites.

The Cameron River volcanic rocks have been described as forming a west facing homocline with minor folds on its eastern side by Henderson (1985), and as forming a simple homocline with steep to overturned beds (Fortier, 1947 ;Henderson,1939; Moore, et.al.,1951 and Lambert, 1977). Lambert (1988) indicates the presence of folds within the Cameron River volcanic belt to the south of the Fenton Lake area.

The predominant foliation in the volcanics is parallel to belt trends over much of the mapped area. This fabric is enhanced by the flattening of pillows in the foliation plane (Lambert, 1977, 1988). Lambert(1977, 1988) also notes that a northwest trending foliation in the volcanics is axial planar to open folds in the main foliation. This fabric may be temporally related to the S_{3A} northwest striking foliation documented locally within the Yellowknife metasedimentary domain by Fyson (1984a).

1.4.6

Depositional and Evolutionary Models

Models for the deposition and deformation of the volcanic and sedimentary rocks of the Slave Province have been suggested by Henderson (1981, 1985), Lambert (1977, 1988), Hoffman (1986), Kusky (1986) and Kusky (1987). Henderson (1981, 1985) and Lambert (1977), both favored the existence of an early sialic crust which underwent extension and rifting. The volcanic belts could have been deposited during this rifting by extrusion of mafic lavas from mantle sources. Deformation in the rocks would ensue as basins created by the downsagging of the sialic platform closed. Hoffman (1986) suggests that the greenstone belts may represent remnants of exotic terrains within an oceanic plate that were sheared off during subduction of this plate beneath some precursor to the Slave province.

Kusky (1986) cites the outcropping of ultramafic rocks along the contact between gneissic rocks and overlying volcanics and evidence for dykes intruding dykes in the Yellowknife belt (sheeted dykes, described by Helmstaedt, et.al., 1987 and discussed by Kusky, 1987) as evidence that greenstone belts are ophiolitic in origin and represent primordial seafloor. In a 1989 paper (Kusky,1989) he suggests that mylonite zones along granite, volcanic contacts in the Cameron River belt could have been the focus of the transport of ophiolites as these mylonites could represent many kilometers of movement. However, Lambert (1988) has observed that the dyke swarms along the margins of the Sleepy Dragon Complex cross felsic igneous and metamorphic rocks and are therefore not part of an oceanic ophiolite complex. He also suggests that the ultramafic rocks described by Kusky (1986) are volumetrically unimportant and could be intrusive.

1.5

FIELD AND LABORATORY WORK

Field work for this thesis was carried out from early June to late August of 1985 and during the first two weeks of July, 1986 with the help of an assistant.

Loop traverses supported by inflatable outboard motor boat were made from base camps on Fenton Lake and a large lake to the east of the volcanic rocks in 1985 and 1986 respectively. Over 200 rock samples were collected, the majority oriented, for thin section study and laboratory analysis.

Approximately 140 thin sections were cut and analysed by microscopy (for structure and mineralogy), staining (for feldspars) and microprobe (for mineral chemistry). Laboratory work was ongoing from

1985 through 1987, involving thin section study and X-Ray flouresence work at the University of Ottawa, X-Ray diffraction at Carleton University and microprobe analysis, performed by Mr. Bonardi at the Geological Survey of Canada on Booth Street in Ottawa.

CHAPTER 2

GENERAL GEOLOGY

Henderson (1939) described the Cameron River belt as extending; "from the northeast shore of Ross Lake northwest to Cameron River and thence northeast , parallel to the northeast branch of the river, to the northern boundary of the area." This describes the Cameron River belt up to the midpoint of Fenton Lake at which point it bends again to trend northwest and then north to the boundary of the area mapped in this study (Fig. 1.1).

Within the map area, dominantly pillowed basaltic rocks intercalated with pillow breccias, massive flows and cut by dykes (Unit 2, Map 1) are overlain by generally coarser, poorly sorted sedimentary rocks (Unit 3, Map 1) to the west and overlie the Sleepy Dragon granite/gneiss terrain (Unit 1, Map 1), located in the southeastern part of the area. The supracrustal and basement succession is intruded by a late Archean granite (Unit 4, Map 1) in the northeastern part of the mapped area. Top determinations indicate that pillows generally face to the west, away from the granite/gneiss terrain (Units 1 and 4 combined, Map 1). A reversal in pillow top facing in the central part of the Fenton Lake map area and to the south of the area, reported by Lambert (1988), within the metavolcanic rocks may indicate small scale folding within the volcanic rocks. The pillowed flows and sedimentary rocks are steeply inclined to overturned.

2.1

Metamorphism

The sedimentary and volcanic rocks in the western and southern part of the map area have been metamorphosed to the greenschist grade. Within 3 km of the northeastern granite (Unit 4, Map 1), low pressure high temperature (575c +/-30c: see Chap. 7) amphibolite grade metamorphism has produced cordierite, biotite and garnet porphyroblasts within sedimentary rocks and hornblende and garnet porphyroblasts within the volcanic rocks. Less common high grade minerals within the volcanic rocks include cummingtonite, anthophyllite, calcic pyroxene, andesine and oligoclase.

2.2

Deformation

Deformation of the supracrustal rocks has taken place in at least 4 phases, each marked by distinctive structures. Notable are steeply inclined, kilometer - scale F_1 folds in the metasedimentary rocks that are overprinted by small, meter to centimeter scale, asymmetrical F_{3A} and F_{3B} folds and associated cleavage foliations throughout the map area. Progressive deformation of basement granitoid rocks has resulted in creation of and locally folding of mylonites (Fig 2.1) about northwest and northeast striking F_{3A} and F_{3B} axes.

Post Archean tectonism (younger than 2500 Ma) or metamorphism appears to be minimal. Intrusion of the northeast striking Proterozoic Dogrib Dyke swarm (Henderson, 1985) which crosses the Slave Province is represented by a northeast trending dyke that cuts the sediments in the central part of the map area. This dyke, apparently undeformed internally, was traced through the metasedimentary rocks and outcrops on the western and eastern shores of Fenton Lake, with some dextral offset, but could not be traced into the volcanic rocks, against which it appeared to terminate.

Figure 2.1 Photograph of folded mylonitic foliation along the east striking contact between the Sleepy Dragon Complex and metavolcanic rocks. The axial plane parallel foliation strikes toward 316° parallel to S_{3A} in the overlying metavolcanics.

FIG. 2.1

Chapter 3

GRANITIC ROCKS

3.1

SLEEPY DRAGON COMPLEX

The Sleepy Dragon Complex (Henderson, 1985) in the Fenton Lake area underlies the southeastern and parts of the eastern portion of the map area (Map 1). The rock varies from a light pink to white and has three morphologies; medium to coarse grained granite, (where undeformed), well foliated augen gneiss and mylonite. Dykes and irregular shaped bodies of amphibolite , usually foliated and often folded, intrude the granitoid rocks. Davidson (1972) has defined 8 units within the complex showing a range of composition from granite to granodiorite and tonalite.

The least deformed portion of the Sleepy Dragon granite, from the southern part of the map area, (Fig. 3.1) is composed of large microcline crystals, retrograded along fractures to fine muscovite and quartz aggregates, in a matrix of smaller albite and quartz crystals with interlocking grain boundaries. Accessory phases are muscovite, surrounded by light colored reaction rims (within which the mineralogy is unknown) and euhedral, light blue/grey tourmaline crystals, probably schorolite.

In augen gneisses feldspar and quartz aggregates with interlocking grain boundaries,

Figure 3.1 Photomicrograph of Sleepy Dragon Complex granitic rock. The rock is composed of large microcline crystals with smaller albite and quartz. Interlocking grain boundaries are visible between all phases. Accessory minerals are muscovite, chlorite and tourmaline. Sample from the southern part of the map area.
PP - plane polarized; CP - cross polarized

Figure 3.2 Photomicrograph of mylonite in Sleepy Dragon granitoid rock. Large feldspar grains are in the area of greatest grain size reduction in quartz. Accessory minerals are biotite and hornblende. Sample from near the northern striking contact of the Sleepy Dragon Complex and metavolcanics.
PP - plane polarized; CP - cross polarized

Figure 3.3 Photomicrograph of northern granite. Equigranular microcline, albite and quartz make up the bulk of the rock. Accessory minerals are biotite, some sericite (alteration of plagioclase), chlorite (alteration of biotite) and epidote. Sample from the northern part of the metavolcanic/granite contact, near the strike change from NW to N.
PP - plane polarized; CP - cross polarized

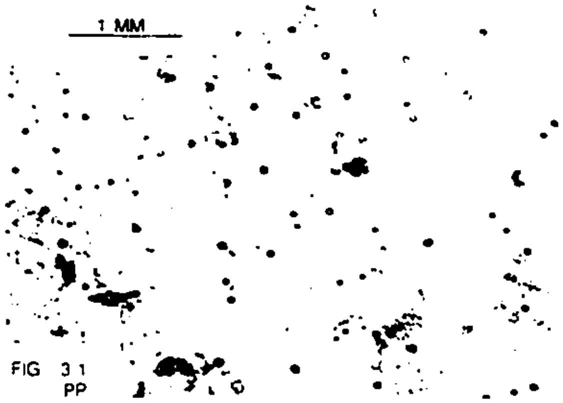

FIG 3.1 PP

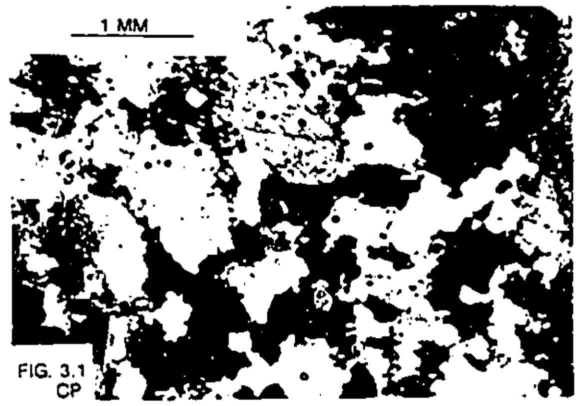

FIG. 3.1 CP

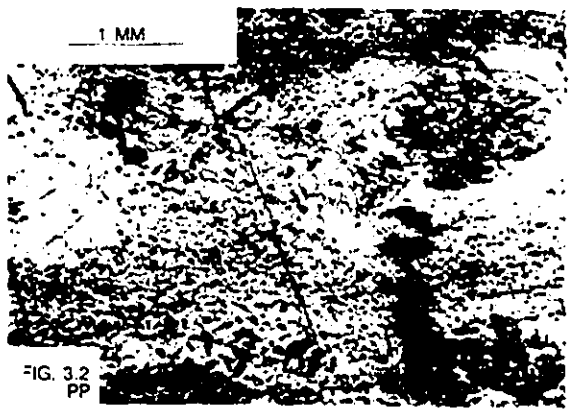

FIG. 3.2 PP

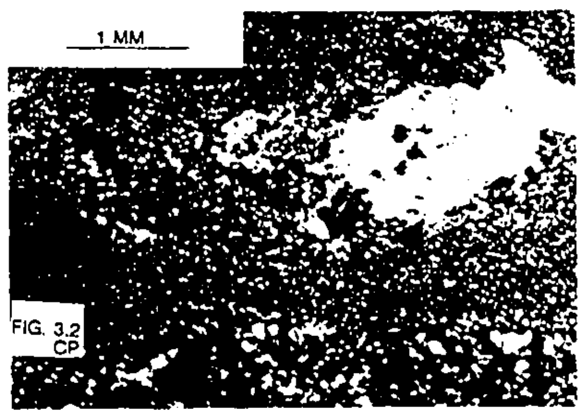

FIG. 3.2 CP

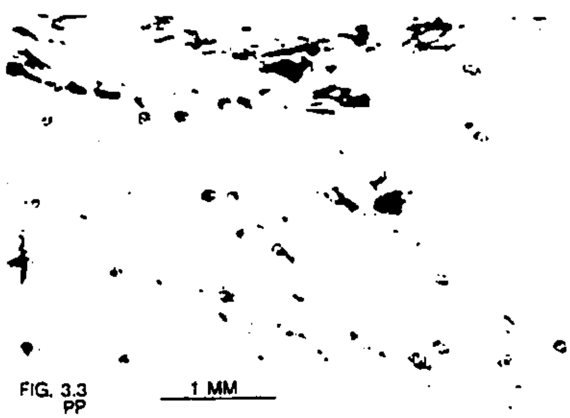

FIG. 3.3 PP

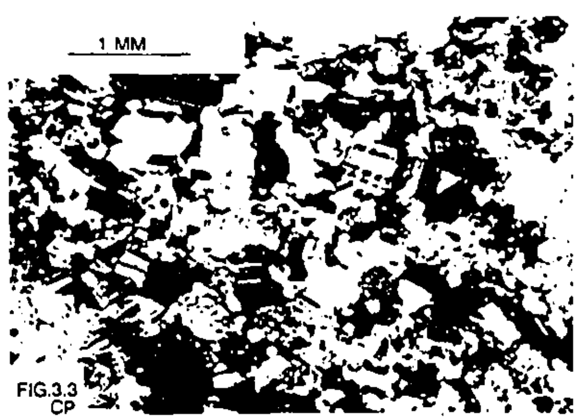

FIG.3.3 CP

ranging in size from mm to cm scale, have a micro-crystaline matrix of recrystallized quartz with .1mm or less grain size. In some examples, possibly retro-grade(?), muscovite, biotite and chlorite occupy intergranular spaces and lie parallel to foliations. Elsewhere biotite accompanies hornblende. Euhedral grains of tourmaline are visible in even the most deformed rocks.

In mylonitic rocks, zones of fine quartz grains a few hundredths of a millimeter across contrast with zones where larger grain sizes are tenths of millimeters across (Fig. 3.2). The fine grains were probably derived from coarser grains during deformation. Feldspar is relatively resistant to grain size reduction although relict grains have been reworked and rounded.

As in the volcanic rocks (see; Chap.4: VOLCANIC ROCKS) steep mineral lineations are seen even where the horizontal section appears undeformed. Quartz ribbons and amphibole crystals have a preferred orientation parallel to lineations (Fig. 8.18b, 8.19b).

3.2

NORTHERN GRANITE

In the eastern and northeastern part of the map area a younger granite intrudes the Sleepy Dragon

Complex gneisses and supracrustal rocks. This granite is a pink weathered , medium to coarse grained rock, little deformed except close to contacts where it has a weak LS fabric defined by alignment of quartz ribbons and micaceous minerals (biotite, muscovite and chlorite) (Fig. 8.20a).

Granitic and pegmatitic dykes associated with the intrusion outcrop over much of the metavolcanic succession within domain D and in domain C north of the Sleepy Dragon Complex. Dykes, both parallel to foliations and crosscutting are up to 2 meters wide and may be visible for 50 meters before pinching out or being lost in vegetation. Granitic dykes are not folded but are often offset along foliations.

Granite from two locations contain roughly equal parts of quartz, microcline and albite with muscovite, biotite and epidote. (Fig. 3.3) Patchy alteration of plagioclase to fine grained muscovite and chlorite interleaved with biotite indicate some retrograde alteration of the granite.

Chapter 4

VOLCANIC ROCKS

4.1

MAP PATTERN

The volcanic belt extends for 12 km across the map area, including a major change in trend from northeast in the southern portion to northwesterly in the northern portion.(Fig. 1.1)

4.2

CONTACTS

4.2.1

Volcanic rocks (Unit 2) and Granitoid gneisses (Unit 3)

Volcanic rocks overlie gneissic rocks and granite of the Sleepy Dragon Complex located to the east and southeast. The volcanic, gneiss contact is angular in map view curving sharply from a northerly strike to an easterly strike for about 3 km, at the southern boundary of the map area before curving to a northerly strike again (Map 1). Contact parallel mylonite zones in granitoid rocks are often folded (Fig. 2.1). One east striking mylonite zone appears to be continuous within the volcanic rocks in the southern part of the area (Map 2)

The volcanic, gneiss contact is obscured along much of its length by overburden. Where exposed, gossanous alteration is generally present, reducing the volcanic rocks to unconsolidated, rusty, red to yellowish material in widths that vary from less than a meter to more than ten meters. Angular granitic boulders embedded in basal amphibolite rock outcrop in the southern part of the area within 20 meters of the contact (Fig. 4.1).

4.2.2

Sedimentary rocks (Unit 3) and Volcanic rocks (Unit 2)

Greywacke - mudstone graded sedimentary rocks overlie the volcanic rocks to the west. Although the contact is reported to be conformable (Henderson, 1985; Lambert, 1988) limited exposure in the map area makes this interpretation difficult to verify. Where seen, in the 'elbow' area, the contact is marked by rusty weathering of sedimentary and volcanic rocks producing an unconsolidated residuum. Elsewhere the contact is commonly marked by a narrow 1 to 5 meter wide recessive linear zone of no outcrop.

4.2.3

Granite (Unit 4) and Volcanic rocks (Unit 2)

A granite pluton in the northeastern part of the area has an intrusive contact with the overlying volcanic rocks, well exposed locally (Fig. 4.2).

Figure 4.1 Angular blocks of foliated granite within a mafic volcanic matrix, just above the east striking contact between Cameron River volcanics and Sleepy Dragon Complex granite/gneiss on the southern boundary of domain B. The granite blocks appear to be boulders but may represent a poorly exposed granitic dyke. Lens cap is 58mm in diameter. Photo oriented with northwest at the top.

Figure 4.2 Photograph looking northwest along the contact between the Cameron River volcanic rocks (to the left) and the northern granite. Evergreen tree in center of photo is 1.5 meters high. Location at eastern margin of structural domain D.

Figure 4.3 Photograph of pillow structures in mafic volcanic rocks flattened with long dimensions parallel to S_1, a shape fabric in pillowed volcanics and a foliation in more massive lithologies (flows and dykes), from the southern part of domain D. Pillow cusp, above book, indicates stratigraphic top of volcanics is towards the top of the photo. Spine of notebook is 16.5 cm long.

Figure 4.4 Photograph of horizontal outcrop surface which shows a cross section through an extrusive volcanic unit from the central part of domain D. Tops determined nearby from less deformed pillows are west, toward photo top. A strongly foliated breccia or volcaniclastic layer underlies a massive layer (which may be a flow or sill). The upper layer is a pillowed volcanic rock now flattened and extended parallel to S_1 foliation, to form a shape fabric. Fractures in volcaniclastic layer are east striking parallel to S_2. Photograph covers 2 meters of outcrop from bottom to top.

Figure 4.5 Photograph of pink weathered almandine rich garnet porphyroblasts within a quartz rich sandstone from the center of domain B. Garnet shows relative resistance to weathering. Silva compass is approx. 6 cm wide.

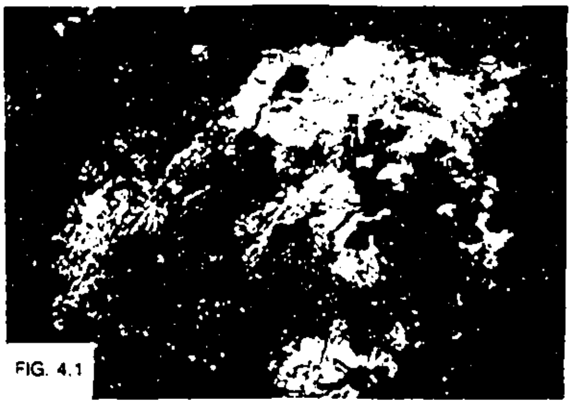

FIG. 4.1

FIG. 4.4

FIG. 4.2

FIG. 4.5

FIG. 4.3

Apophysies of granite in the volcanic rocks at the northern end of the map area and xenoliths of mafic rock within the granite midway along the northwest striking contact between the units (Map 1) indicate the intrusive nature of the contact.

4.2.4

Gneissic rocks (Unit 1) and Granite (Unit 4)

This contact is not well defined being obscured by a lake, overburden and a profusion of granitic dykes in the gneissic rocks. The contact is marked in general by the change over 30 to 40 meters from strongly foliated and mylonitized granitoid rocks to weakly foliated granite (Map 1).

4.3

LITHOLOGY

4.3.1

MAFIC VOLCANICS

Mafic volcanic rocks are dominated by pillowed basaltic rocks (Unit 2a; Map 1 and Fig. 4.3) comprising 60% - 70% of the volcanic domain. Attendant, though less important volumetrically, brecciated pillow lavas (Fig. 4.4), and massive flows complete the suite of mafic volcanic rocks and their derivative lithologies. Gabbroic dykes intrude the volcanic rocks throughout the stratigraphic section.

The mafic volcanic rocks do not exhibit an overall change in character with stratigraphic position. In general the pillowed flows are discontinous both across and along strike where they pinch out. Massive or brecciated flows surround the pillowed flows. Some flows are very thick, up to 400 meters across strike in the central part of the area, with volcaniclastic and pillow breccias up to 100 meters thick locally. One massive unit was measured as 50 meters thick.

Most contacts between pillows, pillow breccias and massive flows are not exposed. Where entire successions are exposed the scale of the flows is small, pillowed portions being 8 to 10 meters thick with pillow breccias measuring 1 to 2 meters thick and massive flows often less than a meter (Fig. 4.6). The succession within one flow unit may vary with massive flows, pillow breccias or volcaniclastic breccias underlying or overlying the pillowed flows.

Relatively undeformed pillows range in size from 10 cm in diameter to large oblate spheroidal shapes with 1m long axes and 0.5m short axes. Some pillows are apparently undeformed in both horizontal and vertical sections. More generally maximum subvertical extension is indicated by elongate pillows and mineral lineations.

Study of thin sections indicates ophitic textures are rarely preserved in volcanic rocks, except

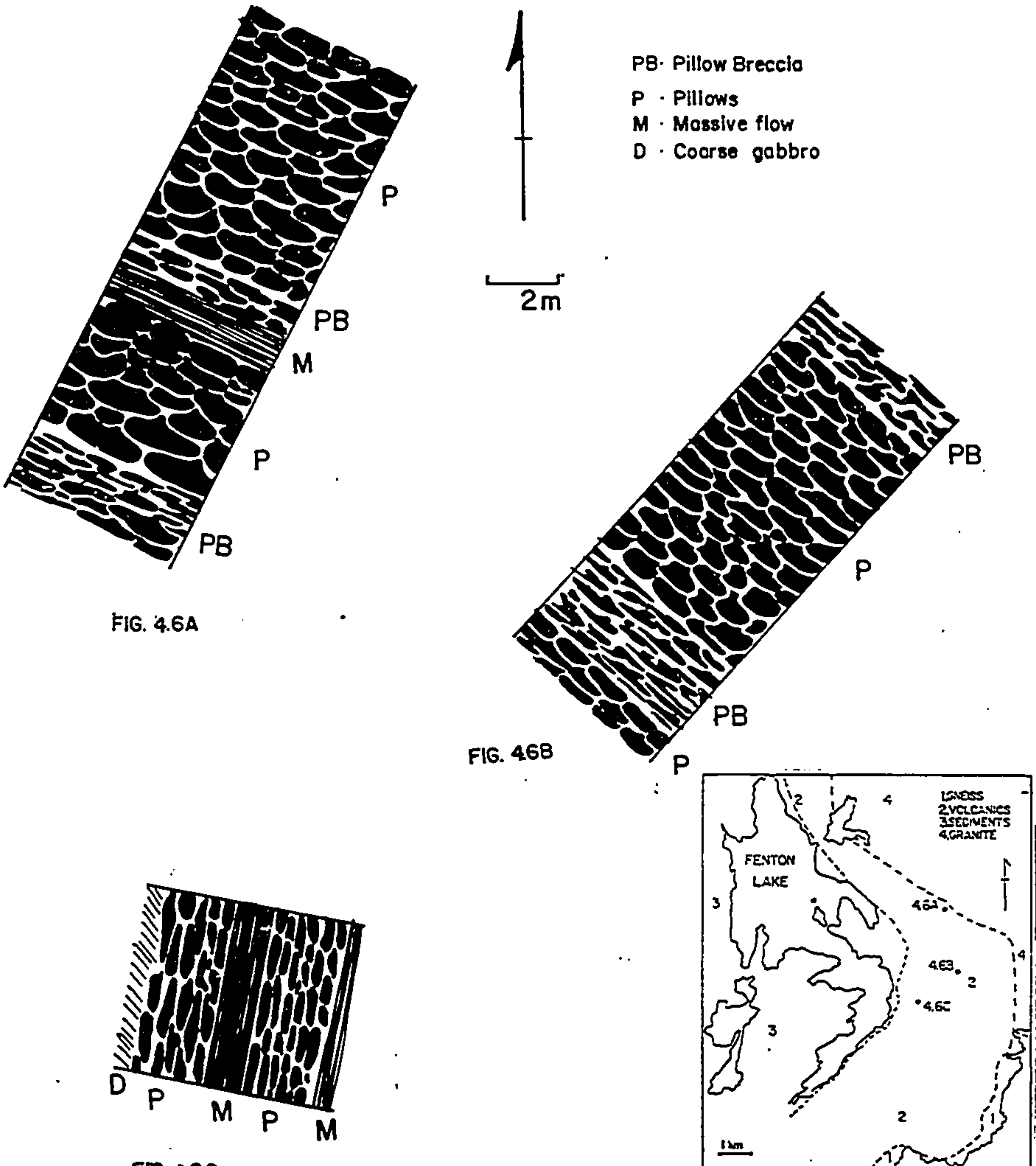

Figure 4.6 Horizontal sections through steeply dipping extrusive mafic volcanic successions of pillowed, brecciated and massive flows. Inset map shows location of section within map area.

in the least deformed examples at the southern end of the volcanic belt below the amphibolite isograd. In general, deformation, alteration of primary pyroxenes to amphibole (actinolite at low grade and hornblende at higher grade), sericitization and epidotization of plagioclase and silicification, has obscured primary igneous microtextures.

4.3.2

FELSIC VOLCANICS

A rhyolite unit (unit 2e, Map 1), descriptively termed "quartz feldspar porphyry" (QFP) underlies a narrow ($\leq$100m wide) recessive zone partially swamp and lake filled, in the south central part of domain D (Fig. 1.3). Outcrops are restricted to frost heaved boulders within the swampy ground and rounded outcrops of a few square meters at the swamp and lake margins. Along strike the rhyolite appears to pinch out to the north for about 3km and then reappears in a narrow steep sided valley, probably underlying a few tens of meters of tree and muskeg covered valley floor, bounded on both sides by mafic volcanic rocks. This unit has been identified in semicontinuous outcrops along strike to the north of the map area for about 15 kms (James, 1989).

QFP has a pale colored matrix in outcrop varying from light brown to creamy white or grey. Bluish quartz phenocrysts and pale orange to white feldspar phenocrysts, up to 3mm in size comprise up to 30% of the rock. Matrix is aphanitic quartz with trace biotite and sericite. In thin section, biotite laths are aligned parallel to the foliation and carbonate infills along foliations and in pressure shadows around phenocrysts.

Mapping of this unit to the north of the study area by BHP-Utah Mines (Cowley et. al., 1988) indicates that thin tuffaceous horizons and meter thick layers of 3cm x 5cm angular cobbles of QFP within a matrix of QFP are present possibly marking flow tops. If such horizons do mark flow tops then individual flows may be tens of meters thick.

4.4

FACING INDICATORS

Pillow facing may be determined using morphology of the pillow in cross section, especially the cusp location, and by observation of internal structure, notably pillow 'shelves' or 'eyebrow' structures (Fig. 4.7) and vesicles.

Pillow 'cusps' are tooth shaped structures formed when a semi solidified pillow begins to settle onto pillows that have been deposited previously and are hardened. Way up of the pillow in outcrop can be determined if cross section exposure of the flow is

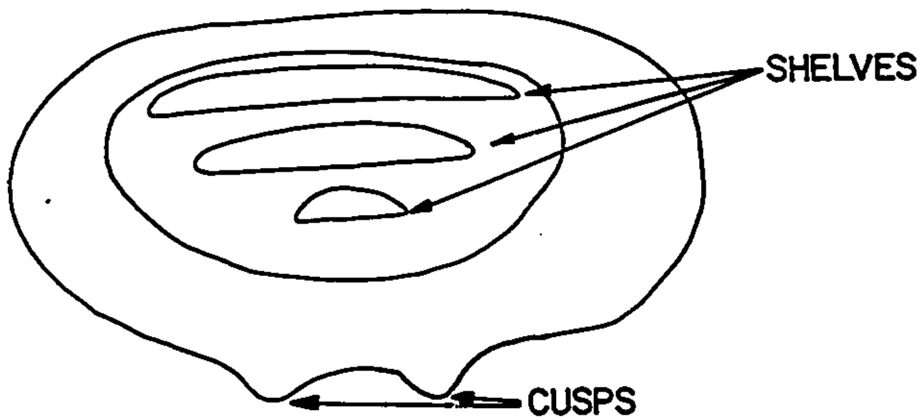

Figure 4.7 Idealized cross section through a pillow structure. Although individual features are indicative of top directions, agreement of three or more geopetal features within a pillowed unit is deemed necessary for top determinations in this study.

available in outcrop. The cusp is subject to reorientation during deformation, so that, in areas of high strain, pillow cusps may be folded into orientations that are not indicative of stratigraphic tops (Borradaile, 1982) (Fig. 4.8). Pillow cusps are distinguishable at up to 4:1 major to minor axis ratios in deformed pillows, however the facing direction determined from the pillow morphology at this state of strain may vary by as much as 45 degrees from the true facing direction (Borradaile, 1982).

Facing directions of pillowed basaltic rocks were determined using pillow cusps, where at least three cusps within an outcrop showed the same facing. In this way, uncertainty in facing due to deformation of pillow structures was reduced.

Pillow 'shelves', are probably created within lava tubes that feed the pillow pile and may be formed when molten lava begins to drain from the center of the hardening shell. The paleo horizontal could then be frozen into the pillow when the cooling rate catches up to the drainage rate, or the drainage channel is cut off. Pillow shelves are probably the most useful feature of pillow lavas in that the ambiguity of the facing found by this method appears to be the least. Top directions are determined by location of shelf structures in the upper part of the

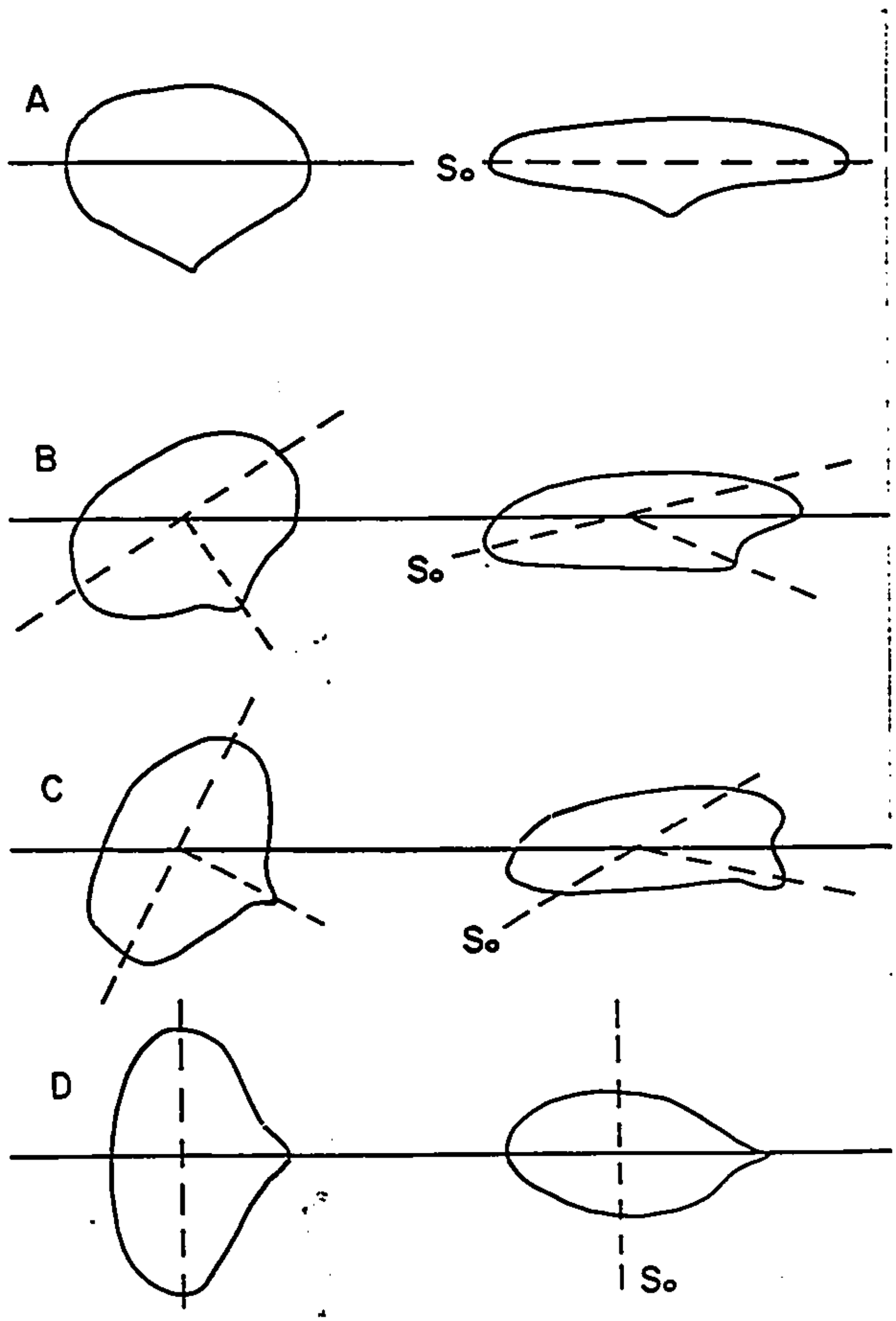

Figure 4.8 Effect of deformation on pillow shape in outcrop. Horizontal line represents plane of flattening. Younging in all cases is perpendicular to S_0 which is not defined by the long dimension of the ovoid pillow profile or normal to the cusp after deformation, unless the principal axes of strain were parallel or perpendicular to the original bedding plane (S_0 as in cases A and D (Figure after Borradaile and Poulsen, 1981.)

pillow (Fig. 4.9). Where deformation has been intense, top directions cannot be determined by this method.

Vesicular pillowed flows are rare. Some vesicles or void spaces, measuring a few millimeters in the long dimension are probably remnant outlines of gas bubbles that rose through the magma as confining pressure dropped during cooling. The vesicles are most heavily concentrated around the pillow rim and, in a few outcrops where other means of determining pillow tops were available, could be shown to concentrate in the upper half of the pillow (Fig. 4.10). Elsewhere, distribution of the vesicles around pillow cores is not strongly polar and in some cases vesicles are distributed all around the pillow margin. Thus, vesicle concentrations within pillow cores was not felt to be a reliable indicator of the pillow facing direction.

4.5

MAFIC DYKES

Amphibolite dykes within the volcanic rocks trend parallel to and at high angles to the layering. Dykes are medium to coarse grained and contrast well texturally with more aphanitic mafic volcanic rocks.

Some dykes may be feeders to the pillowed flows (Lambert, 1977), as shown in one locality, in the

Figure 4.9 Well defined pillow structure, domain C, near eastern edge. The original bottom of the large pillow at photograph center is indicated by the cusp (see text) at lower center. Pillow 'shelf' in upper portion of central pillow gives an orientation subparallel to the paleo horizontal, when deformation has been negligible. Lens cap at center of photograph is 58mm in diameter. Pillow top faces northwest.

Figure 4.10 Photograph of small pillow structure with vesicles, southern edge of domain D. Vesicles are usually most dense in the top half of the pillow. Here top is ambiguous due to the distribution of vesicles around pillow margin. Tops, as determined from weakly deformed pillows within the same outcrop are west. Planar surface in upper portion of pillow structure may be a deformed 'shelf'. Compass ring is 55mm in diameter.

Figure 4.11A and 4.11B Photograph of epidote veins along main northwest striking foliation, eastern edge, structural domain D. The veins become chaotic in detail (4.11B) tracing fine fractures in the volcanic host rock. Notebook is 16.5cm along the spine.

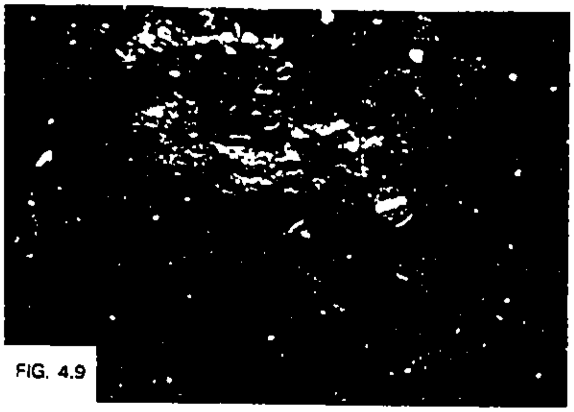
FIG. 4.9


FIG. 4.10


FIG. 4.11A

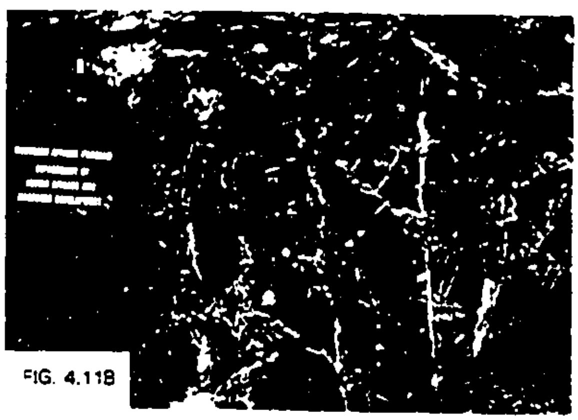
FIG. 4.11B

central eastern part of the map area. Here, a 1.5m wide dyke, branches into narrower dykes, 10 -15 cm wide that interfinger with pillowed flows and appear to bud into pillow lavas. Elsewhere, contacts between coarse grained and medium grained dykes were found indicating that one dyke may have intruded the other. These dykes are not thick, less than 2 meters, and no more than one intrusive event could be documented at any one location.

4.6
ALTERATION

Volcanic rocks are metamorphosed to amphibolite grade (see Metamorphism), over much of the map area. Ophitic textures are obliterated, replaced by porphyroblastic growth of hornblende and garnet and by foliation parallel growth of amphibole and biotite.

Epidote veins parallel foliation planes and microfractures in volcanic rocks adjacent to the northern granite (Fig. 4.11a and b) and epidote defines a subvertical lineation on a cliff face in the southern part of the area, where the volcanics are in contact with the granite/gneiss terrain. Epidote alteration is pervasive in the metavolcanic rocks and probably a late retrograde alteration product.

Gossan zones cross volcanic rocks in several localities. The zones are narrow, ranging from one meter to a few meters across. The orange color of the outcrop appears to be related to hematite veins and oxidation of illmenite. The heavily weathered nature of the gossan zones made sampling for thin section work impossible. As indicated previously, along the contact with the Sleepy Dragon Complex, alteration of the volcanic rocks to rusty weathered unconsolidated material is extensive. No assays of these zones were attempted.

In several locations magnetic disturbances of the compass were such that strike measurements could not be made. The magnetic outcrops do not extend more than a few meters and are usually accompanied by alteration zones. They are not concentrated at any specific stratigraphic interval. Large magnetic anomalies are not visible on 1:50,000 scale aerial survey maps.

CHAPTER 5

SEDIMENTARY ROCKS

5.1

Clastic metasediments (unit 3, Map 1) underlie most of the area west of the volcanic belt. Thin interbeds of metasedimentary rock (Unit 2d) are also present within the volcanic succession. The rocks of unit 3 retain primary sedimentary features such as grain size variations and angularity despite complex deformation and upper greenschist to amphibolite grade metamorphism. The sediments are thus classified on the basis of grain size, sorting and to some extent composition.

Excluding the effects of metamorphism, the sedimentary rocks mainly comprise wackes, both graded and ungraded, and mudstones.

5.2

BEDDING TOP INDICATORS

Bedding contacts and synsedimentary structures are preserved allowing way up determinations to be made over much of the area. Stratigraphic top reversals within the sedimentary rocks were useful in defining axial traces of kilometer scale folds that are not visible otherwise.

Determination of stratigraphic tops was made in outcrops of greywacke - mudstone turbidites (Henderson, 1985), based on fining upward within the A division of the beds (Bouma, 1952) (Fig. 5.1). Color variation across beds is from light colored coarse grained bases to grey and black fine grained tops. Way up determinations assume beds are not reverse graded (Lowe, 1982), though in some cases reverse grading could be present. The coarser portion of the bed is generally the thickest, including up to 3/4 of total bed thickness (e.g., up to 30 cm.). The fine grained, darker, upper parts of graded beds are argillaceous. With increasing metamorphic grade they host biotite and cordierite porphyroblasts.

Other synsedimentary features useful in determining younging directions include foreset beds that are truncated at the top by erosion, scours in bedding tops, rip up clasts of fine sediment within coarser sediments, ball and pillow structures and load structures which accompany the sinking of dense sediment into less dense unlithified substrate.

Where grading is not clearly defined in outcrop, cleavage refraction can be useful as a way up indicator. Cleavage foliations (usually S_{3A} and S_{3B} -see Structural Geology) in graded beds cross finer grained silty layers at oblique angles and curve towards the perpendicular to the bedding plane as sediment coarsens towards the bottom of a bed. In some thick, coarse grained portions of beds the

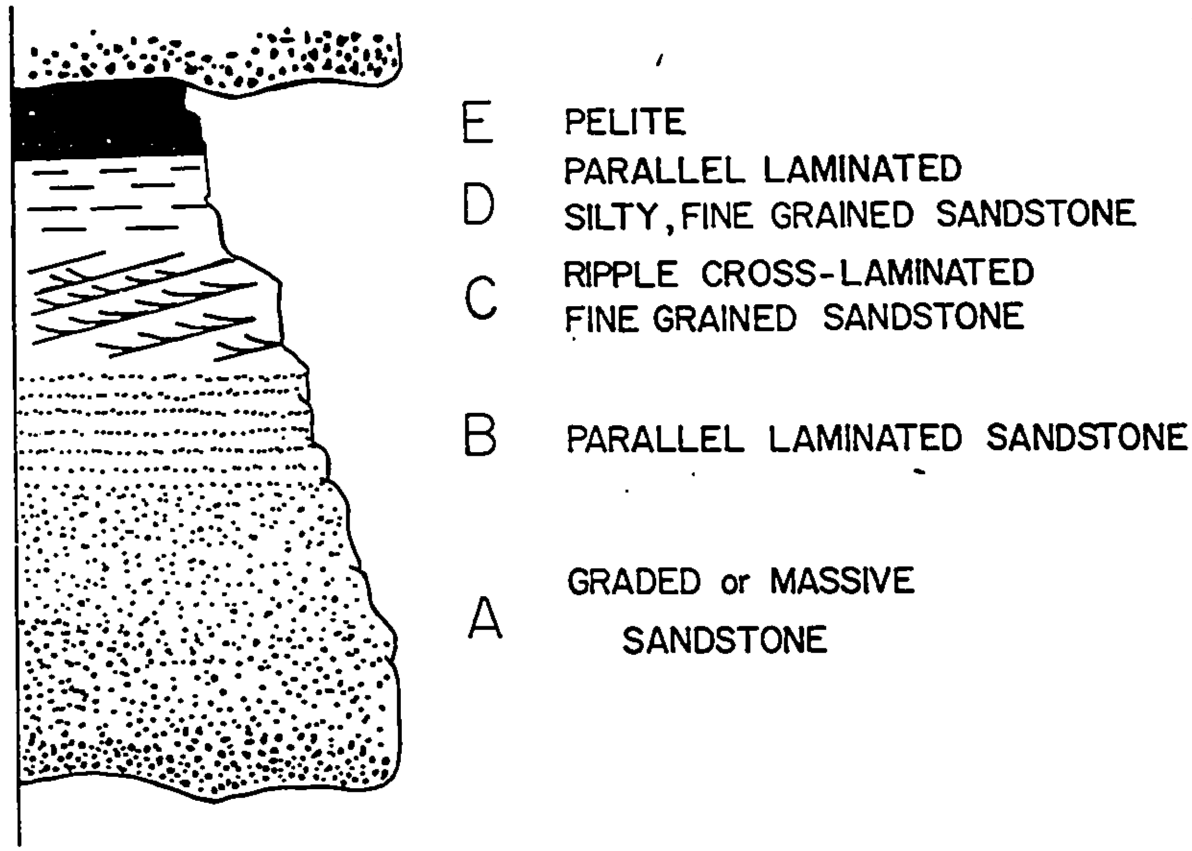

the BOUMA SEQUENCE of deposition from turbidity currents.

FIG.5.1 (after Walker, 1978)

Figure 5.1 Bouma sequence of deposition of sediments from turbidity currents consists of 5 divisions. Only a classic turbidite contains all 5 and most beds include only 2 or 3 different layers. 'A' division is deposited from rapid flowing currents and is considered a proximal to source bed. 'B' and 'C' division beds are deposited from traction currents in upper (B) and lower (C) flow regimes. 'D' and 'E' division layers are fines which are, in part deposited from the turbidity current and in part hemipelagic.

foliation dies out completely (Fig. 5.2).

5.3

LITHOLOGY

5.3.1

SEDIMENTARY DOMAIN

On the west side of Fenton Lake, sedimentary rocks are mainly greywackes and argillites in units 0.3m to almost 1m in thickness. Graded beds commonly exhibit divisions A, B and E of the Bouma sequence, characteristic of turbidites (Bouma, 1952) (Fig. 5.3) while some thinly bedded units display only the B and E divisions (Fig. 5.4).

Ungraded beds of both medium and fine grained wacke (division A) outcrop in thick sequences that are marked by relatively high relief, standing in 50m high bluffs within the sedimentary domain on the western side of Fenton lake near the center of the map area. Bedding contacts are obscured in these sandstones by uniformity of grain size so that thickness of individual beds is unknown. Where interbedded with graded turbidites, ungraded beds vary in thickness from 20 centimeters to more than a meter.

On the eastern shore of Fenton Lake in the 'elbow' region, sedimentary rocks appear to preserve laminated B or D Bouma divisions with thin A and pelitic E divisions (Fig. 5.5). Similar thin pelitic

Figure 5.2 Photograph of a horizontal surface across steeply dipping graded metagreywacke -mudstone beds, western shore of a large lake immediately west of Fenton Lake. S_{3B} curves toward perpendicular to bedding plane and dies out (indicated on photo by solid to dashed lines) Notebook cover is 9cm wide.

Figure 5.3 Photograph of metamorphosed greywacke -mudstone turbidite displaying A, B and E divisions of the Bouma sequence, from a small peninsula, western shore of Fenton Lake. Total thickness of graded unit is about 1/2 meter. Largest cordierite porphyroblasts are present in pelitic E division of the bed. Notebook is 9cm wide.

Figure 5.4 Photograph of thinly bedded metasediments exposed in cross section on a horizontal surface, south end of a large lake immediately west of Fenton Lake. Laminated B and pelitic E divisions of the Bouma sequence form couplets 2.5 - 3 cm thick. Multiple quartz veins parallel bedding traces. Tops of beds toward top of photograph. Mechanical pencil is 12 cm long in photograph.

Figure 5.5 Photograph of thin metasedimentary beds with a coarse grained light grey layer interpreted as a Bouma A division, overlain to the west (left) by a laminated layer of fine pelitic rock which may be a Bouma B or D division. F_{3A} asymetrical fold and S_{3A} northwest trending foliation are prominent. Cordierite forms prominent porphyroblasts. From structural domain E near the metasediment/metavolcanic contact in the center of the map area. Pencil is 12cm long in photo.

Figure 5.6 Photograph of 'quartz eye porphyry', a quartz rich felsic volcanic tuffaceous or sedimentary horizon from the eastern shore of a northwest trending narrow lake in the center of domain D. NW striking fabric, S_{3A}, has quartz 'eyes' elongate parallel to it. Lens cap is 58mm in diameter.

Figure 5.7 Photomicrograph of carbonate rich sandstone from the southern limit of mapping in domain B. Minor biotite and quartz are enclosed in carbonate matrix.
PP - plane polarized; CP - cross polarized


FIG. 5.2


FIG. 5.5

FIG. 5.3

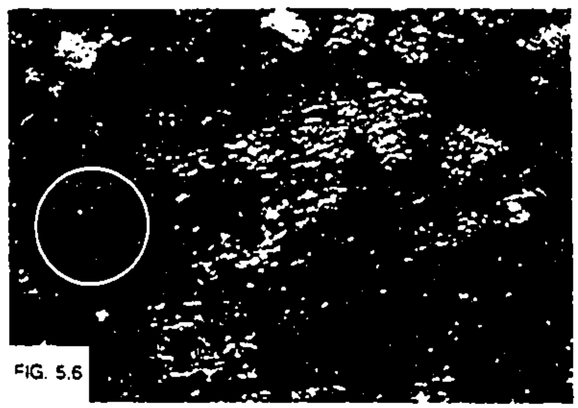
FIG. 5.6


FIG 5.4

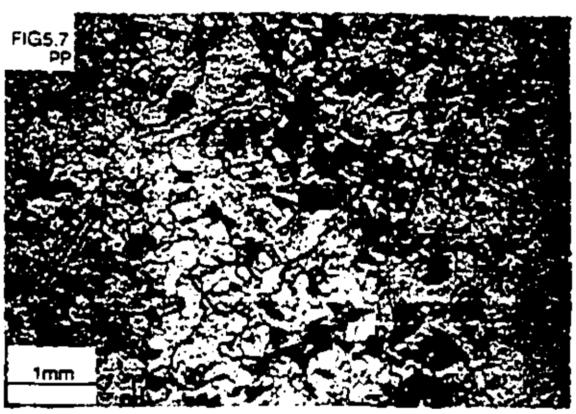
FIG5.7 PP
1mm

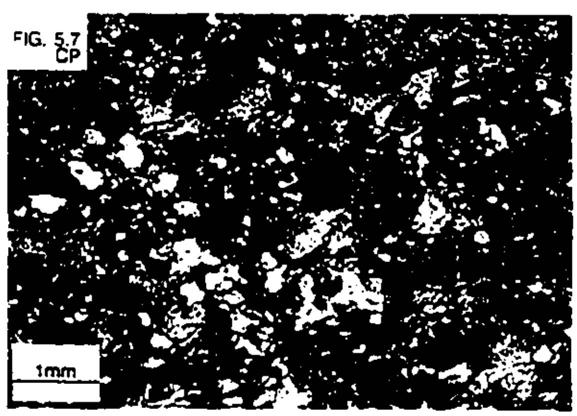
FIG. 5.7 CP
1mm

and fine grained quartz (+/-feldspar) rich (argillaceous) units are common in close proximity to the volcanic rocks along the northeast trending arm and further north in the 'elbow' region.

One outcrop of pebble conglomerate with clasts of mainly mafic volcanic rock up to 4 cm across is located just west of a small lake in the elbow region of the metasediments about 500m west of the contact with metavolcanic rocks (Map 1). The unit is obviously not extensive as no other outcrops were identified.

5.3.2

Intervolcanic sedimentary rocks

Both quartz and quartz carbonate rich sedimentary lenses outcrop along the margins of narrow often muskeg filled recessive zones within the volcanic succession. Coarse, poorly sorted, quartz-rich metasediments (Unit 2d, Map 1) interbedded with metavolcanics often host garnet poikiloblasts that weather dark pink to purple, in outcrops north of the indicated hornblende isograd (see Metamorphism). These rocks are generally strongly foliated parallel to contacts with enclosing volcanics.

Carbonate rich sandstones (unit 2f, Map 1) , overlying the quartz eye porphyry (unit 2e, Map 1), outcrop along the west shore of a narrow northwest striking lake in the northern portion of the volcanic rocks. Carbonate rich sandstones weather recessively and are white to medium grey on exposed surfaces. Weathering texture of this rock is very uneven with narrow, cm thick ridges of resistant more quartz rich stringers seperating relatively recessive, carbonate rich layers. In a few other localities such as near the southern limit of mapping, carbonate rich sediment (Fig. 5.7) is present in small deeply weathered outcrops. This rock is strongly foliated parallel to contacts.

More detailed study of the stratigraphy may allow correlation of some of the sedimentary horizons from north to south within the volcanic domain.

5.4

Petrology

5.4.1

SEDIMENTARY DOMAIN

The major constituent of the coarse grained

portant volumetrically, rock fragments of polycrys-

talline quartz; quartz feldspar intergrowths and mudstone clasts are also present. Some feldspar is preserved within the matrix though mainly altered by metamorphism to cloudy sericitic masses. Primary mineral constituents are less easily defined. Large grains of muscovite and chlorite that are randomly oriented and show some degree of alteration could be primary though late stage retrograde metamorphism of porphyroblastic minerals could have a similar effect. The polycrystalline quartz and quartz feldspar intergrown fragments may be derived from felsic terrains in part granitic (Henderson, 1985).

Most of the metasedimentary rock within the map area lies above the biotite isograd (greenschist facies). At this and higher grades porphyroblastic and poikiloblastic growth of metamorphic minerals, recrystallization of quartz, and loss of primary minerals and primary mineral textures begin to obliterate original rock texture. Deformation causes flattening, brecciation and stretching of rock fragments into foliation parallel orientations, reducing much of the detritus to matrix sized material and making identification of primary clasts and minerals difficult.

According to Henderson (1985), the provenance for rock fragments in the coarsest greywackes are felsic to mafic volcanic rocks and granitic rocks. Henderson (1985) notes that; "While it is clear both granitic and felsic volcanic source terrains were involved, it is difficult to estimate the proportional contribution of each.") Intraformational mudstone clasts indicate derivation of some detritus by reworking of sediments.

Uniform grain sized, reworked sediments are dominantly quartzites and argillites. Quartzites are comprised of over 80 percent quartz with intergranular biotite, chlorite and muscovite. Argillites vary in mica component, with up to 80 percent mica formed during upper greenschist to amphibolite grade metamorphism, similar to fine grained tops of graded beds (Fig. 5.8).

5.4.2

Intervolcanic metasediments

Thin section study of intervolcanic quartz rich sediments reveals coarse angular quartz and quartz feldspar crystals, foliation parallel hornblende and biotite laths, garnet porphyroblasts and rare muscovite within a quartz rich matrix. Carbonate and hematite are vein and fracture filling minerals.

Minerals in calc silicate rocks include syndeformational garnet extending along the S_{3A} foliation (Fig 5.9), hornblende, anthophyllite and epidote in single grains and as alteration margins on hornblende and sphene.

Figure 5.8 Photomicrograph of sedimentary rock showing the contact between the coarser, sandy layer and fine pelitic layers (A and E respectively) of Bouma sequence. Sample from western shore of Fenton Lake, domain A. Fine muscovite and chlorite laths define S_2 east striking foliation, crenulated to S_{3A} northwest striking foliation in pelitic layer. Foliation curves into the sandy layer and becomes less distinct.
PP - plane polarized; CP - cross polarized

Figure 5.9 Photomicrograph of carbonate rich sandstone from intervolcanic metasedimentary horizon in the southern portion of domain D. Garnet (G) is elongate parallel to S_{3A} northwest striking foliation. Other minerals present include hornblende (h), carbonate (d) and quartz (q).
PP - plane polarized

Figure 5.10 Photomicrograph of intervolcanic coarse grained metasandstone. Intergranular biotite and sericite grow parallel to the S_1 or S_{3B} foliation. Foliation strikes 015° and the thin section also contains garnet. Sample from the central area of domain B, about 1km east of the metasediment/metavolcanic contact.
PP - plane polarized; CP - cross polarized

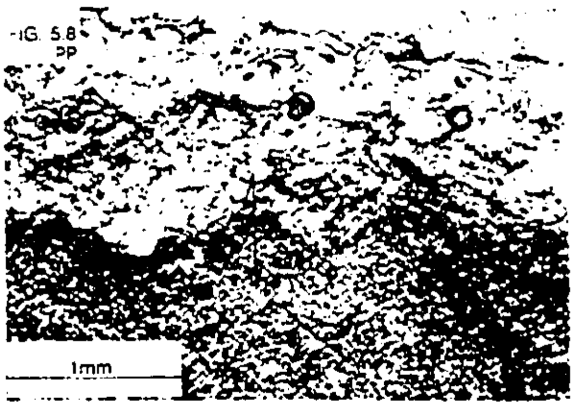

FIG. 5.8 PP

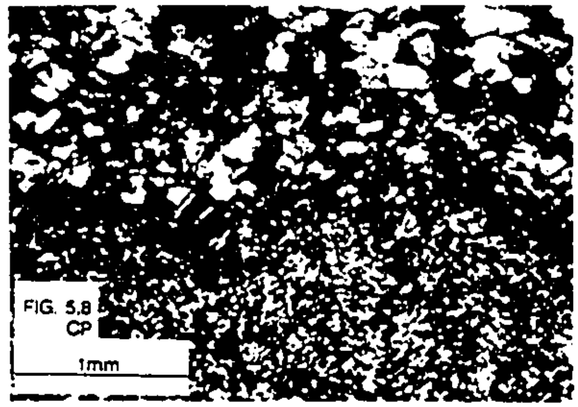

FIG. 5.8 CP

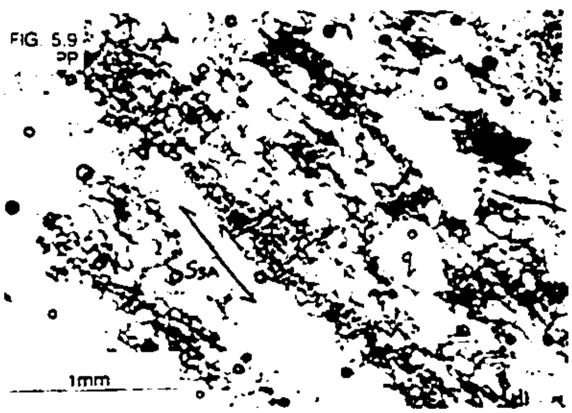

FIG. 5.9 PP

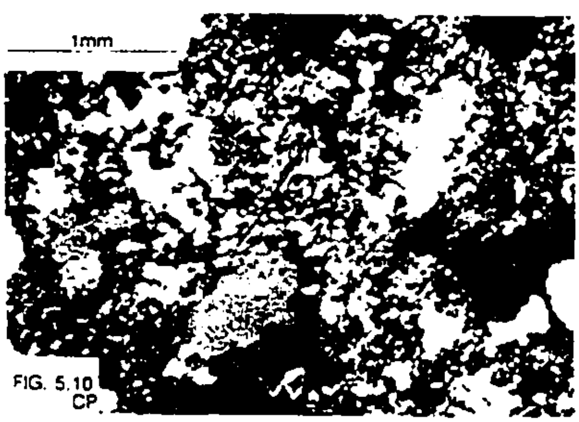

FIG. 5.10 CP

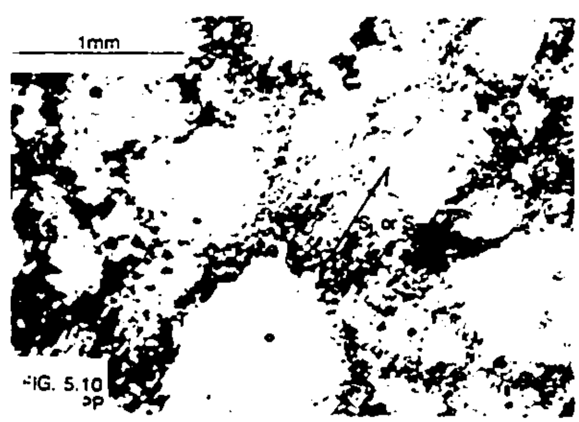

FIG. 5.10 PP

CHAPTER 6

DEPOSITIONAL ENVIRONMENT

6.1

VOLCANIC ROCKS

The metavolcanic rocks outcropping in a steeply dipping, west facing homocline, present a cross sectional view of an extrusive succession. The base of the succession consists of massive volcanic rocks, probably dykes (Lambert, 1977, 1988) along much of the contact with the Sleepy Dragon basement complex, whereas in the northwest trending portion, pillows immediately overlie granitic rocks, perhaps due to stoping and replacement by the younger granitic pluton (unit 4). The volcanics appear to be comprised of a series of discreet subaqueously extruded mafic units of pillowed, brecciated and massive rocks that interfinger along and across strike. Extrusion of these rocks could have taken place along extensional fissures trending NE and NW, reflected by the northeasterly and northwesterly striking arms of the volcanic belt. Together, these fissures could have formed a rift like fracture set.

Small intervolcanic lenses of clastic sediments mark hiatus in volcanism and periods of subaerial erosion. One extensive lens of quartz porphyritic rock marks a relatively short period of felsic volcanism.

6.2

SEDIMENTARY ROCKS

The present study was not detailed enough to clearly determine paleogeographic conditions of sedimentation. Henderson (1972,1975b,1985) concluded that the depositional pattern for the Yellowknife supracrustal domain is indicative of accumulation of sediments on a series of submarine fans that extended into a basin from the margins (Fig. 6.1).

Poor sorting, coarse grain size and the immature, angular to subrounded shapes of much of the sedimentary quartz and feldspar within the coarser grained sedimentary rocks of the map area (Fig. 6.2 and 6.3) suggest the environment of deposition included little opportunity for reworking. Graded bedding, exhibiting the lower two (A and B) and uppermost (pelitic E) divisions of the Bouma sequence indicates deposition from rapidly moving turbidity currents (Walker, 1976). Fragments of quartz and feldspar within the coarse sediments indicate erosion of a felsic volcanic and granitic terrain was an important contributor of sediment to the basin fill.

A conglomerate lens, within 500 meters of the volcanic contact is not considered indicative of pro-

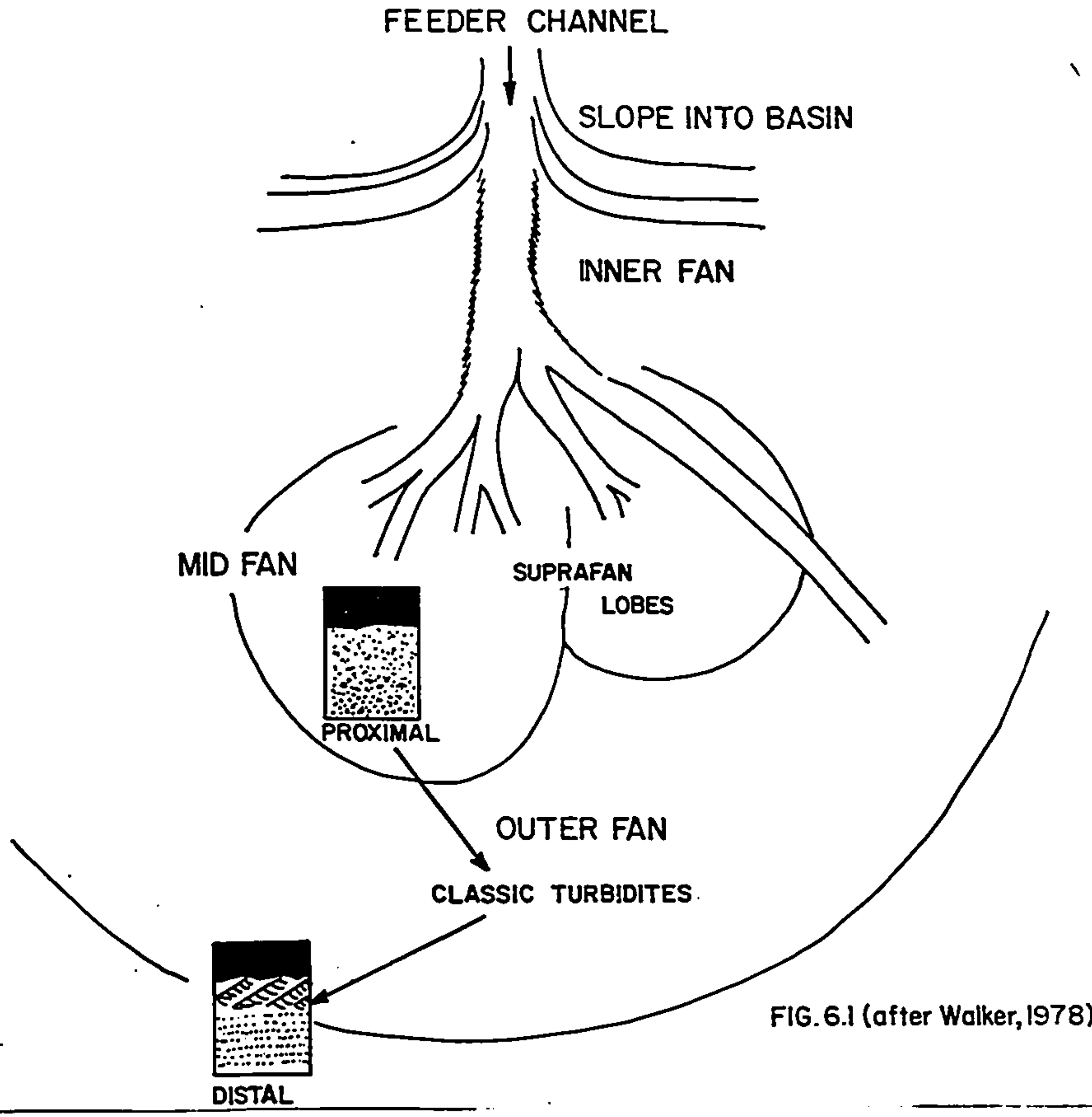

FIG. 6.1 (after Walker, 1978)

Figure 6.1 Distribution of Bouma type turbidity current deposits within a submarine fan environment. Channel deposits and overbank deposits are excluded from the figure. Proximal style turbidites with coarse graded massive 'A' layers are more common on the suprafan lobes while distal types of deposits, excluding 'A' layers are more common on the outer fan and within the abyssal part of the basin. A high incidence of classical turbidite beds containing 4 or 5 of the Bouma divisions probably indicates deposition on the outer fan. Modified from Walker (1978).

Figure 6.2 Photomicrograph of poorly sorted quartz feldspar wacke showing angular outlines of larger sized feldspar clasts (A), intergrowths of quartz and feldspar(B) in some clasts and alteration of feldspar(C) to micaceous minerals. Sample from same location as 5.3, north end of a large lake immediately west of Fenton Lake.
PP - plane polarized; CP - cross polarized

Figure 6.3 Photomicrograph of angular metamorphosed rip up clasts of argillaceous sediment(A) within fine grained wacke. Biotite poikiloblasts(B) are generally irregularly shaped, S_{3A} foliation traverses the slide, striking northwest, weak S_2 parallel orientation of inclusion trails strikes east. Sample from the northern shore of a large lake immediately west of Fenton Lake.
PP - plane polarized; CP - cross polarized

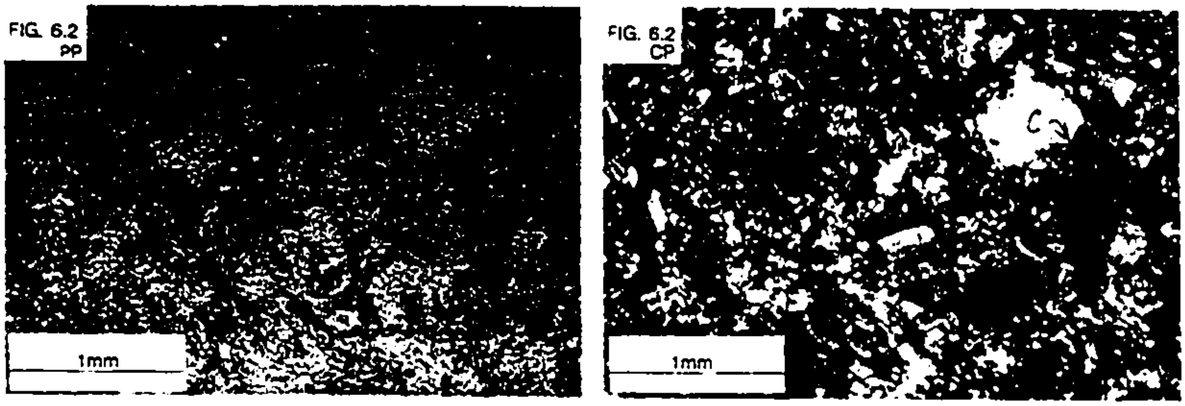

FIG. 6.2 PP FIG. 6.2 CP

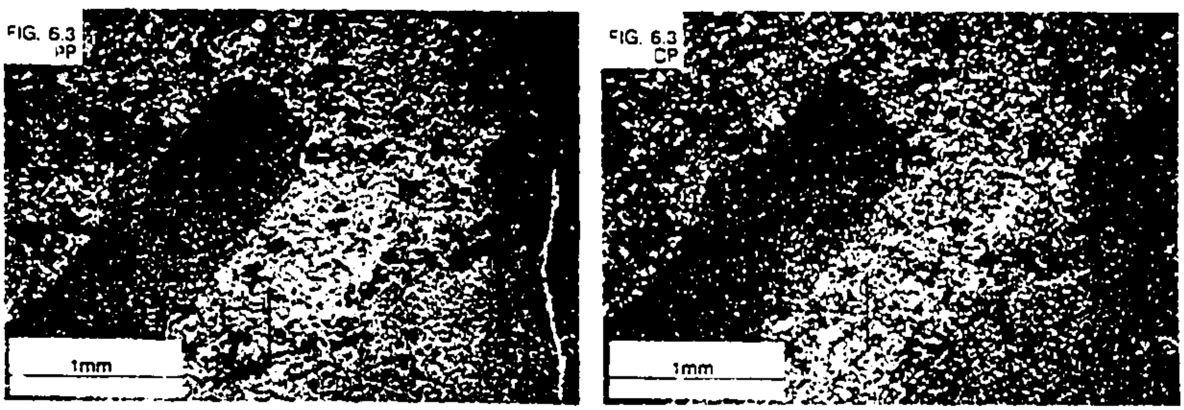

FIG. 6.3 PP FIG. 6.3 CP

ximal sedimentation as conglomerates can be found at almost any point within such a high energy sedimentary basin (Walker, 1978). The mainly mafic volcanic pebbles that constitute the coarse portion of the conglomerate indicate rapid erosion and little reworking of detritus derived from adjacent mafic volcanic source terrain.

Archean greywacke of the Superior Province, similar to that within the map area is described by Pettijohn (1943) as a "microbreccia". Poorly sorted relatively unreworked (immature) wackes, such as those at Fenton lake, are associated with turbidity currents that carry sediment down steep valleys across a depositional fan in rapidly moving debris flows. These flows may travel great distances across the basin floor at the base of the fan before deposition begins (Walker,1978).

The location of fine grained argillaceous metasediment adjacent to the metavolcanic rocks in several places along the contact suggests a quiescent subaqueous environment existed along the present metasediment, metavolcanic contact.

CHAPTER 7

METAMORPHISM

7.1

Introduction

Metamorphism in Yellowknife supracrustal rocks such as at Fenton Lake, has characteristics associated with both contact and regional, dynamic metamorphism. For example, some minerals (chlorite, biotite, cordierite, hornblende, garnet) are randomly oriented, apparently unaffected in growth by the influence of directed stress, whereas elsewhere the same minerals plus muscovite are aligned along foliations and evidently grew during deformation.

In rocks within 3 km of the outcrop of the northeastern granite, isograds mark the appearance of metamorphic minerals of increasing grade as the contact is approached (Fig. 7.1, in pocket). These isograds are generally associated with broad thermal domes, the cores of which are marked by granites, possibly products of partial melting (Thompson, 1978).

7.2

METASEDIMENTS

7.2.1

GREENSCHIST FACIES

Greenschist facies, or low grade metamorphism in pelitic rocks is indicated by the assemblage biotite, muscovite, chlorite albite and quartz. This assemblage implies temperatures in excess of 350°c but less than 550°c at pressures of 3 to 3.5 kilobars (Winkler, 1979). In metasedimentary rocks of the Fenton Lake area, cleavage foliations (S_1, S_{3A} and S_{3B}) are partly defined by preferred dimensional orientation of muscovite and chlorite in rocks below the cordierite isograd.

7.2.1.1

Muscovite and Chlorite

Muscovite is usually lath shaped, aligned parallel to and partly defining foliations and persists into the cordierite grade rocks. Chlorite, also lath shaped, is parallel and sometimes oblique to foliations; it may be interleaved with biotite (Fig. 7.2), or porphyroblastic. Ramsay (1973a, 1974) reports 5 distinct morphologies of chlorite in Slave metasediments. Chlorite and muscovite abundance appears to decrease as metamorphic grade increases.

7.2.1.2

Biotite

Biotite in metasediments forms foliation parallel laths and irregularly shaped poikiloblasts. These morphologies are reported in previous studies which grouped biotite crystals into two distinct phases, distinguished morphologically (Kretz, 1968; Ramsay, 1973a, Fyson, 1975) and chemically (Ramsay, 1973 a and b; Kamineni and Carrara, 1973). In this study, four generations of biotite were recognized, with respect to deformational events. First generation biotites are lath shaped and oriented parallel to S_2 foliation (Fig. 7.3). Second generation crystals are poikiloblastic, sometimes oriented parallel to S_{3A} foliation and contain quartz inclusion trails (Fig. 7.4). Third generation biotites are lath shaped to ragged and parallel later foliation generations at higher metamorphic grades. Randomly oriented, lath shaped, porphyroblastic biotites represent a fourth generation (Fig. 7.5).

Microprobe work by Ramsay (1973 a and b) and Kamineni and Carrara (1973) indicates that the two biotite groups originally recognized (poikiloblastic and foliation parallel) are also chemically different. Ramsay (1973b) notes that as temperatures increase, biotite composition changes, with mineral chemistry approaching stochiometric biotite at higher

Figure 7.2 Photomicrograph of S_{3A} northwest striking foliation defined by layer parallel biotite and chlorite laths between quartz rich domains. S_2 parallel quartz inclusion trails within biotite poikiloblasts are indicated. Chlorite interleaved with biotite may be a late stage alteration. Sample from metasediments on the eastern shore of Fenton Lake near the northern boundary of domain A.
PP - plane polarized; CP - cross polarized

Figure 7.3 Photomicrograph of biotite (B) poikiloblasts within a larger cordierite (Co) poikiloblast (outlined in the plane polarized photomicrograph). Biotite preserves S_2 parallel quartz inclusion trails while cordierite has S_2 parallel biotite laths, and some muscovite (M). Sample from the western shore of Fenton Lake in the southern part of domain A. PP -plane polarized; CP - cross polarized

Figure 7.4 Photomicrograph of biotite, muscovite, chlorite schist from the western shore of Fenton Lake near the southern part of domain A. S_2 parallel phyllosilicates are crenulated in open warps about northwest striking S_{3A} foliation. Biotite poikiloblasts that overgrow east striking S_2 include quartz inclusion trails that parallel S_2. The poikiloblasts show a weak preferred orientation parallel to S_{3A}.
PP - plane polarized; CP - cross polarized

FIG. 7.2 PP

FIG. 7.2 CP

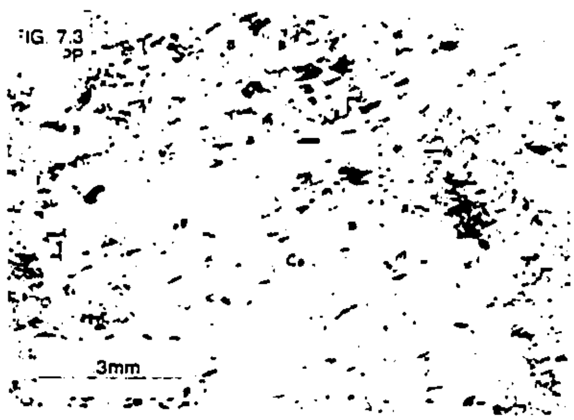

FIG. 7.3 PP

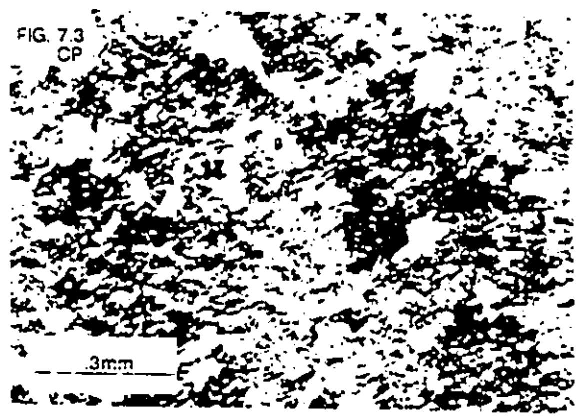

FIG. 7.3 CP

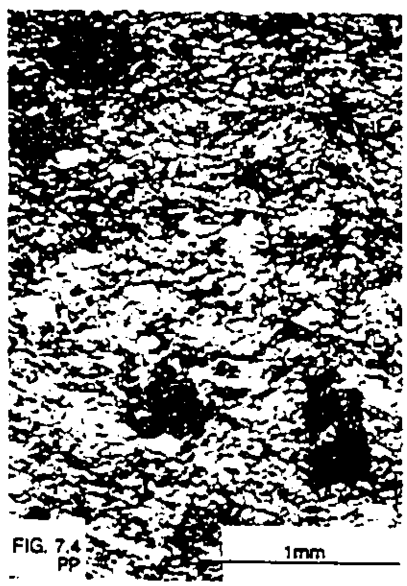

FIG. 7.4 PP

FIG. 7.4 CP

grades.

Ramsay(1973a) proposes the biotite forming reaction:

(1) chlorite + muscovite(1) + ilmenite <-> biotite + muscovite (2) + H_2O + [quartz + rutile + K feldspar]

Growth of biotite poikiloblasts could have consumed muscovite(1), muscovite (2) represents the composition of the remaining muscovite (Ramsay,1973a). Number designators simply denote presence of muscovite before and after the reaction has taken place. Other workers omit such distinctions (R.Kretz, pers. com., 1988)

Ramsay (1973a) indicates a pressure range of 2.5 to 3.5 kb. for the biotite forming reaction. No temperature of reaction is mentioned but, in Abukuma type metamorphism, biotite zone temperatures are given as greater than 300°c. In this study, the four groups of biotites recognized are thought to grow during progressive stages of a single metamorphic event, each group being distinguishable by association with a tectonic fabric and/or morphology.

Figure 7.5 Photomicrograph of S_{3A} foliation parallel growth of biotite laths in high grade metasediment. Note random growth of some biotite crystals, suggesting post deformation metamorphism. Sample from the eastern shore of Fenton Lake near the metasediment/metavolcanic contact.
CP - cross polarized

Figure 7.6 Photomicrograph displaying the mineralogy in a greenschist grade metavolcanic rock. Chlorite laths (C), chlorite interleaved with biotite (B), white mica (M), quartz (Q), actinolite (A), plagioclase (P) and zoisite (Z). Also present in this thin section are calcite and net textured sulphides (pyrite and pyrrhotite).
PP - plane polarized; CP - cross polarized

Figure 7.7 Photomicrograph of feldspar (albitic (F)) altering to very fine white mica along foliation planes. Matrix contains actinolite, hornblende and chlorite (C). Sample from the southern part of domain B within the metavolcanic rocks.
PP - plane polarized; CP - cross polarized

Figure 7.8 Photomicrograph of hornblende (H) consumed within a field of chlorite (C). Sample from domain D within 24m of the granite/metavolcanic contact.
CP - cross polarized

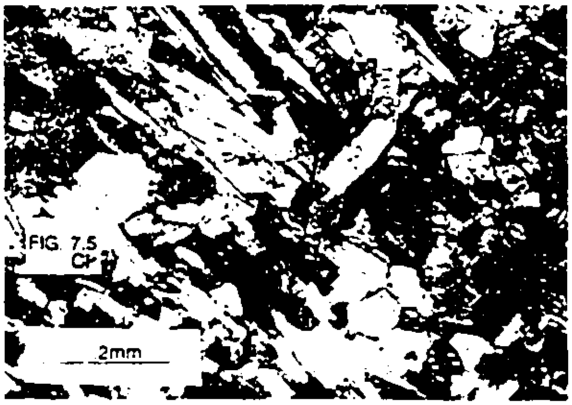
FIG. 7.5 CP 2mm

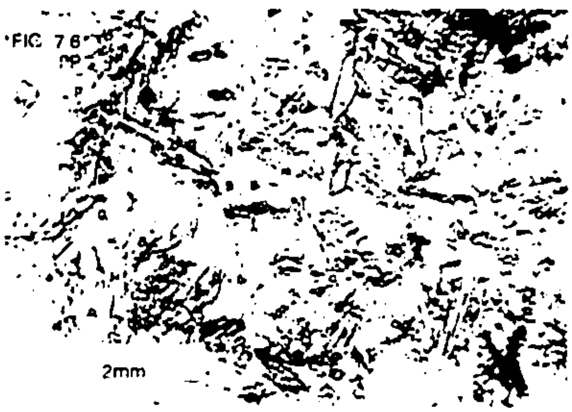
FIG. 7.6 PP 2mm

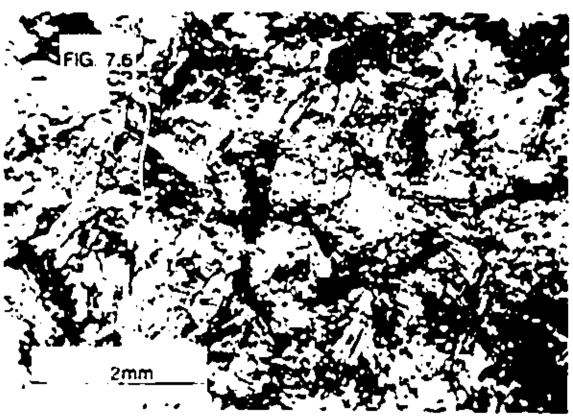
FIG. 7.6 CP 2mm


FIG. 7.7 PP 1mm

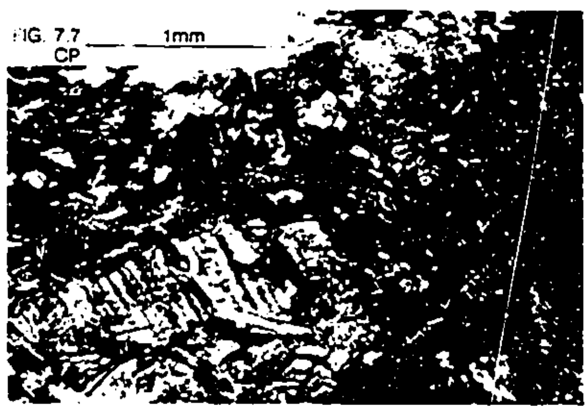
FIG. 7.7 CP 1mm

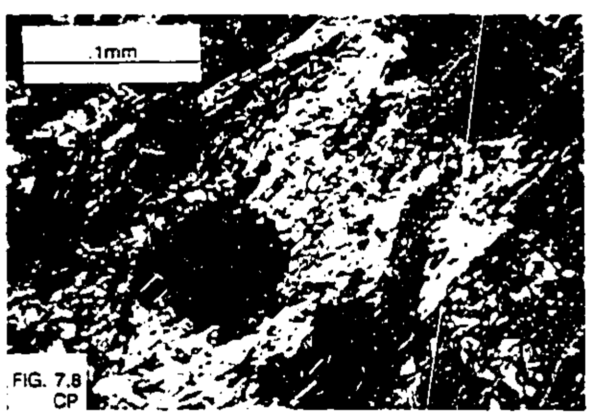
.1mm FIG. 7.8 CP

7.2.2

AMPHIBOLITE FACIES

7.2.2.1

Cordierite Isograd

The boundary between low and medium (amphibolite) grade metamorphism for pelitic rocks, suggested by Winkler (1979), is marked by the first appearance of cordierite, indicated in the study area by the trace of the cordierite isograd (Fig. 7.1, in pocket). Cordierite is regarded as a mineral of low pressure, contact or Abukuma type thermal, metamorphism (Hietanan, 1967).

In the Fenton lake area, cordierite porphyroblasts are most common within 3 kilometers of the sediment/volcanic contact. Cordierite here is often concentrated in finer grained portions of graded beds (Fig. 5.3) where phyllosilicates (chlorite, muscovite and biotite) predominate. The cordierite probably gained necessary elements for formation from the dissolution of some of these phyllosilicates at elevated temperatures.

Ramsay (1974) and Ramsay and Kamineni (1977) propose the reaction:

(2) 1.22 C + 0.74 M + 1.96 B(1) + 1.44 Q + 0.08 A + 0.09 I -> 1.0 Cord + 2.83 B(2) + water

A - albite; B - biotite; C - chlorite; Cord -

cordierite; I - ilmenite; M - muscovite; Q - quartz

(approx. reaction conditions; 3 kb. and 550°c. Seifert, 1970)

Ramsay (1974) suggests that the biotite has changed in composition across the reaction contributing Si and K while becoming enriched in Na and Al(iv)/(Mg + Fe^{3+} + Fe^{2+}) and that biotite increases in abundance across the reaction, therefore it is required that two biotites one a reactant, the other a product, be represented in this reaction. Chlorite and muscovite, at the cordierite in isograd, do not show marked alteration and persist above the isograd (Ramsay, 1974; this study).

Cordierite may be porphyroblastic and form large, net textured poikiloblasts containing relict, foliation parallel phyllosilicates (Fig. 7.3).

Retrogression of cordierite to sericite at crystal margins is common. Rarely, poikiloblasts are almost completely replaced. Sericite alteration is not related to distance above the cordierite isograd and thus, does not appear to be related to any particular point within the metamorphic framework.

Other minerals above the cordierite isograd are biotite and decreased amounts of muscovite and chlorite, often interleaved with biotite or as discreet crystals within cordierite.

Of note in the Fenton Lake high grade metasediments is the absence of both almandine rich garnet and staurolite, two common minerals of the amphibolite facies (Winkler, 1979). Low Mg/(Mg + Fe) ratios are required for the growth of these two phases (Winkler, 1979) with the additional constraint on almandine garnet growth that pressure must be at or above 4 kb. (Winkler, 1979). Apparently these conditions were not met in the metasedimentary domain at Fenton Lake.

7.3

METAVOLCANIC ROCKS

7.3.1

GREENSCHIST FACIES

7.3.1.1

Chlorite, Actinolite, Biotite, Albite

In the southern part of the mafic metavolcanic succession at Fenton Lake, the mineral assemblage contains phyllosilicates, amphiboles, quartz and plagioclase species that are diagnostic of low grade low temperature metamorphism in mafic metavolcanic rocks (Winkler, 1979).

Chlorite crystals are lath shaped (Fig. 7.6) or in felted masses. Actinolite forms acicular masses of clear to light green, weakly pleochroic crystals (Fig. 7.6), and porphyroblast size masses intergrown with hornblende, giving the large crystals a mottled light/dark green color in thin section.

Biotite is a minor phase often interleaved with chlorite (Fig. 7.6) or clinozoisite and is often reddish brown or green in thin section. Plagioclase, mostly albitic (based on determinations made on symmetrically twinned examples) is usually clouded with inclusions and altered marginally and internally to fine grained mica, possibly phengite (Fig. 7.7).

Quartz is a minor phase at low metamorphic grade. Epidote crystals are apparent in some samples though more commonly epidote is massive textured with no crystal faces. Carbonate (probably calcite), and some sphene, in brownish, high relief amorphous masses, are ubiquitous though volumetrically unimportant. Opaque minerals include pyrite, pyrrhotite, illmenite and chalcopyrite in varying quantities.

In one thin section, biotite and chlorite are distinctly interleaved phases within a field of actinolite and fine grained white mica. Similar paragenesis led Turner (1981) to propose the reaction:

(3) Muscovite + Actinolite + Chlorite ->
Biotite (Mg rich) + Epidote

On the eastern side of the metavolcanic belt, metavolcanic rocks from within 50 meters of the southern part of the Sleepy Dragon gneiss, metavolcanic contact (samples 86/22, 86,/7; Fig. 1.3) are composed of greenschist grade minerals. The assemblage contains chlorite in felted masses, actinolite, in clear slightly pleochroic laths, biotite laths, quartz, epidote and accessory sulfides.

7.3.2

AMPHIBOLITE FACIES

As the contact with the northern granite is approached from the southwest the mineral assemblage in metavolcanic rocks becomes increasingly dominated by hornblende in laths, parallel to foliations and as porphyroblasts growing at the expense of actinolite, which decreases in abundance. Chlorite is no longer a distinct phase beyond location 11 (Fig. 7.1) although chlorite may be found at even the highest grades of metamorphism as a late stage alteration of biotite or hornblende (Fig. 7.8).

7.3.2.1

Hornblende Isograd

The hornblende isograd (Fig. 7.1), marking an isotherm of approximately 500°c and the change from low to medium grade metamorphism (Fig. 7.9) (Winkler, 1979), is placed approximately where chlorite crystals are consumed and no longer appear as a distinct phase (although chlorite persists at higher grades as

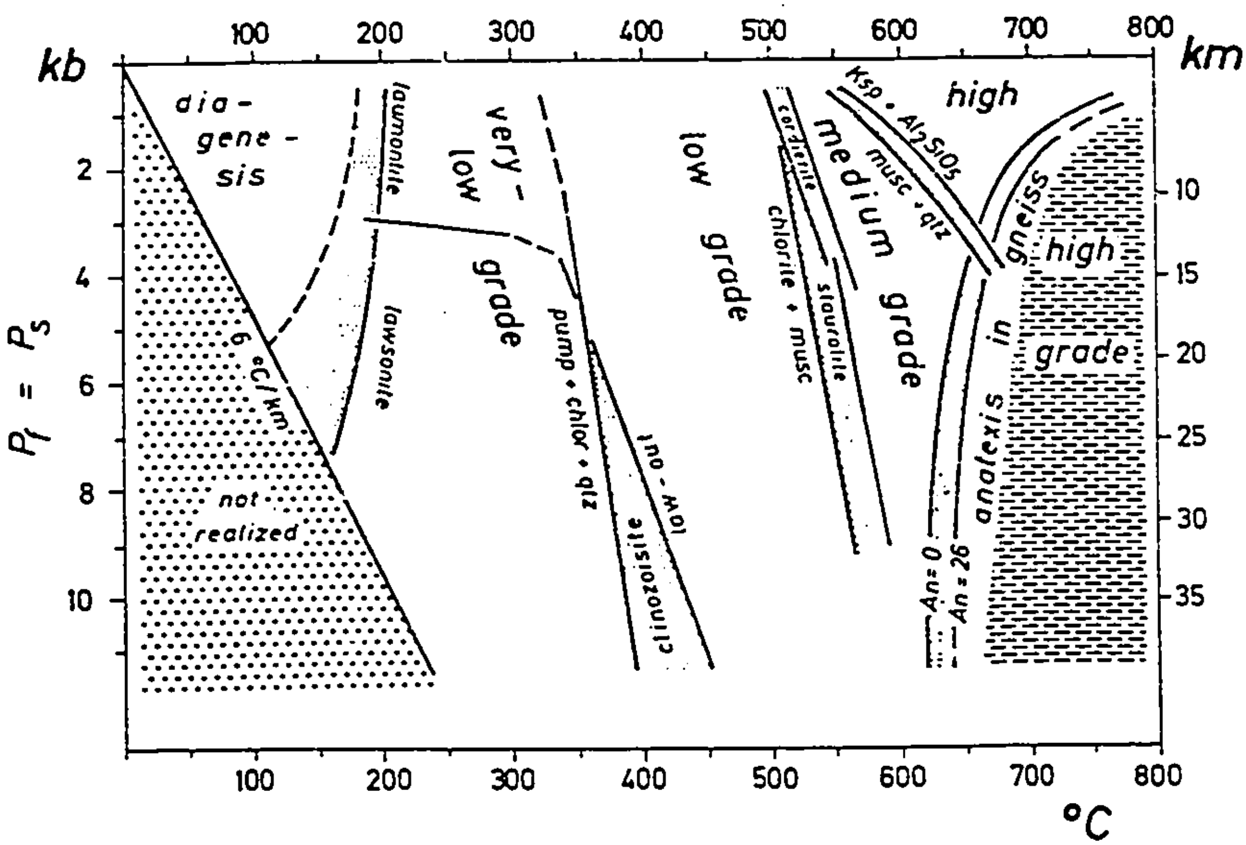

Figure 7.9 Four divisions of metamorphic grade with temperature and pressure constraints included (Figure from Winkler, 1979)

alteration rims and felted masses around hornblende crystals (Fig 7.8)), and actinolite is no longer a major constituent, although still evident as a distinct phase within hornblende.

The approximate position of the isograd probably falls between sample localities 83/32 (chlorite, actinolite, albite) and 85/45 (hornblende) (Fig. 1.3) on the western side of the metavolcanic rocks and north of sample 86/7 (actinolite, chlorite) but south of sample 86/17 (hornblende) on the eastern side of the metavolcanic rocks (Fig. 1.3). The assemblage of minerals beyond this isograd changes towards the northeast to include; garnet, cummingtonite, An richer plagioclase, calcic pyroxene some anthophyllite and locally tourmaline (Fig. 7.10), with a concomitant reduction in the amount of fine white mica and clinozoisite.

Mineral reactions of particular interest in this region are:

1. Transformation of actinolite to hornblende and of albite to An richer plagioclase.

2. Appearance of garnet, cummingtonite, anthophyllite and calcic pyroxene.

The boundary between low and medium grade metamorphism, a temperature of 500°c to 510°c at 3 to 3.5 kb in mafic volcanic rocks (Winkler, 1979), is the approximate point at which actinolite changes to

Figure 7.10 Photomicrograph of metavolcanic rock, within 1 km of the northern granite contact containing tourmaline (T) euhedral crystals, hornblende (A), anomalous blue zoisite (Z) and chlorite (C) in large felted masses. Sample is from structural domain D near the metavolcanic, metasediment contact.
PP -plane polarized; CP - cross polarized

Figure 7.11 Photomicrograph of garnet poikiloblast (G) within metavolcanic rocks. Poikiloblast overgrows and includes 2 foliations defined by hornblende laths. Sample from the vicinity of the metasediment/metavolcanic contact 1km northwest of the Fenton 'elbow'. The early foliation, probably S_2, is crenulated with hornblende growth parallel to S_{3A} crenulations striking northwest. Garnets are elongate parallel to S_{3A} indicating either syndeformational or mimetic growth.
PP - plane polarized; CP - cross polarized

Figure 7.12 Photomicrograph of hornblende (H) cummingtonite (A) assemblage in metavolcanic rocks of the northwestern part of domain D. Sample is unoriented.
PP - plane polarized; CP - cross polarized

Figure 7.13 Photomicrograph of calcic pyroxene (P), possibly augite, in mafic volcanic rock. Pyroxene, which is undeformed, may have grown along a fracture or parting in the rock parallel to the foliation, which strikes 020°, subparallel to both S_{1B} and S_{3B}. Sample 85/86 from the eastern part of the metavolcanic succession, within domain C.
PP - plane polarized; CP - cross polarized

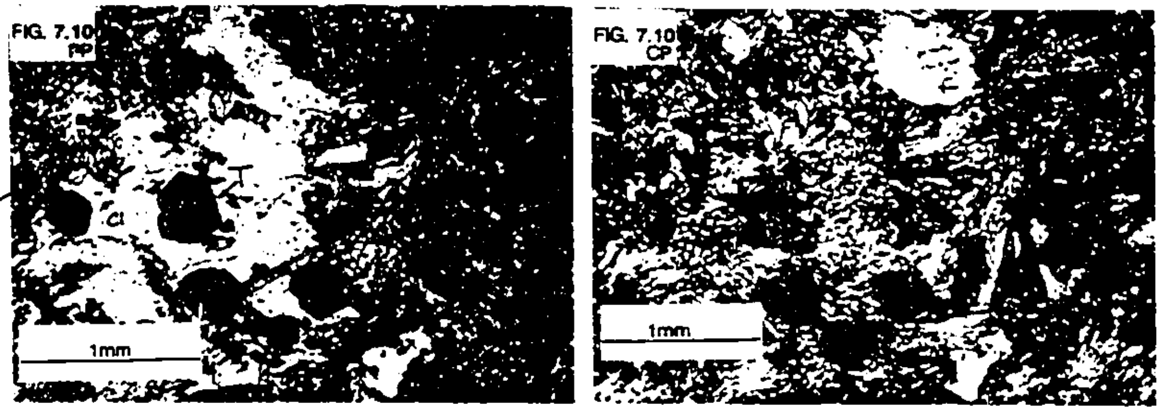

FIG. 7.10 PP
FIG. 7.10 CP

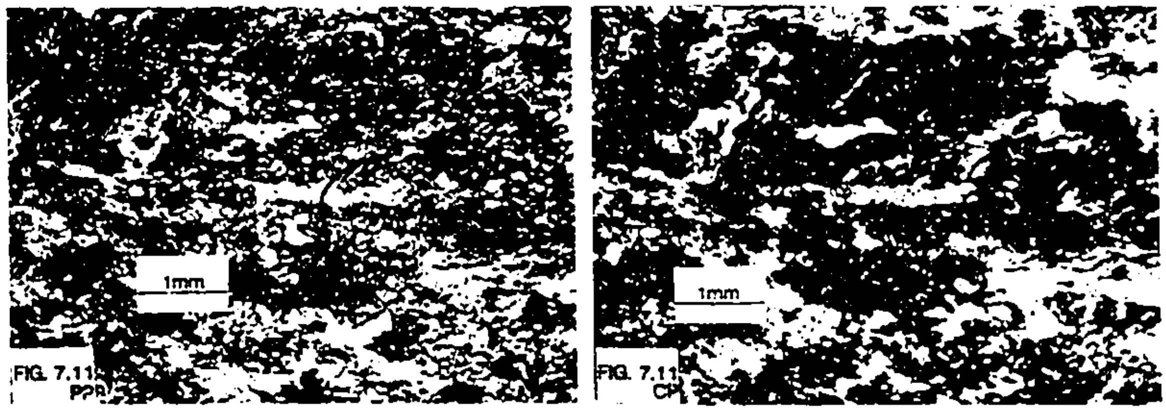

FIG. 7.11 PP
FIG. 7.11 CP

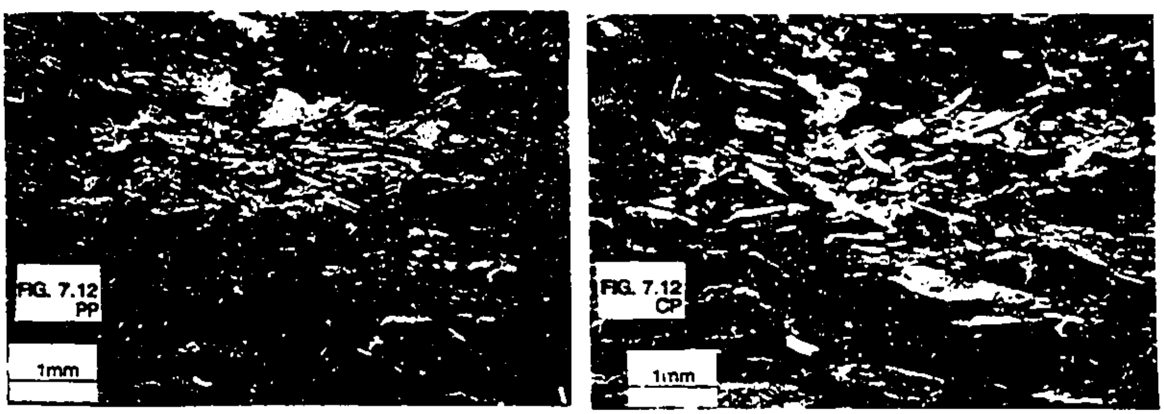

FIG. 7.12 PP
FIG. 7.12 CP

FIG. 7.13 PP
FIG. 7.13 CP

hornblende, although there is hornblende below the isograd and some actinolite above it (Winkler, 1979). The hornblende isograd thus reflects the anticipated trace of the 500°c to 510°c surface.

Possible reactions to produce hornblende have been proposed by Kretz (1963) and include:

for quartz free rocks

(4) Actinolite + Epidote(Al) + Ilmenite + Quartz -> Hornblende + Anorthite + Sphene + H_2O
(Quartz, if present, is consumed in the reaction)

for quartz bearing rocks

(5) Chlorite + Epidote(Al) + Quartz -> Anorthite + Hornblende + H_2O

Winkler (1979) proposes the more general reaction:

(6) Actinolite + Clinozoisite + Chlorite + Quartz -> Hornblende

7.3.2.2

Anorthite

Winkler (1979) reports that the change in composition of albite to An richer oligoclase takes place across the 520°c - 530°c isotherm. With reference to the sample map (Fig. 1.3), sample 85/90 on the western side of the metavolcanic rocks contains oligoclase and sample 85/86, on the eastern side of the metavolcanic rocks, contains plagioclase up to An 40 (approx. andesine) indicating placement of this isotherm somewhere south of samples 85/90 and 85/86 but north of sample 35/45 (albite).

Increase in the anorthite content of plagioclase is probably facilitated by reactions (4) and (5), liberating An by breakdown of epidote (Rambaldi, 1973).

7.3.2.3

Garnet

Garnet in intervolcanic metasedimentary rocks at location 9 (Fig. 7.1), appears as mm. size, purple crystals on weathered surfaces in outcrop (Fig. 4.5) and as ragged edged porphyroblasts in thin section (Fig. 7.11). Garnet is part of the mineral assemblage in intervolcanic metasedimentary horizons north of location 9, in metavolcanic assemblages just south of the narrow lake in the center of domain D (sample 85/93 Fig. 1.3) and northward from this point.

Microprobe analysis of garnets in three samples (locations 3,4 and 9, Fig. 7.1) indicates that almandine component does not exceed 68 wt% and that in each case, spessartine component is always greater than 10 wt%. The large amount of spessartine within the garnet means that it may form at temperatures and pressures well below those for medium grade metamorphism (Winkler, 1979).

7.3.2.4

Cummingtonite

The appearance of cummingtonite in the mineral assemblage as small lath shaped crystals that are clear and non pleochroic (Fig. 7.12), indicates medium grade in metavolcanic rocks and temperatures in excess of 550°c (Winkler, 1979). Cummingtonite in samples 85/91 (Fig. 1.3) on the western side of the metavolcanic rocks, near the northern boundary of structural domain B and on the eastern side of the metavolcanic rocks, in sample 85/88 (Fig. 1.3) is accompanied by small needle like crystals of anthophyllite.

Limited sampling makes location of the cummingtonite isograd, therefore the 550°c isotherm, in metavolcanic rocks arbitrary. The 550°isotherm, the equivalent to the cordierite isograd in the metasediments, may be extended into the metavolcanic rocks, parallel to the hornblende isograd, from a point near the intersection of the cordierite isograd and the metavolcanic succession to a point south of sample locality 85/88 (Fig. 1.3).

7.3.2.5

Calcic Pyroxene

East of sample 85/88 (Fig. 1.3), temperatures may have exceeded 550°c as calcic pyroxene, apparently unaltered, in stringers parallel to foliation in the assemblage of sample 85/86 (Fig. 7.13), indicates temperatures in excess of 600°c (Winkler, 1979). The plagioclase in sample 85/86 is about An 45, a higher grade (approx. labradorite) than at location 85/91 (Fig. 1.3) on the western side of the metavolcanic succession. The 550°c isotherm may therefore curve southward at this point (Fig. 7.1) to include sample 85/86.

Microscope analysis of thin sections from north of location 2 and 3 in the northwest trending arm of the metavolcanics along the granite contact (Fig. 7.1) indicates that amphibolite grade is maintained to the northern limit of mapping. The mineral assemblage is dominated by large hornblende porphyroblasts and includes quartz, clinozoisite, plagioclase (An 30 -40) and often fine white mica and carbonate. Accessory phases are biotite, garnet and sphene. No further evidence of cummingtonite, anthophyllite or calcic pyroxene is seen, suggesting that temperatures were slightly lower in this portion of the metavolcanics relative to locally high grade portions.

7.4

SLEEPY DRAGON COMPLEX - METAMORPHISM

Analysis of gneissic rocks from the Sleepy Dragon terrain in the eastern part of the area indicates a possible metamorphic trend in these rocks from south to north. A sample from within 1 km. of the suggested contact with the younger granite contains euhedral hornblende crystals growing parallel to a steep lineation. The sample is located immediately adjacent to a mafic dyke which may have influenced growth of the hornblende.

To the south, still within Sleepy Dragon gneisses and within 50 meters of the contact with the metavolcanic rocks, gneissic rocks are composed mainly of biotite, plagioclase and quartz.

7.5

MICROPROBE ANALYSIS

Microprobe analysis of samples from within the metavolcanic succession was undertaken, in a sequence from northeast to southwest. Eleven sample locations are numbered sequentially from a mafic volcanic xenolith within the northern granite, southward to below the hornblende isograd (Fig. 7.1). The samples analyzed were from both metavolcanic rocks (locations 1,2,3,6,7,8,10,11: Fig. 7.1) and intervolcanic metasedimentary rocks (locations 4,5 and 9: Fig. 7.1).

Analyzed minerals included amphibole, garnet, biotite, chlorite, epidote and pyroxene.

Six discrimination plots for amphibole composition allow determination of elemental distribution changes (Fig. 7.14), species analyzed (Fig. 7.15) and metamorphic grade (Fig. 7.16). Temperature of crystallization was calculated for three samples from within the metavolcanic succession containing biotite-garnet pairs (Table 3). Analyzed samples were from both intervolcanic metasediments (85/46, 85/94) and mafic metavolcanic rock (86/26).

7.5.1
Amphibole

Variation plots after Studemeister (1983) are designed to show straight line correlations between Al_2O_3 wt% and wt% TiO_2, FeO_t, SiO_2, and MgO respectively (Fig. 7.14a, b, c, d). Al_2O_3 content is thought to increase with increasing metamorphic grade, as are Fe (total) and to a lesser extent TiO_2; content of SiO_2 and MgO should decrease in the prograde direction (Studemeister, 1983).

On these plots, changes in composition of the amphiboles within mafic volcanic rocks from location 11 up to location 6 (Fig. 7.1) appear systematic. Beyond sample 6 the amphibole composition loses distinct amounts of Al_2O_3 and falls back toward the

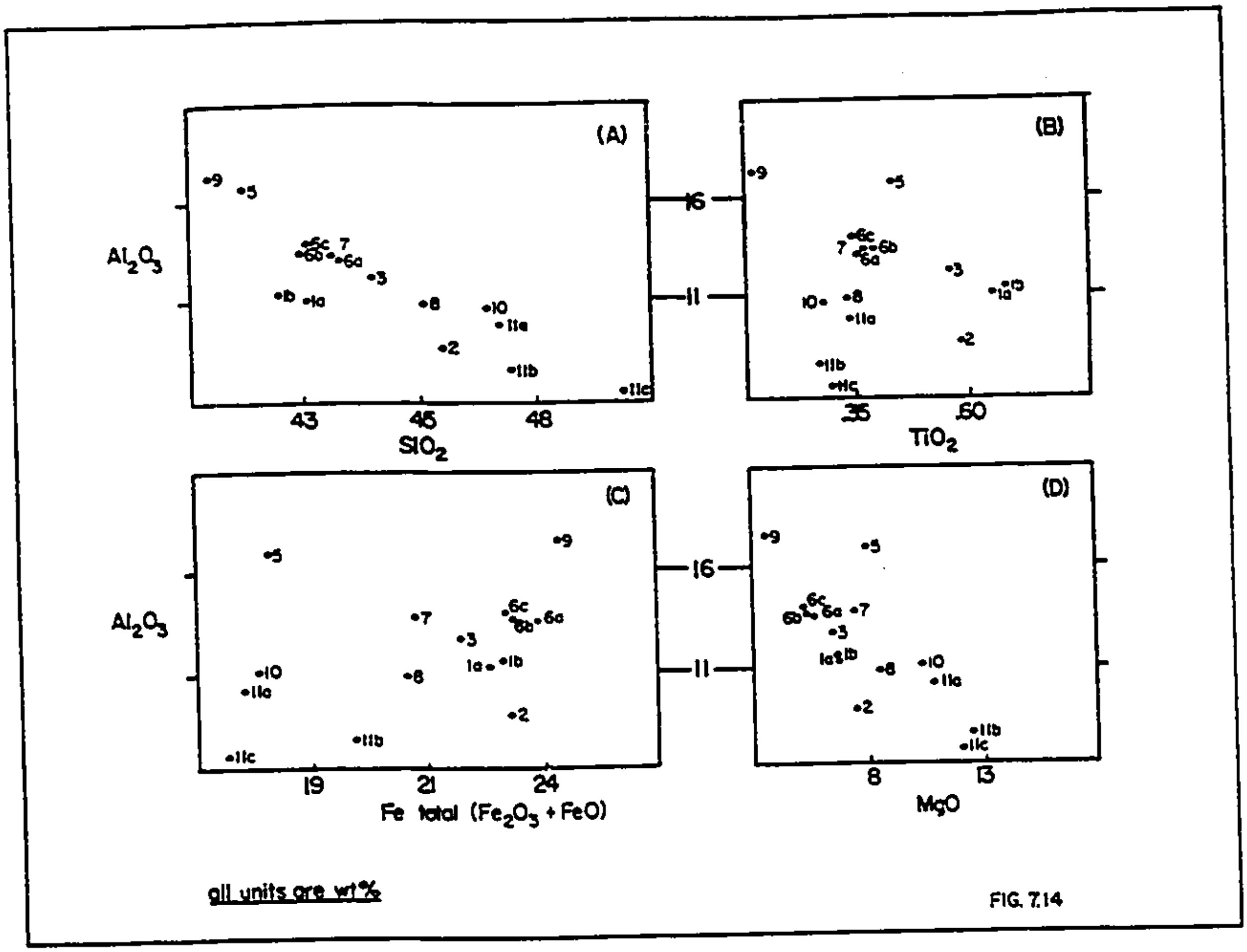

Figure 7.14 Discrimination plot for amphibole composition from Studemeister (1983). Each plot attempts to create a straight line correlation which mat be attributable to increasing or decreasing metamorphic grade based on increasing Al_2O_3 content in relation to SiO_2, TiO_2 Fe total and MgO.

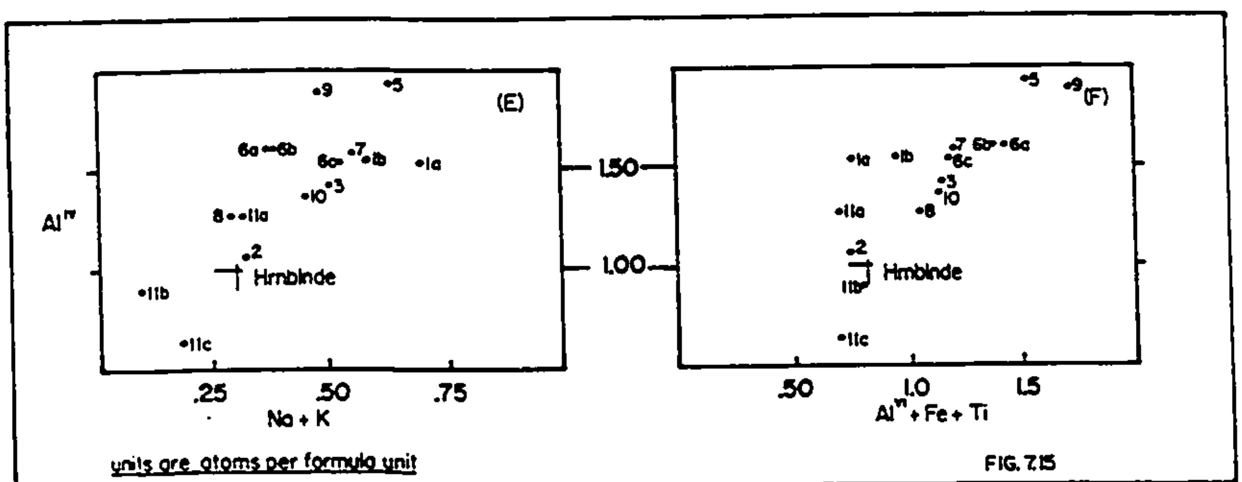

Figure 7.15 Discrimination plot for amphibole compositions from Deere, Howie and Zussman (1980) indicating increasing Al^{iv} content with respect to Na + K and Al^{vi} + Fe + Ti, with increasing metamorphic grade.

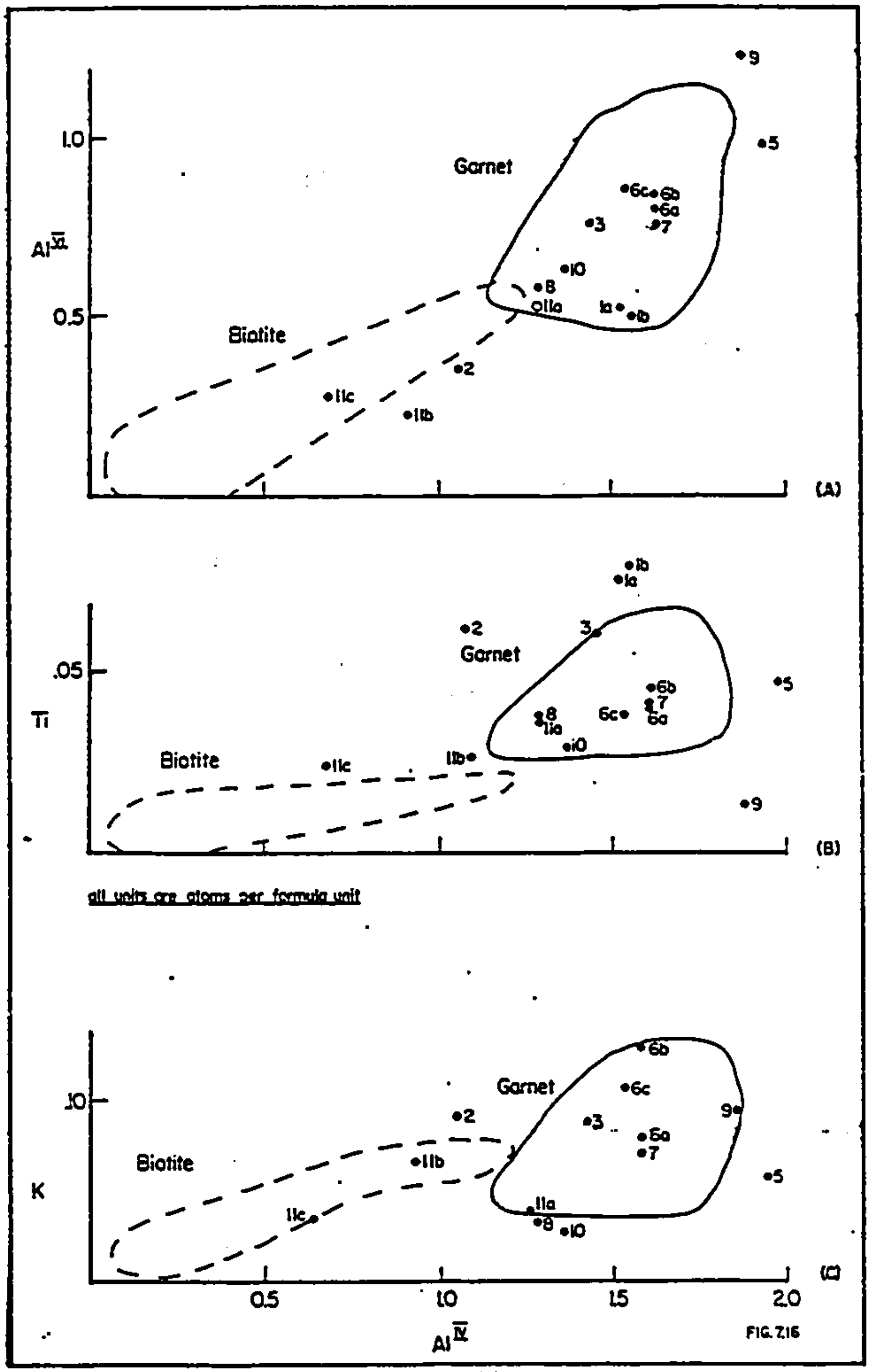

Figure 7.16 Discrimination plot for separation of amphibole by composition into metamorphic zones characterized by biotite, garnet and staurolite/kyanite. The envelopes are suggested by Laird and Albee (1981). These plots are indicative of increasing grade determined by thin section work. The use of this plot requires that the assemblage chlorite, epidote, plagioclase, quartz, Ti bearing phase (biotite), +/- K mica, carbonate and Fe^{3+} oxide.

lower grade compositions. The break in trend takes place across the boundary between structural domains B and D where trends of pillow shape fabrics (S_{1A}, Fig. 1.3) change from NE to NW, and may indicate compositional differences between the metavolcanic rocks within these domains. Samples from intervolcanic metasedimentary rocks plot at the high end of the scale and appear anomalous.

Separation of analyzed amphiboles into species was attempted by use of two discrimination plots suggested by Deere, Howie and Zussman(1980). Variation in Na + K total atoms and Al(vi) + Fe^{3+} + Ti atoms with respect to the number of Al(iv) atoms (Fig. 7.15) indicate that the majority of the amphiboles sampled were hornblendic. Two of three amphibole analysis from location 11 plot below the hornblende position and one plots above indicating coexistence of hornblendic and actinolitic amphibole in lower grade rocks. Once the hornblende composition has been achieved, further compositional changes at anticipated higher temperatures close to the intrusive granite contact are not markedly systematic. Amphiboles from intervolcanic metasediments again plot in anomalously high positions.

In a third type of discrimination plot, based on compositional changes in amphibole with increasing metamorphic grade, Laird and Albee (1981) suggest that when the assemblage chlorite, epidote, plagioclase, quartz, Ti phase (biotite), +/- K mica, carbonate, Fe^{3+} oxide is present, increasing metamorphic grade is reflected by an increase in edenite (Na,K,Al), tschermakite (Al) and glaucophane (Na, K, Si) in amphibole phases. Their discrimination plot is separated into biotite, garnet and staurolite, kyanite metamorphic zones (Fig. 7.16). The plots show a reasonable separation of the data by temperature, reflecting the general metamorphic progression determined by thin section work. Amphibole from location 1 begins to show anomalous chemical changes in plot 7.16b and, due to the elevated K content of the analyzed mineral, rises outside the range of plot 7.16c. As in previous plots, anomalous, apparently out of sequence samples from location 5 and 9 (intervolcanic metasediments), remain so.

7.5.2

GARNET BIOTITE GEOTHERMOMETRY

7.5.2.1

Introduction

Within the metasedimentary domain, the first appearance of cordierite is an accepted indicator of temperature and pressure conditions in the range of 550°c at 3 kb (Ramsay, 1974). Comparable isotherms within the metavolcanic rocks are not as easily defined due to the small sample population and the lack of suitable minerals.

Although the increase in the aluminum content of amphibole (Studemiester, 1983), increase in the An content of plagioclase (Winkler, 1979) and presence of cummingtonite, anthophyllite and calcic pyroxene indicate that the metamorphic grade of the volcanic rocks is increasing with proximity to the northern granite, there are no reliable temperature determinations indicated by these changes beyond the general boundaries of low and medium grade metamorphism set out in various calibrations of regional metamorphic plots (Hietanen, 1967, Winkler,1979).

To better model temperature increases with proximity to the northern granite, geothermometry based on microprobe analysis of garnet, biotite pairs was undertaken. These minerals have been studied for partitioning of the elements Fe (to garnet) and Mg (to biotite) during metamorphism by several authors (Kretz, 1968; Ferry and Spear, 1978; Hodges and Spear, 1982). When activity coefficients and free energy interactions (Margule's parameters) are constrained by assuming cordierite isograd conditions (550c at 3000 bars)for the analyzed samples, temperatures of metamorphism may be calculated using the method of Ferry and Spear (1978), as modified for the garnet solid solution series by Hodges and Spear

(1982).

7.5.2.2

Methods

Using data obtained by microprobe analysis of garnet rims and/or cores and biotite crystals in three samples, temperatures of equilibration may be calculated. It is important for these analyses that garnet be analyzed at the core and rim and if the grain is large enough, at some intermediate point between the core and rim. Garnet is slow to homogenize (very small diffusion rate, Turner, 1981) and the composition may vary greatly across the grain, possibly due to the changes in the metamorphic conditions as the grain grows. Biotite grains sampled should be in contact with the garnet grains (Hodges and Spear, 1982) and rim analysis made at points near the mutual contact.

Following the method of Hodges and Spear (1982), the mole fraction of four garnet components; Almandine (al), Pyrope(py), Spessartine(sp) and Grossular(gr) within each sampled point is calculated by formulae in table 1. The mole fractions of Annite(ann) and Phlogopite(ph) within sampled biotite are also calculated.

With reference to the free energy interaction for the binary end points of the garnet solid solu-

Table 1 Formulae used to calculate mole fractions of phase components. (Hodges and Spear, 1982)

$X_{al} = Fe/(Fe + Mg + Ca + Mn)$

$X_{py} = Mg/(Fe + Mg + Ca + Mn)$

$X_{gr} = Ca/(Fe + Mg + Ca + Mn)$

$X_{ann} = Fe/(Fe + Mg + Ti + Al^{VI})$

$X_{ph} = Mg/(Fe + Mg + Ti + Al^{VI})$

al = almandine, py = pyrope, gr = grossular,
ann = annite, ph = phlogopite

Table 2. Margules parameters for garnet solid solutions. (after Hodges and Spear, 1982)

Margules parameter	Source
$W_{FeMg} = 0$	Newton and Haselton (1981)
$W_{CaMg} = 3300 - 1.5T(K)$	Newton, *et.al.* (1977)
$W_{MgMn} = 0$	Hodges and Spear(1982)
$W_{CaFe} = 0$	Cressey *et.al.* (1978)
$W_{CaMn} = 0$	Ganguly and Kennedy (1974)
$W_{FeMn} = 0$	Ganguly and Kennedy (1974)

tion series (Margules Parameters; W), which are tested for their effect by comparison of results obtained to the expected temperature of the alumino-silicate triple point, Hodges and Spear (1982)(Table 2), determined that the only interaction that was non zero was the mixing of grossular and pyrope in garnet (W_{CaMg} = 3300 -1.5T(Kelvin) from Newton, et. al., 1977).

The formula for the equilibrium coefficient K_1 of the garnet biotite exchange reaction is calculated in formula 1:

$$K_1 = \frac{(X_{py})^3(X_{ann})^3}{(X_{ph})^3(X_{al})^3} \cdot \frac{(Y_{py})^3}{(Y_{al})^3} \qquad (1)$$

The values of Y_{al} and Y_{py} are obtained by substituting Margules parameters into formulae 2 and 3 (after Ganguly and Kennedy, 1974);

$$\ln Y_{py} = \frac{W_{CaMg}(X_{gr}^2 + X_{gr}X_{sp} + X_{al}X_{gr})}{RT(\text{Kelvin})} \qquad (2)$$

$$\ln Y_{al} = \frac{W_{CaMg}X_{py}X_{gr}}{RT(\text{Kelvin})} \qquad (3)$$

The value for the equilibrium coefficient is inserted into formula 4: $0 = 12454 - 4.662T_1(\text{Kelvin}) + 0.057P(\text{bars}) + RT(\text{Kelvin})\ln K_1$ (4)

and the equation is solved for T_1.

7.5.2.3

Results

Results are tabulated in table 3. The garnet compositions for rim and core in two thin sections, 85/46 and 85/94 were analyzed and showed Mn higher in cores than rims and a general zoning with spessartine rich cores and almandine rich rims. A third thin section, 86/26 was treated only for the rim composition of the garnet. Temperatures were computed assuming that biotite compositions were near ideal.(This assumption is considered reasonable by Ferry and Spear(1978) as long as the Ti content of biotite is not signifigant. No minimum value for the significance of this element is suggested.) Three biotites within one slide (85/94) were analyzed, temperatures obtained varied by only 10c regardless of the location of the biotite with respect to the garnet.

TABLE 3
Results of microprobe analysis as applied to the garnet biotite geothermometer. Hodges and Spear, 1982

Sample 85/46: <u>Biotite analysis</u>
46-2

X_{ann} .5812
X_{ph} .3049

Sample 85/46: <u>Garnet analysis</u>

	46-1 core	46-3 core	46-1 rim	46-3 rim
X_{gr}	.1451	.1467	.1511	.1522
X_{al}	.6560	.6700	.6439	.6611
X_{py}	.0319	.0340	.0352	.0369
X_{sp}	.1671	.1493	.1697	.1497

<u>Temperatures in degrees centigrade</u>

	46-1 core	46-3 core	46-1 rim	46-3 rim
	432	388	500	494

Sample 85/94: <u>Biotite analysis</u>

	94-3	94-4	94-9
X_{ann}	.6307	.6374	.6342
X_{ph}	.2196	.2163	.2222

Sample 85/94: <u>Garnet analysis</u>

	94-1 core	94-6 core	94-2 rim	94-5 rim	94-7 unspecified	94-8 unspecified
X_{gr}	.1776	.1779	.1987	.1733	.1522	.1754
X_{al}	.4815	.4477	.6597	.6837	.5772	.4870
X_{py}	.0069	.0070	.0244	.0216	.0143	.0131
X_{sp}	.3340	.3674	.1172	.1521	.2564	.3246

<u>Temperatures in degrees centigrade with biotite #:</u>

	94-1	94-6	94-2	94-5	94-7	94-8
94-3	299.4	313	573	454	390	415
94-4	309	317	580	460	395	420
94-9	298.5	312	570	452	389.3	413.8

Sample 86/26: <u>Biotite analysis</u> <u>: Garnet analysis</u>

Biotite analysis		Garnet analysis	
X_{ann}	.5158	X_{gr}	.1202
X_{ph}	.3000	X_{al}	.6793
		X_{py}	.0548
		X_{sp}	.1457

<u>Temperature in degrees centigrade:</u> 570

7.5.2.4

Conclusions; Garnet, Biotite Geothermometry

Temperatures obtained using the core composition of the garnets were consistently lower than temperatures obtained using the rim compositions. It appears that spessartine rich cores were generated at temperatures as low as 300c, assuming no diffusion of elements within the garnet porphyroblast. The almandine rich rim composition gave temperatures as much as 280c higher than core temperatures and more closely matched the result anticipated, after consideration of the mineral assemblage.

Temperatures obtained from garnet rim compositions are indicative of increasing temperature of metamorphism as the contact with the northern granite is approached (Map Unit 4; Fig. 7.1). Sample 85/46 (location 9, Fig 7.1) at a distance of approx. 3 km. from the nearest contact with the granite gave a value of 500c for the garnet rim composition and 395c to 400c for the garnet core composition. Within 2 km. of the contact, sample 85/94, (location 4, Fig. 7.1) garnet rim compositions for two porphyroblasts gave temperatures of 450c and 580c. These garnets give temperatures of about 300c to 315c for core compositions, indicating that the temperatures under which the garnets began to grow were, within the error of the method, exactly the same. The discrepancy in temperatures obtained from rim analysis may be due to the proximity of these two garnets to each other. During growth the diffusion of elements to the growing crystal may have gradually favored one of the poikiloblasts over the other, effectively stopping the growth of the smaller garnet below peak temperatures.

The third sample analyzed is within 1 km. of the Morose granite contact (sample 86/26, location 3, Fig. 7.1). Garnet was analyzed for rim composition only and gave a temperature of 570c. This is virtually the same temperature that was obtained at location 4, 1.7 km. from the contact. Although the temperature closer to the mapped contact with the northeastern granite could be assumed to be higher, the measured distance is in plan view only. In the third dimension these samples may be closer to equidistant from the granite contact than the map view would indicate.

7.6

Conclusions

Cited evidence for prograde metamorphism in the supracrustal rocks within the map area indicates a broad thermal aureole surrounded the intrusion of a younger granite in the northeastern part of the map area. Temperatures of 500°c were reached in supracrustal sediments up to 3 km. from the contact between the granite and the metavolcanic rocks. Higher temperatures adjacent to the contact are indicated by higher grade metamorphic mineral assemblages and by garnet, biotite geothermometry.

Estimates of peak pressures during metamorphism are restricted to the determination of Ramsay (1974) and Winkler (1979) of about 3 kb for the cordierite isograd. Presence of almandine garnet within intervolcanic metasediments suggests pressures there may have reached 4 kb.

Garnet-biotite geothermometry indicates that temperatures were increasing during genesis of garnet porphyroblasts. In one instance, sample 85/94, the temperature appears to have risen about 200°c between beginning and end of porphyroblast growth.

As temperatures fell, retrograde reactions produced low grade minerals within otherwise medium grade assemblages. The retrograde nature of these minerals (chlorite, sericite and epidote) is indicated by their disposition as rims and halos around higher grade phases.

Chapter 8

STRUCTURAL GEOLOGY

8.1

Introduction

Polyphase deformation of the supracrustal metavolcanic and metasedimentary rocks of the Fenton Lake map area has created structures that may be separated, on the basis of style, orientation and overprinting into 3 distinct generations. During D_1 and D_3 subsets of structures appear to have formed at approximately the same time. These subsets are seperated into A and B generations indicating a best estimate of time relations, based on overprinting relationships, between otherwise morphologically identical foliations. Proterozoic faulting has not been considered within the deformation framework (Fig. 8.1).

First generation structures vary in style across the three major lithologic units. Within the metasedimentary domain, folds (F_1), defined by bedding top reversals, and generally lacking well defined axial surface foliations, are traceable along strike for kilometers. The metavolcanic succession was tilted during first phase deformation (D_1) to form a steeply dipping, westward facing homocline which curves from a NE trend in the southern half of the map area to NW and then to N. Layer parallel

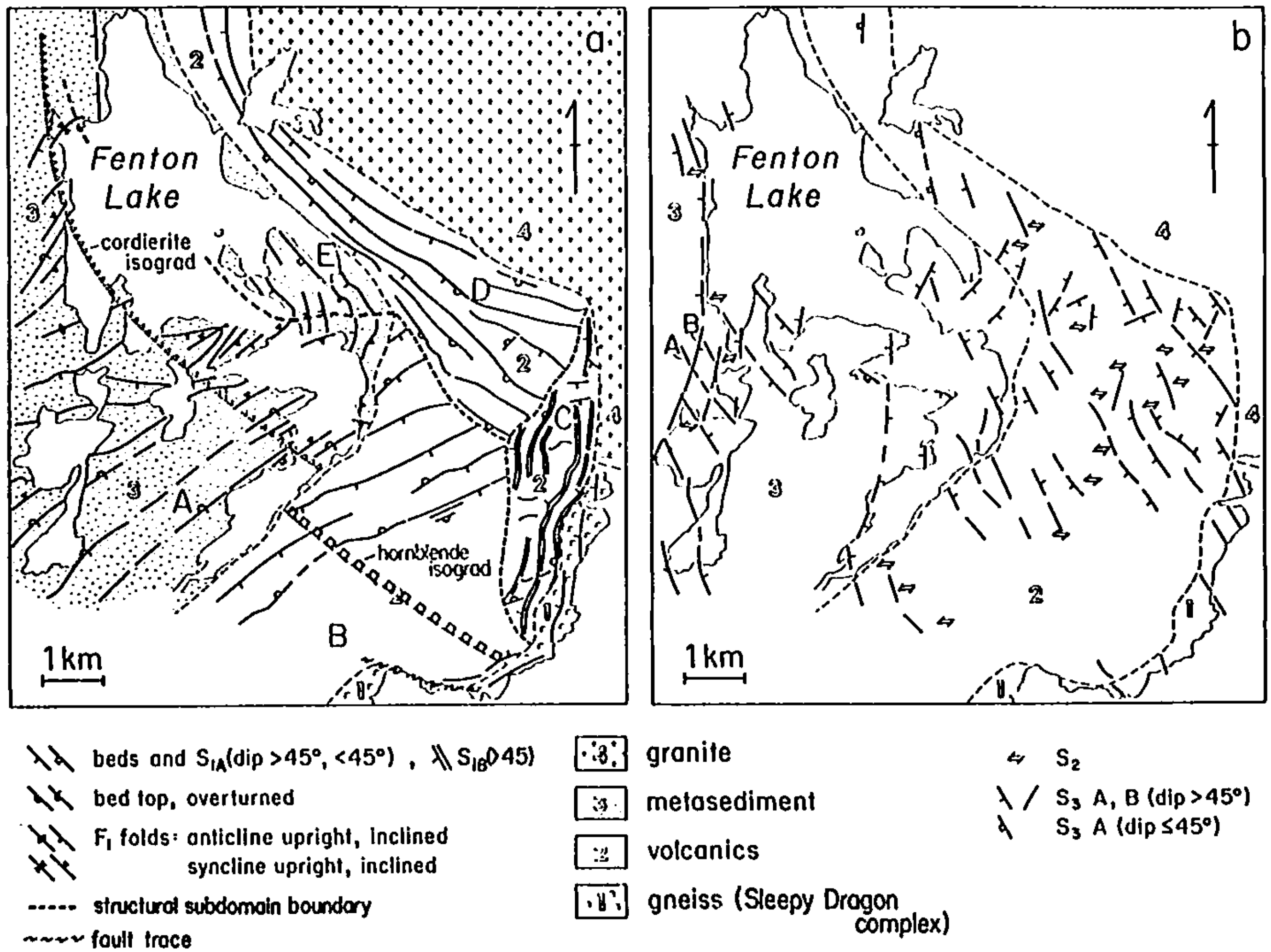

Figure 8.1a Outline map of the Fenton Lake area indicating major lithological boundaries, major structural domains (A to E), trend lines of bedding in metasedimentary rock, S_1 foliation in metavolcanic rocks and metamorphic isograds.

Figure 8.1b Outline map of the Fenton Lake area indicating major lithological boundaries and trends of S_2, S_{3A} and S_{3B} foliations.

foliation (S_{1A}) in the metavolcanics is attributed to D_1. Foliation parallel to the north striking contact between the metavolcanics and the eastern granitic terrain is grouped as S_{1B} (Fig. 8.1a). S_{1A} foliations appear to be transposed into a N - S, S_{1B} parallel orientation in this area. Contact parallel foliations in the Sleepy Dragon basement gneiss, including local mylonite zones are probably D_1 structures.

The map area is divided into 5 structural domains labelled A to E (Fig. 8.1a), based on variations, in trends of tight F_1 folds and fold limbs in metasedimentary rocks and S_1 layer parallel foliation in metavolcanic rocks.

Second generation structures are represented by an easterly striking S_2 foliation (Fig. 8.1b). S_2 is commonly transposed and obliterated by later foliations. Map scale F_2 folds are not recognized.

D_3 structures are small scale F_3 asymmetrical folds and S_3 axial -planar foliations, divided into A and B generations based on a few examples of overprinting relationships observed in the metasedimentary domain. S_{3A} is a northwesterly striking foliation and S_{3B} strikes northeasterly (Fig. 8.1b).

8.2

D_1 STRUCTURES

8.2.1

METASEDIMENTARY ROCKS

8.2.1.1

Folds

The sedimentary rocks display a series of tight to isoclinal F_1 folds with limbs over a kilometer in length. Few hinges are exposed and the folds are mainly defined by reversals in the facing directions of parallel striking beds. One exception is a fold evident in thick bedded sandstone on a promontory on the western shore of Fenton Lake; convergent bedding on the limbs of a syncline is well defined on airphotos (Fig. 8.1a, domain A).

F_1 fold trends are not uniform but vary through almost 90 degrees from northeast (Fig. 8.1a, domain A), parallel to the southern homocline in the volcanic rocks, to northwest and north (Fig. 8.1a, domain E), parallel to the northern homocline in volcanic rocks.

F_1 folds in domain A vary slightly in orientation but the dominant northeasterly trend is clearly shown in equal - area net projections of the poles to bedding (Fig. 8.2, 8.3). Dips are dominantly subvertical to steep southeasterly. Facing directions (Map 2 and Fig 8.1a) indicate that beds and folds in

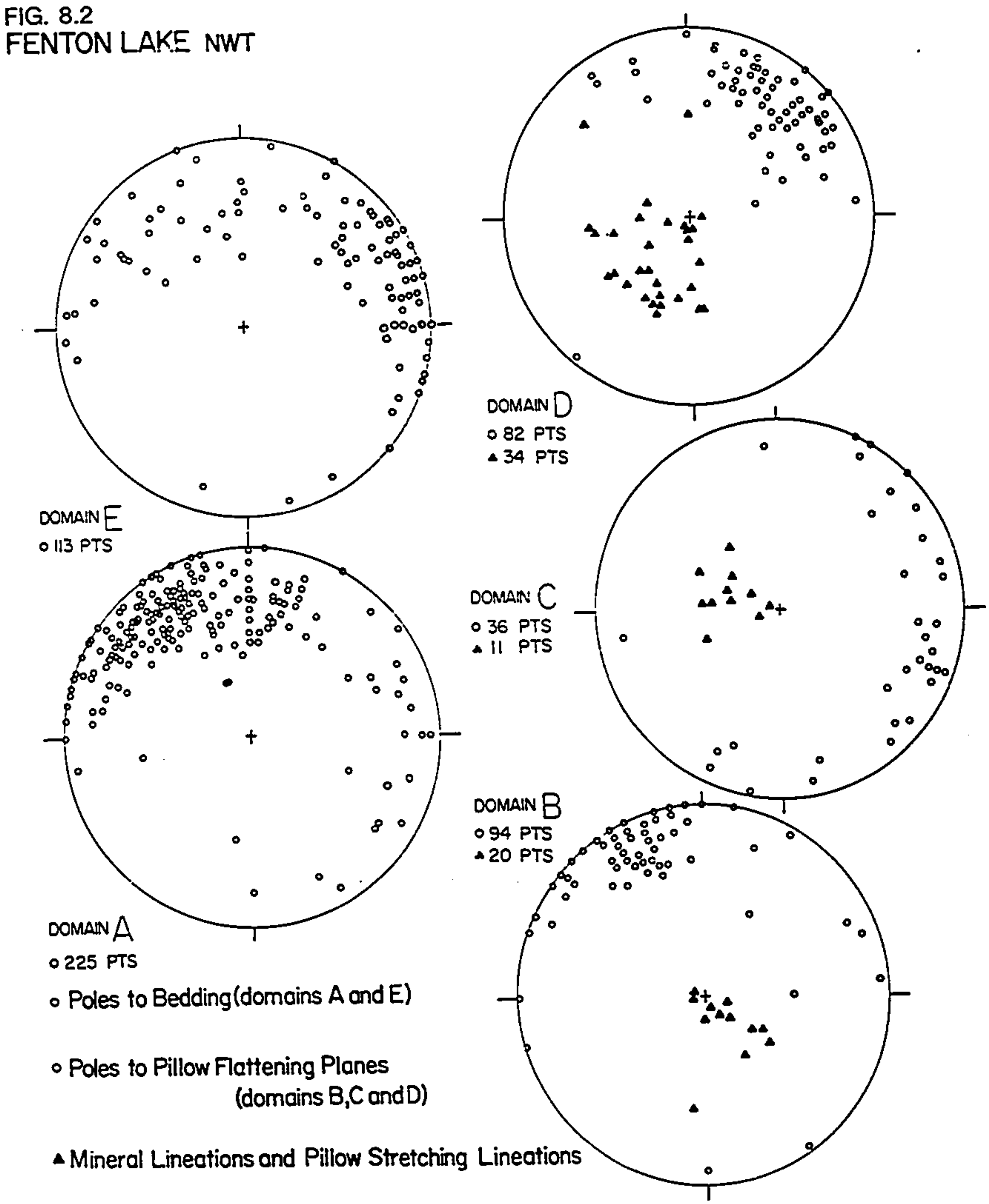

Figure 8.2 Schmidt equal area plots of poles to bedding (S_0) for metasedimentary domains A and E, S_1 pillow flattening planes for metavolcanic domains B, C, and D.

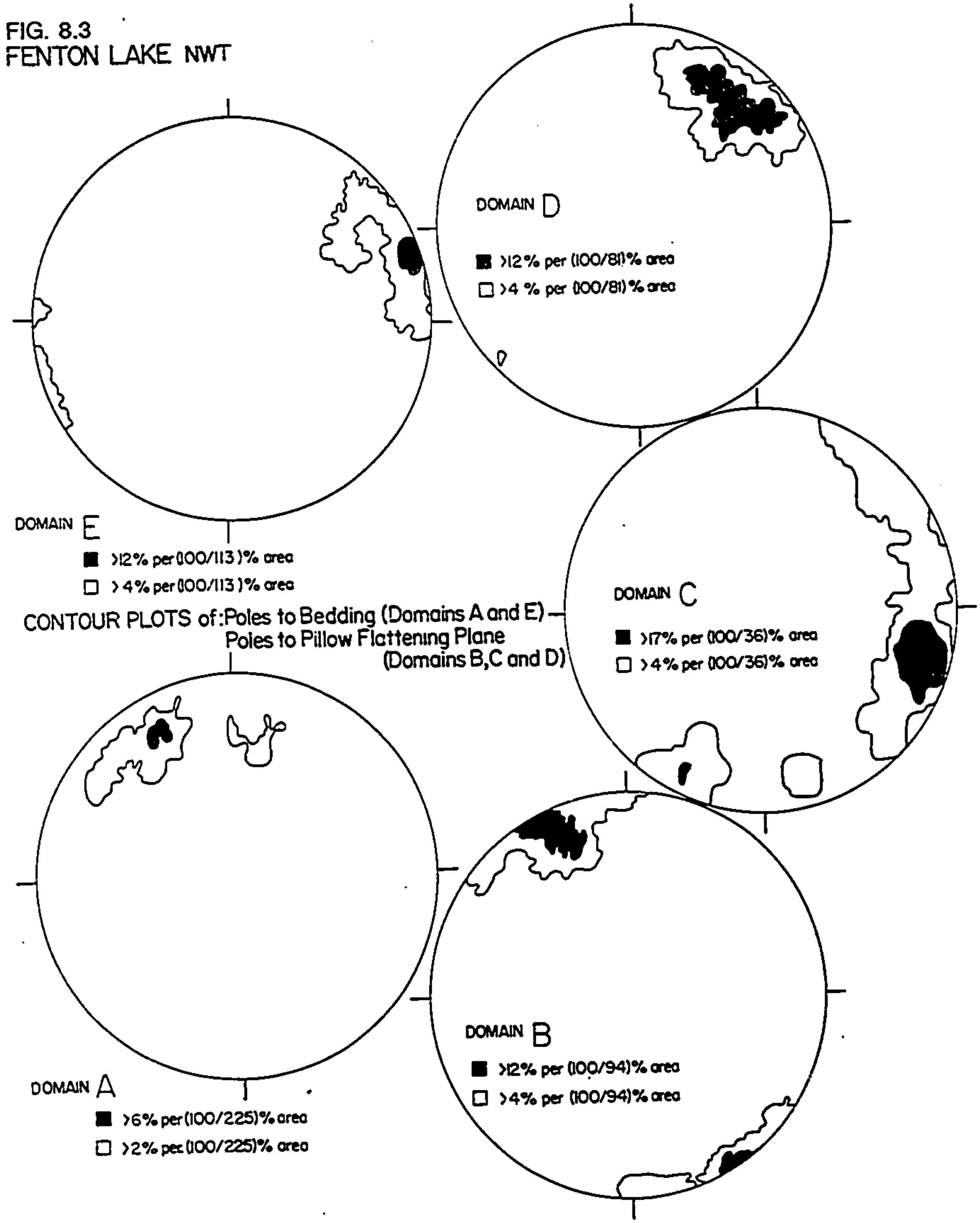

Figure 8.3 Contoured equal area net plots of poles to S_0 and S_1. Plots contoured according to Starkey's (1976) method

domain A are commonly overturned to the northwest.

As in domain A, bedding and folds within domain E vary in orientation (Figs. 8.1a and 8.2). Northwest to northerly trends and steep westerly to vertical dips predominate (Fig. 8.3).

Adjacent to where the volcanic belt curves from northeast (domain B) to northwestward (domain D), lack of continuous outcrop makes the pattern of folding in the sedimentary rocks difficult to establish. It appears that F_1 folds in the metasedimentary rocks conform to the large scale change in trend of the metavolcanic rocks, thereby defining an apparent refold of F_1 as fold hinges curve through the 'elbow' region.

On the western shore of Fenton Lake the change in trend of F_1 structures is less dramatic. The axial - surface traces of folds and parallel bedding on the limbs swing gradually from a northeast to a northerly trend, the latter conforming to the trend of volcanic rocks in the northern part of domain D (Fig. 8.1a).

8.2.2

METAVOLCANIC ROCKS

8.2.2.1

F_1 Folds

The volcanic rocks form steeply dipping, gener-

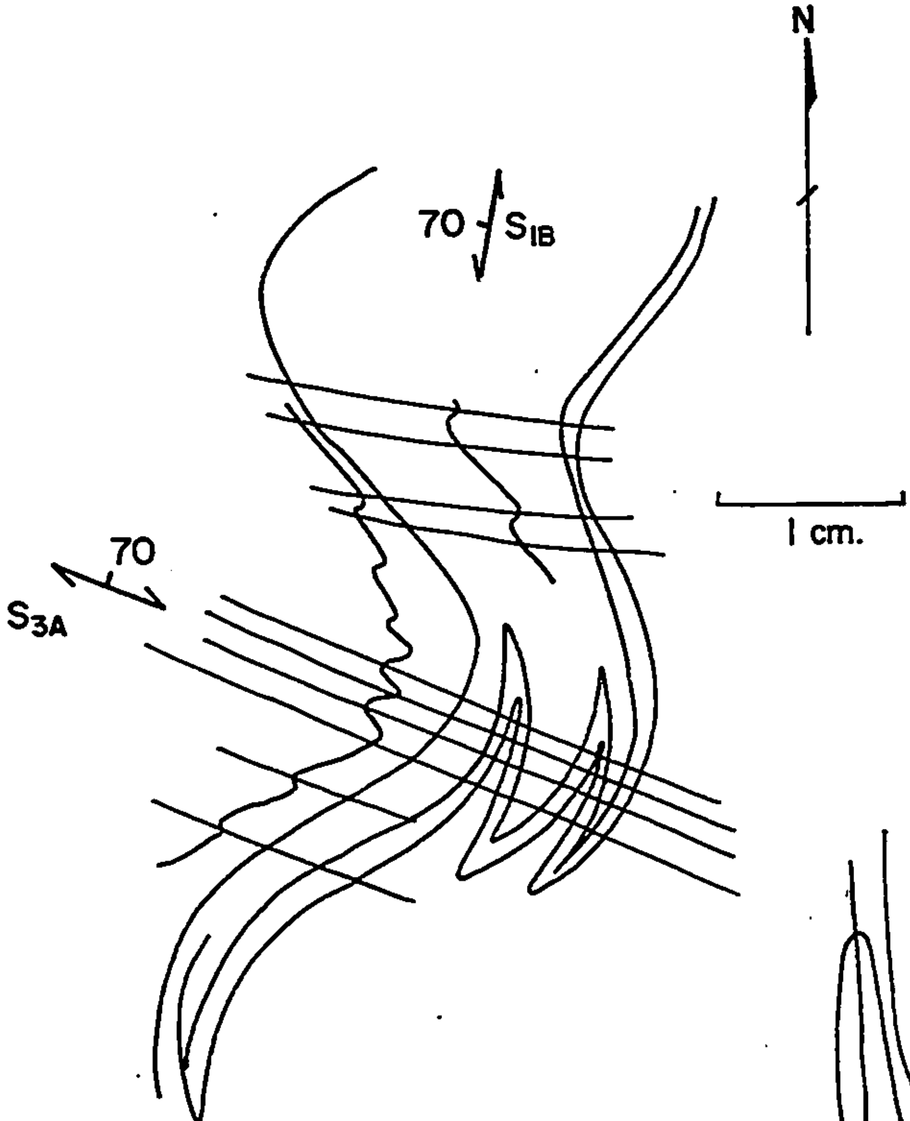

FIG. 8.4A

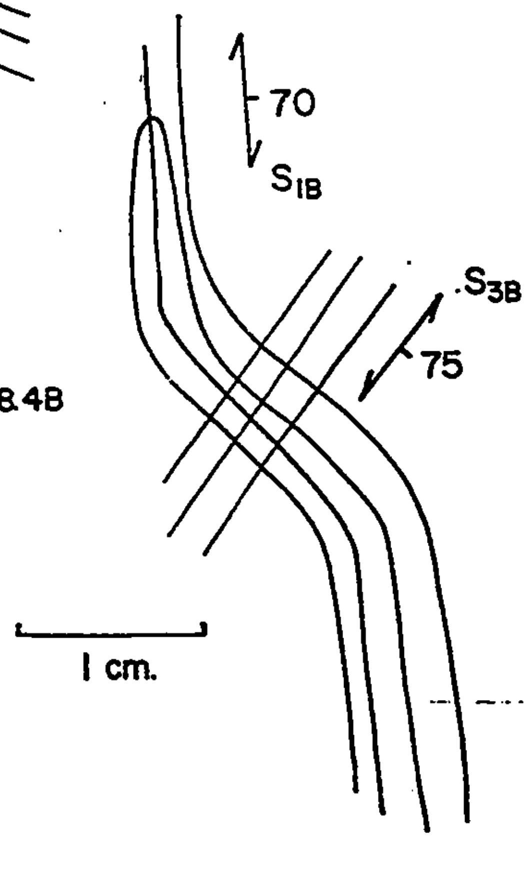

FIG. 8.4B

Figure 8.4 Sketches of small scale features discernible within metavolcanic rocks of domain C and domain D. Intrafolial isoclines are refolded by younger folds and overprinted by foliations. S_{1A} foliation is folded about S_{1B} (north striking) parallel axial planes and refolded about S_{3A} and S_{3B} foliations.

ally homoclinal, successions. A rare outcrop of easterly facing pillows near eastern shore of a narrow northwest striking lake in the south central part of domain D (Map 2) suggests a possible small scale F_1 fold. Minor, tight intrafolial folds in foliation (Fig. 8.4a and b) with axial traces parallel to the granite, metavolcanic contact in domain C are related to the S_{1B} foliation. These rare, minor folds do not significantly affect the map pattern.

8.2.2.2

S_1 Foliation

The S_{1A} foliation is commonly defined in outcrop by the layer parallel orientation of the long dimensions of flattened pillows (Fig. 8.5) and by mineral foliations and spaced cleavages within massive volcanics and within intervolcanic metasedimentary and volcaniclastic rocks. S_{1A} in the interflow metasedimentary rocks conforms to contacts with enclosing, more competent metavolcanic rocks.

S_{1A} and later foliations are locally traced by hematite and epidote veining, especially in close proximity to the northern granite (Fig. 4.11a and b).

Thin sections reveal that S_{1A} is defined by aligned amphiboles (actinolite, hornblende and cummingtonite) in metavolcanic rocks and by aligned biotites and hornblende in the interflow metasedimen-

Figure 8.5 Photograph of flattened pillow structures defining an S_1 shape fabric in horizontal section. The lens cap is 55mm in diameter. Thin quartz vein parallels the flattening plane. Outcrop is midway across the northwest trending arm of the volcanics near the northern end of a long narrow lake.

Figure 8.6 Photograph of subvertically elongated pillows in mafic volcanic rocks, southeastern part of domain C. Quartz veins and light colored alteration of selvages define pillow margins.

Figure 8.7 Photomicrograph of metavolcanic rock from the southernmost part of domain D showing lineation parallel amphiboles, ilmenite and pyrite. PP - plane polarized; CP - cross polarized.

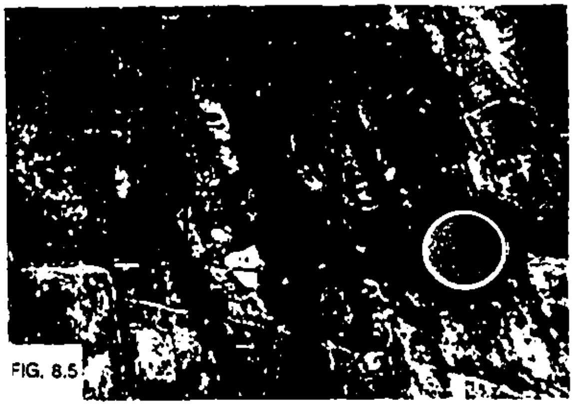

FIG. 8.5

FIG. 8.6

FIG. 8.7 PP

FIG. 8.7 CP

tary rocks.

8.2.2.3

Lineations

A lineation defined by mineral elongation and pillow selvage extension (Fig. 8.6) within each of the volcanic structural domains B, C, and D (Fig. 8.2) commonly plunges 60 degrees or more within the S_{1B} plane (Fig. 8.2). Sulfides are sometimes aligned in down dip stringers parallel to L_1 (Fig. 8.7).

Net projections for each domain show that L_1 clusters at about 90 degrees to the strike of S_1 (Fig. 8.2), in other words, in the down dip direction.

8.2.2.4

Orientation of S_1 and F_1

S_{1A} changes strike abruptly across the boundary between structural domains B and D (Fig. 8.1a) within the metavolcanic rocks and is probably folded and transposed into a granite/gneiss contact parallel orientation (S_{1B}) within structural domain C (Fig. 8.1a).

In structural domain B, northeast striking S_{1A} shape fabrics and local layering follow the map trace of the metasediment/metavolcanic contact in the southern part of the domain. Further northeast, although the contact swings northward, S_{1A} continues northeast, deviating by approximately 45° from the contact (Fig. 8.1a). Thus, the major change in trend of the metavolcanic rocks is not due to folding after S_{1A} had developed. S_{1A} in domain B varies in dip from steep southeasterly to vertical (Map 2).

Pillow tops show that the volcanics face dominantly northwesterly to westerly away from the granite/gneiss terrain to the east. The metavolcanics of domain B are overturned northwestward at the southern end of the metasediment/metavolcanic contact, varying to near vertical further north and subvertical along the metavolcanic/gneiss contact.

Structural domain C occupies a narrow zone along the eastern boundary of the volcanic terrain where the contact with the granitic and gneissic rocks to the east strikes northerly. Pillow flattening trends within the domain are variable with abrupt changes in orientation suggesting that S_{1A} strikes, extending northeastward from domain B, are locally preserved, but generally curve to strike parallel to the contact with the granitic and gneissic rocks to the east. The northerly striking shape fabrics and foliations, designated as S_{1B}, are steeply west dipping (Figs. 8.2/8.3). Where pillows are visible they face predominantly west with the indicated exception in the elbow region of the metavolcanics

(Map 2).

Conforming to the map pattern of the granite, metavolcanic contact, S_1 within domain D curves from northwest to strike northerly at the northern end of the map area (Fig. 8.1a). Dips of S_1 are from 40 to 80 degrees southwest to westerly with the average being about 60 degrees, slightly shallower than dips in the southern part of the belt (Fig. 8.2). West facing pillow structures in the least strained flows at the southern end of domain D indicate that the volcanic belt is probably homoclinal along its mapped length and faces southwest (Map 2 and Fig. 8.1a).

8.2.3

STRUCTURAL DOMAIN RELATIONSHIPS

Strike changes of bedding and S_{1A} foliation between structural domains take place sharply over distances of a few tens of meters in the volcanic succession. The boundary between domains B and D, where S_1 abruptly changes strike from northeast to northwest, is therefore best termed a "fabric front" (Fyson, 1984b). The domain boundary (fabric front) parallels northwest striking S_1 in domain D, which conforms to the contact between the metavolcanic rocks and the northern granite. At the southeastern corner of domain D, S_{1A} strikes northeast, parallel to S_{1A} further south in domain B. The arrangement suggests that northeasterly striking S_{1A} is locally preserved from transposition into the northwesterly direction characteristic of domain D. From the map pattern (Fig 8.1a) S_{1A} striking northwest in domain D appears to truncate NE striking S_{1A} in domain B. However, overprinting relationships are not clearly defined. Lacking evidence to the contrary and considering the similar morphologies and textures, the S_{1A} foliation in the two domains is assumed to have formed sequentially but close in time.

The boundary of domain C with domains B and D is less distinct. It is placed where S_{1A} extending from both domains B and D becomes irregular in orientation and a northerly trending apparently cross -cutting foliation (S_{1B}) is prominent. As indicated previously S_{1B} is parallel to the contact of metavolcanic rocks and granite/gneiss terrain.

8.3

D_2 Structures

8.3.1

METASEDIMENTARY ROCKS

The second phase of deformation, D_2, produced few recognizable folds but is represented by a regionally developed, easterly striking S_2 foliation (Fyson, 1975, 1982, 1984a) (Fig. 8.1b and 8.8). Where preserved at lower metamorphic grades, S_2 is defined

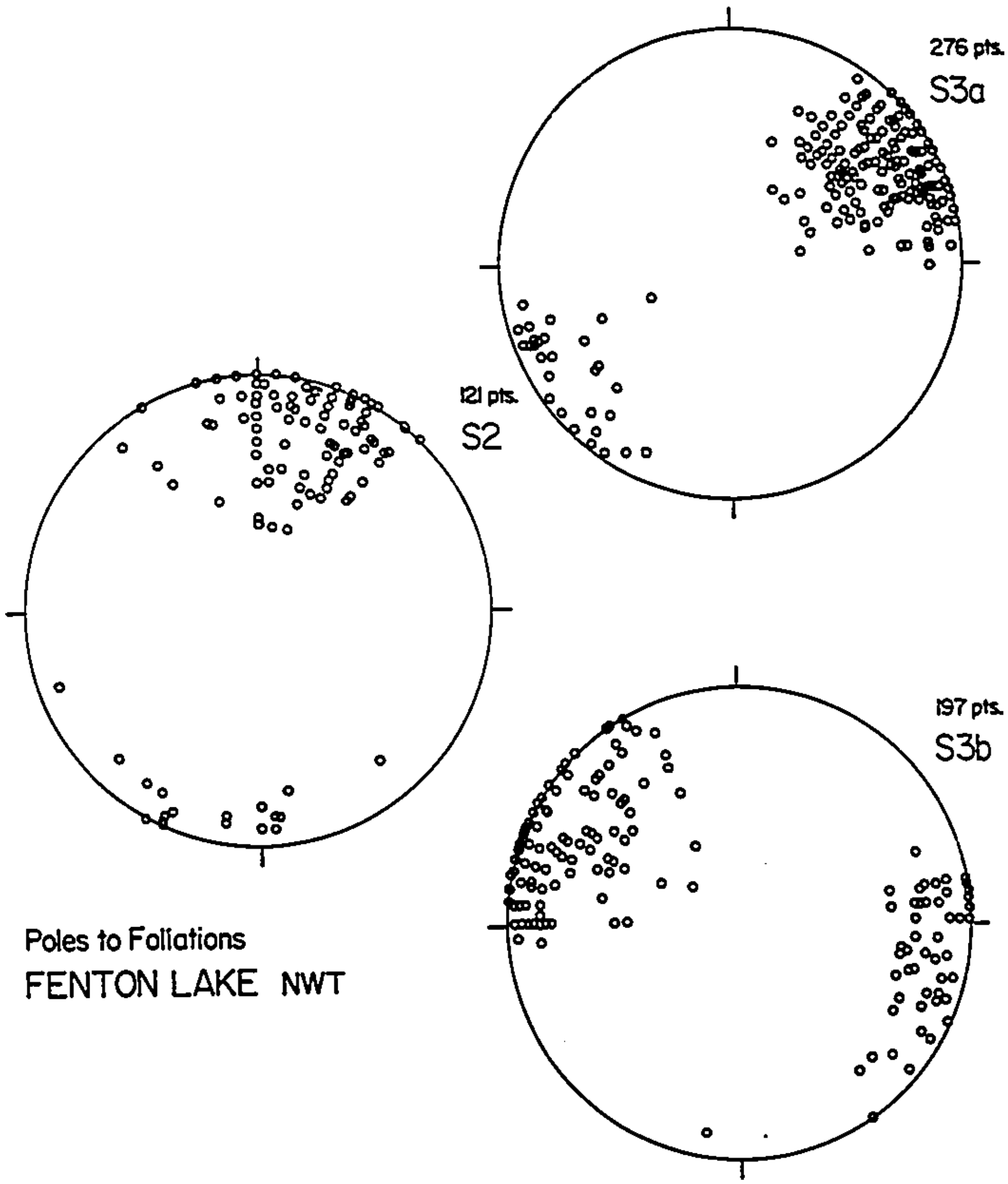

Figure 8.8 Equal area net-plots of poles to S_2 and S_3 foliations for the Fenton Lake area supracrustal rocks.

by a mineral alignment of chlorite, muscovite and/or biotite between quartz rich domains, and by remnant quartz inclusion trails within biotite poikiloblasts, as metamorphic grade increases. Exterior to these biotite porphyroblasts S_2 parallel muscovite and biotite are tightly crenulated and transposed into S_3 cleavages. At cordierite grade the S_2 foliation is locally defined by aligned biotite muscovite and minor chlorite where it is preserved undeformed within cordierite poikiloblasts.

Although the enclosing rocks have been affected by later D_3 structures, S_2 inclusion trails within biotite and cordierite poikiloblasts retain a dominantly easterly strike. Resistance of poikiloblastic minerals to reorientation during D_3 deformation is discussed by Fyson (1980a).

8.3.2

METAVOLCANIC ROCKS

Easterly striking S_2 spaced cleavage in the metavolcanic rocks is most strongly developed in the central part of the map area although S_2 parallel crenulation cleavage was measured at one locality near the southern limit of mapping. A shape fabric parallel to S_2 is not common, however, some of the shape fabrics designated as S_1 in domain C based on easterly strikes, may be D_2 structures.

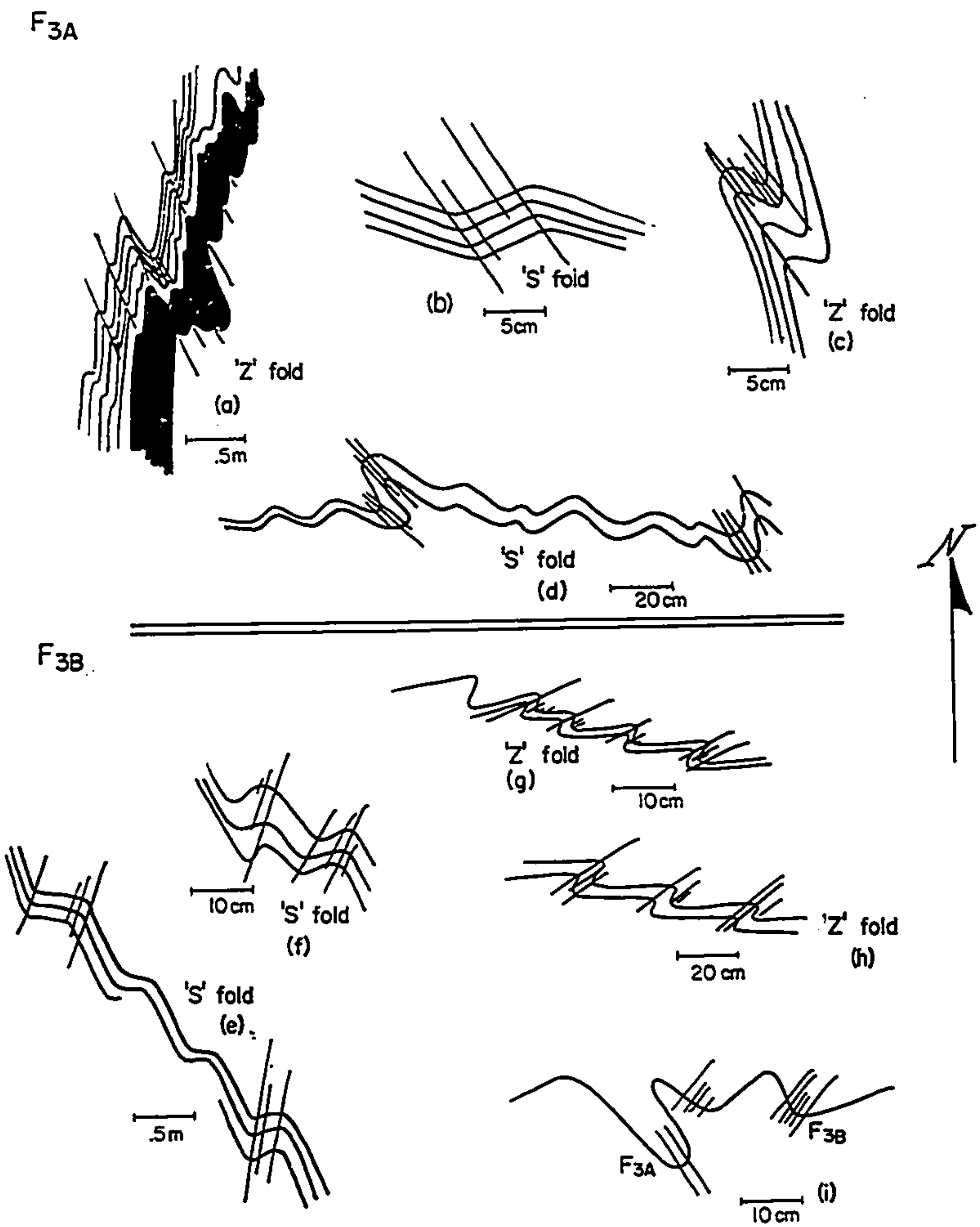

Figure 8.9 Sketches from horizontal outcrops of F_{3A} and F_{3B} generation folds illustrating changes in style and asymmetry within one generation with orientation changes in the folded surface. F_{3A} and F_{3B} generations within one area are shown in Fig. 8.9i.

Sketch locations:

Fig. a, e, h	Sleepy Dragon Gneiss Terrain
Fig. d, f, i	Domain D Metalvolcanics
Fig. b, g	Domain D Metalvolcanics
Fig. c	Domain E Metasediments

8.4

D_{3A} Structures

8.4.1

INTRODUCTION

D_{3A} deformation has produced folds with limbs varying from a centimeter a few meters in length. The folds are open to tight and plunge steeply. A steep S_{3A} axial planar foliation strikes northwest across both the supracrustal and gneissic rocks. F_{3A} folds have both 'S' and 'Z' asymmetries (Fig. 8.9), probably reflecting varying orientations of the S_1 surfaces before D_3 deformation.

8.4.2

METASEDIMENTARY ROCKS

F_{3A} folds with limbs a few centimeters long are propagated sporadically within fine grained and thinly bedded pelitic rocks and are prominent locally in bedding parallel quartz veins (Fig. 8.10). Coarser beds rarely display F_{3A} folds.

S_{3A} foliation is developed in the sedimentary rocks as either a crenulation cleavage or a spaced to penetrative cleavage defined by aligned micas.(Figs. 8.11a and b). S_{3A} refracts within the sediments as it crosses boundaries between coarser and finer beds and may change strike by as much as 10 degrees. Dips are steep to vertical with few exceptions (Fig. 8.8, Map

Figure 8.10 F_{3A} asymmetrical folds in a bedding parallel quartz vein. S_{3A} spaced cleavage strikes northwest (approx. 165°). Resistant layers within metasedimentary rocks parallel bedding and may be sandy laminae found within division B or D of the Bouma sequence. Outcrop on the western shore of a large lake immediately west of Fenton Lake. North toward top of photo. Pencil is 14cm long.

Figure 8.11A Photomicrograph of S_{3A} parallel muscovite (M) and sparse biotite (B) rich domains (strike 170°) separated by quartz rich domains in metasediments from the southern part of domain E. This sample is above the cordierite isograd, yet muscovite is preserved defining the foliation which is parallel to local bedding. The foliation forms open warps whose axial planes are parallel to S_{3B} foliation striking 035°.
PP - plane polarized; CP - cross polarized

Figure 8.11B Photomicrograph of biotite muscovite schist from western shore of a large lake immediately west of Fenton Lake. S_{3A} foliation defined by parallel alignment of muscovite and biotite strikes northwest. F_{3B} folding of S_{3A} produces an S_{3B} parallel kink in the large biotite poikiloblast, open warps in the S_{3A} foliation and realignment of quartz inclusion trails to a northeasterly strike.
PP - plane polarized

FIG. 8.10

FIG. 8.11a PP

FIG. 8.11a CP

FIG. 8.11b PP

2)

8.4.3

METAVOLCANIC ROCKS

F_{3A} folds in the metavolcanic rocks are similar in style and orientation to F_{3A} structures in the metasedimentary rocks. Though scattered throughout the metavolcanic rocks, F_{3A} folds predominate at the southeastern end of structural domain D and in structural domain C.

A spaced cleavage parallel to axial planes of F_{3A} folds, S_{3A} strikes predominantly northwestward, and dips steeply, commonly southwest (Fig. 8.1b, 8.8, Map 2). It affects all volcanic rock types and changes strike only slightly where the volcanics of domain D swing from a northwest to a northerly trend.

S_{3A} is defined by the preferred dimensional orientation of hornblende and actinolite, +/- cummingtonite and opaque minerals, usually ilmenite, in mafic volcanic lithologies (Fig. 8.12) and by the preferred orientation of biotite, hornblende and chlorite (retrograde from biotite) in the intervolcanic metasedimentary rocks (Fig. 8.13a and b). Within the volcanic succession, folded and fractured amphibole grains suggest that S_{3A} was formed by the crenulation of an earlier foliation.

Figure 8.12 Photomicrograph of metavolcanic rock from the northern part of domain D showing S_{3A} parallel hornblende laths which anastamose around hornblende porphyroblasts. Cross sections of hornblende are present in the bottom center of the photograph.
PP - plane polarized; CP - cross polarized

Figure 8.13A Photomicrograph of large polycrystalline quartz clast with S_{3A} parallel biotite and hornblende laths. S_{3A} curves around the clast. Sample from intervolcanic metasedimentary rocks in the northwest trending arm of the metavolcanic rocks.
PP - plane polarized; CP - cross polarized

Figure 8.13B Photomicrograph of intervolcanic metasediments displaying poor sorting and angular to semirounded quartz grains. S_{3A} foliation is defined by the parallel alignment of biotite and amphibole. Black spots are bubbles trapped in the mounting medium
PP - plane polarized; CP - cross polarized

Figure 8.14 Photograph of bedding contact between coarse sandstone, bottom and pelitic sediment showing development of northwest striking foliation in sandstone transposed into northwest S_{3B} foliation in the pelitic rock. S_{3B} dies out in the coarse sediment at the upper left of the photo. Outcrop at the north shore of a large lake immediately west of Fenton Lake. Pencil is approximately 14cm long.

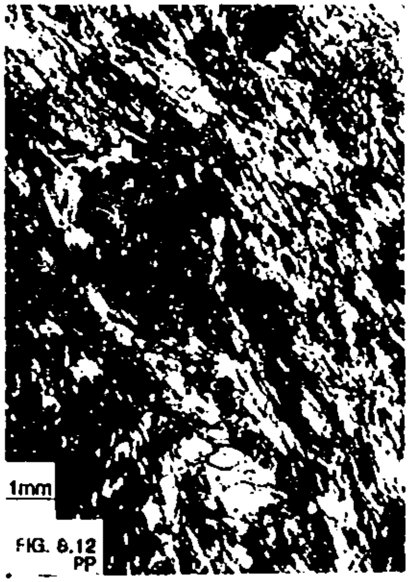

FIG. 8.12 PP

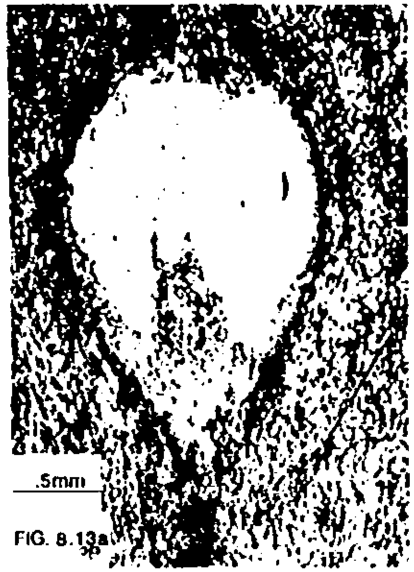

FIG. 8.13a PP

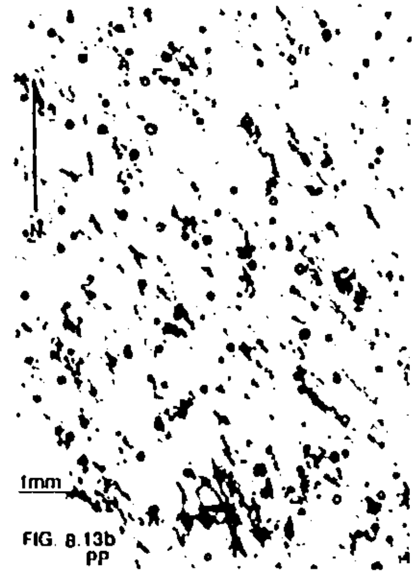

FIG. 8.13b PP


FIG. 8.14

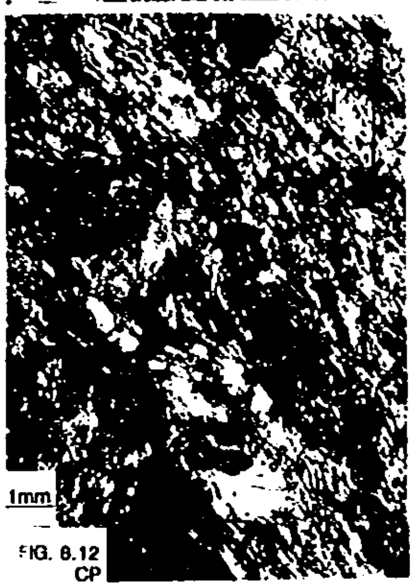

FIG. 8.12 CP

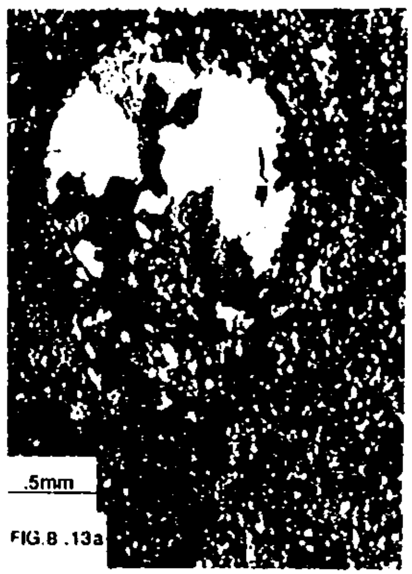

FIG. 8.13a

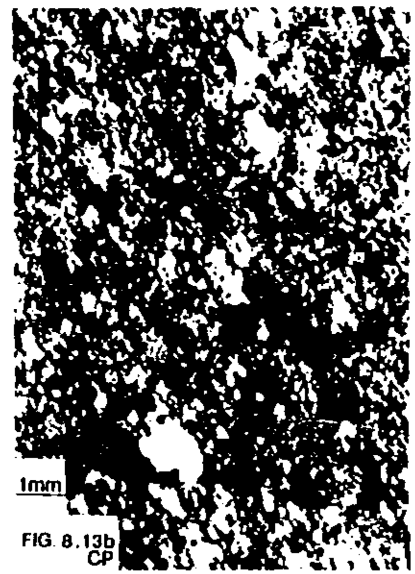

FIG. 8.13b CP

8.5

D_{3B} STRUCTURES

8.5.1

INTRODUCTION

D_{3B} generation structures are similar morphologically to D_{3A} structures. The only distinguishing feature is the northeast to northerly trend of the axial planar S_{3B} foliation (Fig. 8.1b). Where F_{3A} and F_{3B} folds are preserved in the same outcrop they exhibit opposite senses of asymmetry (Fig 8.9i) and were not seen to overprint one another. As for F_{3A}, F_{3B} folds are discontinuous structures which die out rapidly along axial surfaces.

However, in a few localities, S_{3B} crenulations are seen to affect S_{3A} foliations (Fig. 8.14), establishing their time relationship.

8.5.2

METASEDIMENTARY ROCKS

Steeply plunging F_{3B} folds are common in the metasedimentary rocks, especially in thinly bedded units and in bedding parallel quartz veins.

In addition to contrasting strikes, S_{3A} and S_{3B} may be distinguished by relative intensities of development in pelitic (argillaceous) and sandstone units (Fig. 8.14). S_{3A} is preserved in coarse grained sandstone beds in which S_{3B} is either weak or absent, whereas in the pelitic rock S_{3A} is completely overprinted by S_{3B}. Where (as in fig. 8.14) the bedding approximately bisects the angle between S_{3A} and S_{3B}, the consequent chevron pattern of cleavages is distinctive (see also Fyson, 1984b).

Thin sections indicate that S_{3B} is a crenulation of S_2 or S_{3A} with no apparent new mineral growth along the axial surfaces of the crenulations.

8.5.3

METAVOLCANIC ROCKS

A spaced cleavage, S_{3D} is axial planar to asymmetrical S and Z verging cm scale folds in the metavolcanic rocks (Fig. 8.9). S_{3D} foliations are steeply inclined and vary in strike from N to NE (Fig. 8.8) perhaps reflecting variations in directions of shortening controlled by local anisotropy in the rock.

8.6

CRYSTAL GROWTH AND DEFORMATION

The relationship between crystal growth and deformation is well displayed in metasedimentary rocks where structures and fabrics of various generations are readily distinguished. Similar interpretations are more difficult in the metavolcanic rocks where identical mineral species are aligned along successive foliations with relict fabrics (crenulation or folding) rarely preserved.

8.6.1

METASEDIMENTARY ROCKS

Thin section evidence suggests temperatures within the metasedimentary rocks were rising during D_2 deformation, causing growth of biotite parallel to the S_2 fabric. Peak temperatures, pre D_{3A}, saw growth of biotite and cordierite poikiloblasts preserving quartz inclusion trails in biotite and mineral laths in cordierite. The trails in biotite remain parallel to the east striking S_2 foliation (Fig. 8.11b) during D_3 deformation.

Temperatures within the metasedimentary rocks may have been decreasing during and after D_{3A} as minerals aligned parallel to or overgrowing S_{3A} are generally lower grade muscovite and biotite (Fig. 8.11).

Little new mineral growth parallel to S_{3B} suggests a continued drop in temperatures within the metasediments during D_{3B}.

8.6.2

METAVOLCANIC ROCKS

Within the metavolcanic rocks, overprinting relationships are rarely preserved, probably as a result of almost continuous mineral growth during deformation at medium to high metamorphic grades. A rare case of preserved overprinting in the extreme southern part of the area shows S_2 and S_{3A} are locally defined by crenulation of earlier foliations (Map 2). S_{3B} parallel fabrics seen in one thin section from the northeastern part of domain B appear to be related to development of an asymmetrical fold or shear band through S_1 or S_2 parallel hornblende laths (Fig. 8.15).

Temperatures compatible with the growth of hornblende and spessartine to almandine garnet (see metamorphism) were effective over much of the metavolcanic domain above the hornblende isograd (Fig. 8.1a). One sample, 85/9, from within 1 km of the northwest striking metavolcanic/metasediment contact shows a garnet poikiloblast that overgrows a crenulated, east striking foliation (S_2) and the new foliation (S_{3A}), defined by the alignment of hornblende laths (Fig 7.11). S_{3A} anastomoses around garnet elsewhere in the same thin section, suggesting that the garnet grew pre to syn S_{3A}, the latest foliation visible in the thin section.

Lack of good thin section examples of S_{3B} makes it difficult to adequately describe the foliation and relate it to temperature conditions within the metavolcanic rocks.

Figure 8.15 Photomicrograph of metavolcanic rock from the northeastern part of domain B displaying S_1 or S_2 parallel hornblende with cross cutting S_{3B} parallel hornblende laths and F_{3B} asymmetrical fold or shear band. From the northeastern part of domain B, just south of the domain boundary.
PP - plane polarized; CP - cross polarized

Figure 8.16 Photograph of Sleepy Dragon Complex gneiss displaying northerly striking layering and foliation defined by sparse micas anastamosing around quartz and feldspar augen. Possible fold in layering at the center of photograph suggests that some pre D_1 folding may be present in the gneissic rocks. Lens cap is 58mm in diameter.

Figure 8.17 Photograph of structures in Sleepy Dragon Complex gneiss. Boudinaged quartz vein forms a 'Z' fold. The vein is offset in a dextral sense along a shear band type of structure. Both the fold and shear band suggest dextral shear along the foliation. White bear flare attached to launcher is 5cm long.

Figure 8.18A Photomicrograph of a horizontal section through mylonitized granitoid rock near the east striking contact between the Sleepy Dragon gneissic rocks and the metavolcanic rocks. Recrystallization of quartz has removed evidence for grain size reduction.
PP - plane polarized; CP - cross polarized

FIG. 8.16

FIG. 8.15
PP

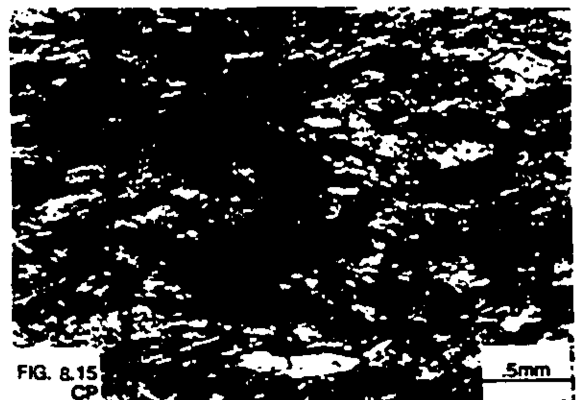

FIG. 8.15
CP

FIG. 8.17

Detail for Fig.8.17

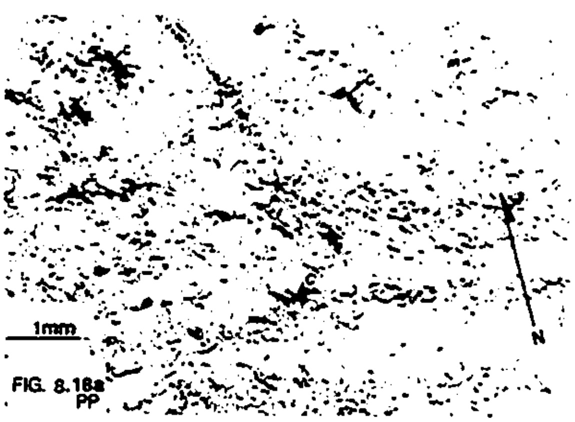

FIG. 8.18a
PP

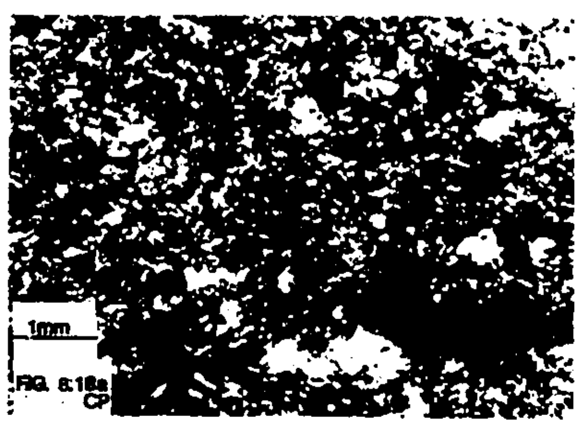

FIG. 8.18a
CP

8.7

STRUCTURES WITHIN THE SLEEPY DRAGON COMPLEX

8.7.1

INTRODUCTION

Rocks of the Sleepy Dragon complex (Henderson, 1985) (Unit 1, Fig. 8.1a) display folds and fabrics close to the volcanics that are similar in orientation to those within the supracrustal rocks, with the exception of the easterly striking S_2 foliation. From limited mapping of the complex within the thesis area, it is not clear whether any structures predate deformation of the supracrustal rocks. Elsewhere, structures trending northeast to eastward within gneisses and foliated granite of the Sleepy Dragon complex appear to be truncated by the volcanic belt. (Davidson, 1972; James, 1989) 8.7.2

8.7.2

FOLIATIONS AND MYLONITES

Gneissic foliation (Fig. 8.16) and mylonite zones parallel the north striking contact with the volcanics and are subparallel to the S_{1B} foliation (Fig. 8.16). These foliations are deformed by discontinuous asymmetrical folds that resemble the F_{3A} generation, based on style and northeasterly orientation; they are also deformed by northeasterly trending shear bands locally along the north striking contact between the Sleepy Dragon complex rocks and the metavolcanics (Fig. 8.17). The asymmetry of these structures suggests a component of dextral strike slip movement along the northerly striking foliation during or post D_{3A}.

An east south east trending mylonite zone is developed parallel to the east striking contact between the metavolcanic rocks and the Sleepy Dragon terrain in the southeastern part of the mapped area (Map 2). This mylonite zone varies in width along strike and affects the granitoid rocks in a zone up to 2 meters wide, marked in outcrop by a linear pink to whitish, mm to cm scale, color banding in the rock. The east striking mylonitic foliation is folded locally, giving rise to a north northwesterly striking foliation that is subparallel to S_{3A} (Fig. 2.1).

Mylonites in granitic rocks are formed of 0.5cm to 1cm wide bands, of alternating microcrystalline quartz and larger recrystallized (0.2mm) quartz rich bands. Relatively large feldspar crystals are locally preserved within quartz rich domains. Muscovite, biotite, actinolite, hornblende and locally chlorite are aligned along the mylonitic foliation. (Fig 8.18b, 8.19a and b)

Figure 8.18B Photomicrograph of vertical quartz ribbon lineation in Sleepy Dragon Complex gneissic rocks. Quartz ribbons are polycrystalline with intergrain serrate margins. Muscovite, actinolite and chlorite are aligned parallel to lineation. Sample from the area of the east striking contact between the Sleepy Dragon Complex and the metavolcanic rocks.
PP - plane polarized; CP - cross polarized

Figure 8.19A Photomicrograph of mylonitized Sleepy Dragon Complex granitoid rock. Horizontal sections through amphibole (hornblende) indicate a strong down dip preferred alignment of long axes. Sample from the central part of the Sleepy Dragon Complex near the metavolcanic contact.
PP - plane polarized; CP - cross polarized

Figure 8.19B Photomicrograph of mylonitized Sleepy Dragon Complex granitoid rock. Fine grained quartz on left side of photo suggests grain size reduction. Amphibole (hornblende) and biotite lie parallel to a vertical lineation. Sample from central part of the north striking contact between Sleepy Dragon Complex gneissic rocks and the metavolcanic rocks.
PP - plane polarized; CP - cross polarized

Figure 8.20A and B Photograph of polished granite slab taken from the contact between the granite and the metavolcanic rocks in the northern part of the map area. 8.20A shows subvertical lineation defined by quartz ribbons and some feldspar. 8.20B shows a section perpendicular to the lineation illustrating a weak foliation in an otherwise undeformed rock.

FIG. 8.18b .5mm
PP

FIG. 8.19a .5mm
PP

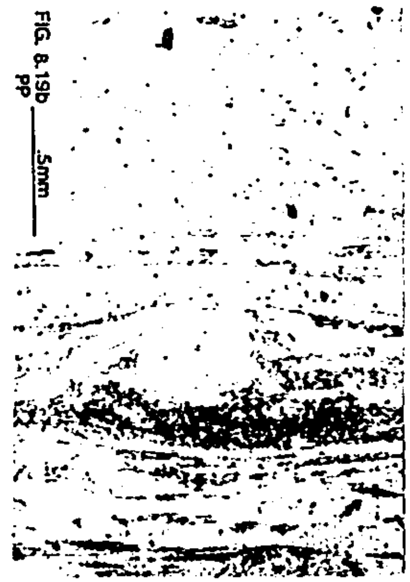

FIG. 8.19b .5mm
PP

2cm

FIG. 8.20a

FIG. 8.18b .5mm
CP

FIG. .19a .5mm
CP

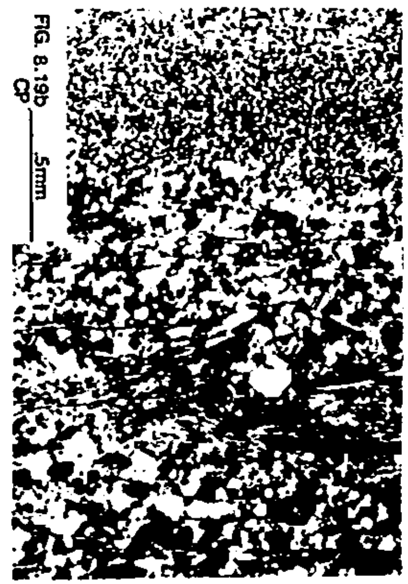

FIG. 8.19b .5mm
CP

2cm

FIG. 8.20b

8.7.3

LINEATIONS

Mineral lineations, defined by quartz ribbons and amphibole (Fig. 8.19b), plunge steeply west to northwest along both north striking and east striking contacts. The lineations generally lie in the plane of the contact parallel foliation, especially where the contact strikes northward, parallel to S_{1a} in the metavolcanics (Map 2).

8.8

STRUCTURES WITHIN THE NORTHERN GRANITE.

The contact between the Cameron River volcanic rocks and the northern granite is visible for short distances in at least three places. Traverses across the volcanic belt and into the granitic terrain, in the northern part of the map area, revealed an intrusive contact with the volcanic rocks resting on the granite. The contact is well exposed on an east sloping exposure north of the elbow region (Fig. 4.2) in the southern part of the northwest striking contact in domain D. The contact is sharp and dips westerly.

Near the contact, a contact parallel, west dipping fabric within the granite is formed in part by the alignment of elongate mineral grains steeply down dip (Fig. 8.20a and b). At a distance of 200m east of the contact, no obvious foliations or lineations were seen within the granitic rocks. Numerous meter scale inclusions of mafic volcanic rocks within the granite preserve foliations parallel to S_{1A}, S_{3A} and S_{3B}, suggesting they represent xenoliths of the supracrustal metavolcanic rocks engulfed by the granite.

The structural relations suggest that the northern granite arrived at it's present level late in the structural history of the area. The contact parallel foliation in the granitic rocks could be related to the emplacement of the granite ("Onion skin fabric"; Fyson and Helmstaedt, 1988) or it may be related to movement of the volcanics downward relative to the granite, by late stage ductile normal faulting (James, 1989).

Chapter 9

Summary and Speculations

9.1

STRUCTURAL GEOLOGY

Narrow belts of predominantly mafic volcanic rock within the Slave Province, exhibit a variety of shapes in map pattern (Fig 1.2). Some belts with rectilinear segments exhibit abrupt changes in trend (Cameron River, Courageous Lake, Takiyuak and other belts). These belts are generally bounded by granite, either intrusive or basement, on one side, and metasedimentary supracrustal rocks on the other.

This study of the Fenton Lake portion of the Cameron River belt where it changes from a northeasterly to northwesterly trend has documented an arrangement of structures that must be accounted for in explanations for the map pattern. Most notable is an early phase foliation (S_1) associated with flattening of pillow structures that changes trend abruptly across a "fabric front", the boundary between structural domains B and D and is cross cut by a similar foliation in domain C (Fig. 8.1A).

A fabric front may also be present south of Fenton Lake where the volcanic belt changes trend from NW - SE (Fig 1.3. Fyson, pers. comm., 1989) The arrangement could have developed as follows.

Volcanics along the western margin of the

Sleepy Dragon Complex were tilted at an early stage of horizontal compression into homoclines facing away from the complex. Continued subhorizontal compressive stresses subsequently imposed steep S_1 flattening fabrics on the inclined volcanics which were further rotated into steep orientations. F_1 folds formed in the sedimentary rocks marginal to the volcanics. Steep stretch lineations in the volcanics and in mylonites, which are present in the basal contact zone and within adjacent gneiss of the Sleepy Dragon Complex, indicate subvertical extension. Additionally, shear bands within mylonite, which indicate a component of N - S oriented dextral slip along part of the contact zone, show that the movement picture within the zone was complex. The S_1 foliations appear to have formed sequentially in northeasterly, northwesterly and northerly directions, each of which conforms to the contacts with bounding granitic rocks. It is suggested that the abrupt changes in trend of these contacts reflect junctions of crustal fractures. The volcanics were rotated and steepened by upthrusting along these fractures, and by compression across them. The fractures acted sequentially as stress guides, hence the sequence of S_{1A} and S_{1B} foliations. During folding of the metasediments, the 'corner' between the northeast and northwest trending volcanic homoclines provided a reentrant into which the folds were moulded against the homocline.

9.2

METAMORPHISM

Metamorphic grade in the area increases with proximity to the northern granite. Although tectonic mineral foliations provide evidence of a dynamic type of regional metamorphism, growth of apparently unstrained poikiloblastic biotite, cordierite and garnet indicate low strains during peak temperature periods, at about the time the granitic bodies were emplaced.

The kilometer scale width of the metamorphic halo associated with the granite is too large to be explained by contact metamorphism whose effects are rarely apparent more than 500 meters from hot contacts (Ralph Kretz, pers. comm., 1988). Thermal doming, suggested by Thompson (1978), whereby large areas of the upper crust are brought under the influence of high temperatures by upward arching of normally surface parallel isotherms could explain the metamorphic pattern described. Peak temperatures at the time of metamorphism are estimated from the partitioning of Fe and Mg between biotite and garnet, based on the experiments of Ferry and Spear (1978) and Hodges and Spear (1982). The range of temperatures appears to be from 300c at which point the first spessartine garnets began to grow, to 570c at the peak of metamorphism, in rocks approximately 1 km. from the granite volcanic contact. The presence of high grade amphibole and pyroxene minerals within 100 meters of the contact suggests that temperatures in the actual contact aureole may have been in excess of 600c.

Chapter 10

SUGGESTIONS FOR FURTHER WORK

10.1

FIELD WORK

More detailed mapping of the metavolcanic terrain to delineate the contacts between lithological units, especially those between the interflow sediments and the metavolcanics, would have greatly improved this field study. The possibility that an intervolcanic sedimentary unit was continuous around the bend of the Fenton Elbow became apparent during compilation of the map. The unit is usually deeply weathered and lack of outcrop in key areas will probably hamper efforts to find its true extent. However, geophysical gravity or magnetic surveys may reveal contrasts with the enclosing volcanic rocks.

More detailed mapping will also delineate the extent of felsic volcanic rocks within the northwest trending arm of the metavolcanics. Outcrop evidence suggests that the rocks are of limited extent, but associated gossans indicate they could be of economic importance.

Sampling within the metavolcanic rocks to better define the metamorphic aureole around the northern granite should be systematic and encompass traverses toward the granite as well as parallel to its margin. Sampling within one volcanic type (i.e. pillowed rocks) throughout the succession would probably best serve the purpose of detecting changes in mineralogy.

The area is being examined for its gold deposit potential at present (1989, 90). Locally anomalous magnetic values, numerous iron alteration zones of small areal extent within the metavolcanic rocks, rusty weathered and probably iron rich zones along both the upper and lower contacts of the metavolcanic rocks suggest the possibility of mineralization which should be further investigated.

Recent discoveries of sedimentary and ultramafic rocks in the contact zone between the Sleepy Dragon gneiss complex and the metavolcanic rocks (Kusky, 1987), have suggested that the metavolcanic belts may include ophiolities (Hoffman, 1986, Kusky, 1986, 1987). Sense of shear along the contact and the possibility of thrusting between the two units (1 and 2) needs further study.

Further mapping within the metasedimentary rocks would serve to better determine the range of depositional environments and help determine the provenance of the sediments. The possibility indicated by fine grained rocks of a quiescent environment of deposition along the metavolcanic metasediment contact should be further investigated.

10.2

Lab Work

This study began limited work on geothermometry for biotite garnet pairs from metavolcanic and inter-volcanic sedimentary rocks, a study which gave interesting results. Microprobe analysis of similar pairs for a wider area would certainly help to complete the picture of metamorphism. Geobarometry was not attempted, but the possibility for successful work is suggested by good constraints on pressures indicated by the coexistence of cordierite, garnet and plagioclase.

REFERENCES

Baragar, W.R.A.

1966: Geochemistry of the Yellowknife volcanic rocks., Can. J. Earth Sci., 3, p. 9-30.

Borradaile, G.J.

1982: Tectonically deformed pillow lava as an indicator of bedding and way up. Can J. Earth Sci., , p. 469-480.

Borradaile, G.J. and Poulsen, K.H.

1981: Tectonic deformation of pillow lava. Tectonophysics, 79, p.17-26.

Bouma, A.H.

1952: Sedimentology of some flysch deposits: Amsterdam, Elsevier, 169p.

Cowley, P., Pollock, T., Cullen, R., Ord, R. and Fournier, J.

1988: Longspur Property 1987 and 1988 Geological, Geochemical and Geophysical Report. DIAND assessment report, NTS85 P/2, 3 and 85 I/15.

Cressey, G., Schmidt,R. and Wood, B.J.
1978: Thermodynamic properties of almandine -grossular garnet solid solutions. Cont. Min. Pet., 67. p.397-404

Davidson, A.
1972: Granite studies in the Slave Province. Geol. Surv. Can., Paper 72-1A, p.109-115.

Deer, W.A., Howie, R.A., Zussman, J.
1980: An introduction to the rock forming minerals; Longman Group Ltd., London, 528p.

Ferry, J.M. and Spear, F.S.
1978: Experimental calibration of the partitioning of Fe and Mg between biotite and garnet; Cont. to Min. and Pet., vol. 66, p. 113-117.

Fortier, Y. O.
1946: Yellowknife - Beaulieu region, Northwest Territories. Geol. Surv. Can., Prelim. Ser. Map 46-23

1947: Ross Lake map area, Northwest Territories. Geol. Surv. Can., Paper 47-16.

Fyson, W.K.

1975: Fabrics and deformation of Archean metasedimentary rocks, Ross Lake - Gordon lake area, Slave Province Northwest Territories. Can. J. Earth Sci., 12, p.765-776.

1980a: Fold fabrics and emplacement of an Archean granitoid pluton, Cleft Lake, Northwest Territories. Can. J. Earth Sci., 17, p.325-332.

1981: Divergent fold overturning and regional tectonics, southern Slave Province, Northwest Territories. Precambrian Research, 14, p.107-118.

1982: Complex evolution of folds and cleavages in Archean rocks, Yellowknife, N.W.T. Can. J. Earth Sci.,19, p.878-893.

1984a: Fold and cleavage patterns in Archean metasediments of the Yellowknife supracrustal domain, Slave Province, Canada. <u>In</u> Precambrian Tectonics Illustrated. A. Kroner ed., Elsevier, Amsterdam, pp. 281-293.

1984b: Basement -controlled structural fronts forming an apparent major refold pattern in the Yellowknife domain, Slave Province. Can J.Earth

Sci.,21, p.822-828

Fyson, W.K. and Helmstaedt, H.

1988: Structural patterns and tectonic evolution of supracrustal domains in the Archean Slave province, Canada. Can. J.Earth Sci., 125,no.2, p.301-315

Ganguly, J. and Kennedy, G.C.

1974: The energetics of natural garnet solid solution: I. Mixing of the aluminosilicate endmembers. Cont. Min. Pet., 48, p.137-148.

Helmstaedt, H., Padgham, W. and Brophy, J.A.

1986: Multiple dykes in the Kam Group, Yellowknife greenstone belt. - evidence for Archean sea -floor spreading. Geology, V14. #7, p.562-566

Henderson, J.B.

1972: Sedimentology of Archean turbidites at Yellowknife, Northwest territories: Can. J. Earth Sci., 9, p.882-902

1975b: Sedimentology of the Archean Yellowknife Supergroup at Yellowknife, District of Mackenzie; Geol. Survey of Can., Bull. 246, p. 62

1981: Archean basin evolution in the Slave Province, Canada; in Precambrian Plate Tectonics, A. Kroner ed., Elsevier, Amsterdam, p. 213-235

1985: Geology of the Yellowknife - Hearne Lake area, District of MacKenzie: a segment across an Archean Basin. G.S.C. Memoir 414, 135p. plus map and sections.

Henderson, J.B., Van Breeman, O. and Loveridge, W.D. 1987: Some U - Pb zircon ages from Archean basement, supracrustal and intrusive rocks, Yellowknife -Hearne Lake area, District of Mackenzie; in Radiogenic Age and Isotope Studies; Report 1, Geological Survey of Canada Paper 87-2, p. 11-121.

Henderson, J.F.

1939: Beaulieu River Area, Northwest Territories. Geol. Surv. Can., Paper 39-1, 16p.+ map.

1943: Structure and metamorphism of early Precambrian rocks between Gordon and Great Slave Lakes, Northwest Territories; Amer. J. of Sci., v. 241, p. 430-446.

Hietanen, A.

1967: On the facies series in various types of metamorphism. J. of Geology, vol. 75, 187-214.

Hodges, K.V. Spear, F.S.

1982: Geothermometry, geobarometry and the Al_2SiO_5 triple point at Mt. Moosilauke, New Hampshire; American Mineralogist, vol. 67, p. 1118-1134.

Hoffman, P.

1986: Crustal accretion in a 2.7-2.5 Ga "granite - greenstone" terrane , Slave Province, N.W.T. : A prograding trench - arc system? Geol. Assoc. of Can., Program with Abstracts, p.82.

James, D.T.

1989: Basement - cover relations between the Archean Yellowknife Supergroup and the Sleepy Dragon Complex north of Fenton Lake, District of Mackenzie, N.W.T. in Current Research, Part C, Geological Survey of Canada, Paper 89-1C, p. 29-36, 1989.

Kamineni, D.C. and Cararra, A.

1973: Comparison of the composition of porphyroblastic and fabric forming biotites in two metamorphic rocks; Can. J. Earth Sci., 10, p948-953.

Kretz, R.

1963: Notes on some equilibria in which plagioclase and epidote participate; Am. J. Sci., 261, p973-982.

1968: Study of pegmatite bodies and enclosing rocks, Yellowknife-Bealieu region; Geological Survey of Canada, Bull. 159, 109p.

Kusky, T.M.

1986: Are greenstone belts in the Slave Province N.W.T. allocthonous? in Workshop on Tectonic Evolution of Greenstone Belts. M.J. deWit and L.D. Ashwal eds. Lunar and Planetary Institute Technical Report 86-10, p. 135-139.

1987: Comment on "Multiple dykes in the lower Kam group, Yellowknife greenstone belt; evidence for Archean seafloor spreading", Geology, V15, no.3, p280-282.

1988: Thrusting between the Cameron River Greenstone Belt and the Sleepy Dragon Metamorphic Complex, Slave Province, District of Mackenzie. Contributions to the geology of the Northwest Territories. Indian and Northern Affairs, Canada, 3, p97-102.

1989: Accretion of the Archean Slave province. Geology, v17, p. 63-67.

Laird, J and Albee, A.L.

1981: Pressure, temperature and time indicators in mafic schist: their application to reconstructing the poly metamorphic history of Vermont. Am. J. Sci., 281, p. 127-175

Lambert, M.B.

1977: Anatomy of a greenstone belt - Slave Province, N.W.T., in, Volcanic regimes in Canada, W.R.A. Baragar, L.C. Coleman and J.M. Hall eds., Geol. Assoc. Can. special paper 16, p.331-340.

1988: The Cameron and Bealieu River Volcanic Belts. Geol. Survey of Can., Bulletin 349.

Lowe, D.R.

1982: Sediment gravity flows: II. Depositional models with special reference to the deposits of high-density turbidity currents. J. Sed. Pet., V52, no.1, p.279-297

Moore, J.C.G., Miller, M.L. and Barnes, R.W.,

1951: Carp Lakes, Northwest Territories. Geol. Surv. Can. Paper 51-8, 1 map with marginal notes.

Newton, R.C. and Haselton, H.T.

1981: Thermodynamics of the garnet - plagioclase - Al_2SiO_5 - quartz geobarometer. In R.C. Newton et.al., Eds., Thermodynamics of minerals and melts. p.131-147, Springer - Verlag, New York.

Newton, R.C., Charlu, T.V. and Kleppa, O.J.

1977: Thermochemistry of high pressure garnets and pyroxenes in the system CaO - MgO - Al_2O_3 - SiO_2. Geochemica et Cosmochemica Acta, 41, p.369-377.

Pettijohn, F.J.

1943: Archean Sedimentation; Bull. Geol. Soc. Amer., vol. 54, pp.925-972.

Rambaldi, E.R.

1973: Variation in the composition of plagioclase and epidote in some metamorphic rocks near Bancroft, Ontario; Can. J. Earth Sci.,10, p 852-868.

Ramsay, C.R.

1973a: The origin of biotite in Archean metasediments near Yellowknife, N.W.T. , Canada; Cont. to Mineral. and Petrol., vol. 42. p. 43-54.

1973b: Controls of biotite zone mineral chemistry in Archean metasediments near Yellowknife, N.W.T.; J. of Petrol., vol. 14, p. 467-488.

1974: The cordierite isograd in Archean metasediments near Yellowknife, N.W.T., Canada variations on an experimentally established reaction; Cont. Mineral. and Petrol., vol. 47, p. 27-40.

Ramsay, C.R. and Kamineni, C.

1977: Petrology and evolution of an Archean metamorphic aureole in the Slave craton, Canada; J. of Petrol., vol. 18, p. 460-486.

Starkey, John

1976: The contouring of spherical data represented in spherical projection; Can. J. Earth Sci., vol. 14, p. 268-277.

Studemeister, P.A.

1983: The greenschist facies of an Archean assemblage near Wawa, Ontario; Can. J. Earth Sci., vol. 20, p. 1409-1420.

Thompson, P.H.

1978: Archean regional metamorphism in the Slave structural province - a new perspective of some very old rocks; in Metamorphism in the Canadian Shield, ed. J.A. Fraser and W.W. Heywood; Geological Survey of Canada, Paper 78-10, p.85-102.

Turner, F.J.

1981: Metamorphic petrology; McGraw - Hill, New York, 403p.

Walker, R.G.

1976: Facies models 2. Turbidites and associated coarse clastic deposits. Geosci. Can., V3, no.1, p.25-36.

1978: A critical appraisal of Archean basin -craton complexes; Can. J. Earth Sci., 15, p.1213-1218

Winkler, H. G. F.

1979: Petrogenesis of metamorphic rocks; Springer Verlag, New York, 348p.

APPENDIX 1: MICROPROBE RESULTS

AMPHIBOLE analyses results

Location	1	2	3	4	5	6	7	8	9	10	11
Sample #	85/73-1	85/70-1	86/26	85/94	85/43	85/90-1	85/88-1	85/100	85/46	85/45	85/30-1
SiO2	42.51	45.44	43.75	N/D	41.13	43.27	43.11	45.06	40.39	46.38	46.71
Al2O3	11.02	8.51	12.45	N/D	16.65	13.34	13.31	10.77	17.41	10.57	9.9
TiO2	0.64	0.57	0.54	N/D	0.42	0.35	0.36	0.32	0.1	0.27	0.33
Cr2O3	0.08	0.08	0.07	N/D	0.64	0.16	0.08	0.1	0.08	0.12	0.2
Fe2O3	2.57	3.03	3.23	N/D	4.19	6.82	4.09	4.27	5.81	3.48	4.5
FeO	19.78	19.73	18.73	N/D	13.37	16.53	16.69	16.24	18.06	13.89	12.54
MnO	0.48	0.59	0.63	N/D	0.18	0.68	0.3	0.41	0.69	0.26	0.34
MgO	6.75	7.44	5.38	N/D	7.95	5.63	7.35	8.44	3.55	10.29	10.89
CaO	11.99	12.02	11.57	N/D	11.39	10.9	11.53	12.08	10.91	12.06	11.85
Na2O	1.08	1.02	1.35	N/D	1.95	0.76	1.64	0.93	1.18	1.04	0.98
K2O	1.32	0.5	0.6	N/D	0.31	0.47	0.38	0.22	0.52	0.16	0.21
Total	98.22	98.93	98.3		98.18	98.91	98.84	98.84	98.7	98.52	98.45

GARNET analyses results

Location	3	4	9
Sample #	86/26	85/94	85/46
SiO2	N/A	N/A	36.84
Al2O3	N/A	N/A	20.44
TiO2	N/A	N/A	0.04
Cr2O3	N/A	N/A	1.18
Fe2O3	N/A	N/A	0.03
FeO	N/A	N/A	0.85
MnO	N/A	N/A	28.96
MgO	N/A	N/A	6.91
CaO	N/A	N/A	5.11
Na2O	N/A	N/A	0.03
K2O	N/A	N/A	
			100.39

BIOTITE analyses results

Location	3	4	9
Sample #	86/26	85/94	85/46
SiO2	N/A	N/A	34.53
Al2O3	N/A	N/A	17.1
TiO2	N/A	N/A	0.75
Fe2O3	N/A	N/A	0
FeO	N/A	N/A	26.22
MnO	N/A	N/A	0.2
MgO	N/A	N/A	7.72
CaO	N/A	N/A	0.04
Na2O	N/A	N/A	0.26
K2O	N/A	N/A	9.12
			95.94

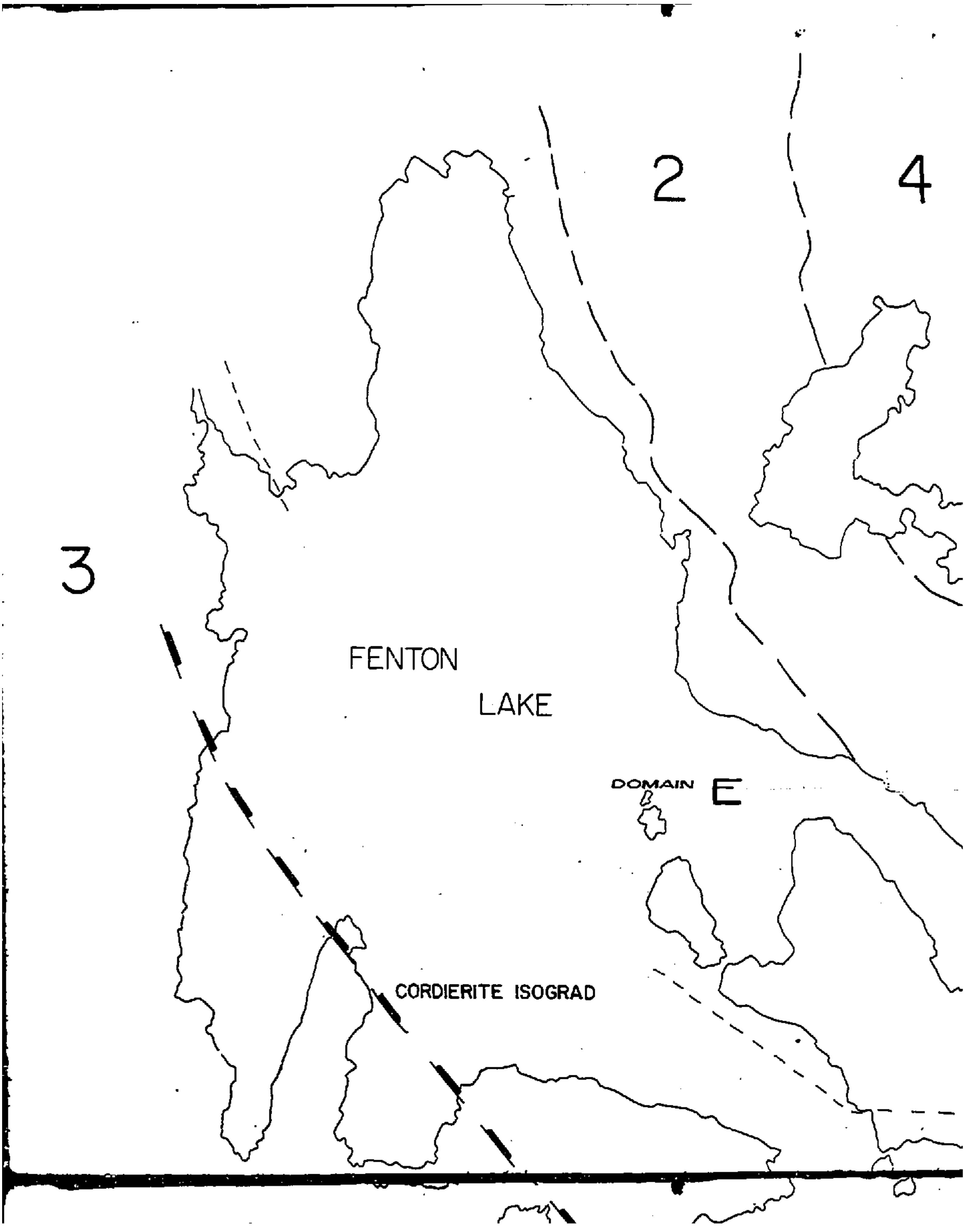
2
4
3
FENTON
LAKE
DOMAIN
E
CORDIERITE ISOGRAD

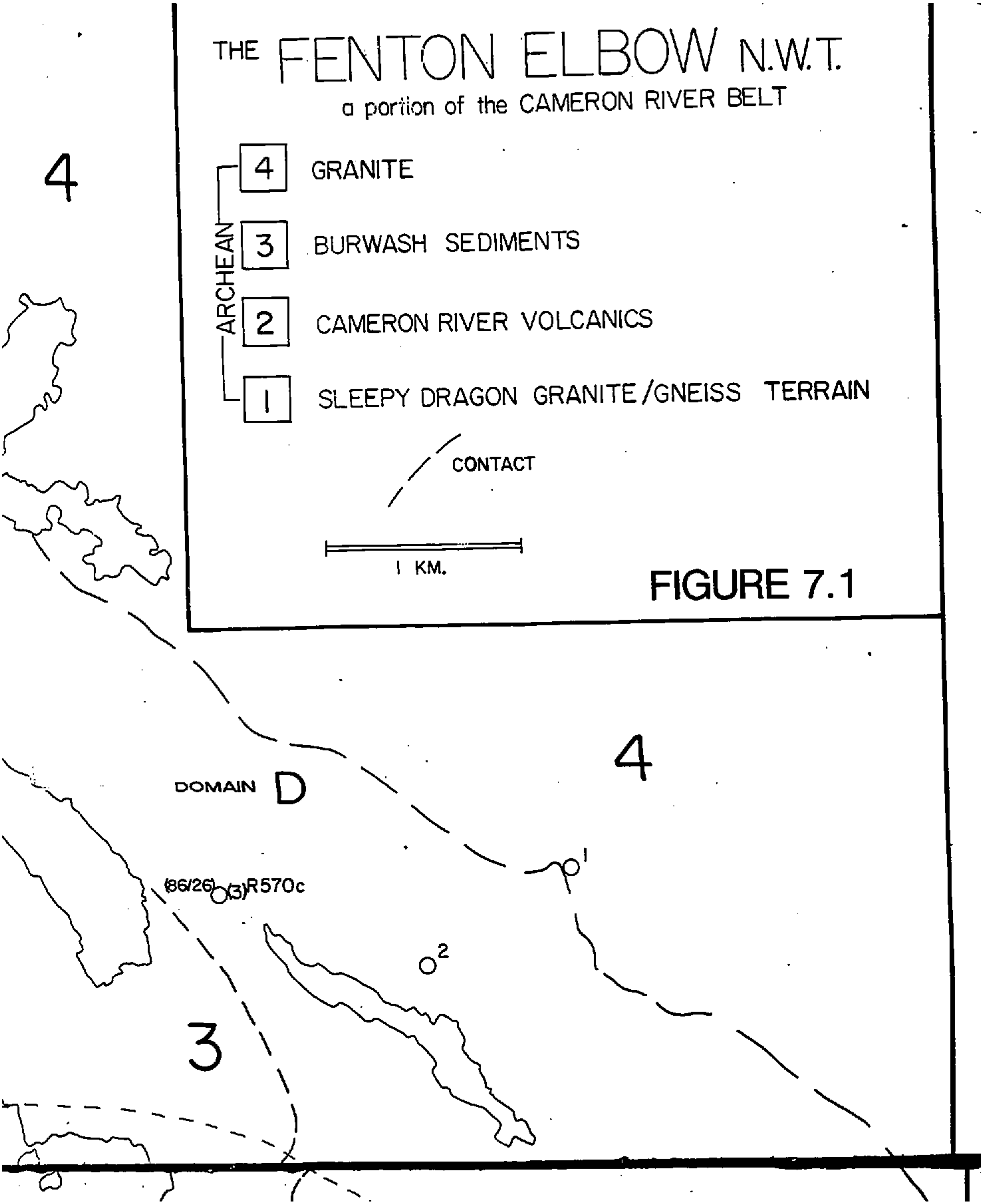
THE FENTON ELBOW N.W.T.
a portion of the CAMERON RIVER BELT
ARCHEAN
4 GRANITE
3 BURWASH SEDIMENTS
2 CAMERON RIVER VOLCANICS
1 SLEEPY DRAGON GRANITE/GNEISS TERRAIN
CONTACT
1 KM.
FIGURE 7.1
4
4
DOMAIN D
(86/26)
(3)R570c
1
2
3

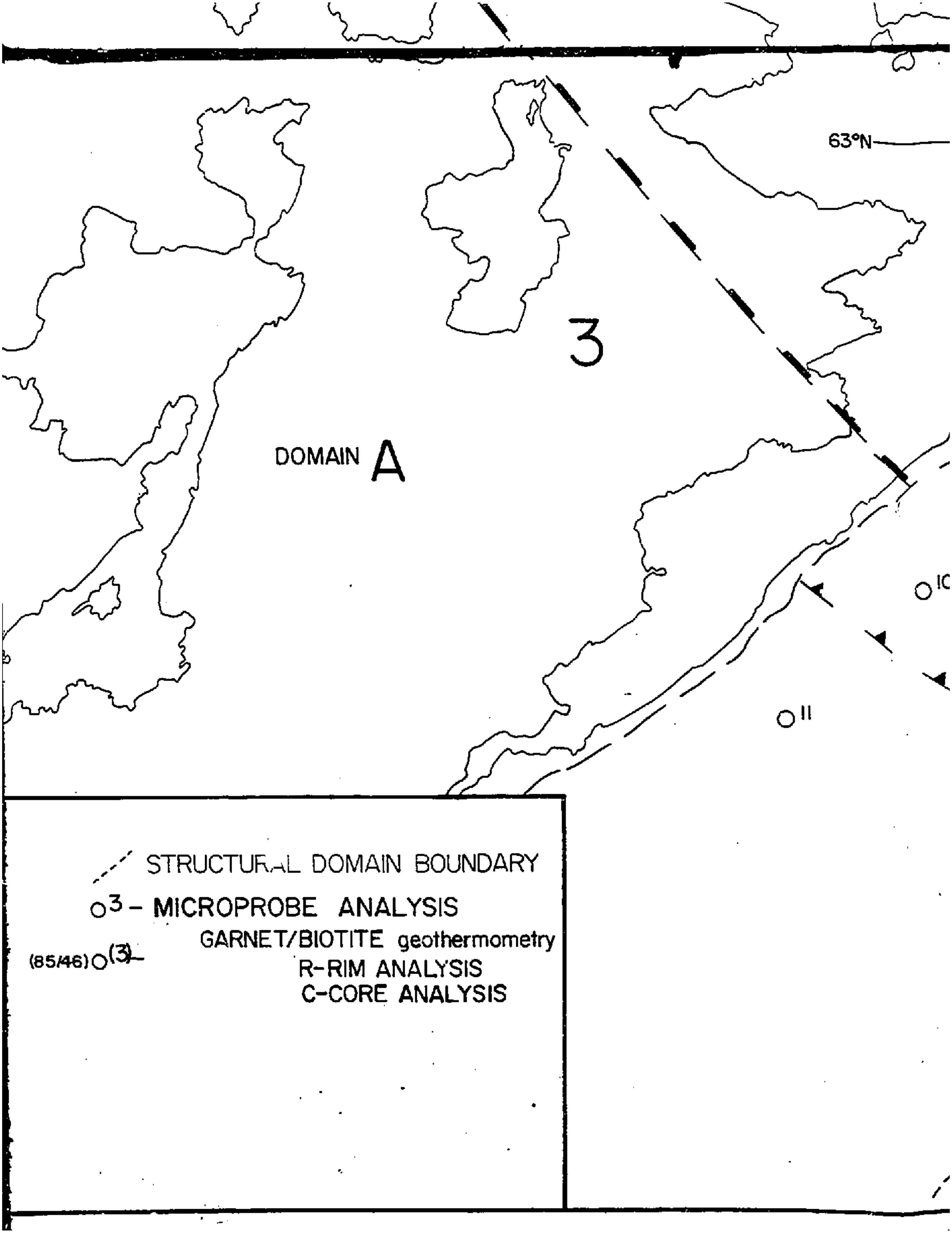
63°N
3
DOMAIN A
11
STRUCTURAL DOMAIN BOUNDARY
3 - MICROPROBE ANALYSIS
GARNET/BIOTITE geothermometry
(85/46) (3)
R-RIM ANALYSIS
C-CORE ANALYSIS

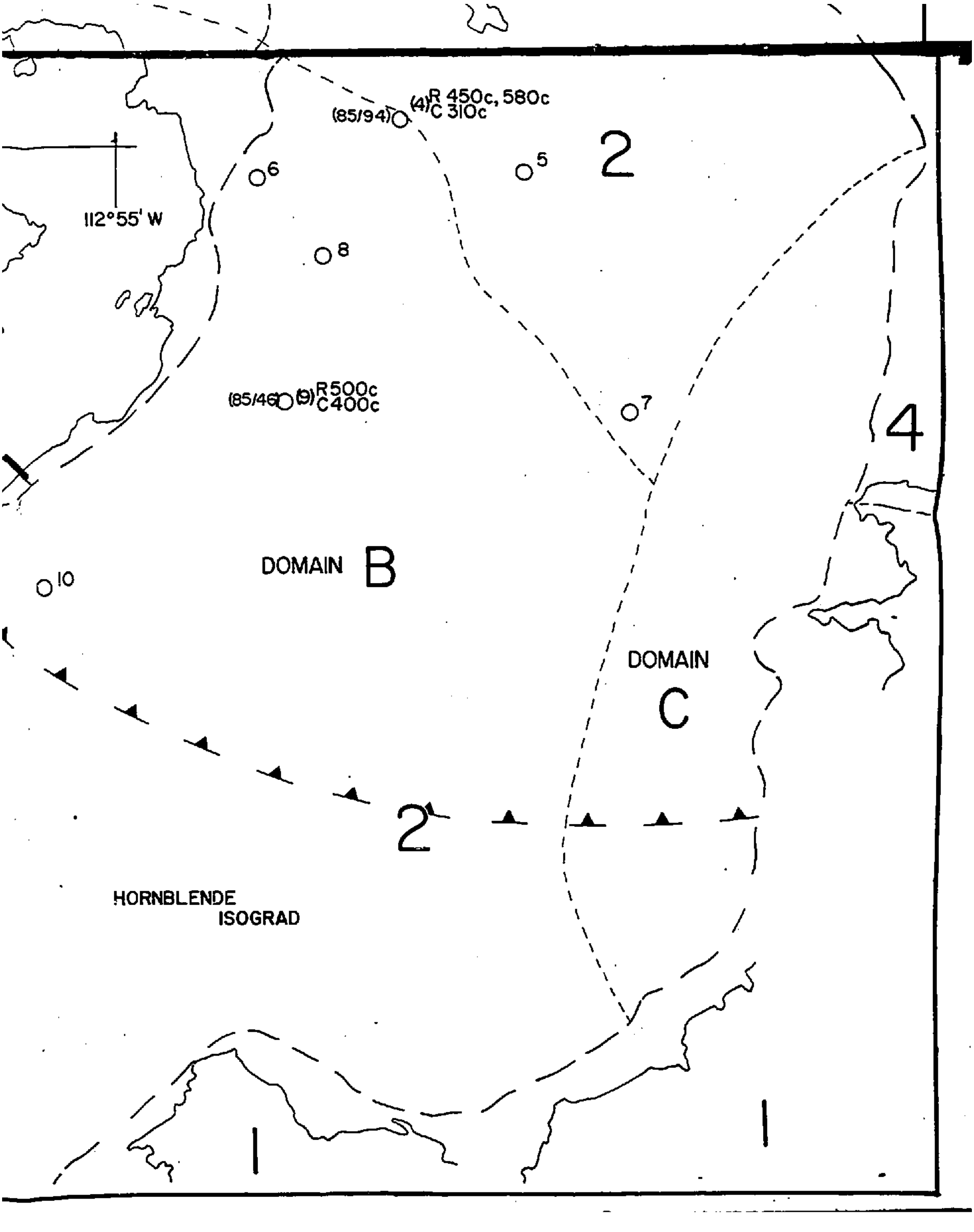

R 450c, 580c
(4) C 310c
(85/94)
2
6
5
112°55' W
8
(85/46) (9) R500c
C400c
7
4
DOMAIN B
10
DOMAIN
C
2
HORNBLENDE
ISOGRAD
1
1

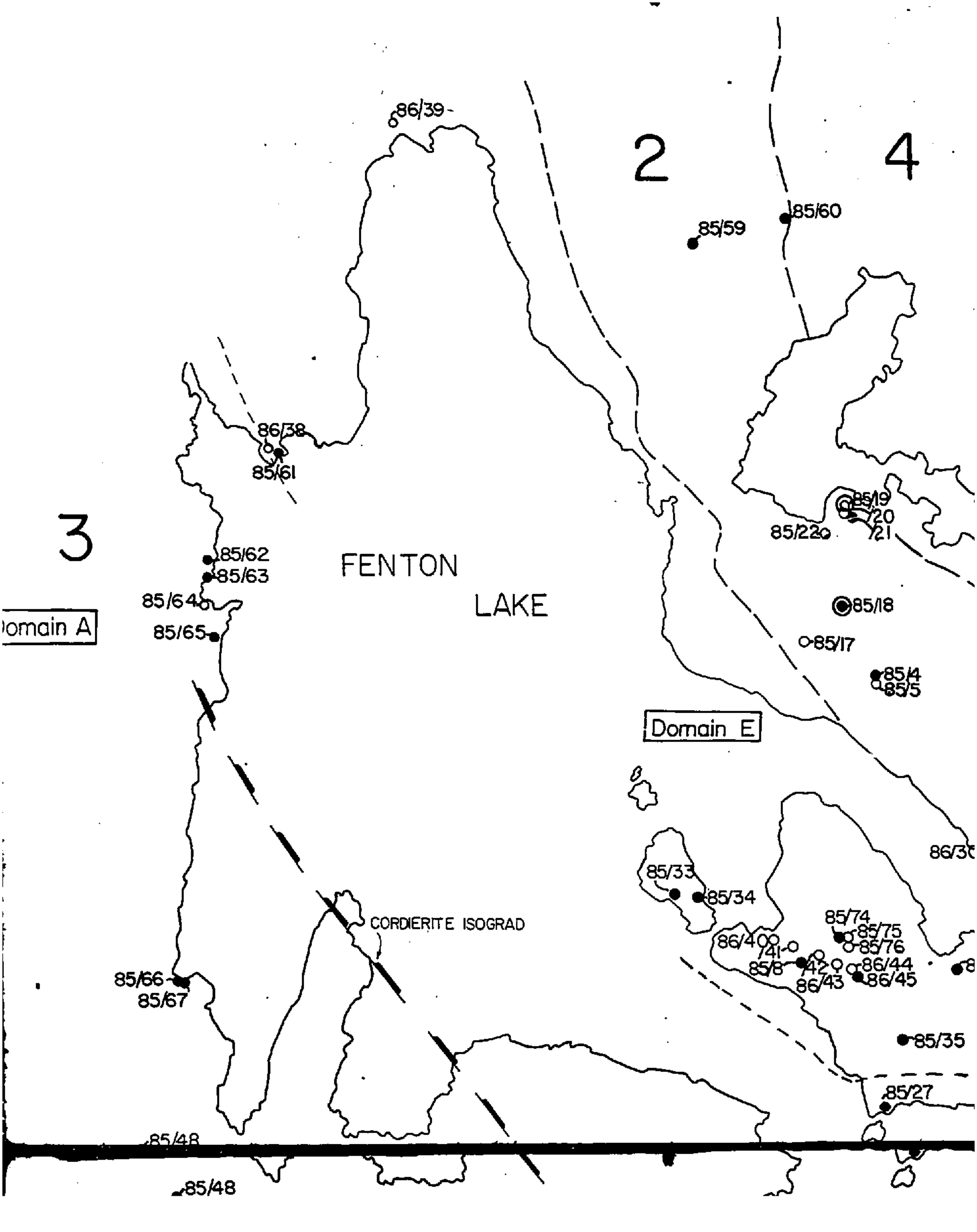
86/39
2
4
85/59
85/60
86/38
85/61
3
85/62
85/63
85/64
85/65
Domain A
FENTON
LAKE
85/19
/20
/21
85/22
85/18
85/17
85/4
85/5
Domain E
86/30
85/33
85/34
CORDIERITE ISOGRAD
85/74
85/75
85/76
86/40
/41
85/8
/42
86/43
86/44
86/45
85/66
85/67
85/35
85/27
85/48
85/48

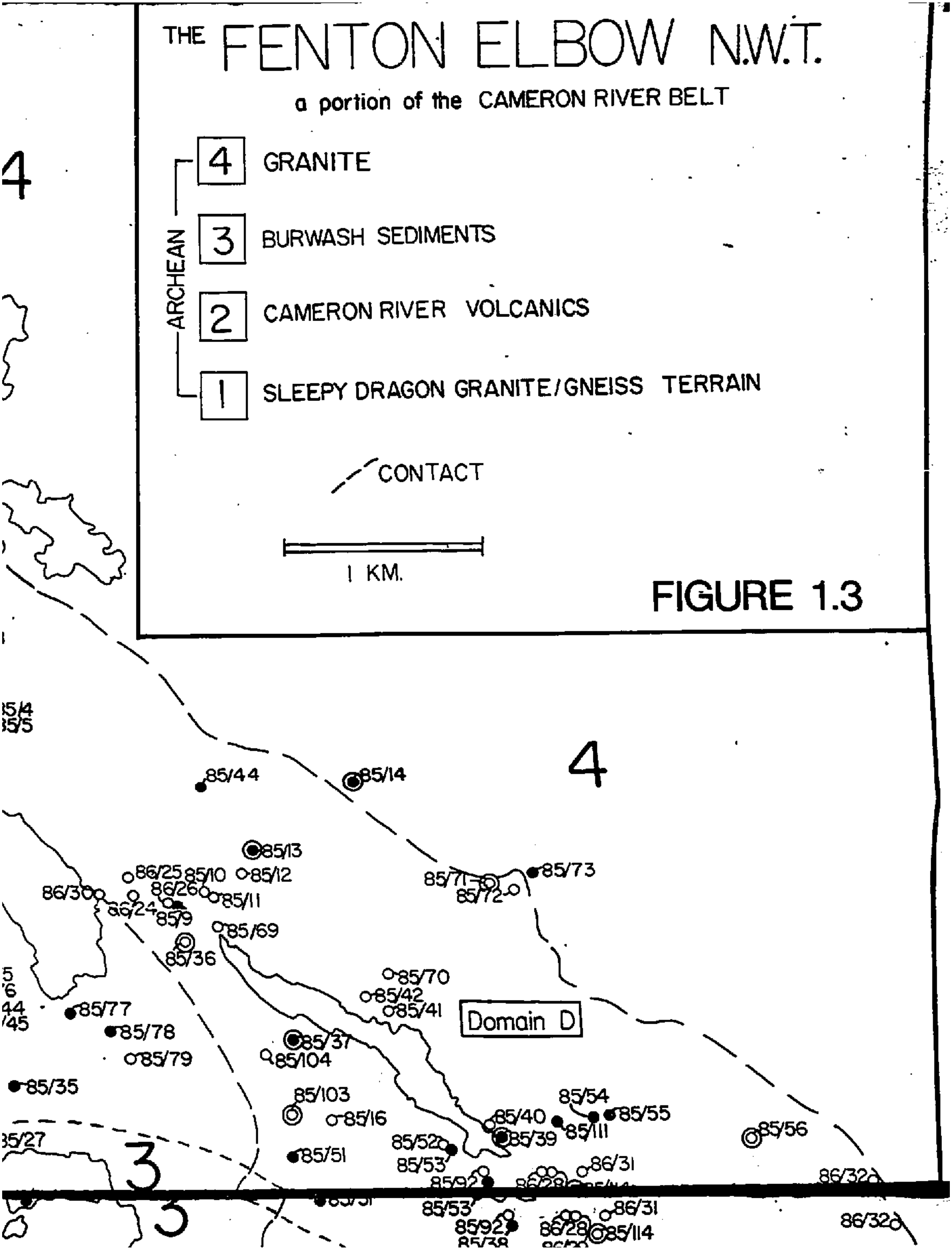
THE FENTON ELBOW N.W.T.
a portion of the CAMERON RIVER BELT
ARCHEAN
4 GRANITE
3 BURWASH SEDIMENTS
2 CAMERON RIVER VOLCANICS
1 SLEEPY DRAGON GRANITE/GNEISS TERRAIN
CONTACT
1 KM.
4
4
3
Domain D
85/44
85/14
85/13
86/25
85/10
85/12
86/30
86/26
85/11
86/24
85/9
85/69
85/36
85/71
85/72
85/73
85/70
85/42
85/41
85/77
85/78
85/79
85/37
85/104
85/35
85/103
85/16
85/51
85/54
85/55
85/40
85/39
85/111
85/52
85/53
85/56
86/31
85/92
86/28
86/32
85/114
85/27

FIGURE 1.3

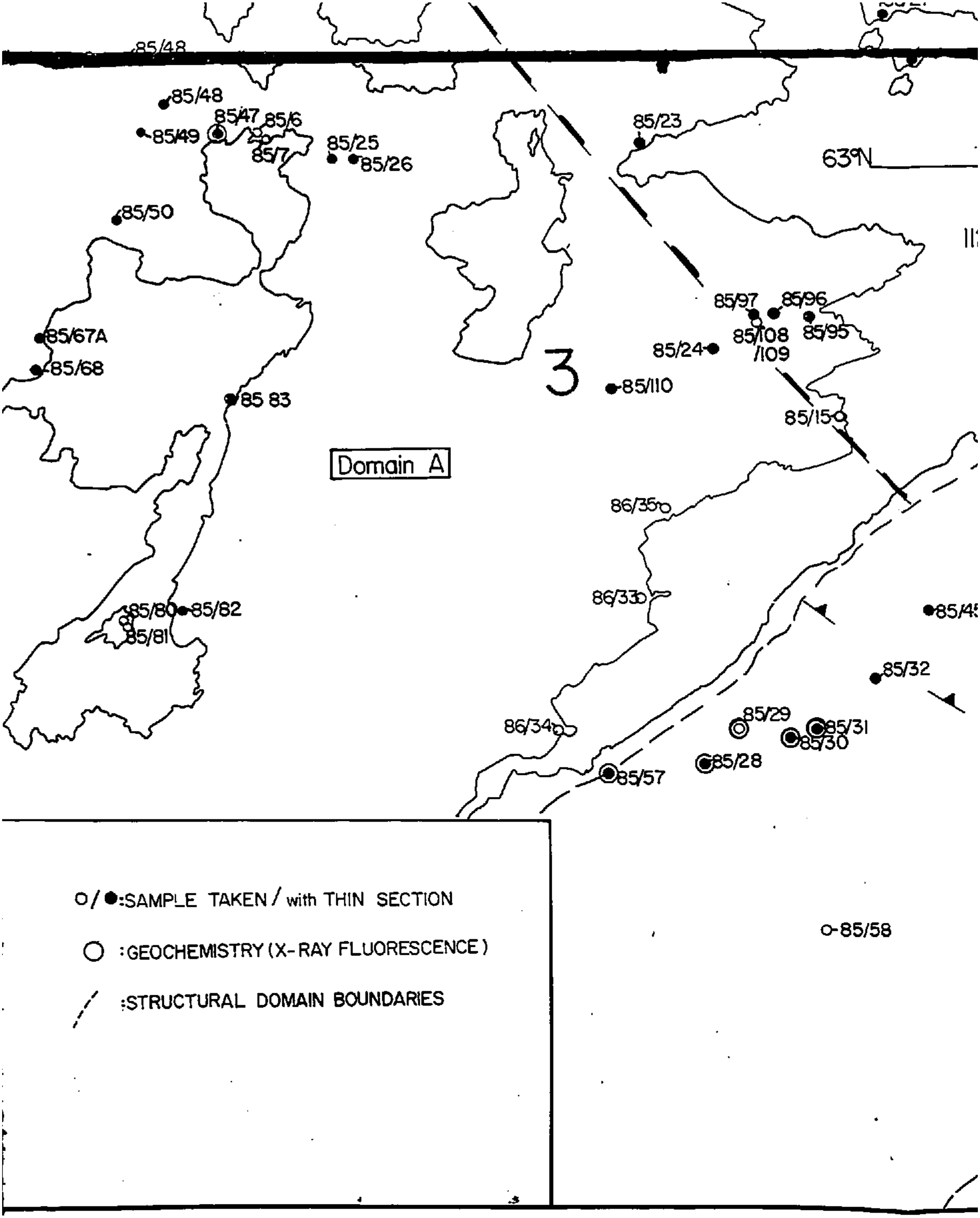

85/48
85/47
85/6
85/49
85/7
85/25
85/26
85/50
85/23
63°N
85/97
85/96
85/108
/109
85/95
85/24
3
85/110
85/67A
85/68
85 83
Domain A
85/15
86/35
86/33
85/80
85/82
85/81
85/32
85/29
85/31
85/30
86/34
85/28
85/57
85/58
o/●:SAMPLE TAKEN / with THIN SECTION
○ :GEOCHEMISTRY (X-RAY FLUORESCENCE)
:STRUCTURAL DOMAIN BOUNDARIES

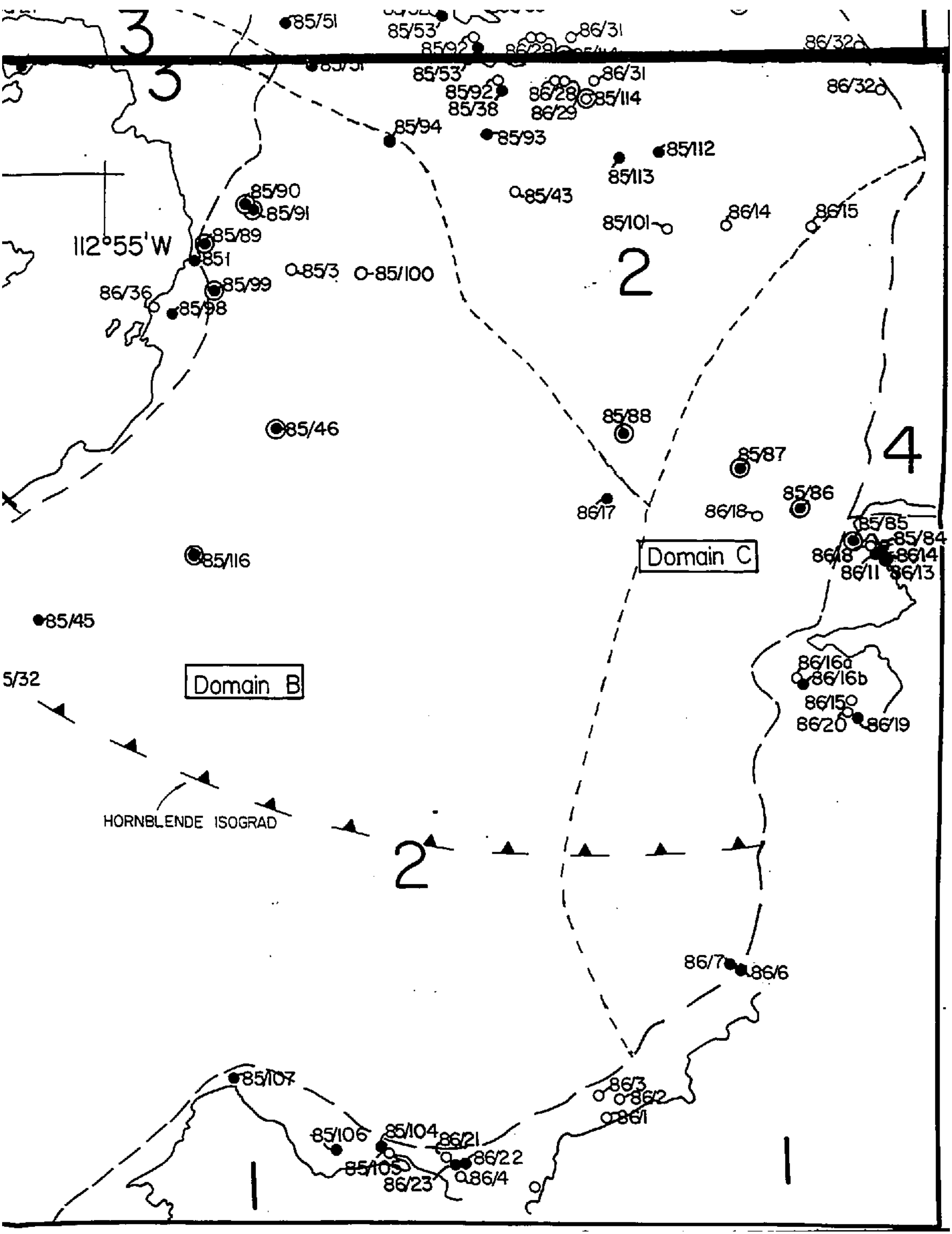

3
85/51
85/53
85/92
86/28
86/31
86/32
86/29
85/114
85/38
85/94
85/93
85/112
85/113
85/90
85/91
85/43
85/101
86/14
86/15
112°55'W
85/89
851
85/3
85/100
2
86/36
85/99
85/98
85/46
85/88
85/87
4
85/86
86/17
86/18
85/85
85/84
Domain C
86/8
86/14
86/11
86/13
85/116
85/45
86/16a
86/16b
86/15
86/20
86/19
5/32
Domain B
HORNBLENDE ISOGRAD
2
86/7
86/6
85/107
86/3
86/2
86/1
85/106
85/104
86/21
86/22
85/105
86/23
86/4

Geology and

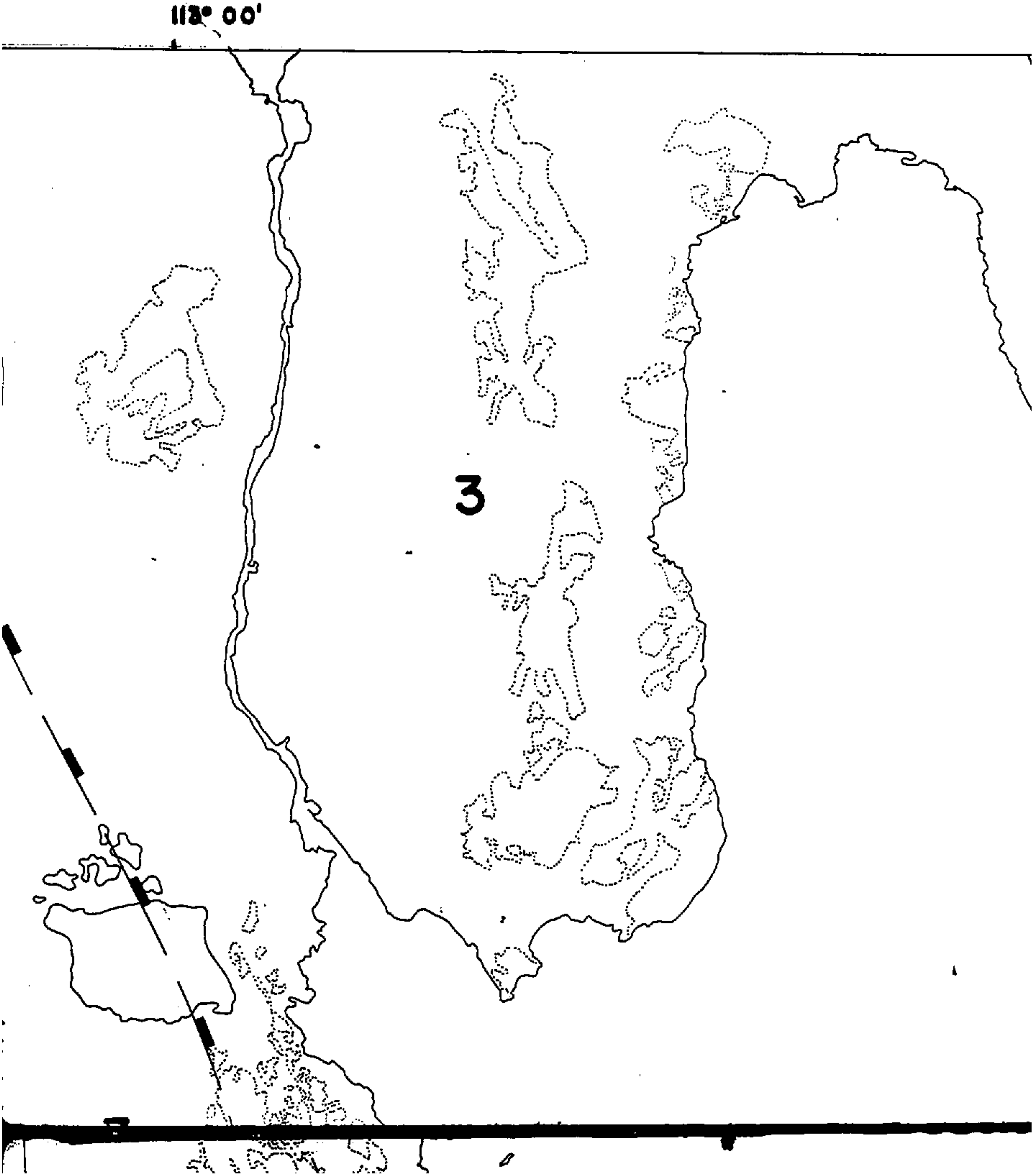

nd Structure of the Cameron

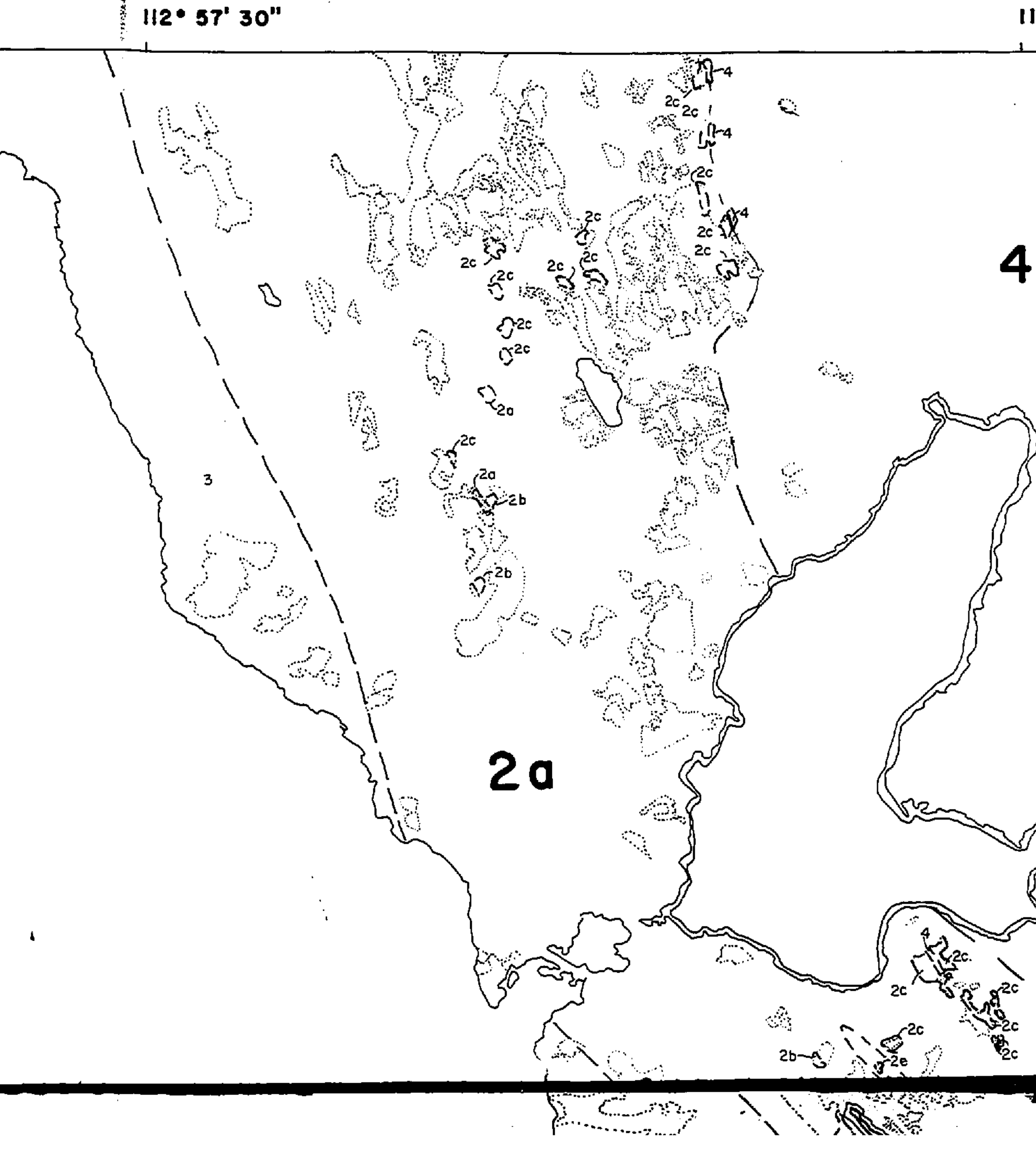

iver Belt, Fenton Lake Area

55'

112° 52' 30"

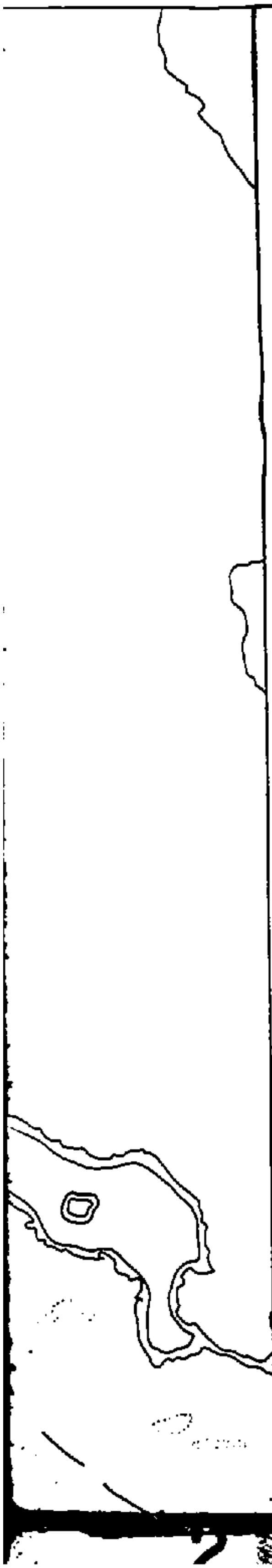

LEGEND FOR LITHOLOGICAL MAP

PROTEROZOIC

5 Dogrib Dykes - coarse gabbro

4 Morose Granite - (muscovite, biotite, quartz, feldspar) granitic and pegmatitic dykes related to the Morose intrusion

ARCHEAN

CAMERON RIVER VOLCANIC BELT

3 Turbidites, coarse sandstones, siltstones, mudstones, a) Conglomerate

2f Carbonate - includes calc - silicate

2e Rhyolite - includes quartz feldspar porphyry quartz porphyry, aphanitic rhyolite

2d Interflow sediments - in part garnetiferous

2c Medium grained amphibolite (metabasalt or gabbro dyke)

2b Pillow breccia and volcaniclastics

2a Pillow basalts

1b Amphibolite dykes in Sleepy Dragon Granitic rocks

1a Sleepy Dragon Basement Complex: granite, granodiorite, granitic gneiss, mylonite

Cordierite Isograd

Hornblende Isograd

G Garnet

g Gossan

M Magnetic

Contact: defined, approximate

Outcrop mapped

Outcrop from airphotos

Xpy Mineral occurrence py-pyrite, po-pyrrhotite, cp-chalcopyrite

SCALE 1:10,000

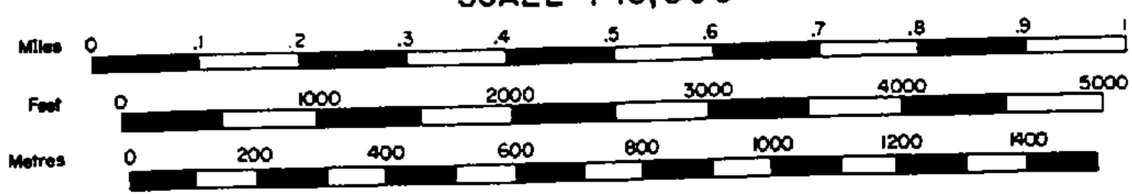

rea; parts of NTS 85 I/15, P

30"

112° 50'

GENERAL GEOLOGY

The Fenton ... area within the Archean Slave Structural Province is underlain by four major rock units as well as mafic and felsic dykes of minor extent.

(1) **Sleepy Dragon Complex**: mainly granitic and gneissic rocks, that occupy the southeastern part of the map area; was interpreted as basement to adjacent volcanic rocks (Davidson, 1972; Henderson, 1981, 1985; Lambert, 1977).

(2) **Cameron River Volcanic Belt**: a predominantly basaltic volcanic pile of pillowed and massive flows with intercalated breccias, volcaniclastics and minor felsic tuffs and sediments.

(3) **Burwash Formation metasediments**: graded coarse to fine, (metagreywacke and argillaceous beds) stratigraphically above and west of the volcanics.

(4) **Morose Granite**: a granitic pluton and dykes (4b) intrude units 1 and 2 in the northeastern part of the map area.

(5) **Dogrib Dykes**: a few gabbroic dykes of the Proterozoic Dogrib swarm trend northeasterly across units 1, 3 and probably 2 and 4.

LITHOLOGY AND STRATIGRAPHIC RELATIONS:

The Sleepy Dragon Complex (1) includes medium grained K-feldspar and plagioclase granitoids with local strongly foliated and mylonitized zones. Amphibolitic dykes (1b) within the complex have been interpreted as feeders to the adjacent volcanic rocks, suggesting that the complex is part of an older basement (Baragar, 1966; Lambert, 1977). Contact relations; however, are obscured by deformation and no dyke has been traced from the complex into the volcanics. An apparent truncation of a strong gneissic fabric in the complex by relatively undeformed volcanic rocks has suggested an unconformable relationship (Davidson, 1972; Henderson, 1985), but tectonic juxtaposition is possible (Kusky, 1985a,b).

The Cameron River Volcanic Belt (2) is composed predominantly of basaltic pillowed flows (2a), massive flows and dykes (2c) and breccias composed mainly of volcanic cataclasts (2b). The dykes within the volcanic pile may be crosscutting or layer parallel and may in part be feeders to the volcanic extrusive rocks. Coarse unfoliated gabbro dykes (2), of uncertain extent also cross the metavolcanics.

Within the volcanic pile, 20 - 40 m wide zones of recessively weathered, medium- to coarse-grained, quartz-rich sediments (2d) outcrop discontinuously along strike, especially in the southern part of the volcanic succession. Sedimentary lenses are foliated parallel to contacts with surrounding volcanic rocks. These sediments are similar texturally to the Burwash Formation sediments to the west, characterized by angular rock fragments and large angular- to sub-rounded quartz grains in a poorly sorted quartz, feldspar matrix. Deposition in a high energy environment with little reworking is indicated.

Quartz feldspar porphyritic rhyolite (2e) outcrops at the margins of a 100 m wide swamp filled valley midway across the northwest trending arm of the volcanics, at the southern end. The unit appears to pinch out 2.2 km along strike to the north, then reappears 2 km further NW in the same stratigraphic position. This unit is semicontinuous for 20 km to the north (James, 1989). The rhyolite has a contact-parallel penetrative foliation throughout; it is especially well developed adjacent to contacts with surrounding mafic volcanic rocks. The rock contains relatively large quartz or feldspar phenocrysts, or both, in a quartz-feldspar matrix. One outcrop is aphyric. This unit appears to extend through the 'elbow' in the volcanic rocks.

A thin unit of carbonate to calc-silicate chemical sediment (2f) is present west of the rhyolite in narrow (<5 m thick) accumulations at the southern end of the northwest trending arm of the volcanics. Carbonaceous sediment also outcrops at the extreme southern limit of mapping.

The Burwash Formation metasediments (3) are mainly poorly sorted quartzofeldspathic greywackes that grade from medium- to coarse-grained basal portions to fine grained tops. A dominantly mafic volcanic clast conglomerate (3b), observed in only one outcrop, lies on the eastern shore of Fenton Lake in the 'elbow' region of the sediments about 500 m west of the contact with the metavolcanics.

Complex abuts the volcanic rocks

METAMORPHISM:

Within the volcanics an equivalent isograd may be represent... the disappearance of chlorite from the metamorphic assembla... actinolite, hornblende, and quartz. As grade increases, acti... is depleted, leaving a predominantly hornblendic composition. ... garnet in the rims and cores of pillows near the vol... sedimentary contact may be controlled by composition of the ... and may indicate a mineral isograd within the volcanic ... Garnet is restricted to the area north of the suggested isog... the volcanic rocks. Geothermometry from garnet/biotite pai... the presence of pyroxene suggest a temperature of 600... 3×10^5 KPa at the contact with the Morose Granite.

Intravolcanic metasediments (2d) in the higher grade rock... marked by purple almandine porphyroblasts. The metasedim... assemblage includes carbonate, sericite, quartz, plagio... biotite and hornblende.

STRUCTURE:

Deformation of the supracrustal rocks has resulted in ... bedding in most places accompanied by development of steep ... zones in the Sleepy Dragon Complex. Earlier fabrics are not ... correlated between lithologies, however, later fabrics ... rocks except the Dogrib Dykes and the Morose Granite.

D_1

The earliest deformation in the metasediments is marked by ... that vary in direction, but close to the volcanics trend paral... the contact, which trends northeast and curves abruptly northw... form an elbow. Directional subsets of folds formed ... successively or at the same time.

In the volcanic rocks the early deformation has created ... foliation, and mineral and stretch lineations in the pillowed ... which lie in steep predominantly monoclinal successions ... northwest and southwest. Minor folds indicated by local chan... the facing directions of pillows may have formed during D_1.

D_2

The second phase of the deformation in the metasedimen... recorded in biotite porphyroblasts as inclusion trails of ... and by a preferred orientation of micas. From limited da... appears to trend variably east-southeast through eas... east-northeast. A similar foliation trending variably easte... present in the metasediments over a wide area of the Yello... domain (Fyson, 1982). Folds related to S_2 are rare in the area.

In the volcanic rocks a weak easterly trending fabric ... elbow region may be related to S_2 in the sediments. Smal... isoclinal intrafolial folds affecting a foliation, therefore ... F_2, are present in both the NE and NW trending portions ... volcanic belt.

D_3

F_3 minor folds and S_3 axial planar foliations cross my... and folded zones in the Sleepy Dragon Complex and the i... amphibolitic dykes. F_3 folds and S_3 foliations are locally pr... in the metavolcanics and the metasedimentary rocks wher... crenulate S_1/S_2. A directional subset (S_{3a}), commonly accompa... open to tight asymmetrical folds, trends northeastward. ... discontinuous subset (S_{3b}), also accompanied by open asymm... folds, trends northeasterly. Locally in the metasediments ... foliation is developed in the coarser grained beds whe... crosses the finer beds probably as a crenulation of S_3, (see ... Fyson, 1982). Elsewhere, time relations between S_{3a} and S_{3b} ... apparent.

ECONOMIC GEOLOGY:

Gold: The Fenton Lake portion of the Cameron River ... Belt hosts gold showings in the northeast trending arm ... volcanic belt at the north end of Bambi Lake, on ground ... formerly staked as the BAMBI claim. The gold is in a qua... that cuts the volcanic rocks. Quartz veins are common ... metavolcanic and metasedimentary rocks. Only one vein ... volcanic rocks, of those visited on the southeastern sh... small lake in the northwest trending arm of the metavolcan... contained sulphides other than pyrite (pyrrhotite, sphalerit...

Pegmatite dykes: These dykes are up to 1 m wide an... traced for 20 m in places in the elbow area and in the nort... trending arm of the volcanics adjacent to the Morose Pl...

... iron enrichment ... magnetic ... volcanic... anomalously magnetic ... massive ... margins of pillowed flows near the c...

5000

1/15, P/2

112° 50'

... an equivalent isograd may be represented by ... of chlorite from the metamorphic assemblage of ... blende, and quartz. As grade increases, actinolite ... ing a predominantly hornblendic composition. Rare ... rims and cores of pillows near the volcanic ... ct may be controlled by composition of the rocks, ... a mineral isograd within the volcanic rocks. ... ted to the area north of the suggested isograd in ... s. Geothermometry from garnet-biotite pairs and ... pyroxene suggest a temperature of 600°C at ... contact with the Morose Granite.

... metasediments (2d) of the higher grade rocks are ... almandine porphyroblasts. The metasedimentary ... carbonate ... quartz, plagioclase ...

... the supracrustal rocks has resulted in steep ... faces accompanied by development of steep shear ... Dragon Complex. Earlier fabrics are not readily ... lithologies, however, later fabrics cross all ... Dykes and the Morose Granite.

... formation in the metasediments is marked by folds ... tion, but close to the volcanics trend parallel to ... trends northeast and curves abruptly northwest to ... Directional subsets of folds formed either ... the same time.

... rocks the early deformation has created steep ... and stretch lineations in the pillowed flows, ... predominantly monoclinal successions facing ... west. Minor folds indicated by local changes in ... of pillows may have formed during D_1.

... of the deformation in the metasediments is ... porphyroblasts as inclusion trails of quartz, ... orientation of micas. From limited data, S_1 ... variably east-southeast through east to ... A similar foliation trending variably easterly in ... metasediments over a wide area of the Yellowknife ... Folds related to S_1 are rare in the area.

... rocks a weak easterly trending fabric in the ... be related to S_1 in the sediments. Small-scale ... folds affecting a foliation, therefore termed ... in both the NE and NW trending portions of the ...

... and S_2 axial planar foliations cross mylonites ... in the Sleepy Dragon Complex and the included ... F_2 folds and S_2 foliations are locally prominent ... volcanics and the metasedimentary rocks where they ... A directional subset (S_{2a}), commonly accompanied by ... asymmetrical folds, trends northeastward. A more ... subset (S_{2b}), also accompanied by open asymmetrical ... northeasterly. Locally in the metasediments the S_{2a} ... developed in the coarser grained beds whereas S_{2b} ... beds probably as a crenulation of S_{2a} (see fig. 8, ... Elsewhere, time relations between S_{2a} and S_{2b} are not ...

...Y:

... Fenton Lake portion of the Cameron River Volcanic ... showings in the northeast trending arm of the ... at the north end of Bambi Lake, on ground that was ... as the BAMBI claim. The gold is in a quartz vein ... volcanic rocks. Quartz veins are common in both ... and metasedimentary rocks. Only one vein in the ... of those visited on the southeastern shore of a ... the northwest trending arm of the metavolcanic rocks ... ides other than pyrite (pyrrhotite, sphalerite (?)).

... dykes: These dykes are up to 1 m wide and can be ... in places in the elbow area and in the northwesterly ... the volcanics adjacent to the Morose Pluton. Of ... ple: for chemical analysis, one near the contact with ...

... presen...

The volcanic rocks are ...

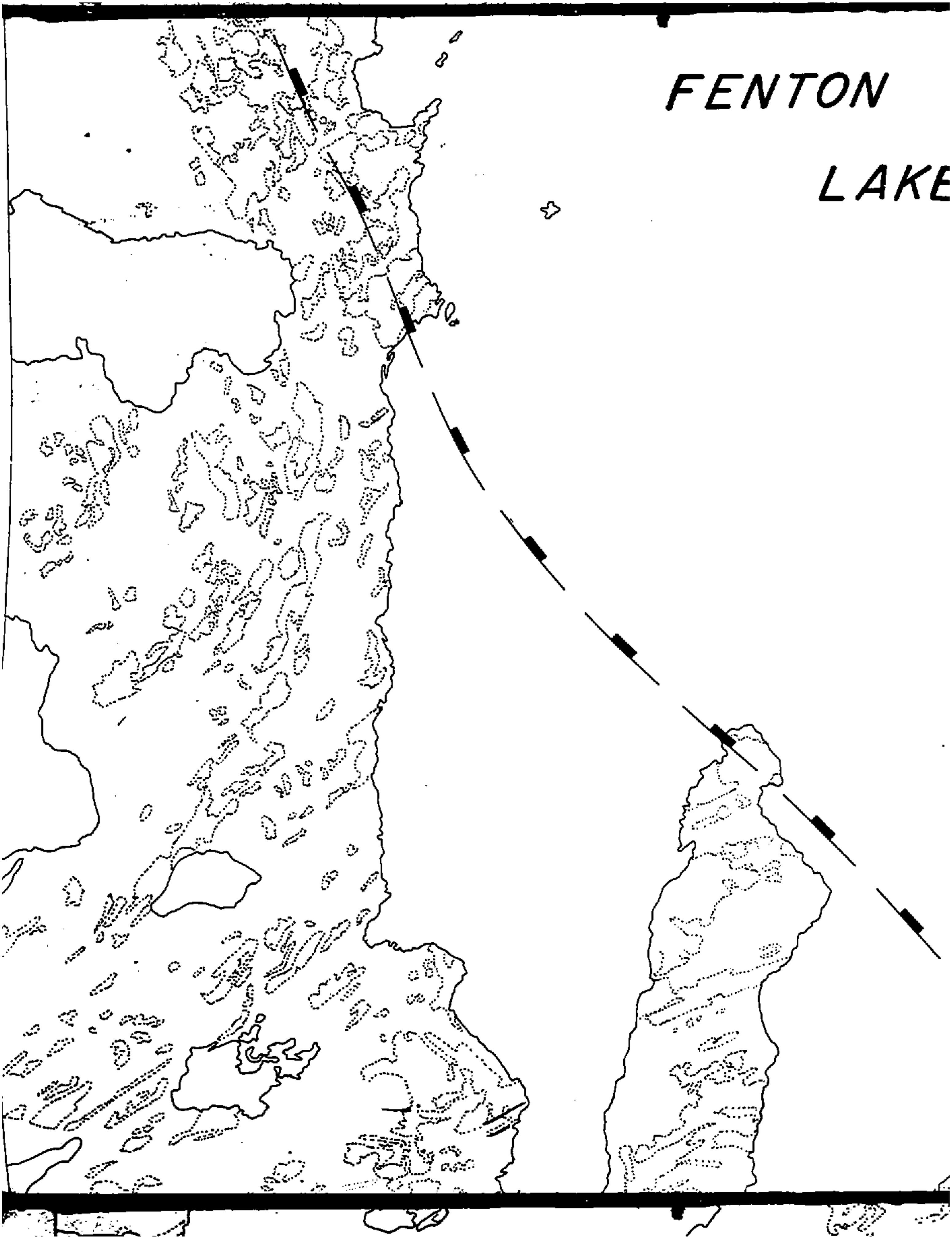
FENTON
LAKE

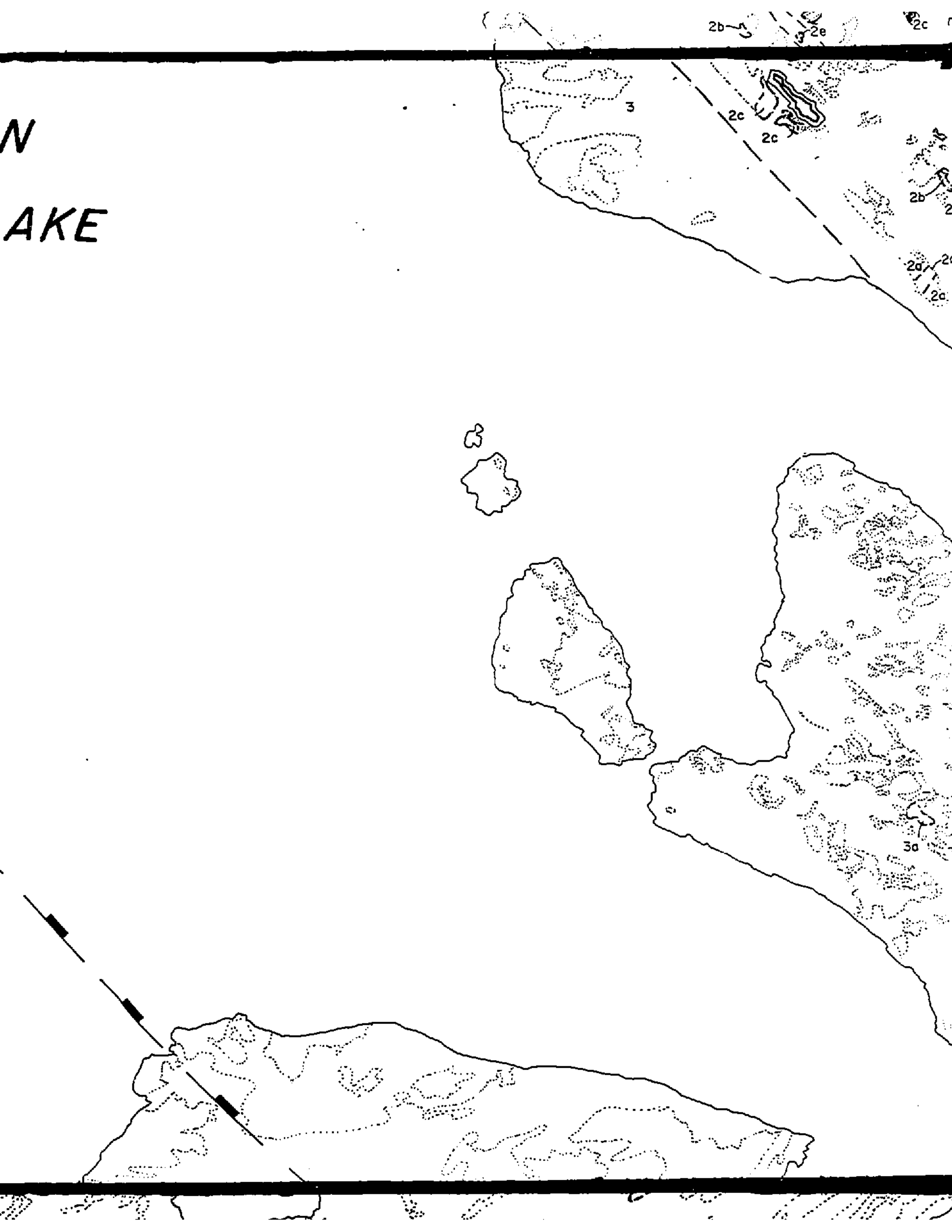
N
AKE
2b
3
2e
2c
2c
2c
3
2b
2a
2c
3a

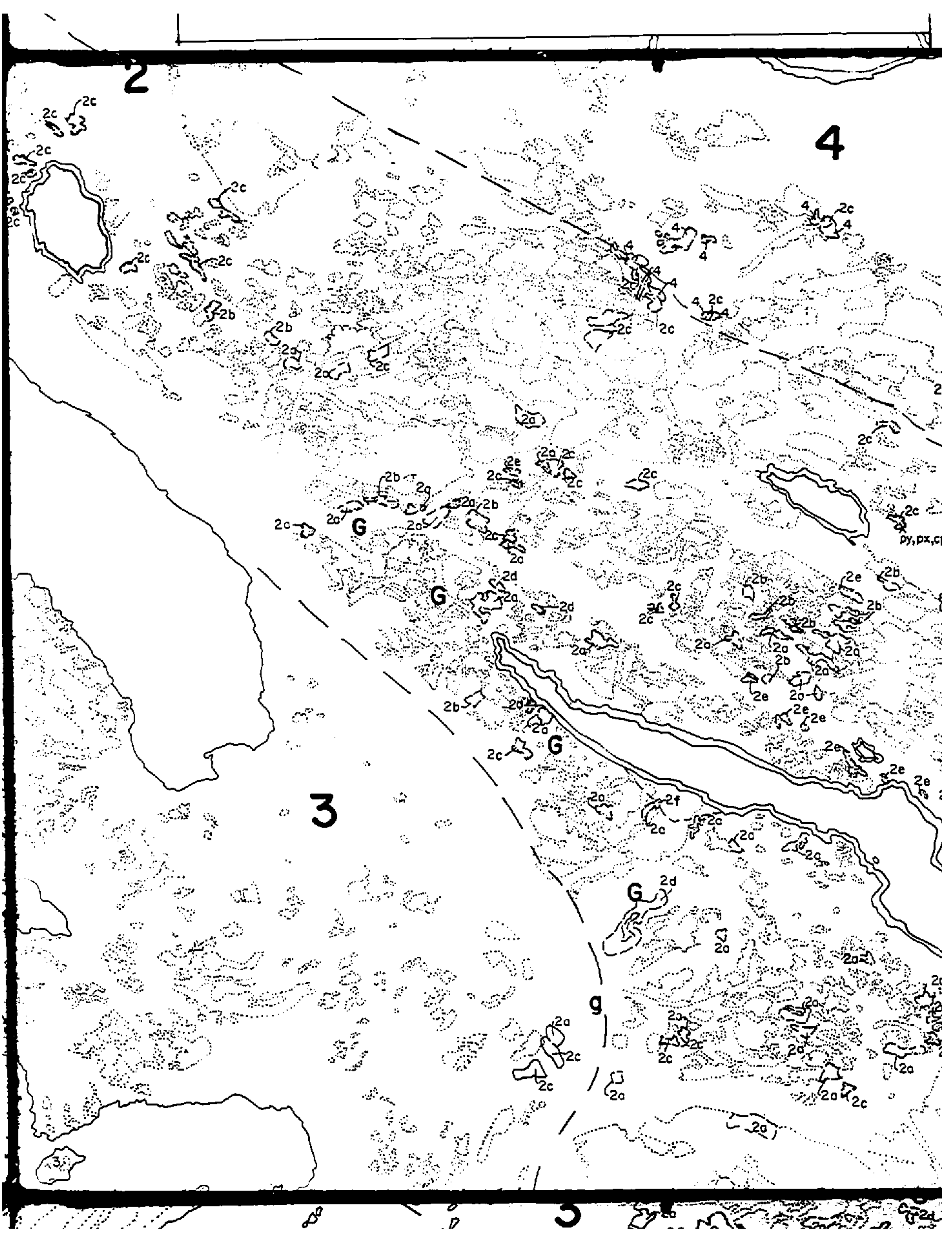
2
4
3
G
g
2a
2b
2c
2d
2e
2f
py, px, c

grained basal portions ... volcanic clast conglomerate ... observed in only one outcrop, ... on the eastern shore of ... Lake in the 'elbow' region ... the sediments about 100 m west ... contact with the metavolcanics.

Pegmatite dykes: These dykes are up to 1 m wide and traced for 20 m in places in the elbow area and in the north ...

Complex abuts the volcani rocks.

METAMORPHISM:

Rocks of sed' entary and volcanic origin are metamorphosed to the greenschi-- and lower amphibolite facies. The development of cordierite ; rphyroblasts, most abundant in finer grained beds, marks a wel defined mineral isograd in the metasedimentary rocks. The isogra: is marked by the loss of muscovite, which is replaced by biotite ir erleaved with chlorite. Locally garnet is present. The cordieri: isograd can be traced from near the northwest corner of the map area southeasterly to include sediments along the western shore : Fenton Lake. It then swings east-southeast and enters the volc ic belt about the midpoint of the southern arm of the vol nics.

Iron enrichment (magnetic outcrop) The volcanic ... anomalously magnetic at three places: within massive ro... elbow region; on the margins of pillowed flows near the co... the Morose Granite (4) where it strikes north; and, fur... near the contact with the Sleepy Dragon Complex. Rusty ... is distinctive in each outcrop.

REFERENCES

Baragar, W.R.A., 1966:
Geochemistry of the Yellowknife volcanic roc... Earth Sci., v.3, pp.9-30.

Davidson, A., 1972:
Granite studies in the Slave Province; Geol. S... Paper 72-1A, pp. 109-115.

Fyson, W.K., 1982:
Complex evolution of folds and cleavages ... rocks, Yellowknife, NWT; Can. J. Earth Sci.... 878-893.

Henderson, J.B., 1985:
Geology of the Yellowknife-Hearne Lake area, D... Mackenzie: a segment across an Archean Bas... Surv. Can. Memoir 414, 135 p.

James, D.T., 1989:
Basement - cover relations between th... Yellowknife Supergroup and the Sleepy Drag... north of Fenton Lake, District of Mackenz... Current Research, Part ...

Lambert, M.B., 1977:
Anatomy of a greenstone belt - Slave Provinc... Volcanic Regimes of Canada; W.R.A. Baragar, L... and J.M. Hall eds.; Geol. Assoc. Can. Specia... , 331-340.

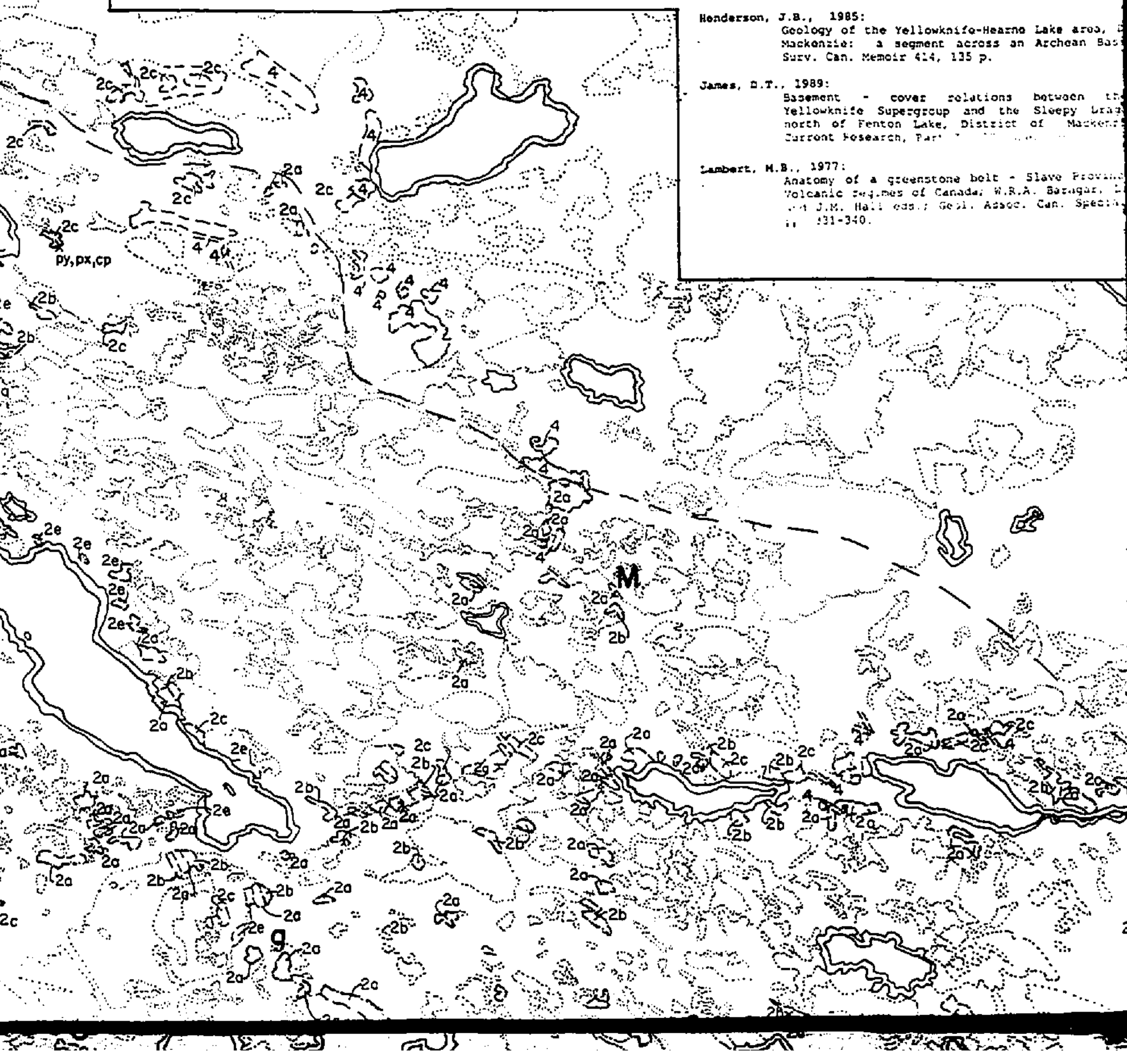

ce and dykes: These dykes are up to 1 m wide and can be
... in the elbow area and in the northwesterly
... the volcanics adjacent to the Morose Pluton. Of
... the chemical analysis ...

anic ... y present ...
ve ro... The volcanic rocks are
the co... within massive rocks in the
l, fur... d flows near the contact with
Rusty ... s north; and, further south
... n Complex. Rusty weathering

ic roc... knife volcanic rocks; Can. J.

eol. S... e Province; Geol. Surv. Can.,

ages ...
Sci., ... s and cleavages in Archean
... n. J. Earth Sci., v.19, pp.

rea, ...
n Bas... Hearne Lake area, District of
... ss an Archean Basin; Geol.

n th...
Drag... ions between the Archean
ackenz... the Sleepy Dragon Complex
... t of Mackenzie, NWT in

Provinc...
gar, L... Slave Province, NWT: in
Specia... H.A. Baragar, L.C. Coleman
... Can. Special Paper 16,

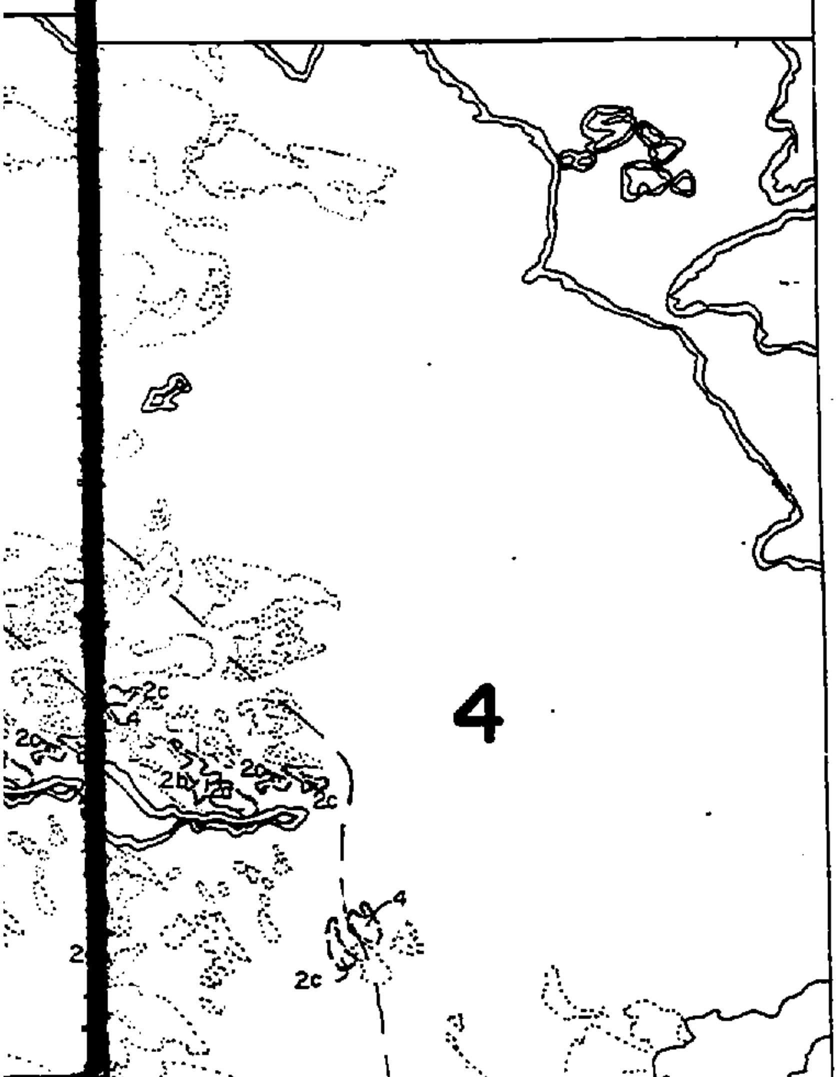

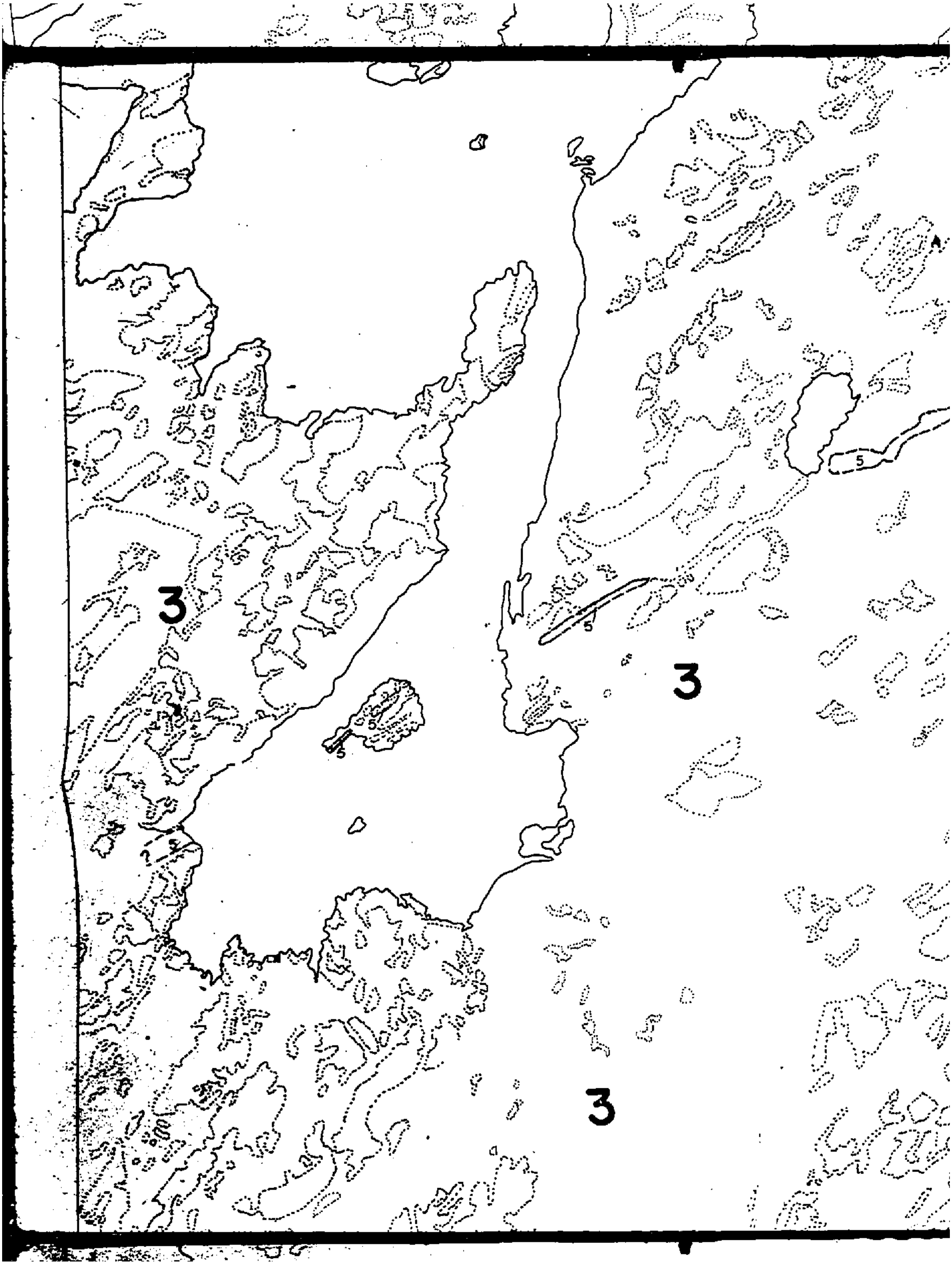
3
5
5
5
5
3
3

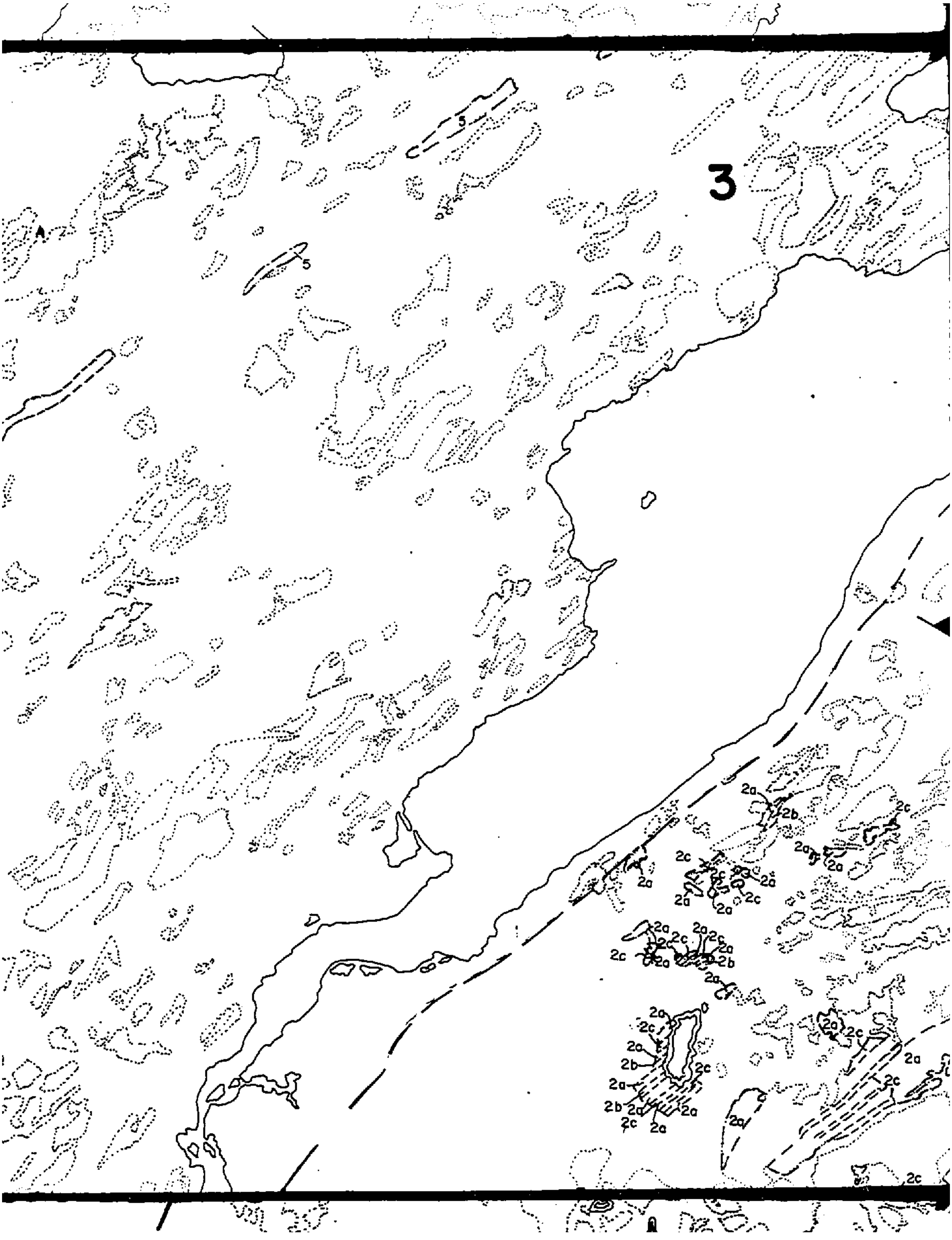
3
5
5
2a
2b
2c
2a
2c
2a
2a
2c
2a
2b
2c
2a
2a
2b
2a
2c
2a
2c
2b
2a
2c
2a
2c
2c

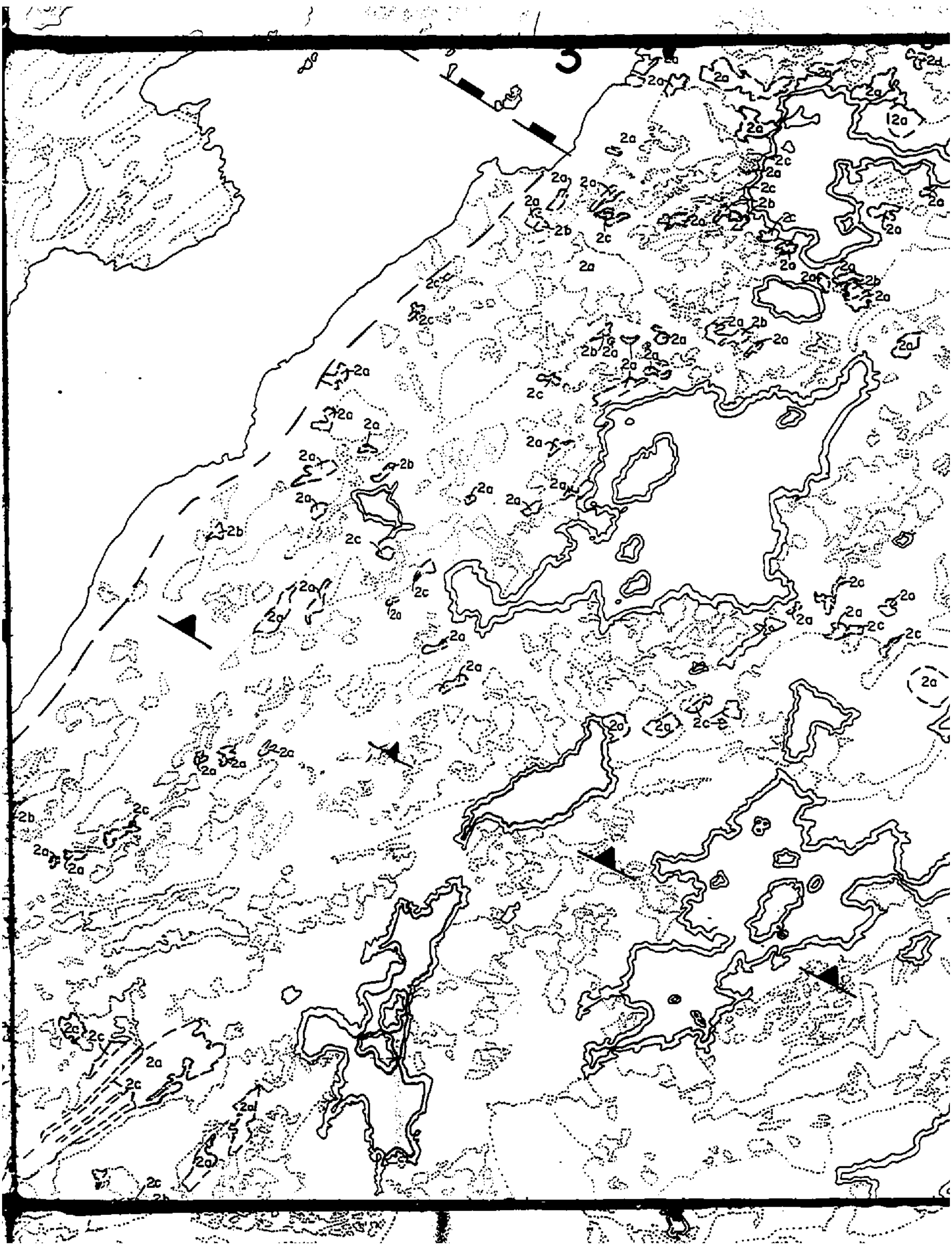
3
2a
2b
2c
2d
12a

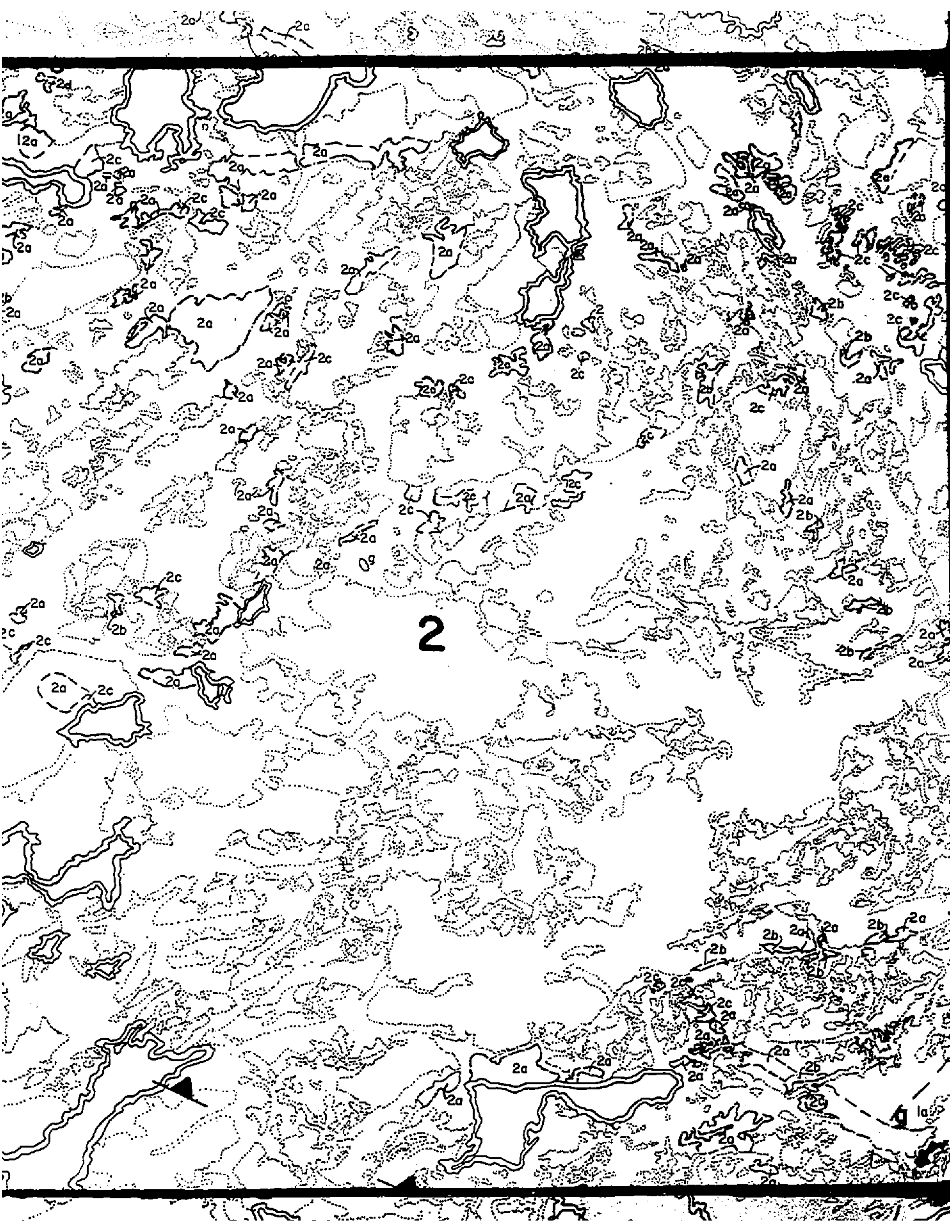

2
2a
2b
2c
2d
1a


4
2c
2a
2b
1
1a
1b
g
1

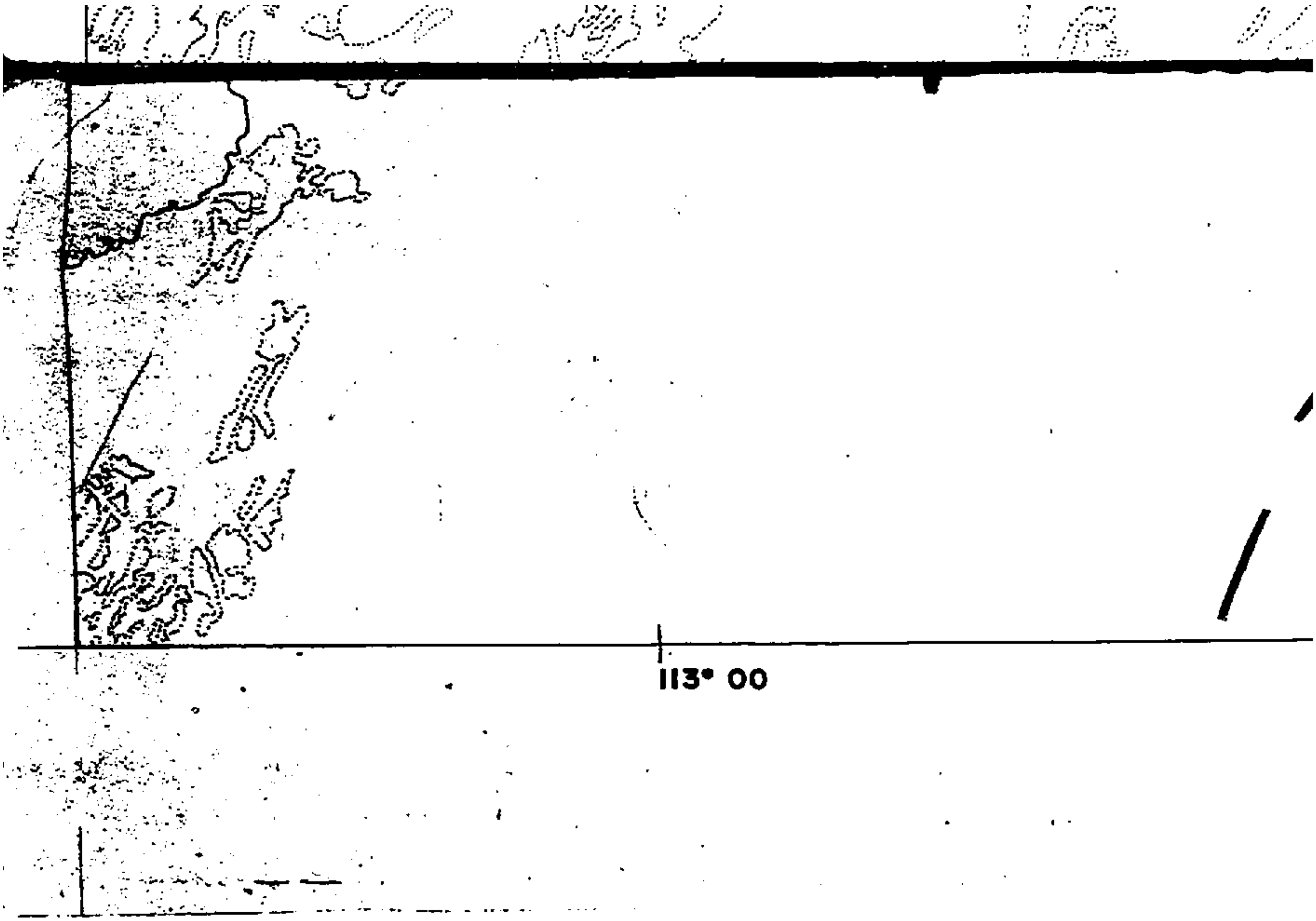
113° 00

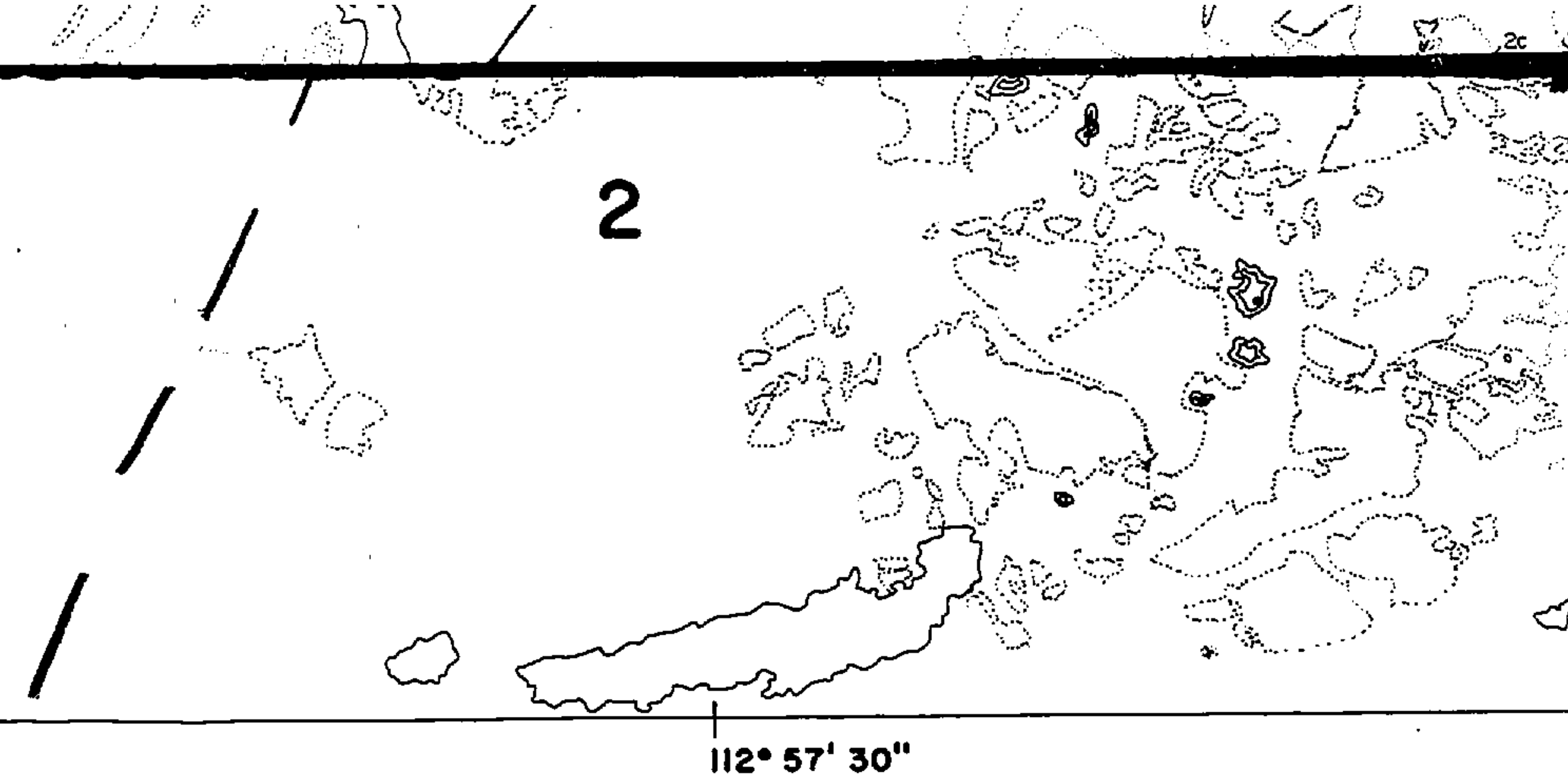
2c
2
112° 57' 30"

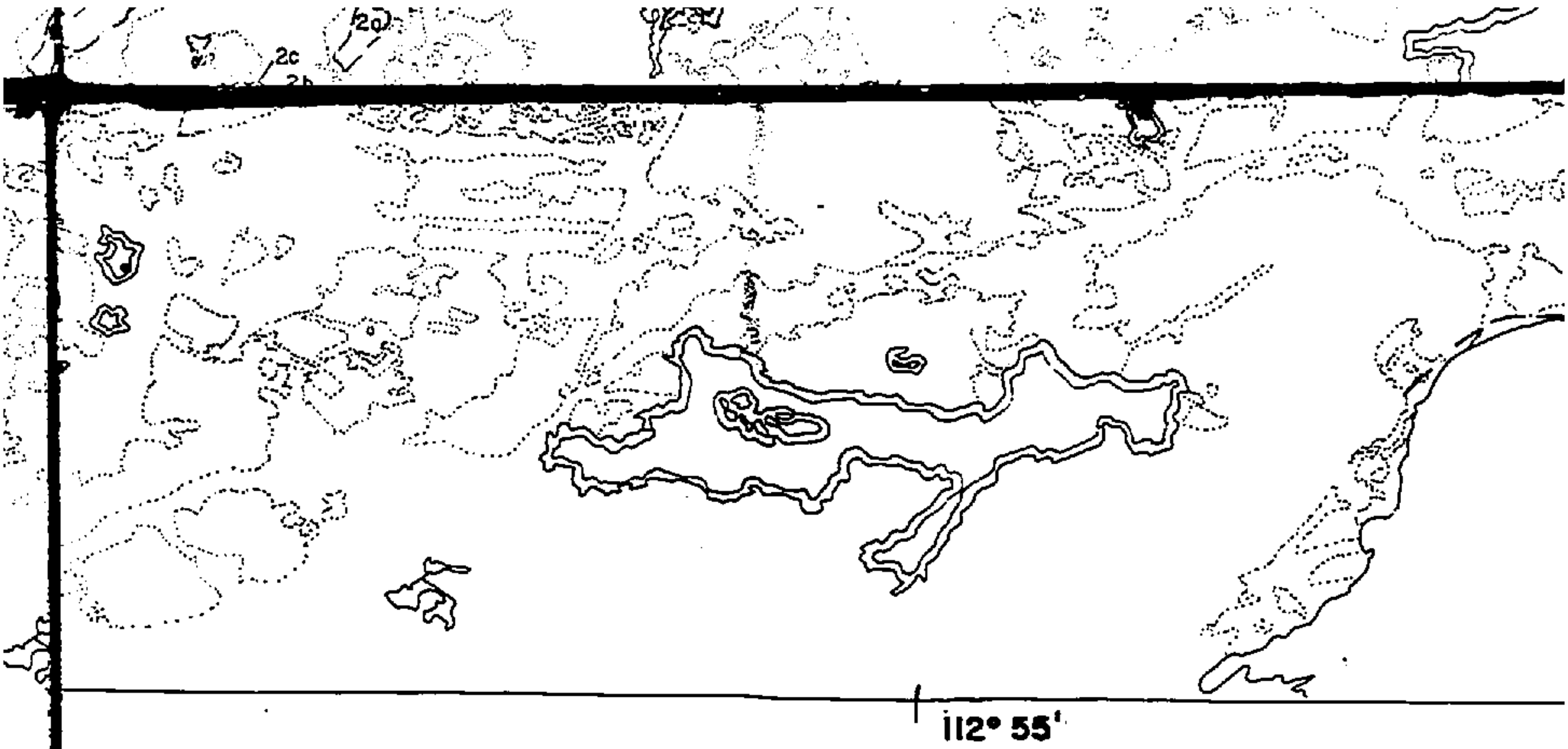

2a
2c
112° 55'

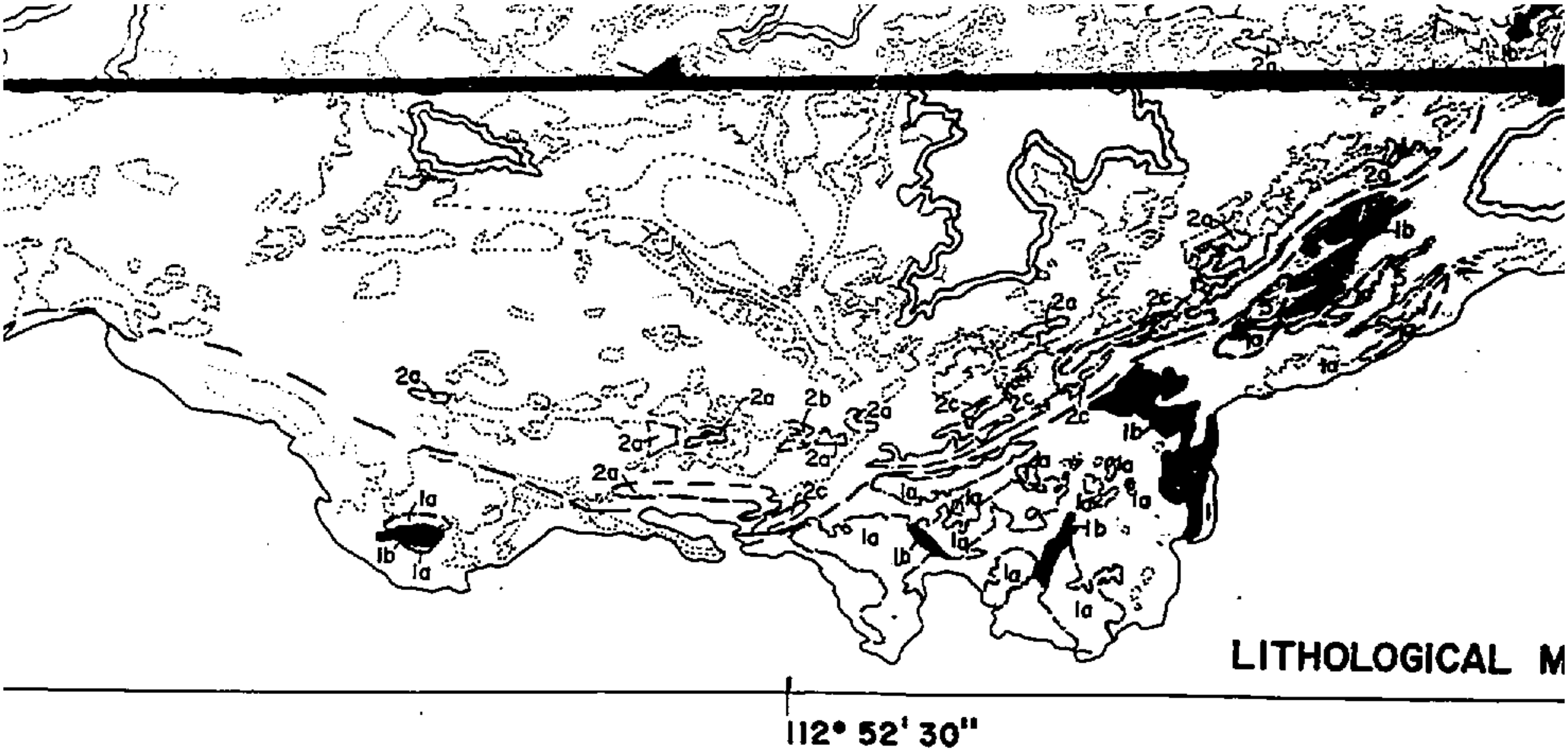
1a
1b
2a
2b
2c
LITHOLOGICAL M
112° 52' 30"

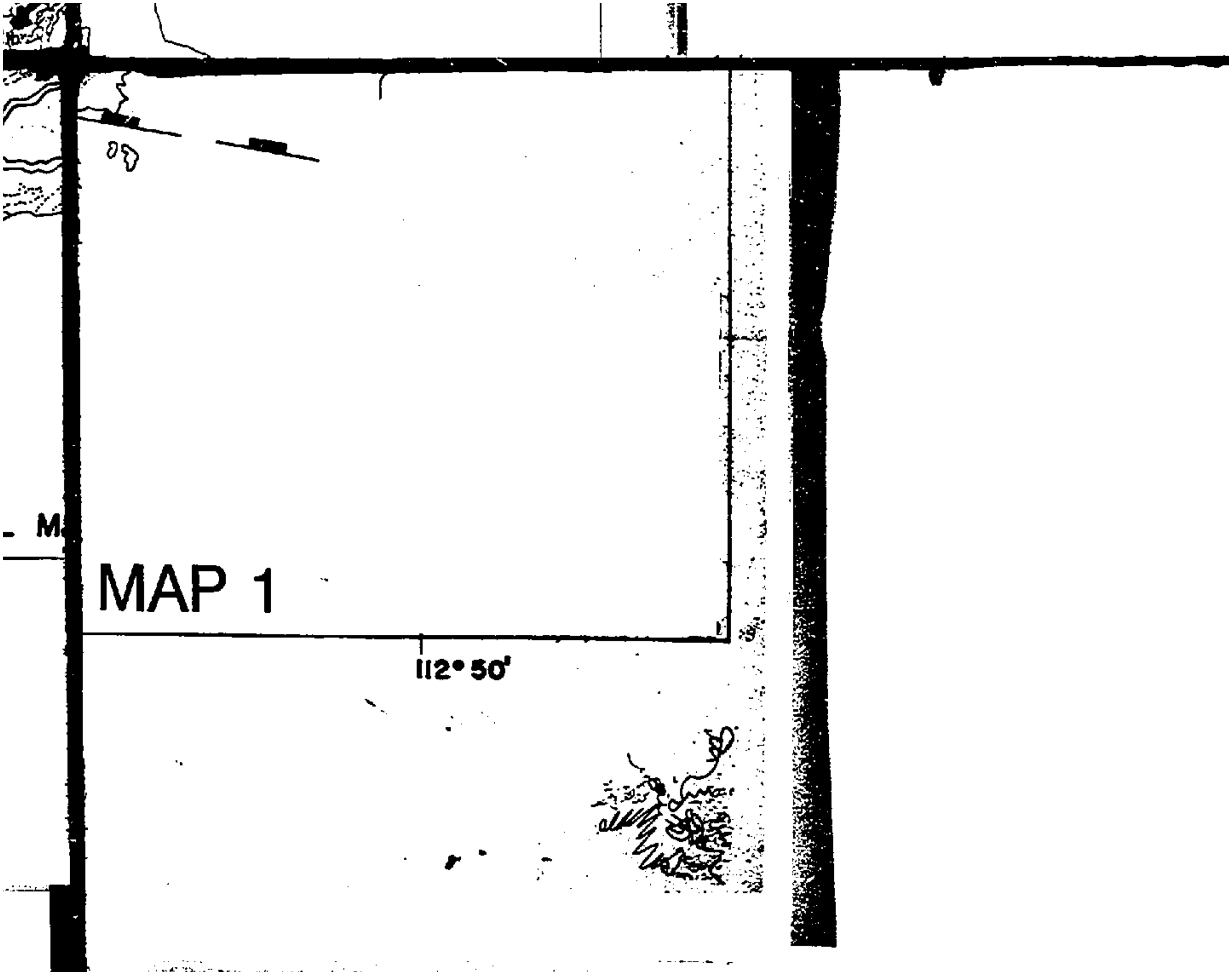
MAP 1
112° 50'

Geology an

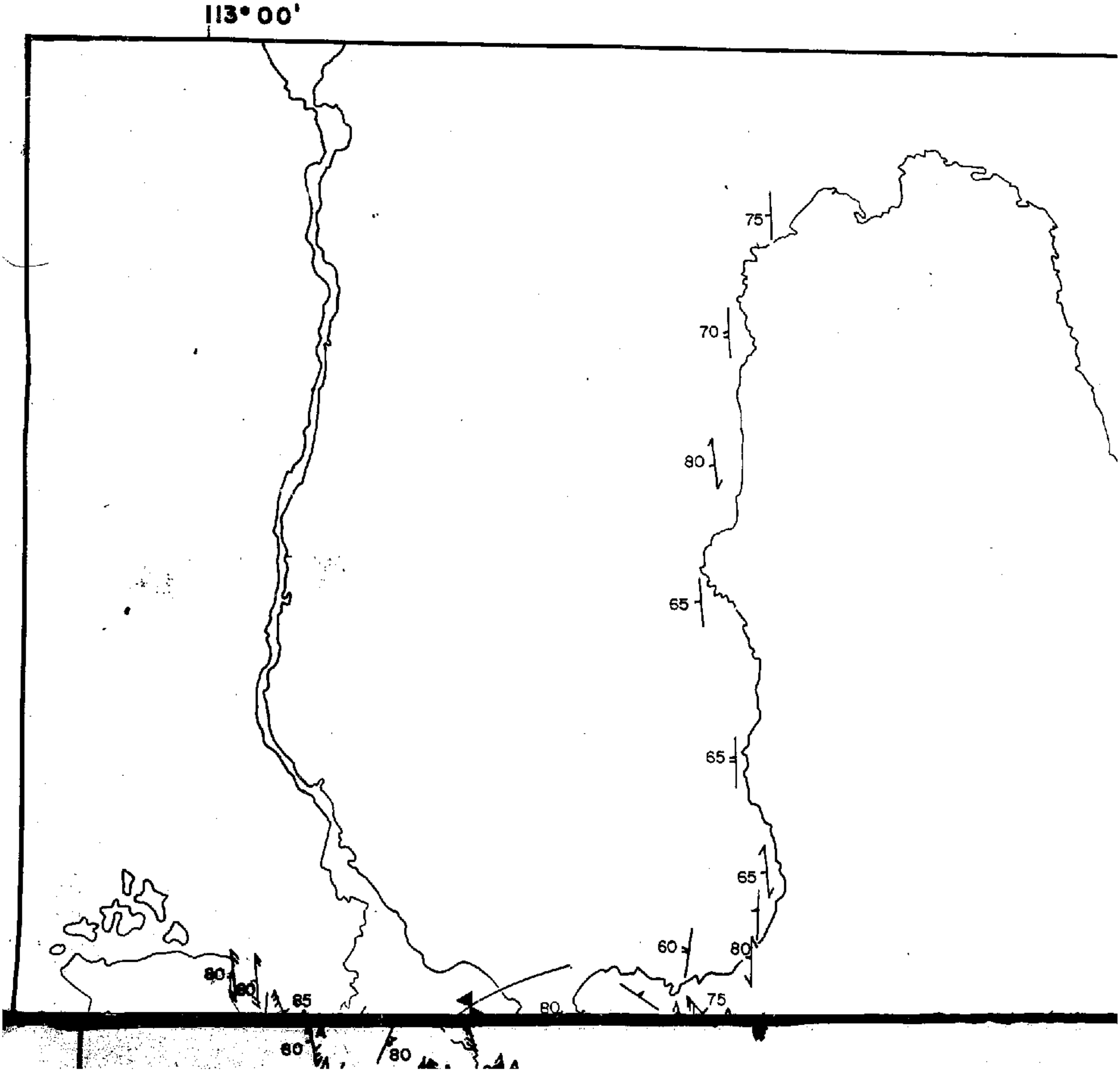

y and Structure of the Camer

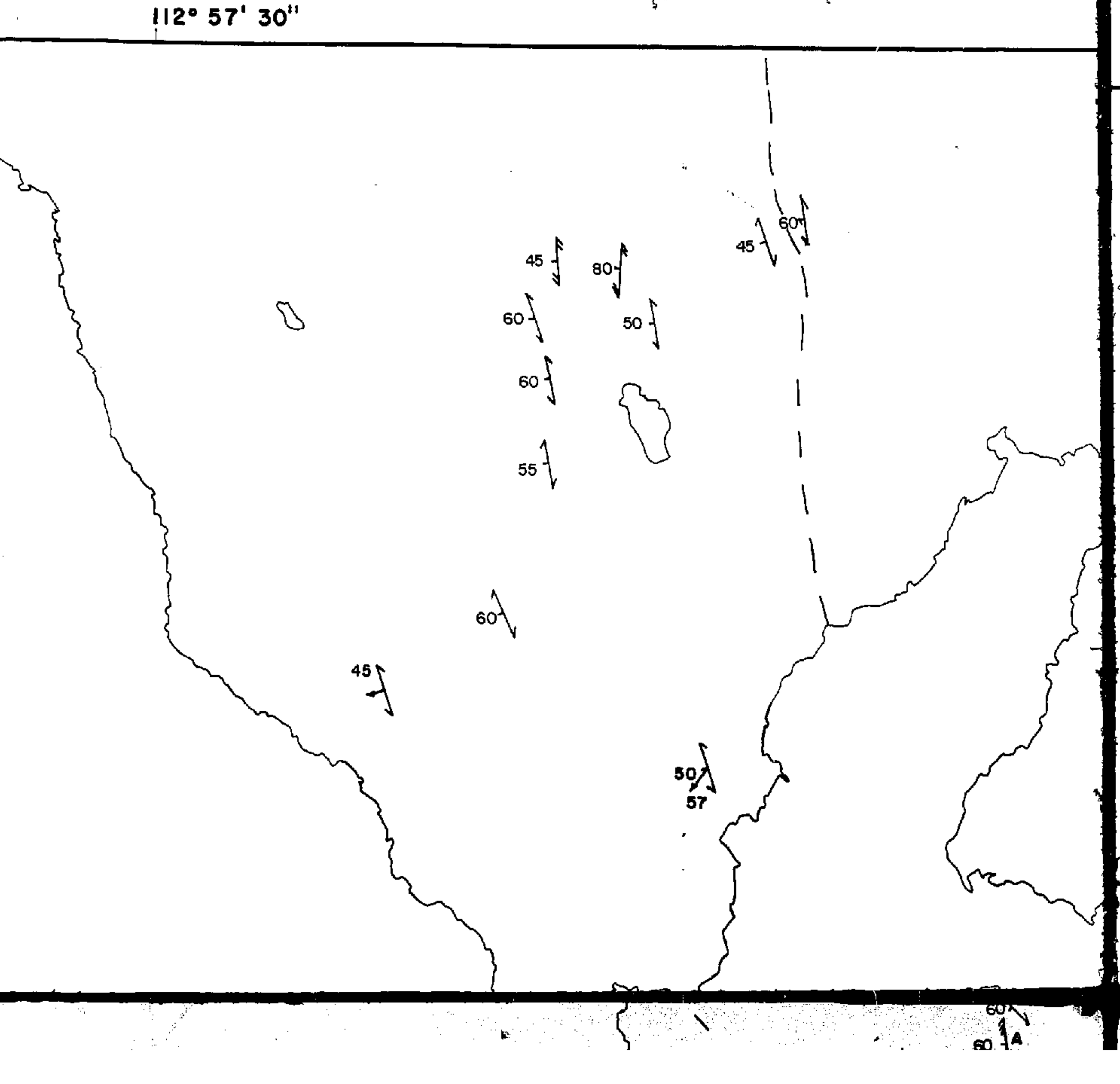

he Cameron River Belt, Fento

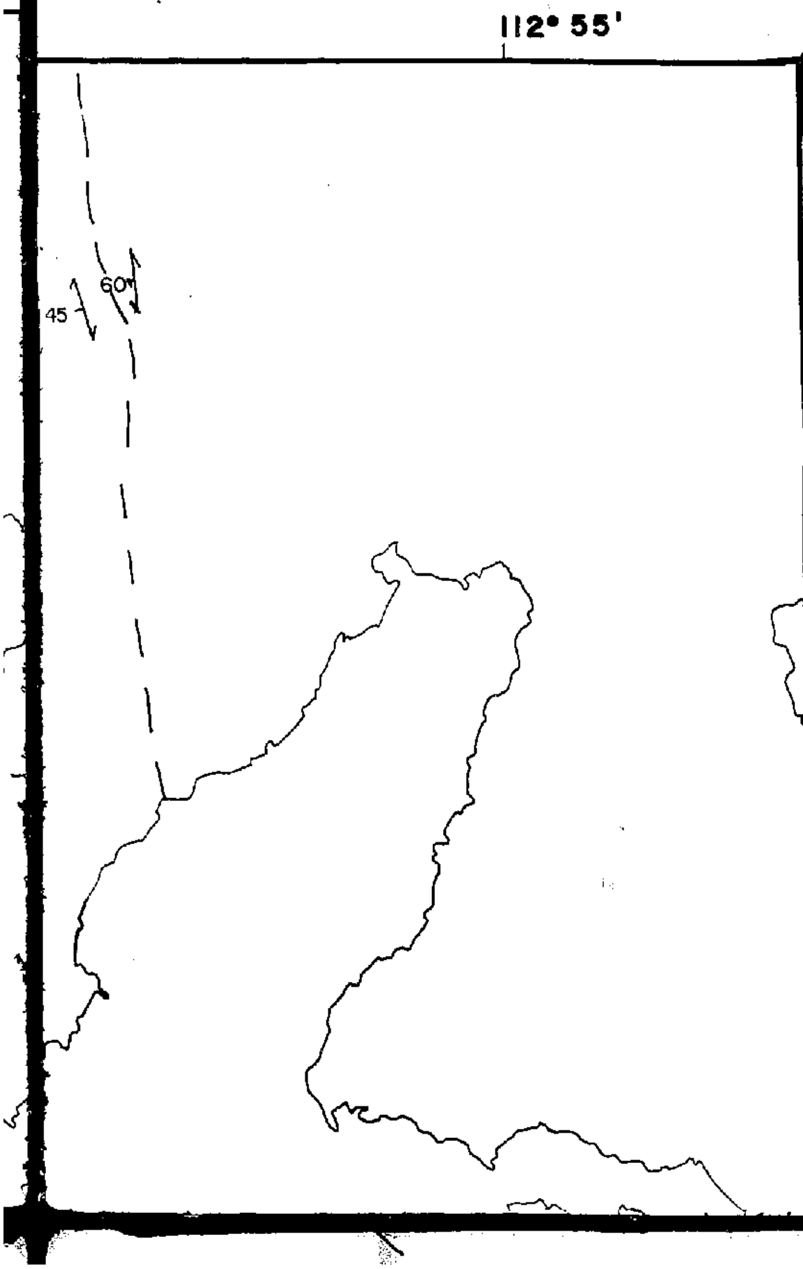

LEGEND

Bedding: tops known; unknown (dip angle indi

Pillow facing: approxi

Foliation: main folia flattering plane; S_1; S_2

A B

Lineation (mineral inte inclined; vertical

Inclusion trails: S_2 where known)

Mylonitic foliation: i

Fold axis: (trend and

Fold axial trace: sy syncline (indicating overturned anticline overturning)

Contact: defined, assu

Lineament from air phot

Geology by R.D. Cullen assisted by C. Massicot
C.D. Gault

SCALE : 1:10

Miles 0 .1 .2 .3 .4 .5

énton Lake Area; parts of NTS

tops known; overturned; vertical; tops
angle indicated)

ng: approximate direction

main foliation (S_1, S_2 or S_3) - pillow
plane; S_1; S_2; S_{3A}; S_{3B}

mineral intersection or stretch direction):
ertical

rails: S_2 (trend only - dips are steep
)

oliation: in granite only

(trend and plunge) F_1, F_2, F_3

trace: syncline; anticline; overturned
(indicating direction of overturning):
anticline (indicating direction of
)

efined, assumed

rom air photos

C. Massicote (1985)
C.D. Gault (1986)

ALE: 1:10 000

.4 .5 .6 .7 .8 .9 1

2'30"

GENERAL GEOLOGY:

The Fenton Lake area within the Archean Slave Structural Province is underlain by four major rock units as well as mafic and felsic dykes of minor extent.

(1) **Sleepy Dragon Complex**: mainly granitic and gneissic rocks, that occupy the southeastern part of the map area; was interpreted as basement to adjacent volcanic rocks (Davidson, 1972; Henderson, 1981, 1985; Lambert, 1977).

(2) **Cameron River Volcanic Belt**: a predominantly basalti[c] volcanic pile of pillowed and massive flows with intercalate[d] breccias, volcaniclastics and minor felsic tuffs and sediments.

(3) **Burwash Formation metasediments**: graded coarse to fine (metagreywacke and argillaceous beds) stratigraphically above and west of the volcanics.

(4) **Morose Granite**: a granitic pluton and dykes (4b) intrude units 1 and 2 in the northeastern part of the map area.

(5) **Dogrib Dykes**: a few gabbroic dykes of the Proterozoi[c] Dogrib swarm trend northeasterly across units 1, 3 and probably [2] and 4.

LITHOLOGY AND STRATIGRAPHIC RELATIONS:

The Sleepy Dragon Complex (1) includes medium grained K-feldspa[r] and plagioclase granitoids with local strongly foliated a[nd] mylonitized zones. Amphibolitic dykes (1b) within the complex hav[e] been interpreted as feeders to the adjacent volcanic rock[s] suggesting that the complex is part of an older basement (Baraga[r], 1966; Lambert, 1977). Contact relations; however, are obscured [by] deformation and no dyke has been traced from the complex into t[he] volcanics. An apparent truncation of a strong gneissic fabric [in] the complex by relatively undeformed volcanic rocks has suggested [an] unconformable relationship (Davidson, 1972; Henderson, 1985), b[ut] tectonic juxtaposition is possible (Kusky, 1986a,b).

The Cameron River Volcanic Belt (2) is composed predominantly [of] basaltic pillowed flows (2a) massive flows and dykes (2c) a[nd] breccias composed mainly of volcanic cataclasts (2b). The dyk[es] within the volcanic pile may be crosscutting or layer parallel a[nd] may in part be feeders to the volcanic extrusive rocks. Coar[se] unfoliated gabbro dykes (5) of uncertain extent also cross t[he] metavolcanics.

Within the volcanic pile, 20 - 40 m wide zones of recessivel[y] weathered, medium- to coarse-grained, quartz-rich sediments (2[...]) outcrop discontinuously along strike, especially in the southe[ast] part of the volcanic succession. Sedimentary lenses are foliate[d] parallel to contacts with surrounding volcanic rocks. Thes[e] sediments are similar texturally to the Burwash Formation sedimen[ts] to the west, characterized by angular rock fragments and lar[ge] angular- to sub-rounded quartz grains in a poorly sorted quart[z-] feldspar matrix. Deposition in a high energy environment with littl[e] reworking is indicated.

Quartz feldspar porphyritic rhyolite (2e) outcrops at t[he] margins of a 100 m wide swamp filled valley midway across t[he] northwest trending arm of the volcanics, at the southern end. T[he] unit appears to pinch out 2.2 km along strike to the north, th[en] reappears 2 km further NW in the same stratigraphic position.

The Burwash Formation metasediments (3) are mainly poorly sorted quartzofeld[spathic] greywackes that grade from medium to coarse ... metavolcanic and metasediment... volcanic rocks, of those visited

...parts of NTS 85 I/15, P/2

...LOGY

... Lake area within the Archean Slave Structural ...lain by four major rock units as well as mafic and ... minor extent.

...Dragon Complex: mainly granitic and gneissic rocks, ... southeastern part of the map area; was interpreted ... adjacent volcanic rocks (Davidson, 1972; Henderson, Lambert, 1977).

...meron River Volcanic Belt: a predominantly basaltic ...e of pillowed and massive flows with intercalated ...clastics and minor felsic tuffs and sediments.

...wash Formation metasediments: graded coarse to fine, ... argillaceous beds) stratigraphically above and ...volcanics.

...rose Granite: a granitic pluton and dykes (4b) intrude ... the northeastern part of the map area.

...grib Dykes: a few gabbroic dykes of the Proterozoic ... trend northeasterly across units 1, 3 and probably 2

...STRATIGRAPHIC RELATIONS:

...py Dragon Complex (1) includes medium grained K-feldspar ... granitoids with local strongly foliated and ...res. Amphibolitic dykes (1b) within the complex have ...eted as feeders to the adjacent volcanic rocks, ... the complex is part of an older basement (Baragar, ... 1977). Contact relations; however, are obscured by ... no dyke has been traced from the complex into the ... apparent truncation of a strong gneissic fabric in ... relatively undeformed volcanic rocks has suggested an ... relationship (Davidson, 1972; Henderson, 1985), but ...position is possible (Kusky, 1986a,b).

...on River Volcanic Belt (2) is composed predominantly of ...wed flows (2a) massive flows and dykes (2c) and ...osed mainly of volcanic cataclasts (2b). The dykes ...canic pile may be crosscutting or layer parallel and ... feeders to the volcanic extrusive rocks. Coarse ...abbro dykes (5) of uncertain extent also cross the

...e volcanic pile, 20 - 40 m wide zones of recessively ...dium- to coarse-grained, quartz-rich sediments (2d) ...tinuously along strike, especially in the southern ...canic succession. Sedimentary lenses are foliated ...contacts with surrounding volcanic rocks. These ...similar texturally to the Burwash Formation sediments ... characterized by angular rock fragments and large ...-rounded quartz grains in a poorly sorted quartz, ...x. Deposition in a high energy environment with little ...dicated.

...dspar porphyritic rhyolite (2e) outcrops at the ...00 m wide swamp filled valley midway across the ...ing arm of the volcanics, at the southern end. The ... pinch out 2.2 km along strike to the north, then ...further NW in the same stratigraphic position. This ...tinuous for 20 km to the north (James, 1989). The

...metasediments (3) are mainly poorly sorted

Within the volcanics an equivalent isograd may be represented by the disappearance of chlorite from the metamorphic assemblage of actinolite, hornblende, and quartz. As grade increases, actinolite is depleted, leaving a predominantly hornblendic composition. Rare garnet in the rims and cores of pillows near the volcanic-sedimentary contact may be controlled by composition of the rocks, and may indicate a mineral isograd within the volcanic rocks. Garnet is restricted to the area north of the suggested isograd in the volcanic rocks. Geothermometry from garnet/biotite pairs and the presence of pyroxene suggest a temperature of 600°C at 3×10^5 KPa at the contact with the Morose Granite.

Intravolcanic metasediments (2d) in the higher grade rocks are marked by purple almandine porphyroblasts. The metasedimentary assemblage includes carbonate, sericite, quartz, plagioclase, biotite and hornblende.

STRUCTURE:

Deformation of the supracrustal rocks has resulted in steep bedding in most places accompanied by development of steep shear zones in the Sleepy Dragon Complex. Earlier fabrics are not readily correlated between lithologies, however, later fabrics cross all rocks except the Dogrib Dykes and the Morose Granite.

D_1

The earliest deformation in the metasediments is marked by folds that vary in direction, but close to the volcanics trend parallel to the contact, which trends northeast and curves abruptly northwest to form an elbow. Directional subsets of folds formed either successively or at the same time.

In the volcanic rocks the early deformation has created steep foliation, and mineral and stretch lineations in the pillowed flows, which lie in steep predominantly monoclinal successions facing northwest and southwest. Minor folds indicated by local changes in the facing directions of pillows may have formed during D_1.

D_2

The second phase of the deformation in the metasediments is recorded in biotite porphyroblasts as inclusion trails of quartz, and by a preferred orientation of micas. From limited data, S_2 appears to trend variably east-southeast through east to east-northeast. A similar foliation trending variably easterly is present in the metasediments over a wide area of the Yellowknife domain (Fyson, 1982). Folds related to S_2 are rare in the area.

In the volcanic rocks a weak easterly trending fabric in the elbow region may be related to S_2 in the sediments. Small-scale isoclinal intrafolial folds affecting a foliation, therefore termed F_2, are present in both the NE and NW trending portions of the volcanic belt.

D_3

F_3 minor folds and S_3 axial planar foliations cross mylonites and folded zones in the Sleepy Dragon Complex and the included amphibolitic dykes. F_3 folds and S_3 foliations are locally prominent in the metavolcanics and the metasedimentary rocks where they crenulate S_1/S_2. A directional subset (S_{3a}), commonly accompanied by open to tight asymmetrical folds, trends northeastward. A more discontinuous subset (S_{3b}), also accompanied by open asymmetrical folds, trends northeasterly. Locally in the metasediments the S_{3a}

metavolcanic and metasedimentary rocks. Only one vein in the volcanic rocks of those visited on the southeastern shore of a

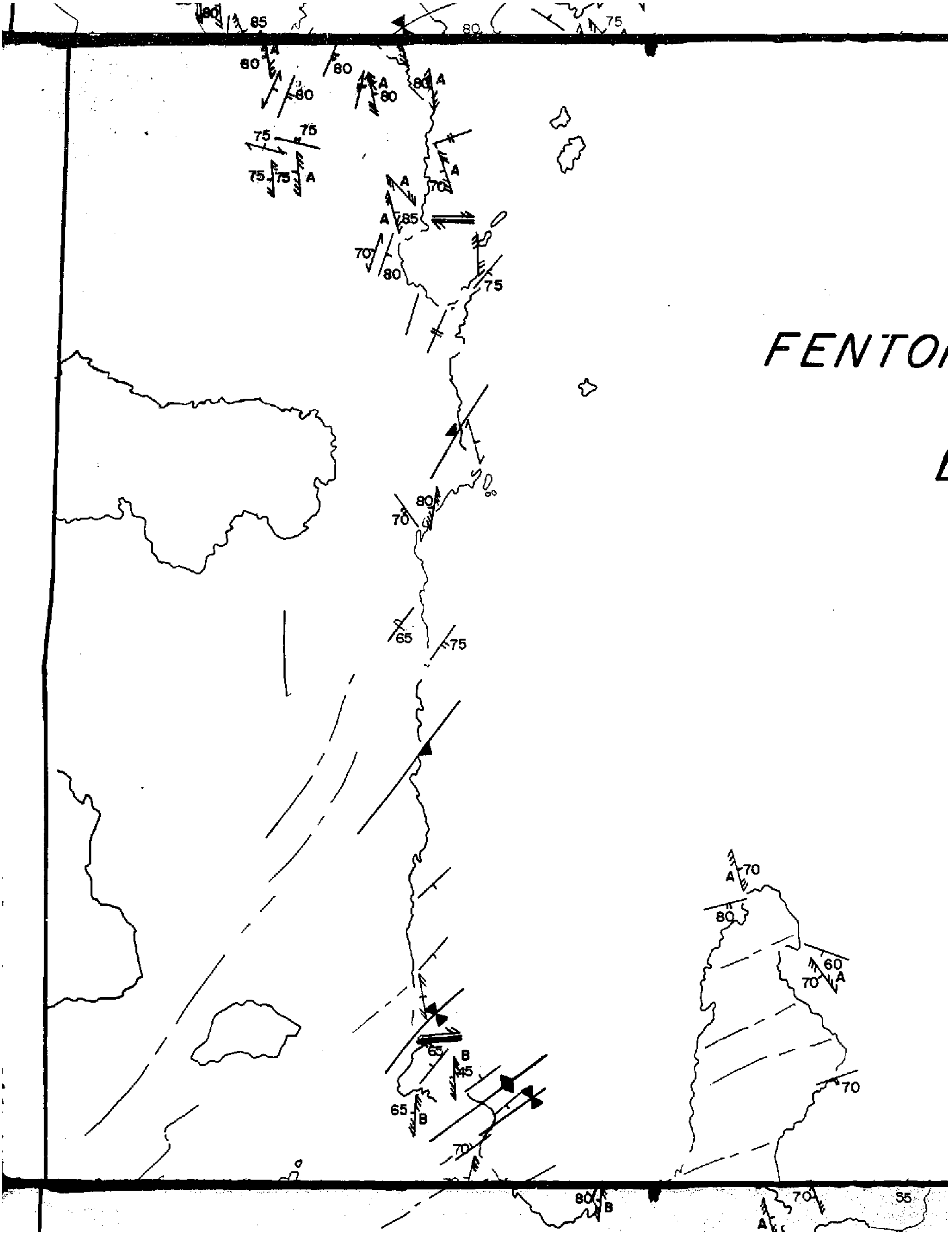
FENTO

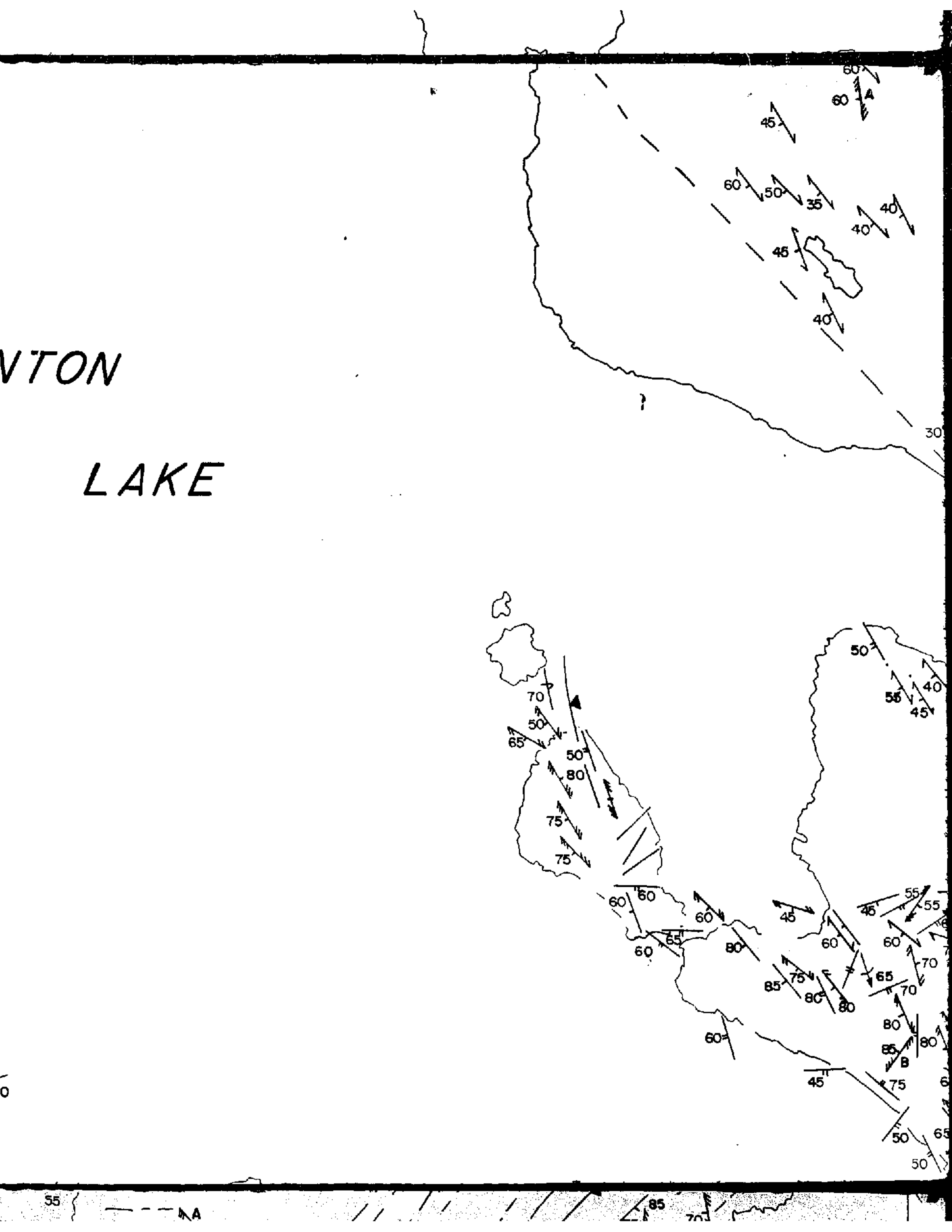
VTON
LAKE

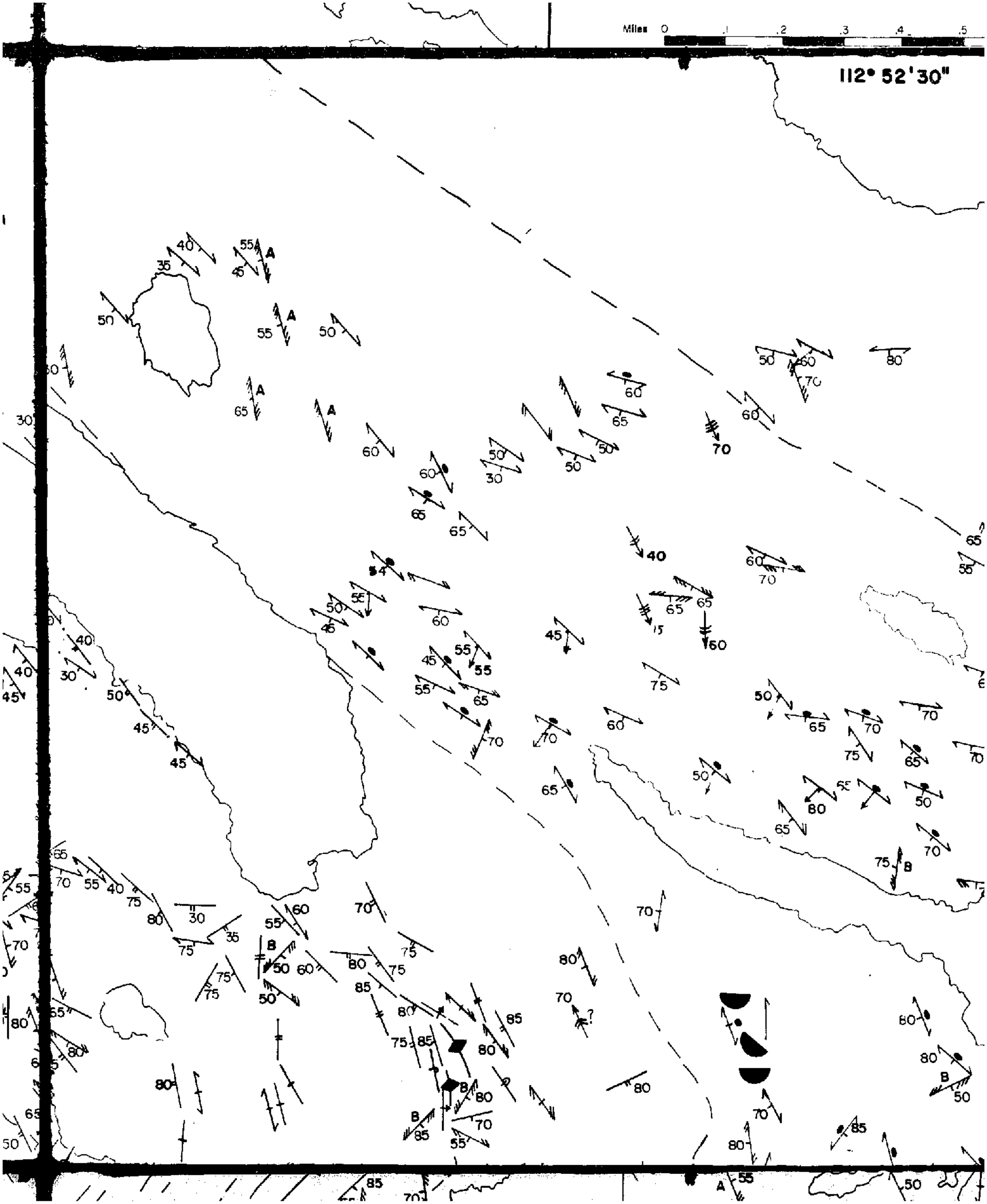
Miles 0 .1 .2 .3 .4 .5
112° 52' 30"

margins of a 100 m wide swamp filled valley midway across t... northwest trending arm of the volcanics, at the southern end. ... unit appears to pinch out 2.2 km along strike to the north, ...

The **Burwash Formation metasediments** (3) are mainly poorly sorted quartzofeldspathic greywackes that grade from medium- to coarse-grained basal portions to fine grained tops. A dominantly mafic volcanic clast conglomerate (3b), observed in only one outcrop, lies on the eastern shore of Fenton Lake in the 'elbow' region of the sediments about 500 m west of the contact with the metavolcanics.

The **Morose Granite** (4) is a plagioclase, K-feldspar, muscovite, biotite granite that is relatively unfoliated except near the volcanic rocks where it displays a contact-parallel foliation. Inclusions of volcanic rocks (2), up to 100 m from the contact, show all the fabrics present in the volcanic belt. A few granitic dykes (4a), some of which are pegmatitic, intrude the volcanic rocks east and north of Fenton Lake and may be off-shoots from the main granitic pluton. The dykes are absent where the Sleepy Dragon Complex abuts the volcanic rocks.

METAMORPHISM:

Rocks of sedimentary and volcanic origin are metamorphosed to the greenschist and lower amphibolite facies. The development of cordierite porphyroblasts, most abundant in finer grained beds, marks a well defined mineral isograd in the metasedimentary rocks. The isograd is marked by the loss of muscovite, which is replaced by biotite interleaved with chlorite. Locally garnet is present. The cordierite isograd can be traced from near the northwest corner of the map area southeasterly to include sediments along the western shore of Fenton Lake. It then swings east-southeast and enters the volcanic belt about the midpoint of the southern arm of the volcanics.

metavolcanic and metasedimen... volcanic rocks, of those visited... small lake in the northwest trend... contained sulphides other than pyr...

Pegmatite dykes: These dyke... traced for 20 m in places in the e... trending arm of the volcanics ad... three dykes sampled for chemical a... the Morose Granite (4), yielded va... zinc and 124 ppm barium.

Gossan: Zones of rusty weat... 40 m along strike, are present in... contact with the Sleepy Dragon C... weathered and sulphide minerals ar...

Iron enrichment (magnetic outcr... anomalously magnetic at three pla... elbow region; on the margins of pi... the Morose Granite (4) where it ... near the contact with the Sleepy ... is distinctive in each outcrop.

REFERENCES

Baragar, W.R.A., 1966:
Geochemistry of the ... Earth Sci., v.3, pp.9-...

Davidson, A., 1972:
Granite studies in th... Paper 72-1A, pp. 109-...

Fyson, W.K., 1982:
Complex evolution of ... rocks, Yellowknife, ... 878-893.

Henderson, J.B., 1985:
Geology of the Yellow... Mackenzie: a segmen... Surv. Can. Memoir 414...

James, D.T., 1989:
Basement - cover ... Yellowknife Supergro... north of Fenton Lak... Current Research, Par...

Lambert, M.B., 1977:
Anatomy of a greenst... Volcanic regimes of ... and J.M. Hall eds.; ... pp. 331-340.

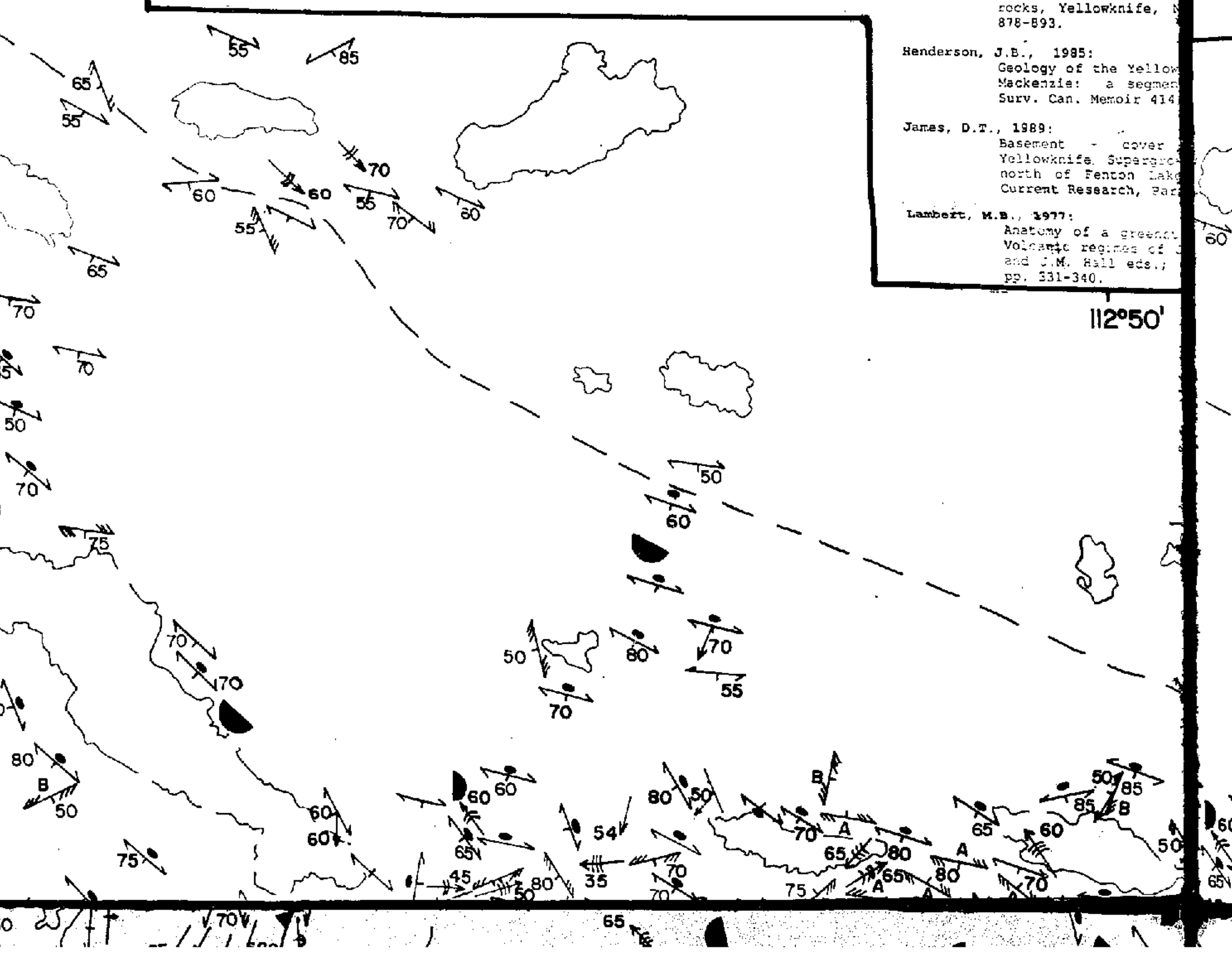

...00 m wide swamp filled valley midway across the ...ng arm of the volcanics, at the southern end. The ... pinch out 2.2 km along strike to the north, then ...further NW in the same stratigraphic position. This ...tinuous for 20 km to the north (James, 1989). The

in the metavolcanics and the metasedimentary rocks where they crenulate S_1/S_1. A directional subset (S_{4a}), commonly accompanied by open to tight asymmetrical folds, trends northeastward. A more discontinuous subset (S_{4b}), also accompanied by open asymmetrical folds, trends northeasterly. Locally in the metasediments the S_{4}

...ormation metasediments (3) are mainly poorly sorted ... greywackes that grade from medium- to coarse- ...tions to fine grained tops. A dominantly mafic ...nglomerate (3b), observed in only one outcrop, lies ...hore of Fenton Lake in the 'elbow' region of the ...00 m west of the contact with the metavolcanics.

...anite (4) is a plagioclase, K-feldspar, muscovite, ...that is relatively unfoliated except near the ...where it displays a contact-parallel foliation. ...canic rocks (2), up to 100 m from the contact, show ...resent in the volcanic belt. A few granitic dykes ...ch are pegmatitic, intrude the volcanic rocks east ...nton Lake and may be off-shoots from the main ... The dykes are absent where the Sleepy Dragon ... volcanic rocks.

...imentary and volcanic origin are metamorphosed to ...and lower amphibolite facies. The development of ...phiblasts, most abundant in finer grained beds, ...ines mineral isograd in the metasedimentary rocks. ...rked by the loss of muscovite, which is replaced by ...ed with chlorite. Locally garnet is present. The ...d can be traced from near the northwest corner of ...theasterly to include sediments along the western ...ake. It then swings east-southeast and enters the ...out the midpoint of the southern arm of the

metavolcanic and metasedimentary rocks. Only one vein in the volcanic rocks, of those visited on the southeastern shore of a small lake in the northwest trending arm of the metavolcanic rocks contained sulphides other than pyrite (pyrrhotite, sphalerite (?)).

Pegmatite dykes: These dykes are up to 1 m wide and can be traced for 20 m in places in the elbow area and in the northwesterly trending arm of the volcanics adjacent to the Morose Pluton. Of three dykes sampled for chemical analysis, one near the contact with the Morose Granite (4), yielded values of 1041 ppm rubidium, 364 ppm zinc and 124 ppm barium.

Gossan: Zones of rusty weathered rock, up to 20 m thick and 40 m along strike, are present in the volcanic rocks and along the contact with the Sleepy Dragon Complex. These zones are heavily weathered and sulphide minerals are rarely preserved.

Iron enrichment (magnetic outcrop) The volcanic rocks are anomalously magnetic at three places: within massive rocks in the elbow region; on the margins of pillowed flows near the contact with the Morose Granite (4) where it strikes north; and, further south near the contact with the Sleepy Dragon Complex. Rusty weathering is distinctive in each outcrop.

REFERENCES

Baragar, W.R.A., 1966:
Geochemistry of the Yellowknife volcanic rocks; Can. J. Earth Sci., v.3, pp.9-30.

Davidson, A., 1972:
Granite studies in the Slave Province; Geol. Surv. Can., Paper 72-1A, pp. 109-115.

Fyson, W.K., 1982:
Complex evolution of folds and cleavages in Archean rocks, Yellowknife, NWT; Can. J. Earth Sci., v.19, pp. 878-893.

Henderson, J.B., 1985:
Geology of the Yellowknife-Hearne Lake area, District of Mackenzie: a segment across an Archean Basin; Geol. Surv. Can. Memoir 414, 135 p.

James, D.T., 1989:
Basement - cover relations between the Archean Yellowknife Supergroup and the Sleepy Dragon Complex north of Fenton Lake, District of Mackenzie, NWT in Current Research, Part C, GSC Paper 1989-1C, pp. 29-36.

Lambert, M.B., 1977:
Anatomy of a greenstone belt - Slave Province, NWT; in Volcanic regimes of Canada; W.R.A. Baragar, L.C. Coleman and J.M. Hall eds.; Geol. Assoc. Can. Special Paper 16, pp. 331-340.

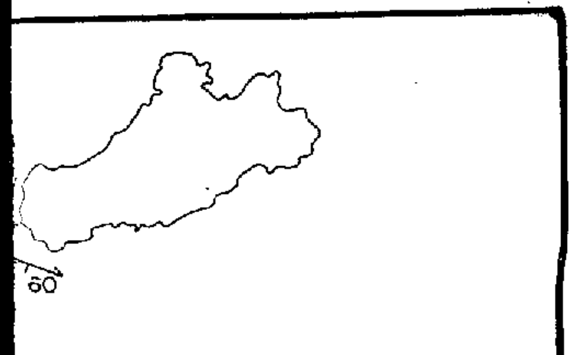
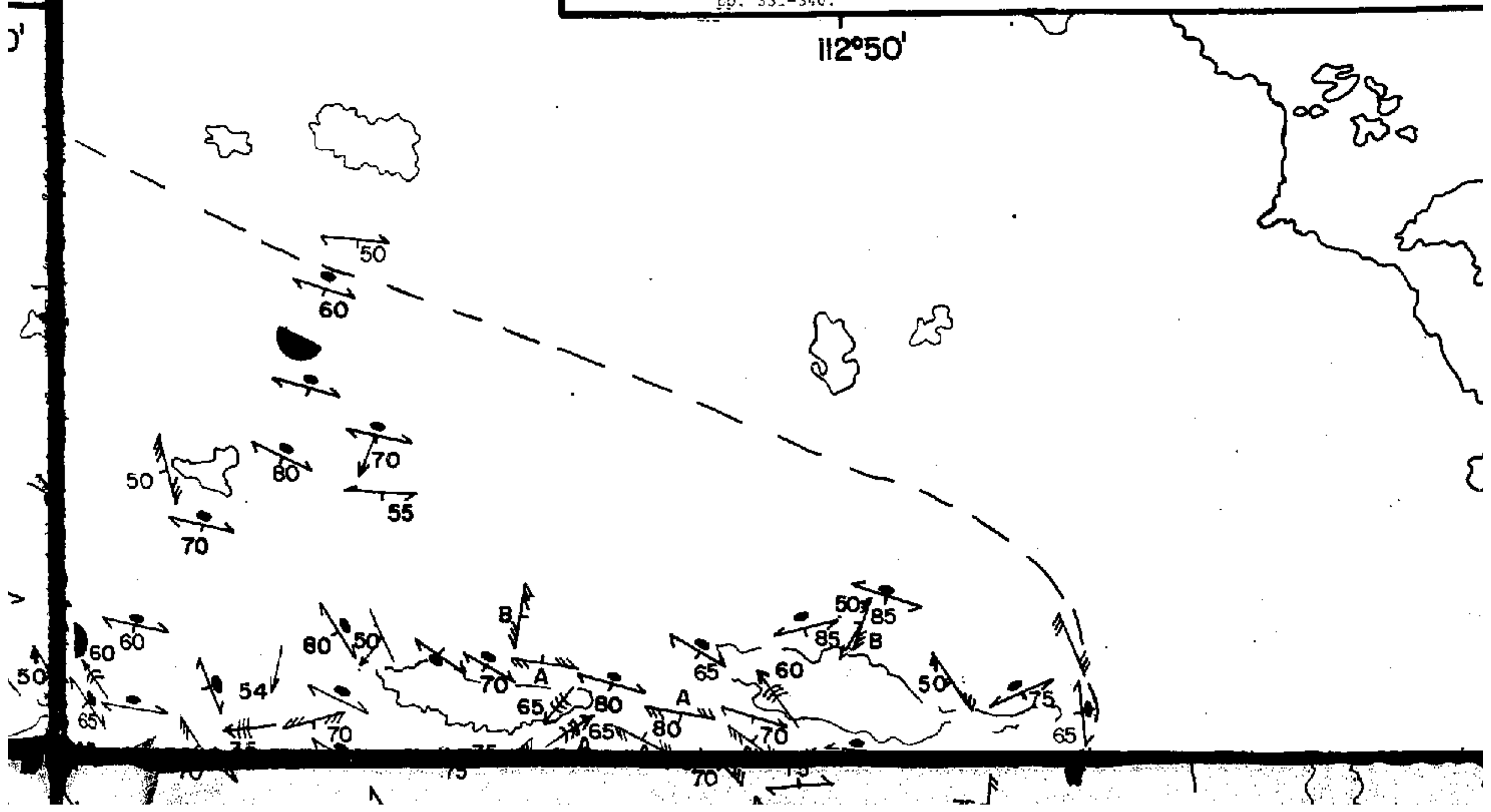

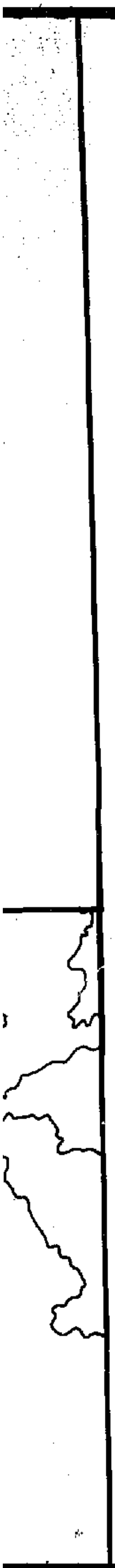

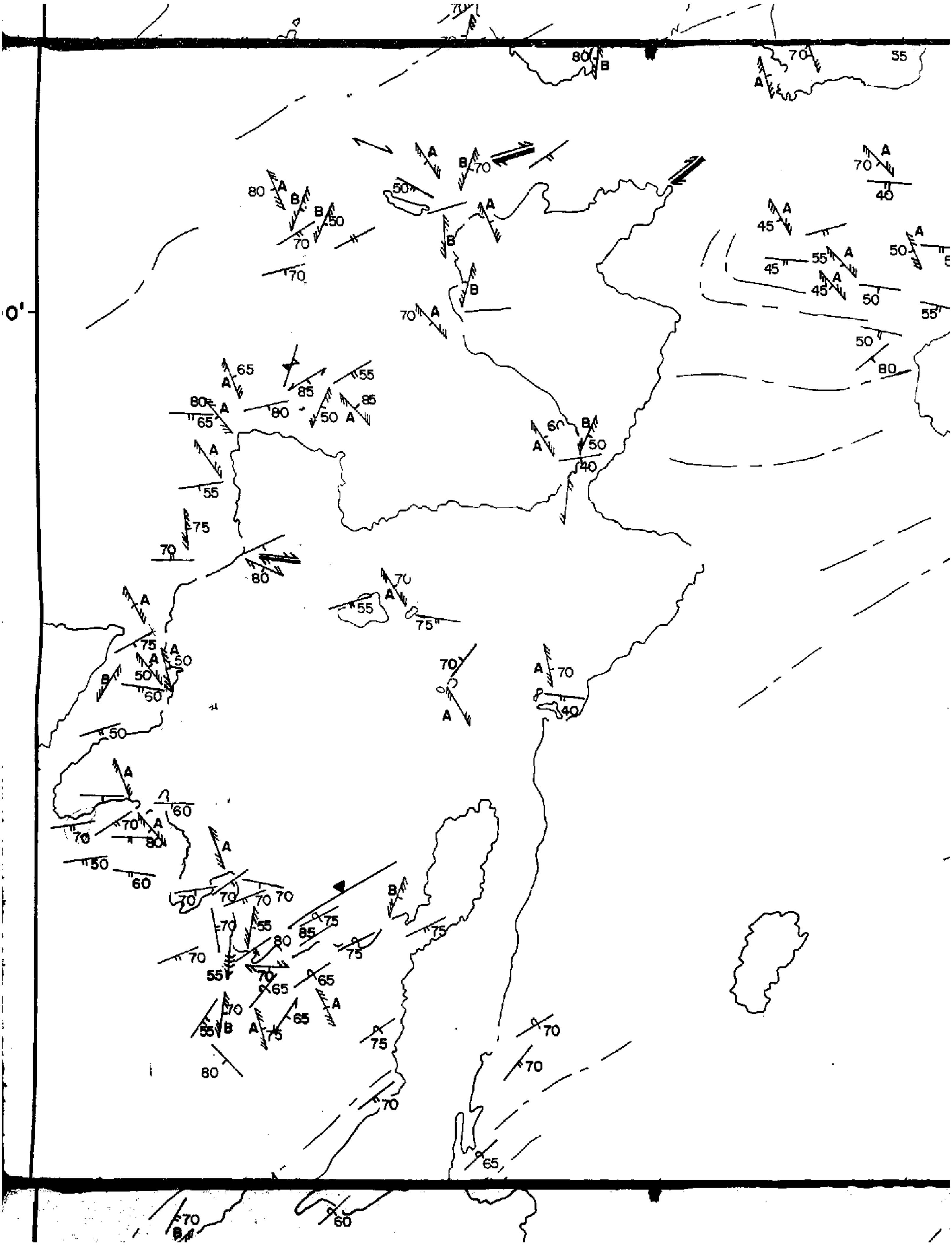

80
B
70
55
A
70
A
B
70
80
A
B
B
50
50
70
A
A
40
45
A
B
50
A
55
A
45
45
A
70
45
50
B
70
A
50
55
50
80
65
A
85
55
80
A
80
50
85
A
65
60
B
A
50
A
40
55
75
70
80
70
A
A
55
75
75
A
A
50
B
A
50
60
70
A
70
A
50
A
60
70
A
70
80
50
60
A
70
70
70
70
B
75
70
55
85
75
80
75
75
70
55
70
65
65
A
70
55
B
A
75
65
75
80
70
70
70
65
70
B
60

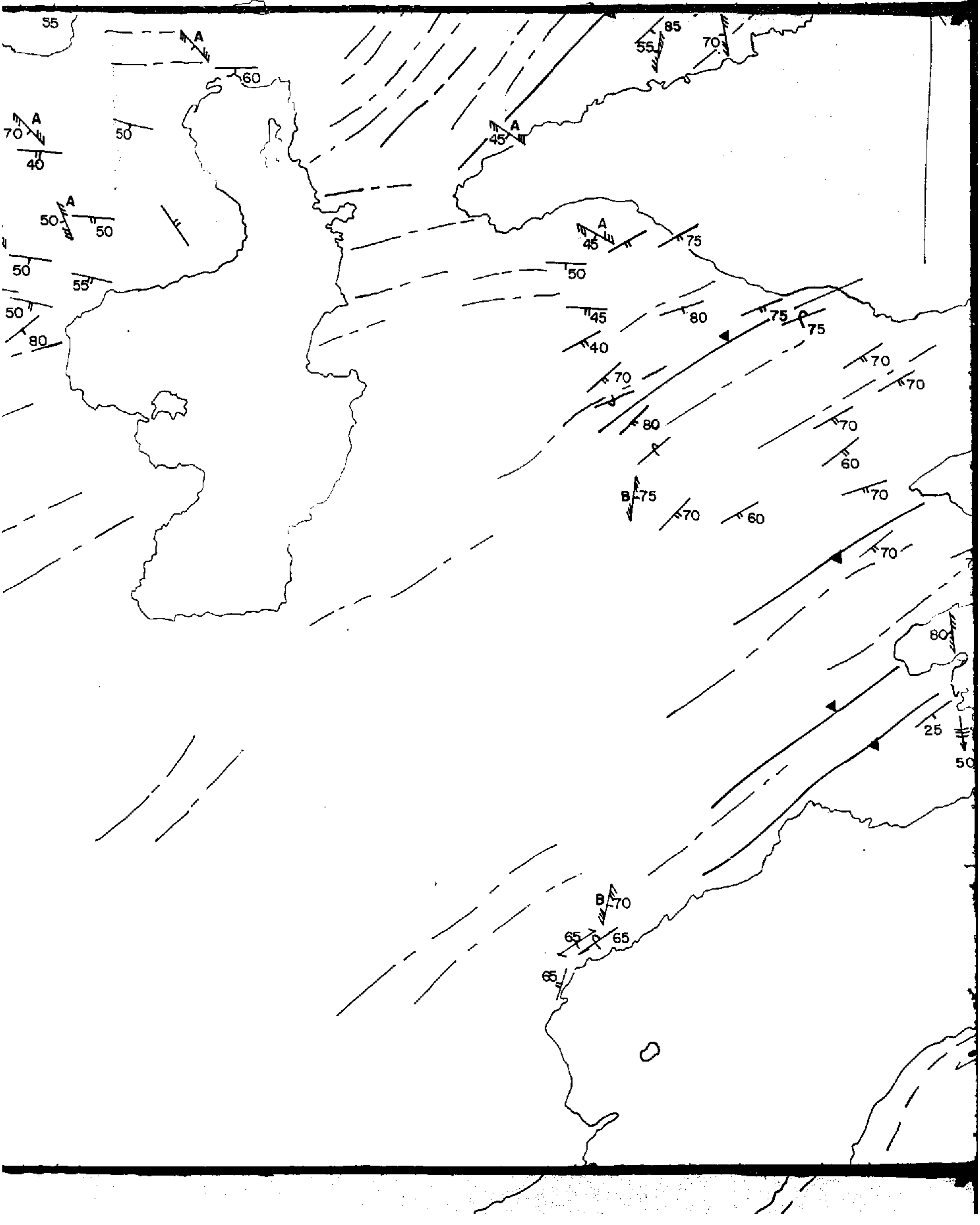
55
A
85
55
70
60
A
70
40
50
A
45
A
50
50
A
45
75
50
50
55
50
80
50
45
80
75
75
40
70
70
70
80
70
60
B
75
70
70
60
70
80
25
50
B
70
65
65
65

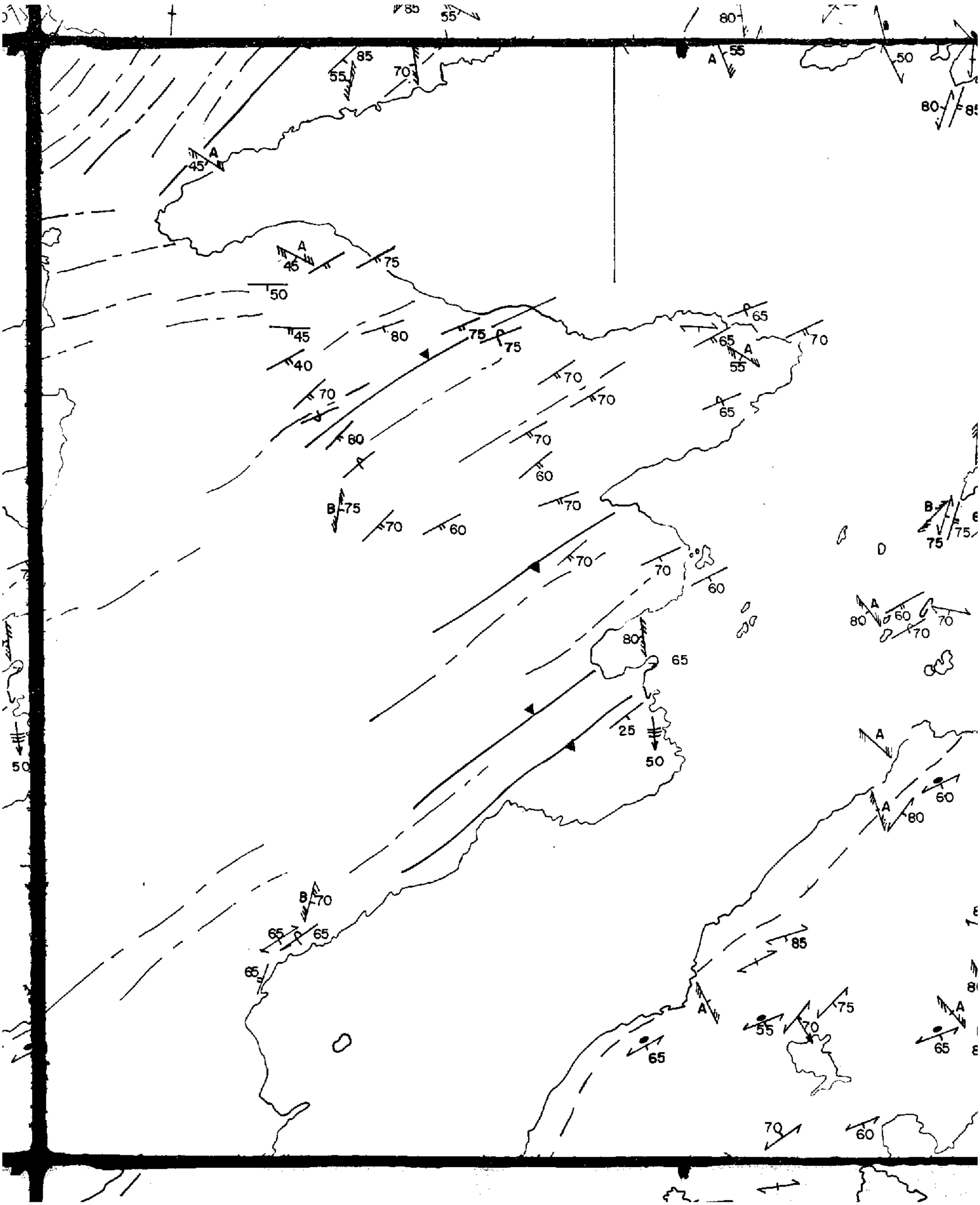

85
55
80
A
55
50
80
85
55
70
A
45
A
45
75
50
65
45
80
75
75
65
A
55
70
40
70
70
70
65
80
70
60
B
75
70
60
70
B
75
75
D
70
70
60
A
80
60
70
70
80
65
25
50
50
A
60
A
80
B
70
65
65
65
85
A
75
55
70
A
65
65
70
60

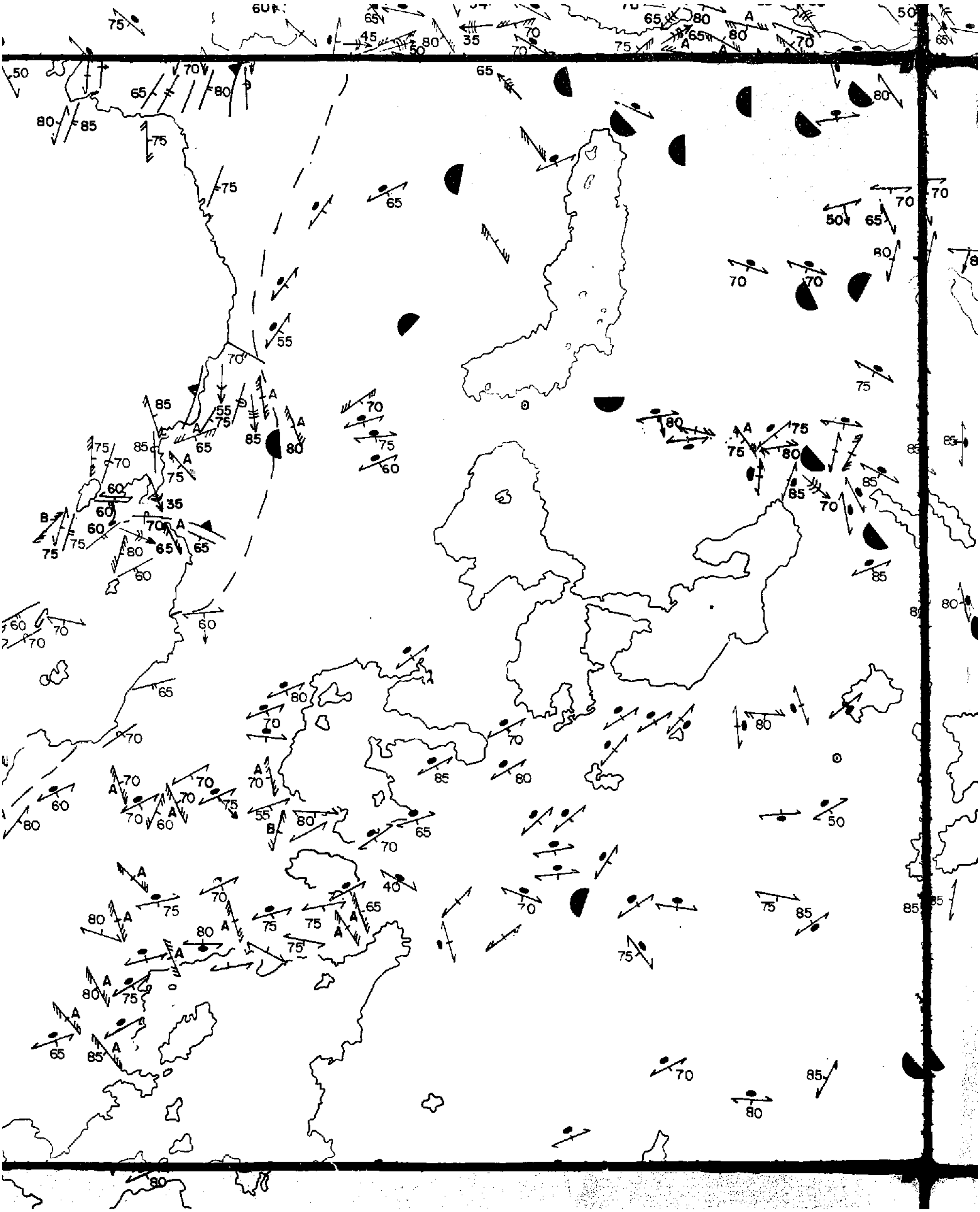

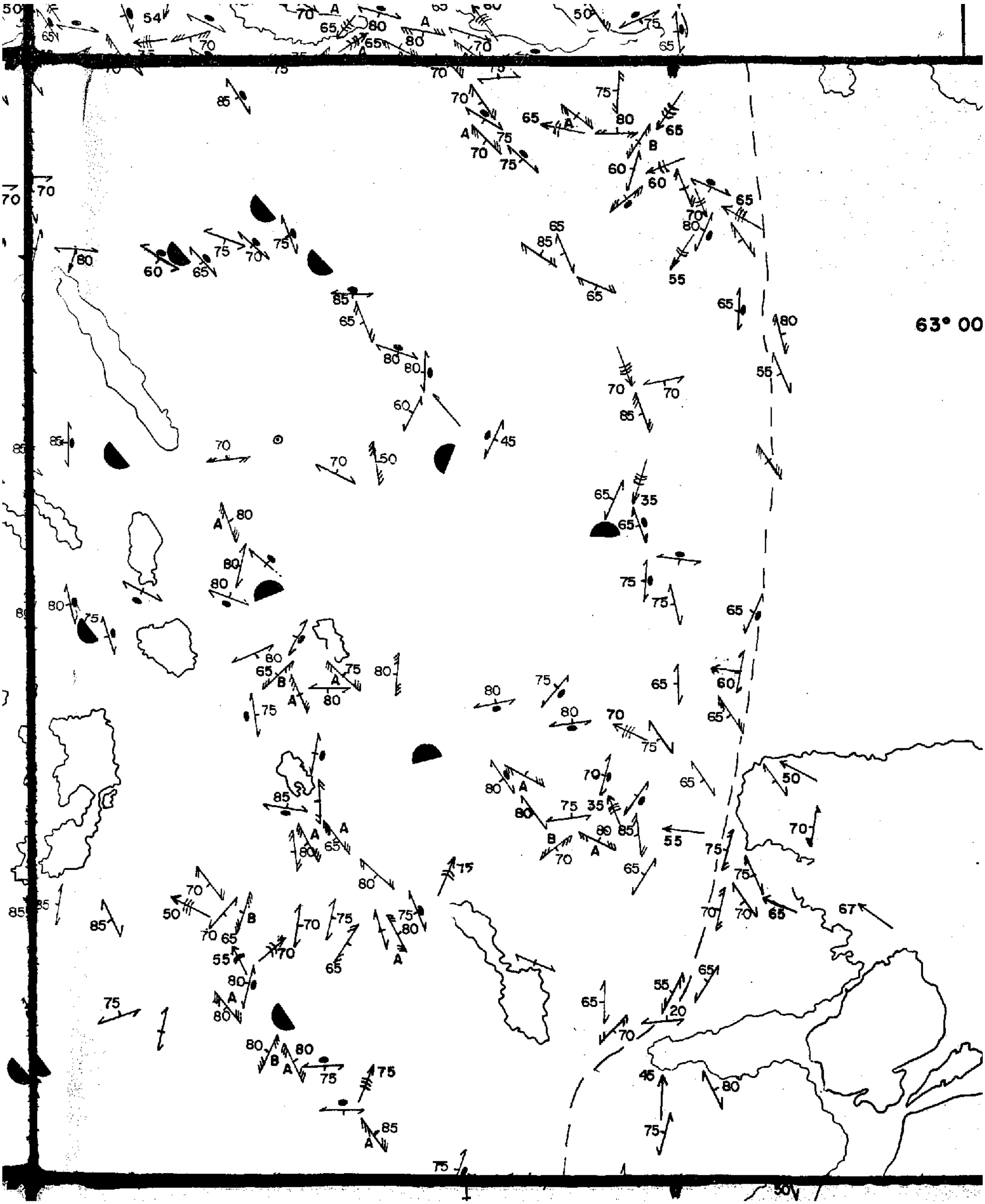
63° 00

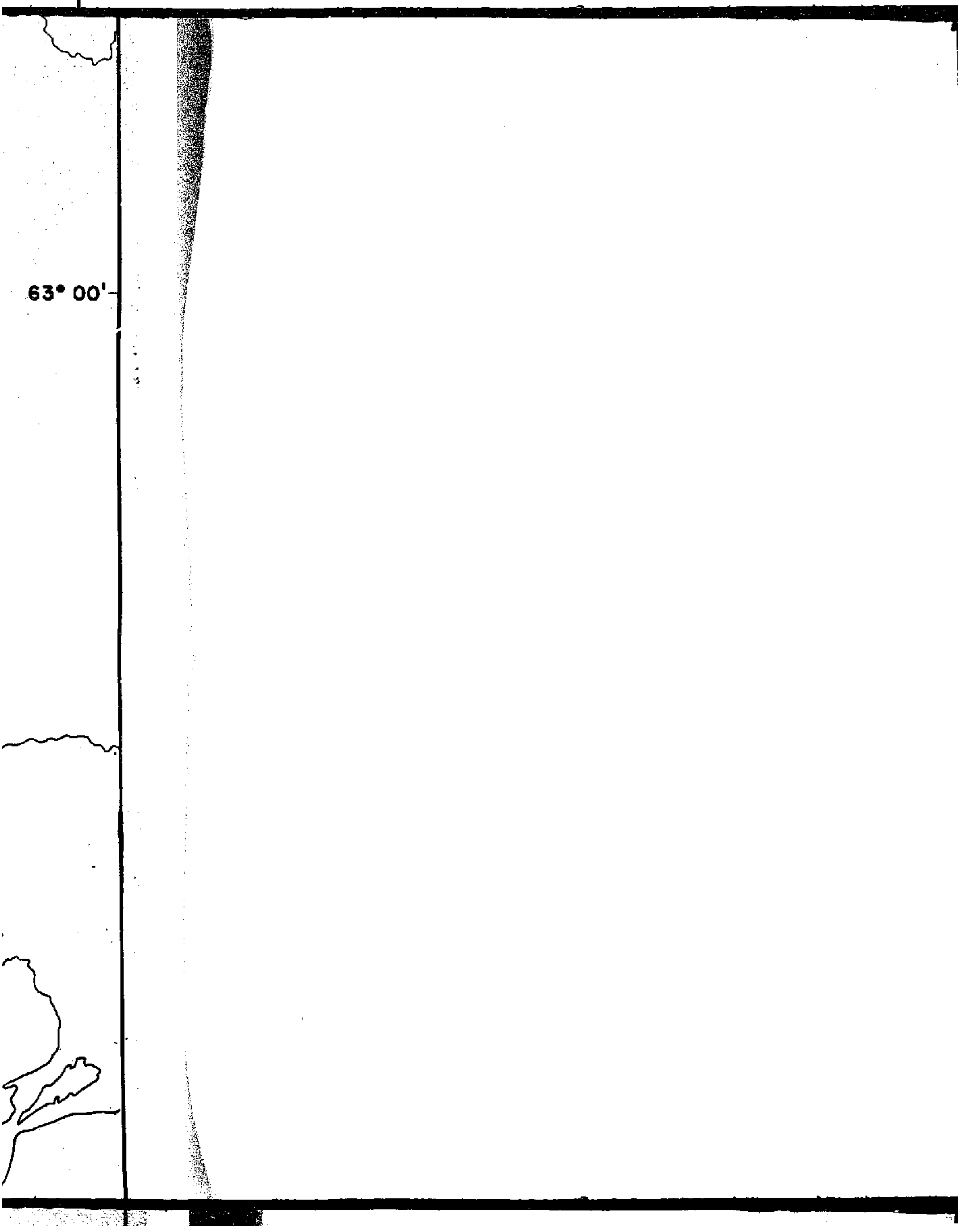
63° 00'

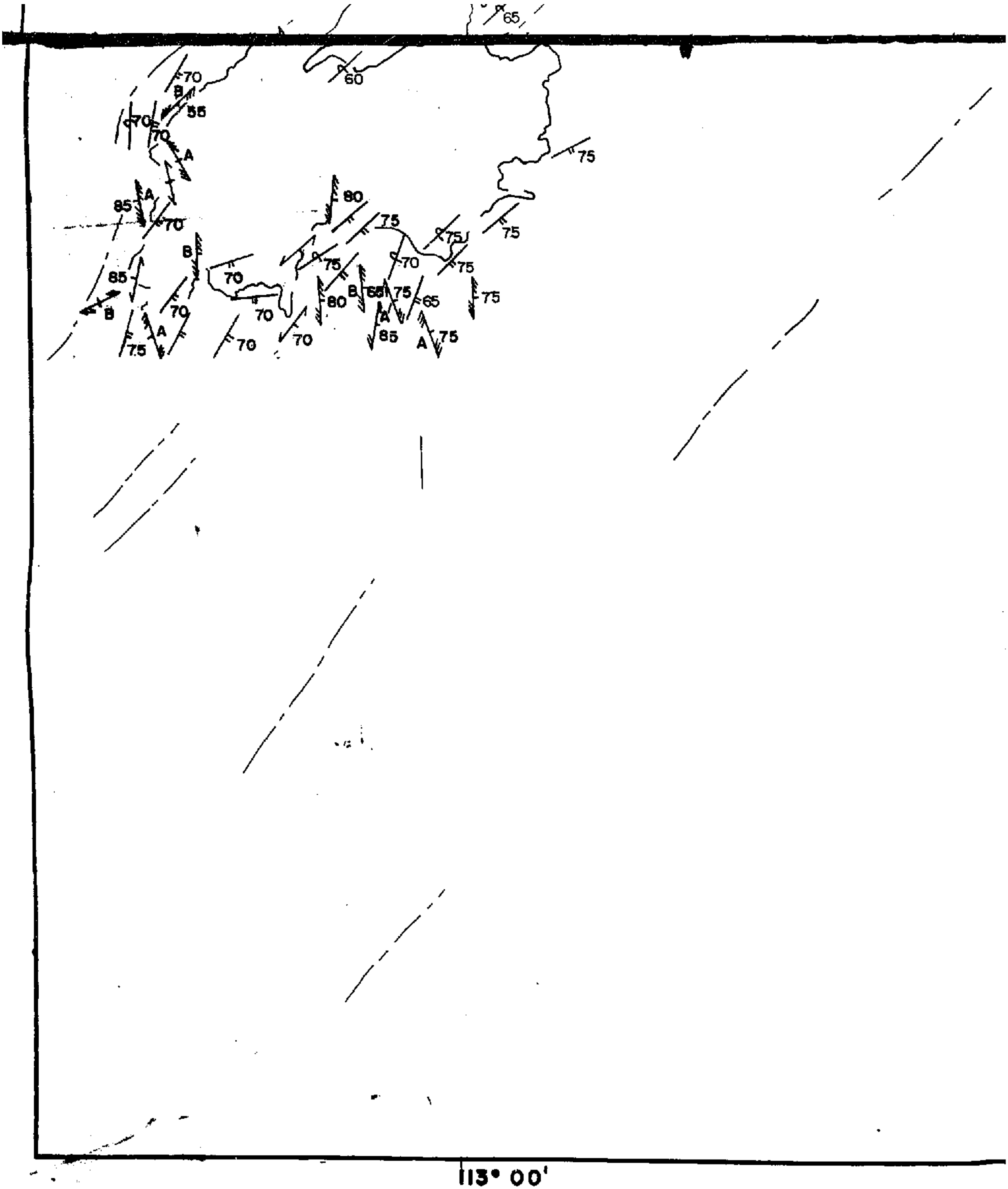
65
60
70
B
55
70
70
A
75
80
85
A
70
75
75
75
B
70
75
85
70
75
B
80
B
65
75
65
75
70
70
B
A
85
70
70
75
A
75
113° 00'

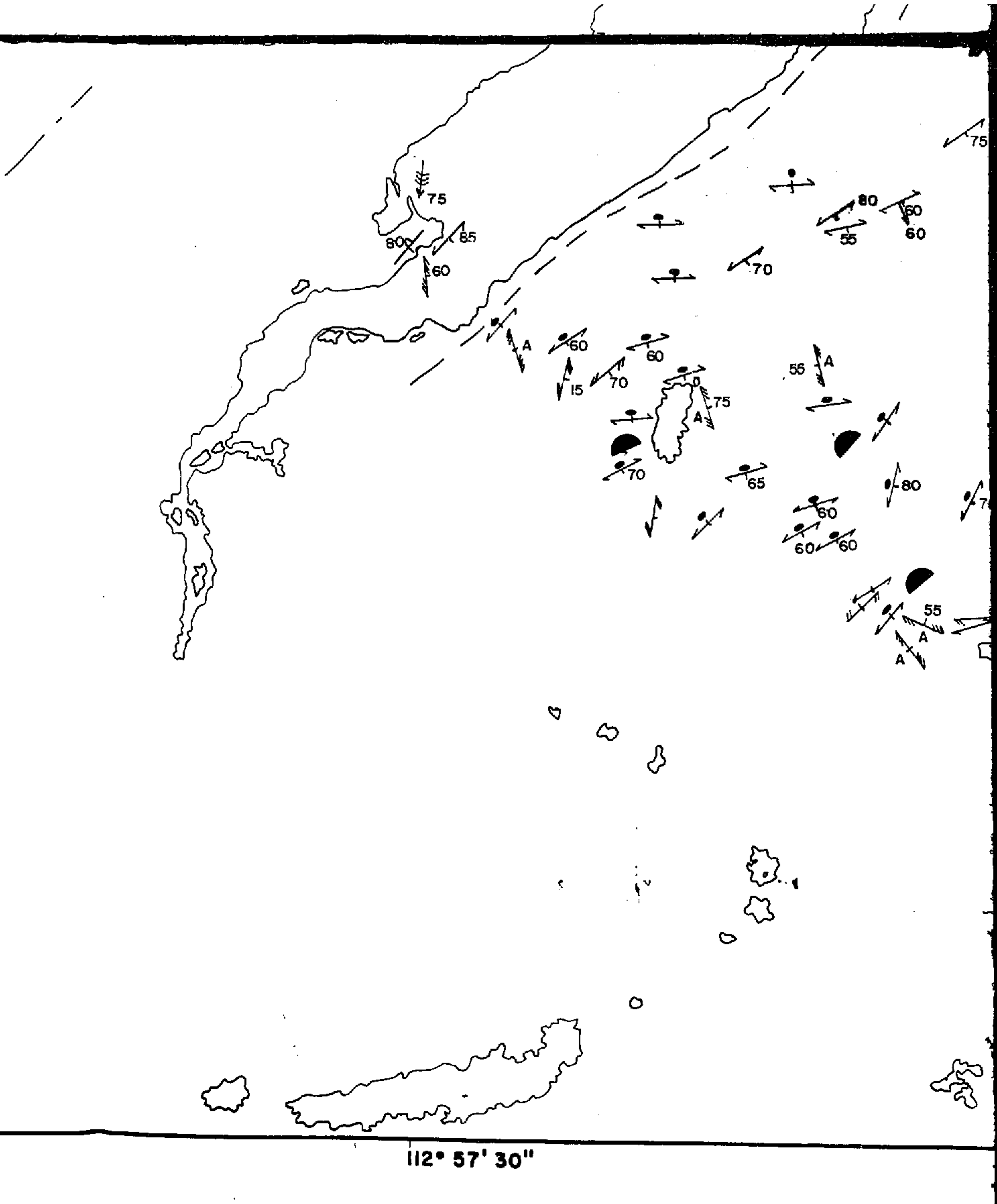
75
80
85
60
75
80
60
55
60
70
A
60
60
55
A
15
70
75
A
70
65
80
60
60
60
55
A
A
112° 57' 30"

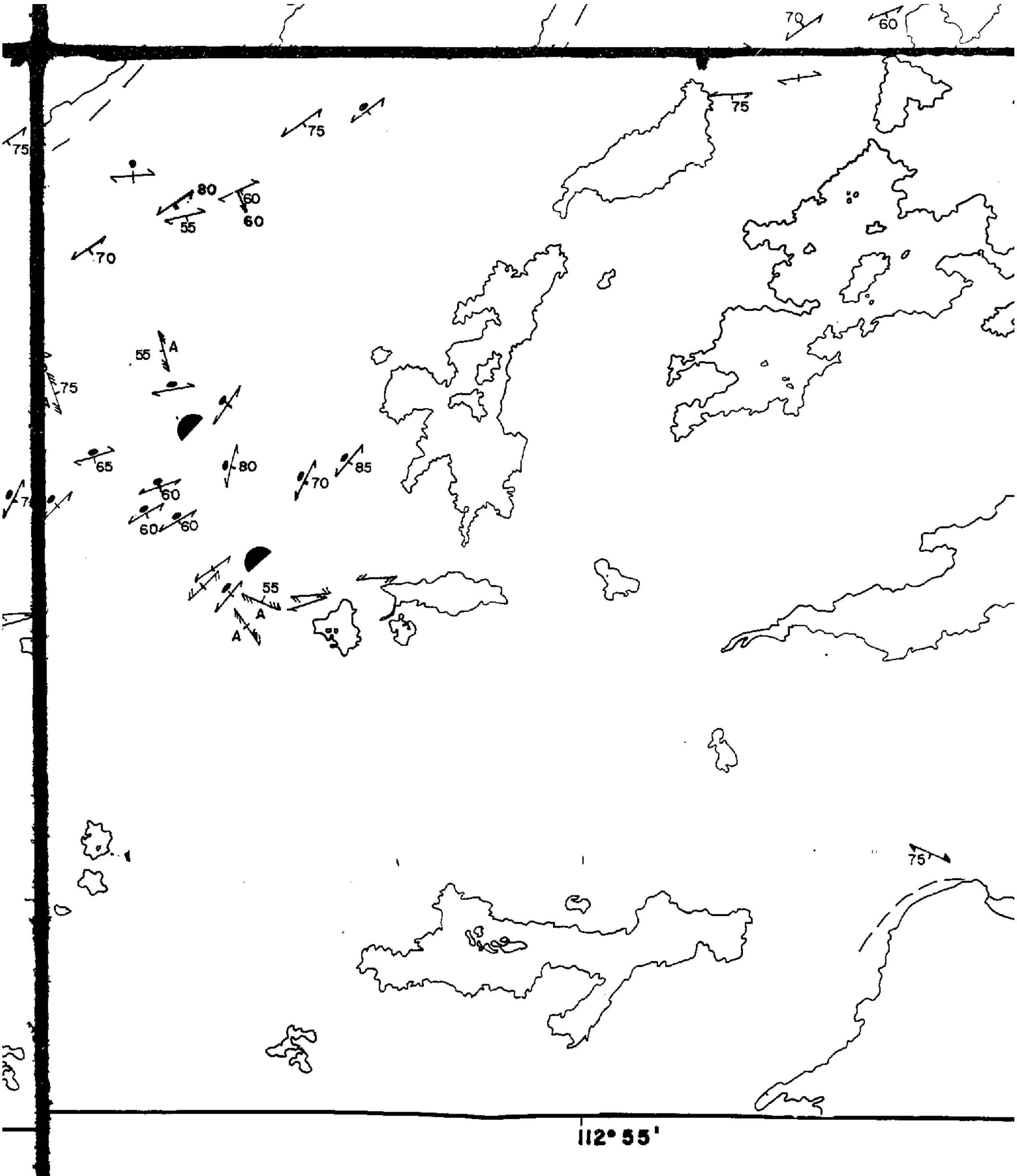

70
60
75
75
75
80
60
60
55
70
55
A
75
65
80
70
85
60
60
60
55
A
A
75
112° 55'

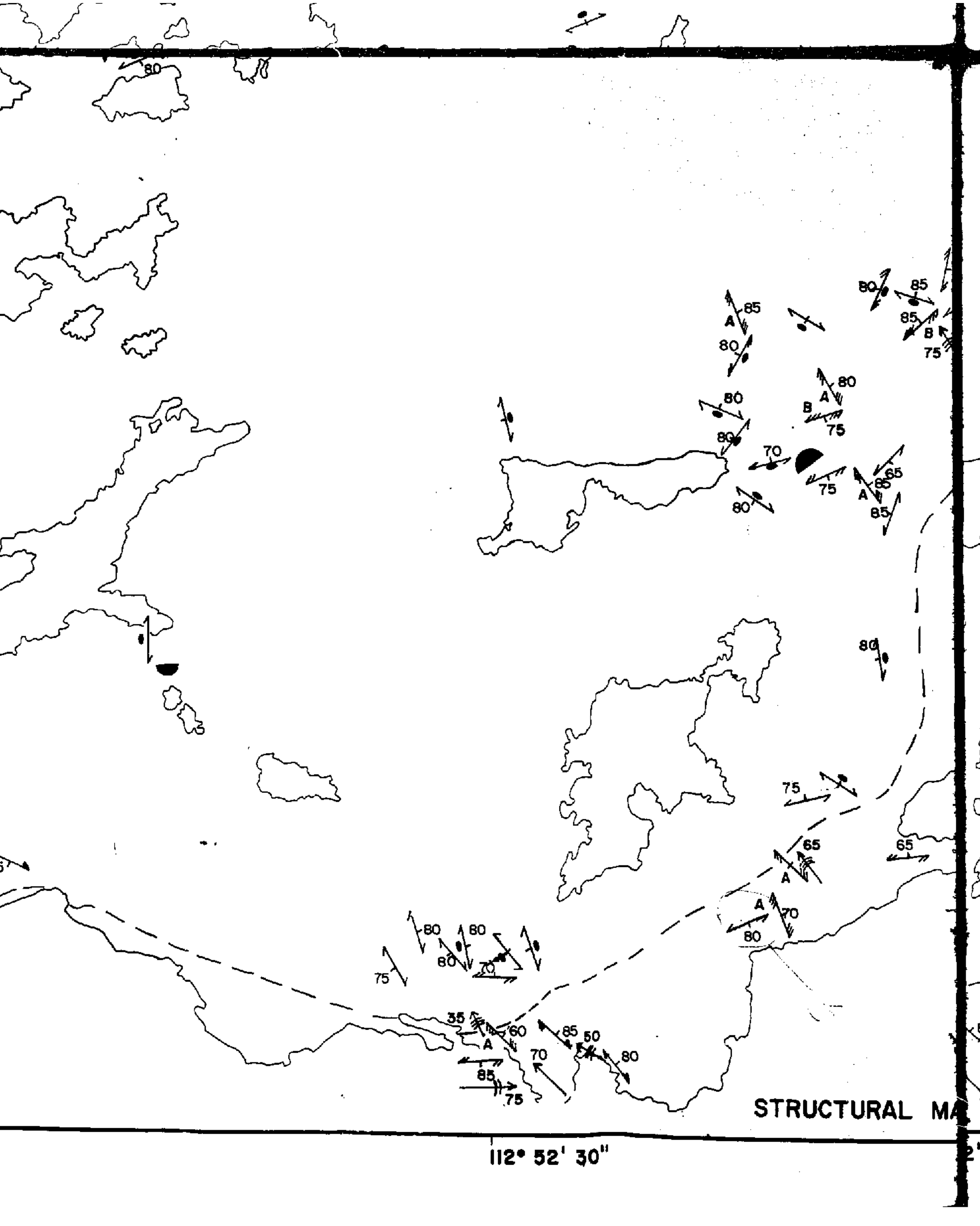
STRUCTURAL MA
112° 52' 30"

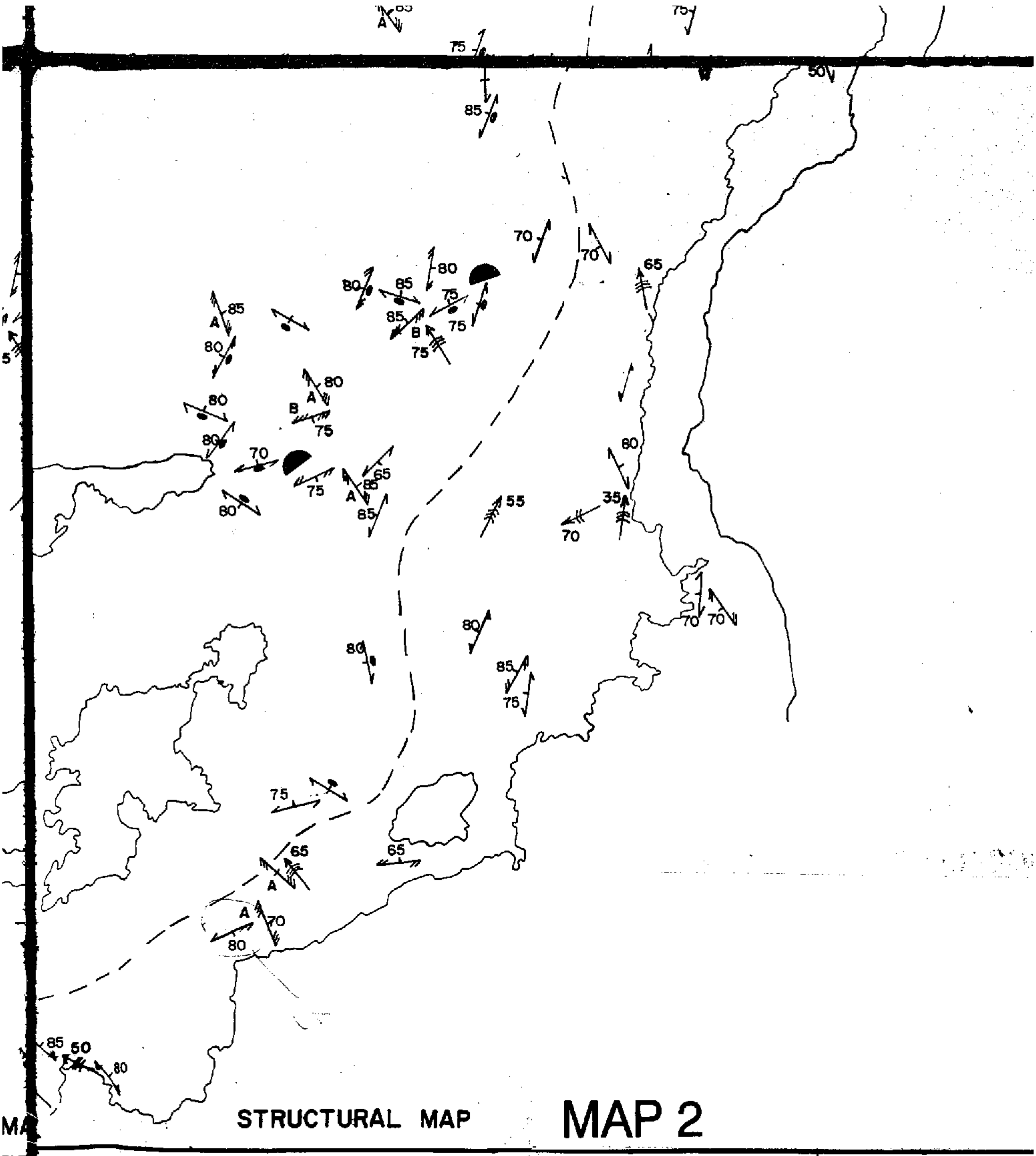

STRUCTURAL MAP

MAP 2

2' 30"

112° 50